



NUI MAYNOOTH

Ollscoil na hÉireann Má Nuad



# Investigating the cellular localisation of DEAD box helicase DDX3

---

**Ruth Brennan B.Sc.**

February 2013

A thesis submitted to  
The National University of Ireland, Maynooth  
for the degree of  
Doctor of Philosophy

Department of Biology  
National University of Ireland, Maynooth  
Supervisor: Dr. Martina Schroeder

This work was funded by the HRB Scholars Programme in Immunology  
(Grand No. PhD/ 20007/9)

## Contents

---

Contents .....	I
Abstract .....	VII
Acknowledgements .....	VIII
List of abbreviations .....	IX
List of Tables .....	XIII
List of Figures.....	XIV
Chapter 1 : Introduction .....	1
1.1. An Introduction to Nuclear Transport .....	3
1.1.2. Nuclear import .....	6
1.1.2.1. Ran dependent nuclear import .....	6
1.1.2.1.2. Importin-Beta .....	9
1.1.2.1.3. Transportins .....	10
1.1.2.2. RAN independent nuclear import .....	11
1.1.2.2.1. Calmodulin/calcium- dependent import.....	11
1.1.3. Nuclear Export.....	12
1.1.3.1. Ran dependent nuclear export .....	12
1.1.3.1. Ran-independent nuclear export.....	17
1.1.4. Regulation of Nuclear transport.....	17
1.2. Introduction to DDX3 .....	20
1.2.1. DDX3's role in RNA metabolism .....	20
1.2.2. Evidence of DDX3's role in Transcription .....	24
1.2.3. Evidence of DDX3's role in Splicing .....	26
1.2.4. Evidence of DDX3's role in RNA export .....	26
1.2.5. DDX3's role in Protein Translation .....	27
1.2.6. Summary of DDX3's nuclear and cytoplasmic functions.....	28
1.3. Aims of this study.....	30
Chapter 2 : MATERIALS AND METHODS.....	31
2.1. Standard Laboratory Procedures .....	31
2.2. Molecular Biological methods .....	31
2.2.1. Preparation of chemically competent cells .....	31
2.2.2. Transformation of chemically competent cells.....	31
2.2.2. Isolation of plasmid DNA .....	32
2.2.2.1. Small-scale DNA amplification .....	32
2.2.2.2. Large-scale DNA amplification .....	32
2.2.2.3. DNA quantification.....	33
2.2.3. Agarose gel electrophoresis.....	33

2.2.4. DNA purification.....	34
2.2.4.1. Gel purification.....	34
2.2.5. Polymerase Chain Reaction (PCR) .....	34
2.2.5.1. End-point PCR.....	34
2.2.5.1.1. Principle.....	34
2.2.5.1.2. Primer design .....	34
2.2.5.1.3. PCR reaction mix .....	35
2.2.5.1.4. PCR cycling program.....	36
2.2.6. Site directed mutagenesis PCR.....	36
2.2.6.1. Principle.....	36
2.2.6.1. Primer Design .....	37
2.2.6.2. PCR reaction mix .....	38
2.2.6.3. PCR cycling conditions.....	39
2.2.6.4. <i>DPN1</i> digestion and transformation .....	39
2.2.7. Gene cloning technology.....	39
2.2.7.1. Principle.....	39
2.2.7.2. Vectors and insert sequences .....	40
2.2.7.3. Cloning protocols .....	41
2.2.7.3.1. Enzymatic digestion of the vector and the insert .....	41
2.2.7.3.2. Dephosphorylation of vector for one enzyme cloning .....	42
2.2.7.3.3. Ligation of the vector and the insert.....	42
2.2.7.3.4. Transformation and selection .....	43
2.2.7.3.5. Screening of the transformants .....	43
2.2.7.3.6. Sequencing .....	43
2.2.7.4. Plasmid construction.....	43
2.3. Protein methods .....	46
2.3.1. One-Dimensional SDS-PAGE.....	46
2.3.2. Coomassie Blue staining.....	46
2.3.3. Western blot analysis .....	46
2.3.3.1. Electroblothing procedure .....	46
2.3.3.2. Immunoblotting procedure.....	47
2.3.3.3. Chemiluminescent detection .....	47
2.4. Mammalian cell culture methods .....	47
2.4.1. Cells culture.....	48
2.4.2. Transient transfection of mammalian cell lines .....	49
2.4.2.1. Calcium Phosphate transfection .....	49
2.4.2.2. Gene juice transfection .....	49
2.4.2.3. SIRNA transfection .....	49

2.4.3. Cell treatments.....	50
2.5. Co-immunoprecipitation (Co-IP) assay .....	51
2.5.1. Principle.....	51
2.5.2. Co-immunoprecipitation (Co-IP) assay .....	51
2.6. <i>In vitro</i> Recombinant protein Pull down Assay.....	51
2.6.1. Expression and purification of recombinant His-tagged Proteins in E.coli ....	51
2.6.2. <i>In vitro</i> Pulldown assay.....	52
2.7. Intracellular protein Co-localisation Studies.....	53
2.7.1. Immunofluorescent staining .....	53
2.7.1.1. Mitochondria staining .....	54
2.7.1.1. Lipid droplet staining.....	54
2.7.3. Low content analysis .....	55
2.7.3. High Content analysis.....	56
2.7.3.1. Preparation of cells for IN Cell Analyzer.....	56
2.7.3.2. Analyzes of High-Content data.....	56
2.8. Nuclear Cytoplasmic fractionation .....	58
2.8.1. Principle.....	58
2.8.2. Method.....	58
2.9. Cell cycle arrest and synchronization .....	59
2.9.1. Principle.....	59
2.9.2. Double thymidine block (G1/S block).....	59
2.9.3. Thymidine/Nocodazole block ( G2/M block) .....	59
2.9.4. Serum starvation (G0/G1 block).....	59
Chapter 3 : Nuclear export of DDX3 .....	61
3.1. Introduction .....	61
3.1.1. DDX3 export via Tip Associated Protein (TAP) .....	61
3.1.2. DDX3 export via CRM-1.....	61
3.1.3. Conclusion .....	64
3.2. Aims .....	64
3.3. Results.....	65
3.3.1. DDX3 localises predominantly in the cytoplasm in a range of transformed cells Lines .....	65
3.3.2. DDX3 is exported from the nucleus in a CRM-1 dependent manner .....	67
3.3.3. DDX3 helicase activity is not required for nuclear export .....	70
3.3.4. Mapping the region of DDX3 required for nuclear export.....	72
3.3.4.1 The C-terminus of DDX3 in not required for nuclear export .....	72
3.3.4.2. The N-terminus of DDX3 is required for nuclear export.....	74
3.3.5. The NES in the N-terminus of DDX3 is required for nuclear export .....	77

3.3.5.1. Disrupting the NES of DDX3 results in impaired nuclear export.....	80
3.3.5.2. The NES of DDX3 is sufficient to restore nuclear export of export deficient mutants.....	84
3.4. Discussion .....	86
Chapter 4 : Investigating the Nuclear import of DDX3.....	89
4.1. Nuclear import of DEAD box helicases .....	89
4.1.1 RAN Dependent- Importins.....	89
4.1.2 RAN Dependent-Transportins .....	90
4.1.3. RAN Independent-Calmodulin .....	91
4.1.4. Inhibitors of nuclear import .....	91
4.1.4.1. Importin $\alpha/\beta$ inhibitors .....	91
4.1.4.2. Importazole (IPZ) small molecule inhibitor.....	92
4.1.4.3. Calmodulin Inhibitors.....	92
4.2. Aims .....	93
4.3. Results.....	94
4.3.1. DDX3 contains two globular RecA-like domains which are imported into the nucleus independently .....	94
4.3.2. Putative NLS found using predication software.....	96
4.3.3. Investigating the nuclear import of DDX3 using import inhibitors .....	103
4.3.3.1. Importazole does not inhibit the import of DDX3 .....	103
4.3.3.2. Bimax inhibitors do not inhibit nuclear import of DDX3.....	107
4.3.3.3. Calmodulin inhibitors do not inhibit nuclear import of DDX3 .....	109
4.3. Discussion .....	111
Chapter 5 : Regulation of DDX3 localisation by viral infection.....	115
5.1. Introduction .....	115
5.1.1. The role of DDX3 in the immune system .....	115
5.1.2. DDX3 is targeted by viruses .....	124
5.1.2.1. DDX3 is a target for Vaccinia virus .....	124
5.1.2.2. DDX3 is a target for HBV .....	124
5.1.2.3. Introduction to HIV .....	125
5.1.2.4. DDX3 is a target of HCV.....	128
5.1.3. Conclusion .....	133
5.2. Aims.....	134
5.3. Results.....	135
5.3.1. High content analysis to investigate change in localisation after a range of stimuli .....	135
5.3.2. Does DDX3 localisation change after overexpression of IKK $\epsilon$ ?.....	136
5.3.3. Investigating the relationship between HIV-Rev protein and DDX3.....	138

5.3.3.1. HIV-Rev changes the localisation of DDX3 .....	138
5.3.3.2. DDX3 interacts with HIV-Rev protein .....	141
5.3.3.3. Overexpression of DDX3 does not affect HIV-Rev mediated expression of Gag protein .....	144
5.3.4. Investigating the relationship of DDX3 and HCV Core protein .....	146
5.3.4.1. HCV Core protein co-localises with endogenous DDX3 in distinct cytoplasmic speckles .....	146
5.3.4.2. HCV Core protein prevents the nucleocytoplasmic shuttling .....	147
5.3.4.3. Core protein inhibits DDX3 shuttling through a direct interaction.....	153
5.3.4.4. DDX3 nuclear shuttling is inhibited in Huh7 cells expressing non-replicating full length HCV genome .....	156
5.3.4.5. HCV infection causes cellular redistribution of endogenous DDX3 in a hepatocyte cell lines .....	158
5.3.4.6. Does HCV Core expression change protein expression of DDX3? .....	160
5.3.4.7. HCV causes redistribution of eIF4E .....	161
5.3.4.7. Does DDX3 localise differently in primary cells compared to transformed cells? .....	162
5.4. Discussion .....	164
Chapter 6 : Regulation of DDX3 localisation by cellular stress.....	168
6.1. Introduction to RNA granules .....	168
6.1.1. DDX3's association with stress granules .....	171
6.1.2. Conclusion.....	173
6.2. Aims .....	173
6.3. Results.....	174
6.3.1. DDX3 localises to cytoplasmic granules in response to stress.....	174
6.3.2. Helicase activity not required for DDX3 to be recruited to stress granules	178
6.3.3. Stress granules inhibit the nuclear import of DDX3.....	180
6.3.4. The eIF4E binding site is not required for recruitment of DDX3 to stress granules .....	182
6.3.5. The C-terminus and the N-terminus of DDX3 play a role in recruitment to SG .....	184
6.4. Discussion .....	189
Chapter 7 : Investigating the role of DDX3 in the cell cycle .....	192
7.1. Introduction .....	192
7.1.1. DDX3's role in cycle control.....	193
7.1.2. DDX3 as a tumour suppressor.....	195
7.1.3. DDX3 as an oncogene.....	196
5.1.4. Conclusion .....	198
7.2. Aims .....	199
7.3. Results.....	200

7.3.1. High content analysis to investigate change in localisation in response to DNA damage .....	200
7.3.2. Localisation of endogenous DDX3 changes during cell cycle.....	202
7.3.3. Phospho-Thr 323 DDX3 antibody co-localised with nuclear speckle marker .....	210
7.3.4. Investigating the role of Cyclin B phosphorylation of DDX3 .....	211
7.3.5. Investigating the expression of DDX3 during the cell cycle .....	214
7.4. Discussion .....	217
Chapter 8 : General Discussion.....	221
Bibliography.....	227
Appendix I.....	249
Appendix II.....	255

## Abstract

---

DDX3 is an RNA helicase that has been shown to have a range of nuclear and cytoplasmic functions, including transcription, translation, splicing and mRNA export. DDX3 has also been shown to play a role in innate immune signalling and tumorigenesis. DDX3 is targeted by multiple viruses: HIV, HCV, HBV and Vaccinia Virus have all been shown to interact with DDX3; either using DDX3 to replicate or inhibiting DDX3's function in antiviral signalling. Human DDX3 was reported to be exported from the nucleus independently of its N-terminal NES and to interact with CRM-1 through DDX3's C-terminal region. It was suggested that DDX3 acts as a CRM-1 cofactor, rather than cargo, and that it mediates Rev-dependent export of HIV RNAs. I confirmed that DDX3 exports in a CRM-1 dependent manner, and DDX3's N-terminus is required for nuclear export.

We have also investigated the nuclear import of DDX3. Putative NLS were found using bioinformatic software, and tested for functionality by mutating key basic residues. We also used a range of nuclear import inhibitors to examine how DDX3 is imported into the nucleus. We found that the DDX3's two Rec-A like domains could be imported independently, and also that DDX3 imported independently of Importin- $\beta$  and Calmodulin. We were also interested as to whether DDX3's cellular localisation was regulated during viral infection, cellular stress and during the cell cycle. We investigated the relationship of DDX3 with HIV and HCV viral proteins, and found that both HIV and HCV target the cellular localisation of DDX3. We found that DDX3 directly interacts with HIV-Rev protein, and also that HIV-Rev recruits DDX3 to the nucleolus. We also found that HCV Core protein recruited DDX3 to cytoplasmic speckles, and prevented the nucleocytoplasmic shuttling of DDX3. We found DDX3 to be recruited to Stress Granules after cellular stress. DDX3's cellular localisation and expression levels were also found to change throughout the cell cycle.

## Acknowledgements

---

First and foremost, I would like to thank my supervisor Dr. Martina Schroeder for all her help over the course of my PhD. This work would not have been possible without your advice, guidance and expertise.

I would like to thank everyone in the Host-Pathogen Interaction Lab, it has been great working with you all and I appreciate all the help and laughs you have given me throughout the years.

I would also like to thank the members of the Cell Signalling Lab, it has been a pleasure working alongside you.

My research would not have been possible without funding from the Health Research Boards (HRB). I would like to thank Prof. Paul Moynagh and the HRB Scholars' programme for giving me the opportunity to do this PhD.

Many thanks to Dr. Nigel Stevenson (Intracellular Immunology, Trinity) and Cormac McKenna (Institute of Molecular Medicine, Trinity) for helping out with the HCV work. Also Dr. Antje Hoff (Institute of Molecular Medicine, Trinity) for her help with the HCA.

To all my friends in Maynooth, thank you so much for supporting me over the last few years, and in particular this last year. Thank you for always cheering me up when my PhD work went awry, and most importantly for always being available for a cup of tea and a chat!

And finally I would like to thank my family for supporting me in all my academic endeavours. Mam and Dad, your ability to embrace life during this last year was inspirational, and I thank you for this. Dad you are never, and never will be far from my mind and to you I dedicate this thesis.

## List of abbreviations

---

Aim2-like receptors (ALRs)

Benzo[a]pyrene diol epoxide (BPDE)

CALcium MODulated proteIN (Calmodulin)

Casein Kinase 1 (CK1)

Cellular Apoptosis Susceptibility protein (CAS)

Chromosome region maintenance 1 (CRM-1)

Classical Nuclear localisation sequence (cNLS)

Constitutive Transport Element (CTE)

C-type Lectin receptors (CLRs)

Cyclin dependent kinases (Cdk)

Danger-Associated Molecular Patterns (DAMPs)

Endosomal sorting complex required for transport (ESCRT)

Epithelial-mesenchymal-like transition (EMT)

Epstein Barr virus Nuclear Antigen-1 (EBNA-1)

Etoposide (ETO)

Five prime untranslated region (5' UTR)

Glioblastoma Multiforme (GBM)

Glutathione S-transferase (GST)

Hepatocellular Carcinoma (HCC)

High content Analysis (HCA)

High-mobility group (HMG)

Human Papillomavirus (HPV)

Hypoxia Inducible Factors (HIFs)

Hypoxia Responsive Elements (HREs)

IFN-regulatory factor (IRF)

Importazole (IPZ)

Importin- $\beta$  binding (IBB)

Interferon (IFN)

Interleukin a (IL-1)

Internal Ribosomal Entry Site (IRES)

I $\kappa$ B (inhibitor of NF- $\kappa$ B) kinase  $\epsilon$  (IKK $\epsilon$ )

laboratory of genetics and physiology 2 (LGP2)

Lemptomycin B (LMB)

Leucine-rich repeat (in Flightless I) interacting protein-1 (Lrrfip1)

Long Terminal Repeat (LTR)

Mammalian orthoreovirus (MRV)

Melanoma differentiation-associated antigen 5 (MDA5)

Multiple cloning site (MCS)

Messenger ribonucleoprotein particles (mRNPs)

Negative effector (Nef)

NOD-like receptors (NLRs)

non-coding region (NCR)

Non-Structural protein 1 (NS1)

Nuclear localisation sequence (NLS)

Nuclear Pore Channel (NPC)

Oral Squamous Cell Carcinoma (OSCC)

Pathogen-Associated Molecular Patterns (PAMPs)

Phosphatase and tensin homolog (PTEN)

Polyinosinic polycytidylic acid (poly I:C)

Pregenomic RNA (pgRNA)

Pre-integration complex (PIC)

Processing Bodies (PB)

Processing Body (PB)

Proliferating Cell Nuclear Antigen (PCNA)

Protein parathyroid hormone related protein (PTHrP)

Regulator of Chromosome Condensation 1 (RCC1)

Regulator of virion expression (Rev)

Retinoic acid inducible gene I (RIG-I)-like receptors (RLRs)

Retinoic-acid inducible genes (RIG-I) receptors (RLRs)

Rev response element (RRE)

Reverse Transcriptase (RT)

RNA interference (RNAi)

RNA polymerase III (Pol III)

Sendai virus (SeV)

Signal Transducers and Activator of Transcription 1 (STAT 1)

Sodium Arsenite (SA)

Sterol regulatory element-binding protein 2 (SREPB2)

Stimulator of interferon genes (STING)

Stress granules (SG)

TANK-binding kinase (TBK1)

Temperature-sensitive (ts)

Tip-associated protein (TAP)

Toll like receptors (TLRs)

Topoisomerase II (TopoII)

Transacting responsive (Tar)

Tumour necrosis factor (TNF)

Vaccinia virus (VACV)

Viral infectivity factor (Vif)

Viral protein r (Vpr)

Viral protein u (Vpu)

## List of Tables

---

Table 1.1: Mammalian Exportins and their cargoes. ....	12
Table 1.2: Human DDX3 regulates transcription of several gene promoters. ....	24
Table 1.3: Human DDX3 interacts with translational initiation factors.....	28
Table 2.1: PCR Master Mix.....	35
Table 2.2: PCR cycling program .....	36
Table 2.3: Site Directed mutagenesis primers.....	37
Table 2.4: PCR Master Mix.....	38
Table 2.5: PCR Conditions. ....	39
Table 2.6: Restriction enzyme digestion reaction.....	41
Table 2.7: Dephosphorylation reaction. ....	42
Table 2.8: Ligation reaction. ....	42
Table 2.9: Primers used for PCR amplification of DDX3 mutants. ....	44
Table 2.10: Cell line information .....	48
Table 2.11: siRNA sequence and Identifier ( <i>Invitrogen</i> ).....	50
Table 6.1 : Known stress granule components and their protein function. ....	169

## List of Figures

---

Figure 1.1: Architecture of nuclear membrane and NPC complex structure.....	5
Figure 1.2: Overview of nuclear protein import.....	8
Figure 1.3: Redefinition of NES consensus sequence into PKI-like NES and Rev-like NES.....	13
Figure 1.4: Nuclear export through the pore.....	16
Figure 1.5: DDX3 belongs to the DEAD-box protein family.....	22
Figure 1.6: Nuclear and cytoplasmic processes involving mRNA.....	23
Figure 1.7: DDX3 is a multifunctional protein with distinct roles in the nucleus and the cytoplasm. ....	29
Figure 2.1: Schematic of NES addition plasmid construction.....	45
Figure 2.2: Nuclear/Cytoplasmic intensity was measured using Olympus Fluoview Software. ....	55
Figure 2.3: High Content microscopy workflow. ....	57
Figure 3.1: Leucine rich NES is conserved in the DDX3 homologues and corresponds to a PKI-like NES.....	63
Figure 3.2: Endogenous DDX3 localises in the cytoplasm. ....	66
Figure 3.3: DDX3 has a cytoplasmic localisation in a range of human cell lines. ....	67
Figure 3.4: CRM-1 is required for the export of DDX3. DDX3 accumulated in the nucleus when treated with 20mM Leptomycin B (LMB) for 2 hours. ....	69
Figure 3.5: Helicase activity of DDX3 is not required for nuclear export. ....	71
Figure 3.6: The C-terminus of DDX3 is not required for export or import of DDX3. ....	73
Figure 3.7: DDX3 has a putative NES at residues 12-22.....	75
Figure 3.8: WT DDX3 localises predominantly in the cytoplasm; whereas N-terminal deletion mutant 139-662 localises predominantly in the nucleus.....	76
Figure 3.9: Removal of putative NES results in nuclear accumulation of DDX3.....	78
Figure 3.10: N-terminal deletion mutants 22-662 and 139-662 are predominantly nuclear, compared to WT DDX3 which is predominantly cytoplasmic.....	79
Figure 3.11: DDX3 NES mutant localises predominantly in the nucleus.....	81
Figure 3.12: WT DDX3 co-IPs with endogenous CRM-1 stronger than NES mutant and 139-662.....	83
Figure 3.13: The N-terminal NES (1-22) is sufficient to mediate export of DDX3. ....	85
Figure 4.1: The DDX3 truncation mutants 139-408 and 409-662 are imported independently into the nucleus, suggesting two distinct regions facilitate nuclear import of DDX3.....	95
Figure 4.2: Mutation of putative NLS predicted by PSORTII did not disrupt nuclear import.....	97
Figure 4.3: NuclImport was used to identify other putative NLS regions in DDX3. ....	98
Figure 4.4: Mutation to putative NLS predicted by NuclImport did not disrupt nuclear import of DDX3.....	100
Figure 4.5: Mutation to putative NLS predicted by NuclImport did disrupt nuclear import of 139-408 mutant. ....	102
Figure 4.6: Nuclear import of endogenous DDX3 is not affected by the Importin $\beta$ inhibitor Importazole (IPZ).....	104
Figure 4.7: Nuclear import of DDX3 truncations is not affected by the Importin- $\beta$ inhibitor Importazole (IPZ).....	106
Figure 4.8: Nuclear import of DDX3 is not inhibited by the Importin $\beta$ inhibitors Bimax 1 or Bimax 2.....	108
Figure 4.9: Nuclear import of DDX3 is not affected by the Calmodulin inhibitor W7. ....	110
Figure 5.1: Antiviral signalling leading to type I IFN production.....	118

Figure 5.2: Structure of K7-DDX3 complex. ....	121
Figure 5.3: DDX3 is required for IFN $\beta$ induction and is a target for viral immune evasion.....	123
Figure 5.4: Organization of the HIV-1 genome. ....	127
Figure 5.5: Schematic of HCV virion structure and genome organisation.....	130
Figure 5.6: Endogenous DDX3 does not change localisation after treatment with various stimuli. ....	136
Figure 5.7: Overexpression of IKK $\epsilon$ does not change the cellular localisation of endogenous DDX3.....	137
Figure 5.8: Endogenous DDX3 co-localises with HIV-Rev protein in the nucleolus....	138
Figure 5.9: Endogenous DDX3 co-localises with HIV-Rev protein in the nucleus.....	139
Figure 5.10: Endogenous CRM-1 co-localises with HIV-Rev protein in the nucleus... 140	
Figure 5.11: Myc-tagged DDX3 co-immunoprecipitates with Ha-tagged HIV-Rev. ....	141
Figure 5.12: DDX3 interacts with HIV-Rev through residues between aa 139-408. ...	143
Figure 5.13: DDX3 interacts directly with HIV-Rev. ....	144
Figure 5.14: Overexpression of DDX3 does not change HIV-Rev mediated expression of Gag.....	145
Figure 5.15: HCV Core protein co-localises with endogenous DDX3 in cytoplasmic speckles in HeLa cells. ....	146
Figure 5.16: HCV Core protein from different genotypes Con1 of HCV virus prevents shuttling of DDX3 into the nucleus.....	148
Figure 5.17: HCV Core protein from different genotypes H77 of HCV virus prevents shuttling of DDX3 into the nucleus.....	149
Figure 5.18: HCV Core protein from different genotypes JC1of HCV virus prevents shuttling of DDX3 into the nucleus.....	150
Figure 5.19: HCV-Con1 and endogenous DDX3 co-localise around lipid droplets in HepG2 hepatocyte cells line. ....	152
Figure 5.20: Con1 Y35A mutant does not cause change in DDX3 localisation. ....	154
Figure 5.21: HCV Con1 Y35A Core protein does not prevent shuttling of DDX3 into the nucleus.....	155
Figure 5.22: HCV Core protein prevents shuttling of DDX3 into the nucleus. ....	157
Figure 5.23: HCV infection causes DDX3 to co-localise with HCV Core protein in cytoplasmic speckles in Huh7 cells. ....	159
Figure 5.24: Expression of Ha-tagged Core protein increased endogenous DDX3 protein expression. ....	160
Figure 5.25: Overexpression of HCV Core protein Con1 causes some eIF4E to co-localise in cytoplasmic speckles with Core protein.....	161
Figure 5.26: DDX3 has a more nuclear localisation in primary cells compared to transformed cells.....	163
Figure 6.1: DDX3 can be placed at multiple levels of the mRNA life cycle. ....	172
Figure 6.2: Overexpressed DDX3 has a distinct cytoplasmic speckle localisation.....	174
Figure 6.3: DDX3 co-localises with stress granules component eIF4E after Sodium Arsenite induced oxidative stress.....	176
Figure 6.4: Cycloheximide inhibits formation of DDX3 and eIF4E-containing granules. ....	177
Figure 6.5: DDX3 helicase mutant K230E co-localises with stress granule component eIF4E after Sodium Arsenite induced oxidative stress.....	179
Figure 6.6: Nuclear export deficient mutants are recruited to stress granules after Sodium Arsenite treatment. ....	181
Figure 6.7: The eIF4E binding site is not required for recruiting DDX3 to stress granules. ....	183

Figure 6.8: The N-terminus is not critical for recruiting DDX3 to stress granules. ....	185
Figure 6.9: The C-terminus is not critical for recruiting DDX3 to stress granules.....	186
Figure 6.10: Residues within the N-terminus are critical for recruitment of DDX3 to stress granules in the absence of the C-terminus. ....	188
Figure 7.1: Schematic of cell cycle.....	193
Figure 7.2: Endogenous DDX3 does not change localisation after treatment with Etoposide. ....	201
Figure 7.3: WT DDX3 localised to the nucleus in a small percentage of untreated cells. ....	202
Figure 7.4: There is no clear change in the localisation and expression of DDX3 during the cell cycle. ....	204
Figure 7.5: Localisation and level of Phospho-Thr323 DDX3 changes throughout the cell cycle.....	205
Figure 7.6: Endogenous DDX3 is predominantly cytoplasmic and Phospho-Thr323 DDX3 is predominantly nuclear at the G1/S block.....	207
Figure 7.7: Endogenous DDX3 becomes more nuclear and Phospho-Thr323 DDX3 remains nuclear at G2/M block. ....	208
Figure 7.8: Endogenous DDX3 is predominantly cytoplasmic and Phospho-Thr323 DDX3 predominantly nuclear at the G0/G1 block. ....	209
Figure 7.9: Phospho-Thr 323 DDX3 co-localises with nuclear speckle marker anti splicing factor SC-35. ....	210
Figure 7.10: The site mutants T204A and T204D have a predominantly cytoplasmic localisation and are exported from the nucleus in a CRM-1 dependent manner .....	212
Figure 7.11: The double site mutants TA2 and TD2 have a predominantly cytoplasmic localisation and are exported from the nucleus in a CRM-1 dependent manner. ....	213
Figure 7.12: Levels of DDX3 and Phos-Thr323-DDX3 changed during different stages of the cell cycle. ....	215
Figure 7.13: Levels of DDX3 are increased at prometaphase.....	216
Figure 7.14: Expression of DDX3 increases during mitosis.....	216

## **Chapter 1 : Introduction**

---

The human cell is a complex structure composed of subcellular compartments that have specialised environments and functions. The nucleus and cytoplasm are the two major compartments of the cell, segregating DNA replication and transcription to the nucleus and protein synthesis to the cytoplasm. The nucleus and cytoplasm are separated by the nuclear envelope, a double lipid bi-layer, which separates genetic material in the nucleus from the cytoplasm. The nuclear envelope is embedded with Nuclear Pore Complexes (NPC) which allow the controlled transport of molecules between the nucleus and the cytoplasm. Many cellular proteins have distinct functions within the cytoplasm or the nucleus, consequently regulation of a protein's nuclear transport can also regulate protein function. The NPC plays an integral role in controlling both gene expression and cell cycle regulation (Ahmed & Brickner 2007; Hetzer & Wente 2009).

In this study, I investigated the cellular localisation of the human DEAD-box RNA helicase DDX3, and the regulation of its nuclear import and export. Since DDX3 has been shown to influence various cellular processes in both the nucleus and the cytoplasm, we hypothesised that its cellular localisation is likely to be regulated and would influence its participation in its different cellular functions. DDX3 has been implicated in all aspects of the RNA life cycle, participating in the nuclear events (transcription, splicing and mRNA export) as well as the cytoplasmic events (translation and ribosome biogenesis) (Chang & Tarn 2009). Hence, it would be expected that DDX3 localisation changes in response to cellular requirements.

Importantly, DDX3 has been reported to regulate transcription and translation of proteins involved in control of the cell cycle, with DDX3 being implicated as both a tumour suppressor and oncogene (Chao et al. 2006; Botlagunta et al. 2008). Interestingly, DDX3 localisation has been suggested to be modified during cancer, switching from a predominantly nuclear localisation in healthy epidermal cells to a cytoplasmic localisation in transformed epidermal cells (Chao et al. 2006). A number of oncogenes and tumour suppressors have also been shown to be mislocalised in cancer cells, as a consequence of incorrect nuclear cytoplasmic transport (Kau et al. 2004).

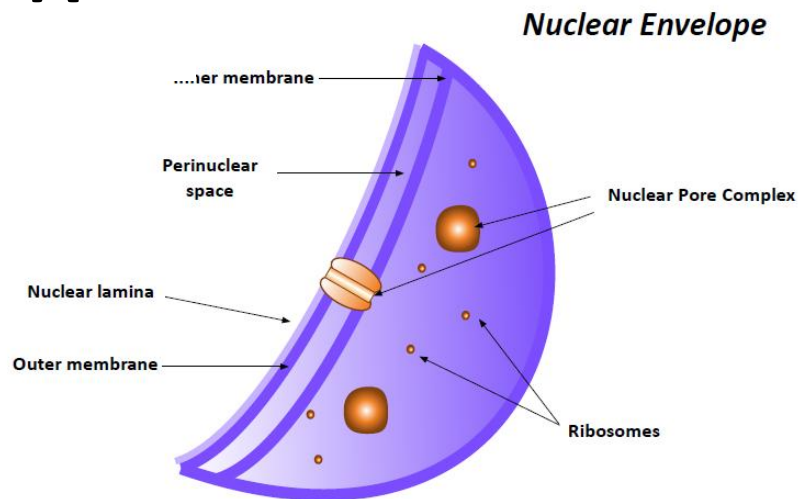
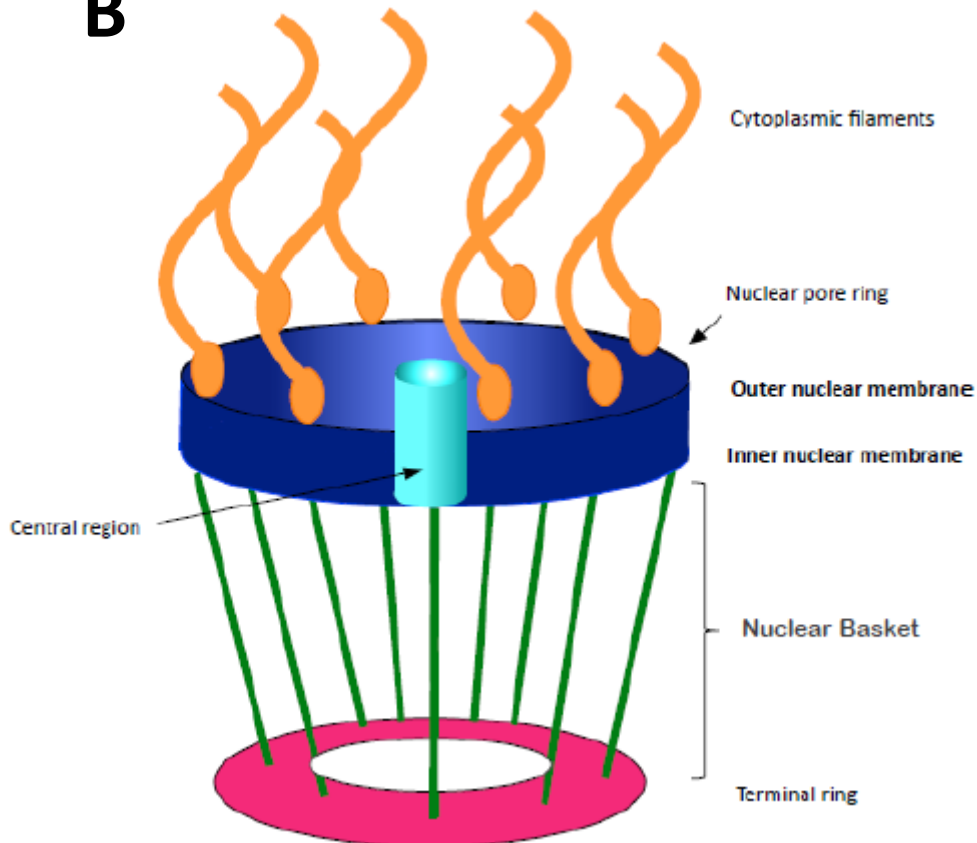
DDX3 has also been shown to be a critical component of innate immune signalling, being implicated in both cytoplasmic and nuclear signalling events (Schröder 2011). DDX3 is targeted by a range of viruses that pose major global health threats, namely Human Immunodeficiency Virus (HIV) (Yedavalli et al. 2004), Hepatitis C Virus (HCV) (Lee et al. 2008; Owsianka & Patel 1999; Oshiumi, Ikeda, et al. 2010), Hepatitis B virus (HBV) (Wang, Kim, et al. 2009; Chang et al. 2006), poxviruses (Schröder et al. 2008), Norovirus (Vashist et al. 2012) and West-Nile virus (Geissler et al. 2012). Various viruses have been linked to an increased risk of tumorigenesis (Carrillo-Infante et al. 2007), for example HCV is the major causative agent of Hepatocellular Carcinoma (HCC) (De Oliveria Andrade et al. 2009). Since DDX3 is a target for various viruses, and has also been implicated in tumorigenesis (Schröder 2010), we speculated that DDX3 localisation could be altered by viruses to impede DDX3's many cellular functions.

## 1.1. An Introduction to Nuclear Transport

The nuclear envelope (NE) separates the nucleus from the cytoplasm in eukaryotic cells and is comprised of two lipid membranes; the inner nuclear membrane and the outer nuclear membrane. Separation of transcription and translation via the nuclear membrane provides eukaryotes with the power to control gene expression; but also necessitates the ability to selectively transport proteins between the cytoplasmic and nuclear compartments (Fahrenkrog & Aebi 2003). The nuclear transport of proteins is often regulated, with post-translational modifications playing an important role in this process. Post-translational modification such as phosphorylation, sumoylation, ubiquitination can regulate the nuclear transport of proteins, and ensure the correct functions of proteins (Rothenbusch et al. 2012; Nardozzi et al. 2010; Geetha et al. 2005).

The transport of molecules greater than approximately 40kDa across the nuclear envelope occurs through the nuclear pore complexes (NPCs), which are imbedded in the inner and the outer nuclear membrane (Fahrenkrog & Aebi 2003) (Figure 1.1). The NPC is comprised of stationary nucleoporins and soluble transport factors which can shuttle between the nuclear and cytoplasmic compartments. The NPC structure consists of two main functional regions: the central domain embedded in the nuclear envelope and the peripheral structures, which extend into the nuclear interior and the cytoplasm. The NPC central domain consists of an eight-fold symmetrical cylindrical assembly, which encases the main nuclear transport channel which is lined with Phe-Gly nucleoporins and functions as a molecular sieve to regulate the bidirectional transport of macromolecules and small metabolites (Figure 1.1).

Karyopherins are nuclear transport factors that bind to proteins containing specific sequences and transport these proteins through the NPC (Fried & Kutay 2003). Karyopherins can be divided into two groups based on their function, Importins import proteins containing Nuclear Localisation Sequences (NLS) and Exportins export proteins containing Nuclear Export Sequences (NES).

**A****B**

**Figure 1.1: Architecture of nuclear membrane and NPC complex structure**

**A:** The nuclear envelope separates the nucleus from the cytoplasm in eukaryotic cells. It consists of an inner and outer membrane, which is embedded with Nuclear Pore Complexes (NPC). **B:** Each nuclear pore complex (NPC) is a cylindrical structure comprised of eight spokes surrounding the central region that connects the nucleus and cytoplasm. The outer and inner nuclear membranes of the nuclear envelope join to form a ring in which the NPC sits. The NPC is anchored to the nuclear envelope by a nuclear pore ring structure that connects to the core scaffold and comprises inner ring and outer ring elements. NPC-associated peripheral structures consist of cytoplasmic filaments, the nuclear basket and a terminal ring. Adapted from (Strambio-De-Castillia et al. 2010).

## 1.1.2. Nuclear import

### 1.1.2.1. Ran dependent nuclear import

---

#### 1.1.2.1.1. Importin alpha

---

The Importin- $\alpha$  family recognises classical nuclear localisation sequences (cNLS). These cNLSs consist of either one or two stretches of basic amino acids. Monopartite cNLSs are illustrated by the SV40 large T antigen NLS (<sup>126</sup>PKKKRRV<sup>132</sup>) and the bipartite cNLSs are illustrated by the nucleoplasmin NLS (<sup>155</sup>KRPAATKKAGQAKKKK<sup>170</sup>). The monopartite motif is typically a cluster of basic residues preceded by a helix-breaking residue; whereas the bipartite motif consists of two clusters of basic residues separated by 9-12 amino acids. The search algorithm PSORT II can be used to detect cNLS from the amino acid sequence of proteins (Gardy et al. 2005).

Importin- $\alpha$  family members contain a flexible N-terminal importin- $\beta$  binding (IBB) domain, which is required for both binding to importin- $\beta$  and dissociation of the cargo complex (Görlich et al. 1995; Fanara et al. 2000). The C-terminus is a highly structured domain containing ten Armadillo repeats which interact with the cNLS containing cargo and also the export factor Cellular Apoptosis Susceptibility protein (CAS) (Conti et al. 1998; Cingolani et al. 1999). There have been six importin- $\alpha$  family members identified, which can be split into three phylogenetically distinct groups; the  $\alpha$ -1s, the  $\alpha$ -2s and the  $\alpha$ -3s (Goldfarb et al. 2004).

The cNLS pathway was the first nuclear import pathway characterised, however it is not necessarily the pathway most prevalently used (Lange et al. 2007). Examples of proteins which are imported via importin- $\alpha$  include p53, which

interacts with importin- $\alpha$  via two bi-partite NLSs (Liang 1999), and Cap Binding Protein 80 (CBP 80) which interacts with importin- $\alpha$  via its N-terminal NLS (Dias et al. 2009). It is important to note that some proteins are transported via importin- $\alpha$  independently of an cNLS that matches the consensus sequence. For example, Signal Transducers and Activator of Transcription 1 (STAT 1) does not contain a cNLS that can be defined using cNLS search algorithms, however upon dimerization each subunit contributes basic residues that form a cNLS recognised by importin- $\alpha$  (Fagerlund et al. 2002).

During nuclear import, importin- $\beta$  forms a complex with importin- $\alpha$  and its cargo in the presence of a high concentration of Ran/GDP. This complex is then transported through the nuclear pore to the nucleus, where a high concentration of Ran/GTP is present. Finally, the complex disassociates at the nuclear side of the pore, with Ran/GTP binding to importin- $\beta$ , displacing importin- $\alpha$  and the cargo protein. As a result, the cargo protein is released within the nucleus. The Ran/GTP-importin- $\beta$  complex is then exported to the cytosol, where the bound GTP is hydrolyzed to GDP, releasing importin- $\beta$  to participate in another cycle of nuclear import. Importin- $\alpha$  is recycled to the cytoplasm by the nuclear export factor CAS, in complex with RanGTP (Stewart 2007) (Figure 1.2).

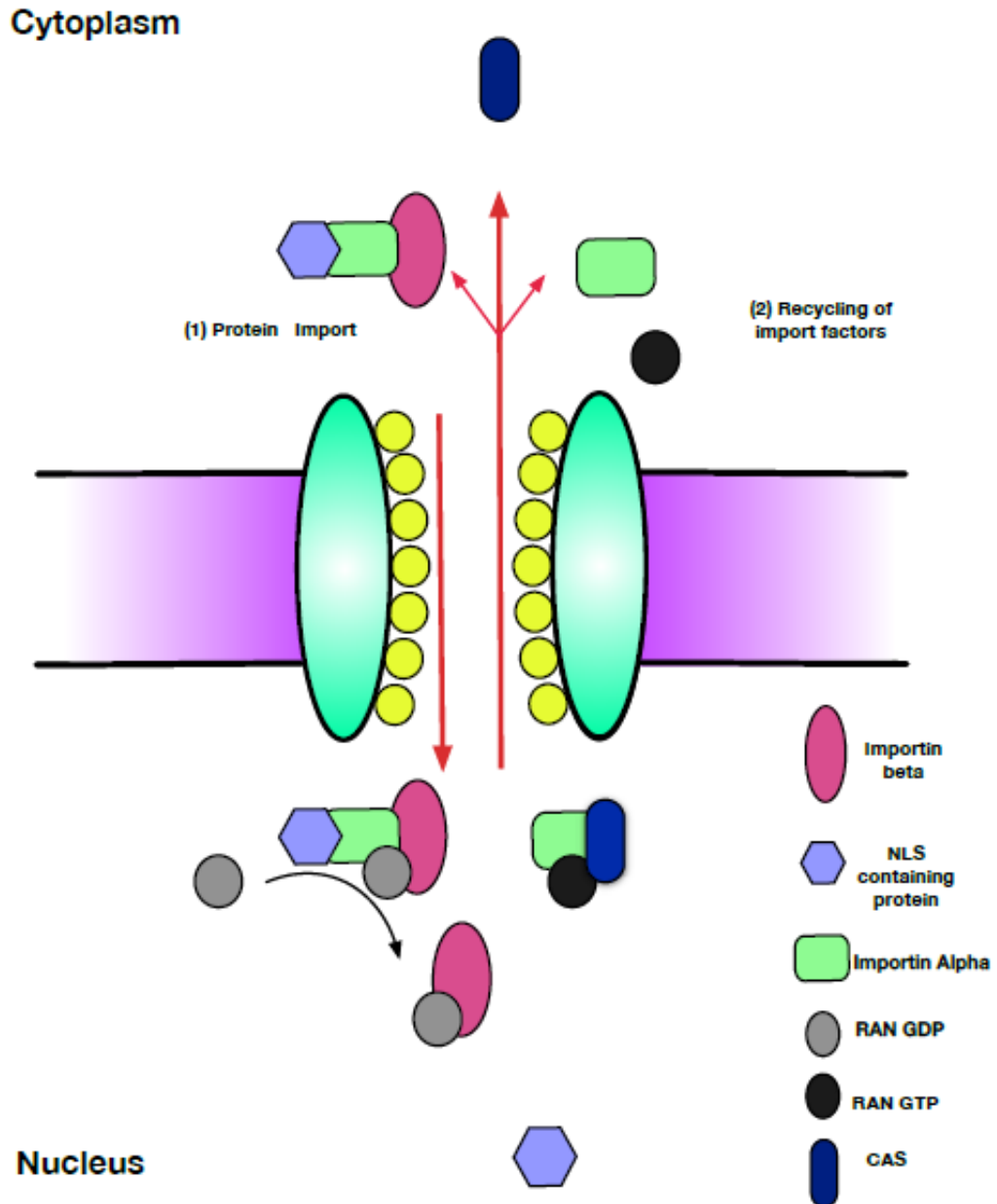


**Figure 1.2: Overview of nuclear protein import.**

An import complex is formed in the cytoplasm between cargoes that contain an NLS, importin- $\alpha$  and importin- $\beta$ . After passing through the nuclear pore complex (NPC), RanGTP binds to importin- $\beta$  resulting in dissociation of importin- $\beta$  from importin- $\alpha$ . The NLS containing cargo is then dissociated from importin- $\alpha$  and importin- $\alpha$  is recycled to the cytoplasm by its nuclear export factor CAS, in complex with RanGTP. In the cytoplasm, RanGAP stimulates GTP hydrolysis, releasing the importins for another import cycle.

#### 1.1.2.1.2. Importin-Beta

---

As stated above, importin- $\alpha$  mediates import of cNLS containing proteins in conjunction with importin- $\beta$ ; however importin- $\beta$  alone can also import non-classical NLS containing proteins. Non-classical NLS proteins are imported by importin- $\beta$  without its adaptor importin- $\alpha$ , in a Ran-dependent fashion. Cargoes that directly bind to importin- $\beta$  include transcription factors such as GAL4 (Chan et al. 1998); retroviral proteins such as HIV-1 Rev and Tat (Truant & Cullen 1999); ribosomal proteins and various others (Cingolani et al. 2002).

Importin- $\beta$  family members have a modular structure consisting of 19 HEAT repeats, with each HEAT repeat made up of two helices connected by a loop. The A helices are located on the outside of the protein forming a convex face; whereas the B helices form a concave face inside (Cingolani et al. 1999). NPC binding sites are found on the convex face (Bayliss et al. 2000), whereas the importin- $\alpha$  IBB binding domain and RanGTP binding sites are located in the C-terminal (HEAT 7-19) and N-terminal (HEAT 1-10) regions of the concave face (Cingolani et al. 1999; Vetter et al. 1999). There are 11 importin- $\beta$  family members in the human proteome (Pemberton & Paschal 2005).

The requirements for non-classical NLS proteins to be recognised by importin- $\beta$  are undefined and the recognised sequences are diverse; containing either three-dimensional epitopes or linear epitopes. It would seem that there are multiple cargo binding sites within importin- $\beta$ , for example the non-classical NLS containing protein parathyroid hormone related protein (PTHrP) binds to importin- $\beta$  in a region distinct from the site to which the importin- $\alpha$  IBB domain binds (Cingolani et

al. 2002), and sterol regulatory element-binding protein 2 (SREPB2) binds to yet another distinct region (aa 343-403) (Lee et al. 2003).

#### 1.1.2.1.3. Transportins

Transportins (also known as Kap $\beta$ 2) are members of the Karyopherin protein family. Transportins have been shown to import proteins involved in mRNA processing, recognising a distinct sequence known as the PY-NLS (also known as M9-NLS) (Lee et al. 2006). More than 20 mRNA processing proteins have been reported as being imported via transportin (Lee et al. 2006). Transportin was first identified as a nuclear import factor for the splicing factor hnRNP A1 protein, which contains a 38 amino acid signal referred to as the M9-NLS (Fridell et al. 1997).

PY-NLSs are often found within structurally disordered regions of proteins, and can be divided into two subclasses: hydrophobic and basic PY-NLS (hPY-NLS or bPY-NLS). PY-NLSs have an overall positive charge and contain either a loose hydrophobic (hPY-NLS) or basic motif (bPY-NLS) at the N-terminus, alongside a R/K/H-X<sub>(2-5)</sub>-P-Y motif at the C-terminus (Lee et al. 2006). A bioinformatic search for PY-NLSs in human SwissPROT database found 81 candidate transportin substrates, of which 61% were involved in transcription or RNA processing (Lee et al. 2006).

### 1.1.2.2. RAN independent nuclear import

#### 1.1.2.2.1. Calmodulin/calcium- dependent import

---

Ran-independent nuclear import pathways have been described, but are poorly understood. Calmodulin (CALcium MODulated proteIN) is a calcium binding messenger protein expressed in all eukaryotic cells, which has been reported to have a role in Ran-independent nuclear import. Calmodulin has been shown to be imported to the nucleus in the absence of cytosolic factors or an ATP-regeneration system, with import being sensitive to the calmodulin antagonist peptide M13, which blocks Calmodulin binding to target proteins (Liao et al. 1999). Calmodulin acts as a transducer of intracellular  $Ca^{2+}$  signals, and can regulate the nuclear transport of Calmodulin-binding proteins in its  $Ca^{2+}$ -bound state, eg. p21<sup>waf1/cip1</sup> (Taulés et al. 1999) , and Cdk4 and Cyclin D1 (Taulés et al. 1998). It must be noted, that the inhibitory effect of Calmodulin on the nuclear import of p21<sup>waf1/cip1</sup> was shown to be caused by Calmodulin preventing phosphorylation of p21<sup>waf1/cip1</sup> at Ser153 , a residue found within the p21<sup>waf1/cip1</sup> classical NLS (Rodríguez-Vilarrupla et al. 2005).

The Calmodulin pathway is suggested to be an evolutionarily ancient pathway, with Calmodulin shown to import a range of evolutionary conserved architectural transcription factors (Hanover et al. 2009; Hanover et al. 2007). For example HMG (high-mobility group) non-histone chromosomal proteins have been shown to be imported via the Calmodulin pathway, (Hanover et al. 2009; Kaur et al. 2010). The HMG-box of SOX (SRY (sex-determining region on the Y chromosome)-related HMG-box)) family members, which play key roles in development, is highly conserved and displays striking homology within the Calmodulin-NLS (Kaur et al. 2010). Defects in

nuclear import of HMG-box of SOX are associated with sex reversal diseases. It was proposed that release of intracellular calcium stores during cellular activation induces the Calmodulin/Ca<sup>2+</sup> import pathway, and inhibits GTP-dependent nuclear transport (Sweitzer & Hanover 1996). The Calmodulin import system could represent another means to facilitate the import of proteins into the nucleus in response to different cellular requirements.

### 1.1.3. Nuclear Export

#### 1.1.3.1. Ran dependent nuclear export

Exportins are required for the nuclear export of proteins. Most exportins, such as CAS (cellular apoptosis susceptibility), Exportin T or Exportin 5, seem to have a restricted number of cargoes (Fried & Kutay 2003); however CRM-1 (Chromosome region maintenance 1, also called Exportin 1 or XPO1) has a broad range of cargoes. Table 1.1 gives an overview of mammalian exportins and their cargoes.

<i>Exportin</i>	<i>Export Cargo</i>
CRM-1	Proteins containing NES, snurportin
CAS	Importin- $\alpha$
Exp-t	tRNAs
EXP4	eIF5A
Exp5	Pre-miRNAs, tRNAs, minihelix RNAs, eEF1A, JAZ
Exp7	p50RhoGAP, 14-3-3 sigma
Imp13b	eIF1A

**Table 1.1: Mammalian Exportins and their cargoes.**

Adapted from Kutay and Güttinger 2005.

CRM-1 is the most important nuclear export receptor for proteins. It interacts with proteins containing a conserved nuclear export sequence (NES). The NES of the HIV Rev protein has helped define CRM-1 function (Askjaer 1998). The NES recognised by CRM-1 is defined as a short amino acid sequence comprised of evenly spaced hydrophobic residues; with leucine usually being most abundant (La Cour et al. 2004). Leucine-rich NESs usually form the consensus sequence  $\phi$ -x<sub>2-3</sub>- $\phi$ -x<sub>2-3</sub>- $\phi$ -x-

$\Phi$  ( $\Phi=L,I,V,F,M$ ;  $x$  any amino acid); where the intervening amino acids are often negatively charged, polar or small (La Cour et al. 2004). Recently it has been suggested that NESs can be split further into two types; PKI-class NESs and Rev-class NESs with different consensus sequences (Güttler et al. 2010). The PKI-class of NESs contain five hydrophobic residues, whereas Rev-like NESs contain four hydrophobic residues (Figure 1.3).

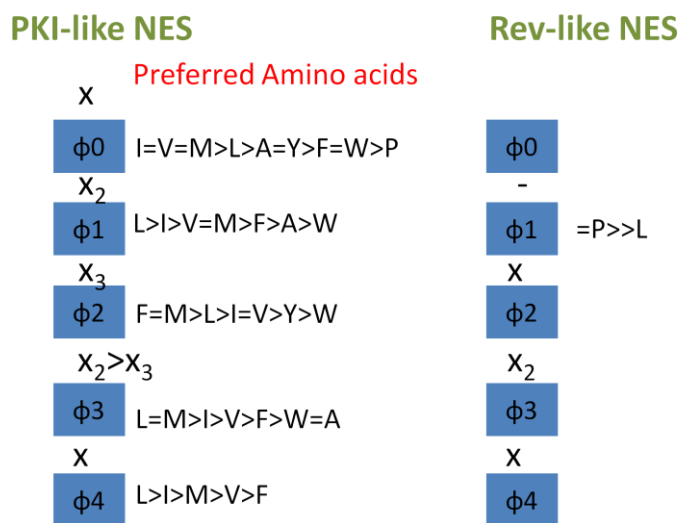


**Figure 1.3: Redefinition of NES consensus sequence into PKI-like NES and Rev-like NES.**

$\Phi$  is key hydrophobic residue with preferential amino acids indicated. Figure adapted from (Güttler et al. 2010).

Binding of NES-containing proteins to CRM-1 is controlled by RanGTP, which predominantly localises to the nucleus. CRM-1 binding to the NES is usually weak; this is to facilitate disassembly of the export complex in the cytoplasm. CRM-1 contains 19 HEAT repeats, the RanGTP interaction has been suggested to occur at an acidic loop within HEAT repeat 8; and this seems to mediate for the cooperative binding of the NES cargo (Hutten & Kehlenbach 2007).

When NESs with strong affinity to CRM-1 were created, these “supraphysiological” NES interacted with CRM-1 in a RanGTP independent manner. These NES-containing proteins localised at the cytoplasmic filaments of the NPC,

suggesting that the efficient release of export complexes from the NPC was impaired (Kutay & Güttinger 2005).

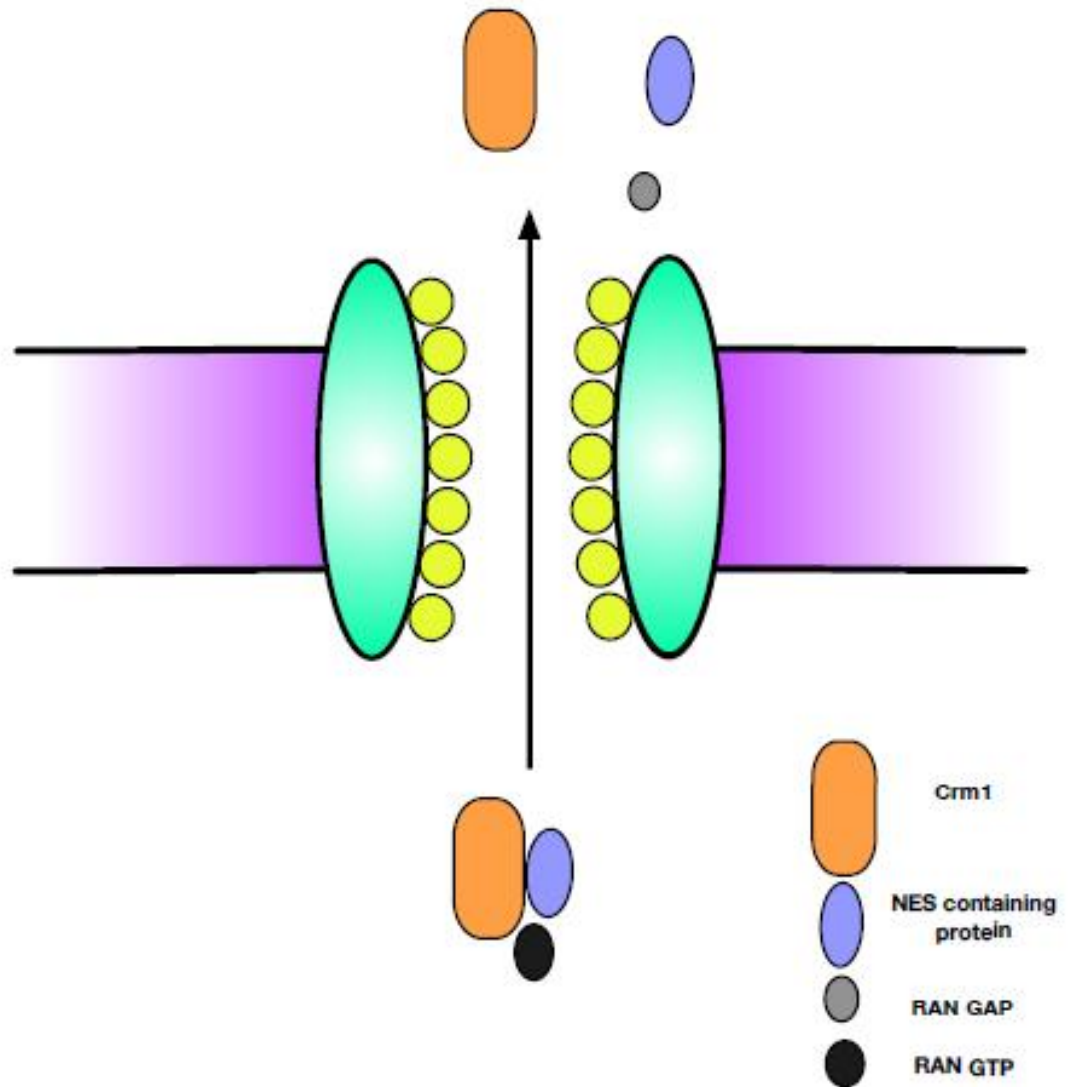
CRM-1 can bind NESs that vary in both length and sequence at a single binding cleft. Guttler et al. showed that NESs bind to a hydrophobic cleft in CRM-1 at five specific hydrophobic pockets regardless of sequence differences; with no single hydrophobic residue essential for either CRM-1 binding or NES function (Güttler et al. 2010). This hydrophobic cleft has a defined conformation which does not adapt to different NESs. NES-like sequence patterns can be found frequently in proteins; however to be functional they must occur within the N- or C-termini or within unstructured regions of the protein.

The exact mechanism of nuclear export through CRM-1 is unclear. During the formation of the export complex, RanGTP binds to CRM-1 with the NES-containing export cargo. As stated earlier, the binding of CRM-1 to NES-containing cargo is weak; RanBP3 is thought to promote the formation of export complexes by linking CRM-1 to Regulator of Chromosome Condensation 1 (RCC1) and also by enhancing the catalytic activity of RCC1 (Nemergut et al. 2002). RanBP3 binds to CRM-1 at the acidic loop, allowing stable binding of both RanGTP and the NES-containing cargo (Englmeier et al. 2001; Petosa et al. 2004). RanBP3 increases the active concentration of RanGTP and promotes the binding of cargo to the CRM-1 central domain. RanBP3 contains FG repeats; and CRM-1 binds to its FG-repeat containing region (Hutten & Kehlenbach 2007).

The exact mechanism of CRM-1 translocation through the pore is unknown (Figure 1.4). Directionality of transport is imposed by the Ran gradient, which favours assembly of export complexes and disassembly of import complexes in the

nucleus (Fried & Kutay 2003; Macara 2001; Pemberton & Paschal 2005; Tran & Wente 2006). CRM-1 has been shown to interact with cytoplasmic nucleoporins, Nup358 and Nup 214, with these being seen as terminal docking sites of the export complex (Hutten & Kehlenbach 2006; Bernad et al. 2004). RanBP1, Nup358, RanGAP (Hutten & Kehlenbach 2006; Englmeier et al. 1999); and NXT1 (Black et al. 2001) are required for disassembly of the export complex from its terminal binding site in the cytoplasm. For disassembly, RanGTP in the complex must be hydrolysed. While RanGTP is interacting with the export complex; hydrolysis is inhibited. However, RanBP1 releases this inhibition and with the aid of RanGAP the export complex can be disassembled.

Cytoplasm



Nucleus

**Figure 1.4: Nuclear export through the pore.**  
NES containing proteins interact with CRM-1 in complex with RanBP3.

#### 1.1.3.1. Ran-independent nuclear export

In human cells the majority of mRNA export occurs independently of the Ran system and the karyopherin family of proteins (Clouse et al. 2001). The Tip-associated protein (TAP), also known as NXF1, and its cofactor Nxt1/p15 are responsible for the nuclear export of most cellular mRNAs (Izaurrealde 2002). TAP contains a PY-NLS, an RNA binding (RNP) domain, and a leucine-rich repeat (LRR) domain in its N-terminus (residues 1–372) (Truant 1999; Lee et al. 2006; Liker et al. 2000). During mRNA export, TAP interacts with the mRNP, forming a heterodimer with p15 and interacts with the FG repeats of nucleoporins via its C-terminus (Fribourg et al. 2001).

TAP was originally found to interact with the Constitutive Transport Element (CTE) of viral RNA, giving viruses the ability to export their unspliced RNAs from the nucleus (Kang & Cullen 1999; Braun et al. 1999). In normal mRNA export, TAP binds to an export adaptor-mRNA complex, causing a transfer of the mRNA to TAP's RNA binding domain. TAP binds to mRNA weakly in the absence of adaptor proteins, however in the presence of a bound adaptor TAP has a 4-fold higher binding affinity with mRNA (Hautbergue et al. 2008). Following transport through the NPC, TAP dissociates from adaptor proteins reverting to a low affinity RNA-binding state, and the DEAD box protein Dbp5 promotes the displacement of the mRNP from the NPC (Tran et al. 2007; Lund & Guthrie 2005).

#### 1.1.4. Regulation of Nuclear transport

Nuclear transport is involved in regulation of critical processes such as gene regulation and cell cycle progression. Proteins that have distinct functions in the nucleus and cytoplasm can be regulated by controlling their nuclear transport.

Nuclear transport can be regulated through post-translational modifications in response to a variety of signals such as hormones, cytokines and growth factors, cell cycle signals, immune challenge and stress (Poon & Jans 2005). Regulation of nuclear import via phosphorylation is the most studied post-translation modification, with phosphorylation regulating import in various ways. Phosphorylation of amino acids within a protein's NLS has been shown to increase binding affinity to importins, with phosphorylation of Ser<sup>385</sup> of Epstein Barr virus Nuclear Antigen-1 (EBNA-1) increasing binding to importin- $\alpha$ 5 and thus increasing nuclear import (Kitamura et al. 2006). Phosphorylation of proteins can also cause structural rearrangement, for example STAT1 phosphorylation induces homodimerisation through a reciprocal SH2-phosphoTyr interaction, which exposes an NLS recognisable by importin- $\alpha$ 5 (Fagerlund et al. 2002; Balagopal & Parker 2009). Phosphorylation of the HBV Core antigen positions the NLS on the exterior of the viral capsid, thus promoting nuclear import (Kann et al. 1999; Rabe et al. 2003).

Ubiquitination and sumoylation can also regulate the nuclear import of proteins. For example, ubiquitination has been shown to regulate nuclear import of the tumour suppressor Phosphatase and tensin homolog (PTEN) (Trotman et al. 2007; Howitt et al. 2012). Sumoylation has been shown to regulate the nuclear import of many different proteins (Wilson & Rangasamy 2001; Pichler & Melchior 2002), including targeting RanGap1 to the nuclear pore complex (Matunis et al. 1998).

Nuclear export of proteins can also be regulated by post-translational modifications. The interaction of the main mammalian exportin CRM-1 with its NES-containing cargo can be regulated by phosphorylation; either positively or

negatively. For example, casein kinase II dependent phosphorylation of PPARgamma results in accumulation in the cytosol (Von Knethen et al. 2010); whereas phosphorylation of c-Fos inhibits nuclear export (Sasaki et al. 2006). Mono-ubiquitination is required for nuclear export of hDCNL1 (Wu, Yan, et al. 2011). Sumoylation has also been shown to regulate nuclear export, with sumoylation of TEL being required for its nuclear export (Wood et al. 2003).

## 1.2. Introduction to DDX3

---

DDX3 is a member of the DEAD-box family of putative RNA helicases which were first described in 1989 (Linder et al. 1989); and there are now over 500 DEAD-box proteins described in protein databases. It was first discovered in 1997 as one of five X-chromosomal genes that have homologues in the non-recombining region of the Y-Chromosome (DDX3Y) (Lahn & Page 1997). All DEAD-box helicases contain nine conserved helicase motifs, including the Asp–Glu–Ala–Asp (D-E-A-D) motif, which is located within a structurally conserved core element forming two recA-like domains. DEAD-box helicases have been implicated in a wide variety of cellular processes involving RNA, including splicing, mRNA export, transcriptional and translational regulation, RNA decay and ribosome biogenesis (Schröder 2010). Interestingly, DDX3 seems to be critical for survival as knockout mice are not viable and stably knockdown DDX3 cell lines are not able to retain knockdown.

In the following sections the various nuclear and cytoplasmic functions of DDX3 will be reviewed.

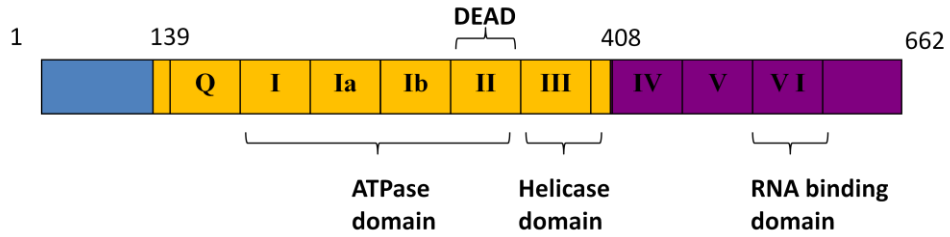
### 1.2.1. DDX3's role in RNA metabolism

---

DEAD-box proteins have been implicated in all aspects of RNA metabolism. DDX3's core helicase domain is comprised of two covalently linked globular domains, each consisting of five  $\beta$ -strands and five  $\alpha$ -helices, connected by a flexible linker. DEAD-box helicases such as DDX3 contain nine conserved helicase motifs, Motif I (Walker A), motif II (Walker B), motif III and motif Q in the sub domain 1, and motif V and VI in the sub domain 2 (Figure 1.5). DDX3 and its homologues share strong similarities as shown in Figure 1.5. The core helicase motifs are involved in ATP binding, ATPase activity, RNA substrate binding and

unwinding. The N- and C- termini of DEAD-box proteins show much more divergence, and are thought to confer functional specificity to the individual DEAD-box helicases (Rocak & Linder 2004).

**A**



**B**



**Figure 1.5: DDX3 belongs to the DEAD-box protein family.**

**A:** A schematic representation of DDX3 protein structure and conserved domains. **B:** Human DDX3 protein sequence alignment with DDX3 homologues: *Mus musculus* PL10 ; *Xenopus* An3; *Drosophila* Belle and *S. cerevisiae* Ded1p and human DDX3. Alignment was performed using CLC Sequence viewer, conservation shown in colour gradient with blue being most identical to red being non identical.

During the mRNA life cycle, mRNA is processed in both the nucleus and the cytoplasm to produce a functional protein. Briefly, mRNA is transcribed from DNA in the nucleus, mRNA is then processed by mRNA processing enzymes (eg. 5' capping, splicing, polyadenylation). Processed mature mRNA is then transported from the nucleus to the cytoplasm in complex with proteins as mRNPs, and in the cytoplasm mRNA is translated at the ribosomes (Figure 1.6). DEAD box proteins have been shown to have roles all of these processes, hence nucleocytoplasmic transport of DEAD box proteins must occur for mRNA processing to occur.

The role of DDX3 in various aspects of RNA metabolism will be discussed in the following paragraphs.

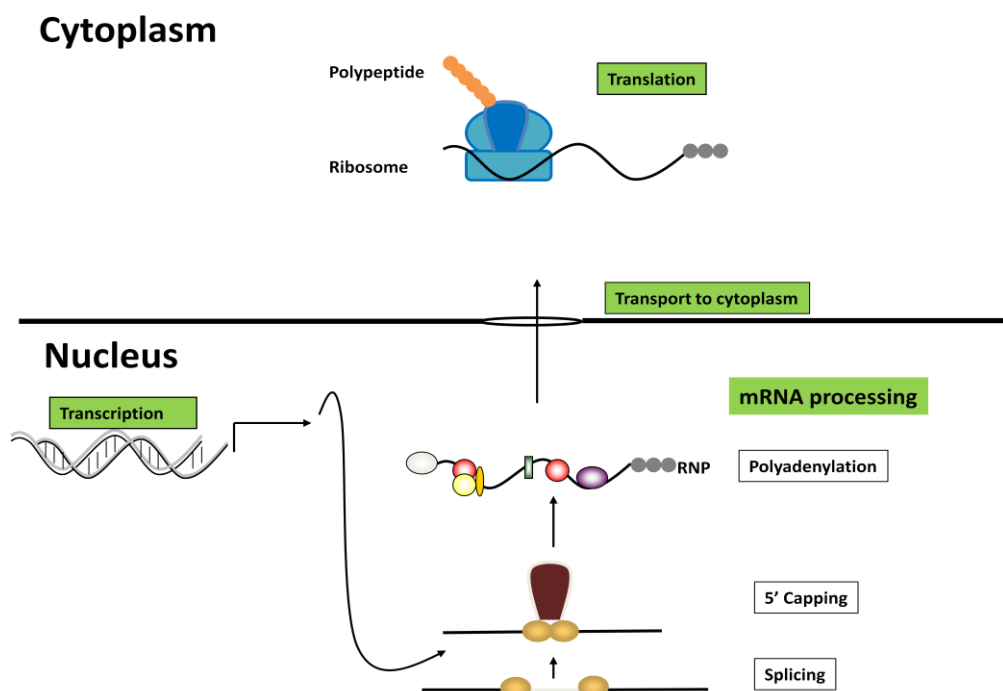


**Figure 1.6: Nuclear and cytoplasmic processes involving mRNA.**

In the nucleus, mRNA is transcribed from DNA into mRNA, mRNA processing occurs (splicing, 5' capping and polyadenylation), followed by transport to the cytoplasm where the mRNA is translated into protein.

### 1.2.2. Evidence of DDX3's role in Transcription

Several DEAD-box proteins have been shown to play a role in gene regulation through interaction with the transcription machinery in the nucleus (Rocak & Linder 2004; Fuller-Pace 2006). DDX3 has been suggested to participate in transcriptional regulation of several genes, ranging from genes involved in cell cycle regulation to genes involved in innate immune signalling (Schröder 2010). DDX3 has been shown to bind to the IFN $\beta$ , p21<sup>waf1/cip1</sup> and E-Cadherin promoters, with the ability to either increase or decrease activation of these promoters (Table 1.2) (Soulat et al. 2008; Chao et al. 2006; Wu, Liu, et al. 2011; Botlagunta et al. 2008).

<b>DDX3 regulates transcription of promoters</b>		
<b>Promotor</b>	<b>↑/↓ activation</b>	<b>Reference</b>
IFN $\beta$	↑	(Soulat et al. 2008)
p21 <sup>waf1/cip1</sup>	↑	(Chao et al. 2006; Wu, Liu, et al. 2011)
E-Cadherin	↓	(Botlagunta et al. 2008)

**Table 1.2: Human DDX3 regulates transcription of several gene promoters.**

DDX3 has been shown to increase activation of the IFN $\beta$  promoter during innate immune responses. Chromatin immunoprecipitation revealed that DDX3 was recruited to the IFN $\beta$  promoter upon infection with *Listeria monocytogenes*, independently of IRF3 (Soulat et al. 2008). DDX3 induced activation of the IFN $\beta$  promoter independently of DDX3's ATPase activity, since the K230E helicase inactive mutant behaved the same as wild type DDX3 (Schröder et al. 2008; Soulat et al. 2008). The K230E mutant has a mutation in the Walker A motif, which disrupts its ability to bind nucleotides, and thus disrupting ATPase and helicase

activity (Yedavalli et al. 2004). Other DEAD-box proteins have also been shown to regulate promoter activity independently of their enzymatic activity (Yan et al. 2003; Rajendran et al. 2003).

DDX3 has been shown to interact and cooperate with Sp1 to up-regulate promoter activity of the cell cycle regulator p21<sup>waf1/cip1</sup> in a ATPase-dependent and helicase-independent manner (Chao et al. 2006). DDX3 has been shown to be down-regulated in human hepatocellular carcinoma (HCC) cancers; suggesting a role as a tumour suppressor gene (Chang et al. 2006). DDX3 has also been shown to regulate transcription of the tumour suppressor E-Cadherin. Loss of E-Cadherin, a cell adhesion protein, has been shown to induce epithelial–mesenchymal transition (EMT) in breast cancer (Botlagunta et al. 2008). DDX3 was shown to reduce activation of an E-Cadherin promoter reporter construct through direct binding to the E-Cadherin promoter, while knockdown of DDX3 by shRNA promoted E-Cadherin expression (Botlagunta et al. 2008). Another study showed that DDX3 positively regulates the transcription factor Snail, with knockdown of DDX3 by shRNA resulting in decreased levels of Snail (Sun et al. 2011). Snail is a transcriptional repressor of E-Cadherin (Batlle et al. 2000).

The role for DDX3 in regulating gene expression at the level of transcription demands that DDX3 must be present in the nucleus. Regulation of DDX3's nuclear import could therefore affect the expression of genes transcriptionally regulated by DDX3, such as p21<sup>waf1/cip1</sup>, IFN $\beta$  and E-Cadherin.

### 1.2.3. Evidence of DDX3's role in Splicing

A role for DEAD-box proteins in splicing has been suggested due to the interaction of DDX3's and the DDX3 homologue Ded1p from *S. cerevisiae* with the spliceosome and mRNPs (Stevens et al. 2002; Merz et al. 2007). In yeast, three-DEAD box proteins have been shown to be required for in vivo splicing; Sub2, Prp28, and Prp5 (Linder 2006). However, neither human DDX3 nor Ded1p have been shown to be required for splicing. In humans, DDX3 has only been shown to be associated with spliced mRNAs in an Exon junction complex (EJC)-dependent manner (Merz et al. 2007), suggesting DDX3 does not play an active role in splicing but associates with the RNPs after splicing has occurred (Schröder 2010).

### 1.2.4. Evidence of DDX3's role in RNA export

DDX3 has been shown to be exported via two nuclear shuttling proteins, TAP and CRM-1 (Lai et al. 2008; Yedavalli et al. 2004). As stated earlier, the nuclear export of mRNA occurs predominantly through a heterodimer of TAP and a small cofactor termed Nxt (Cullen 2003). DDX3 has been shown to interact with TAP independently of RNA binding via its C-terminus, and also to interact with polyA-mRNAs (Lai et al. 2008).

In addition to NES-containing proteins, CRM-1 has been found to export a small subset of inducible RNAs, including IFN- $\alpha$ 1 mRNA and IFN $\gamma$ -induced HLA-A mRNA (Kimura et al. 2004; Browne et al. 2006). DDX3 has been shown to be exported via CRM-1 and to interact with CRM-1 (Yedavalli et al. 2004). Knockdown of DDX3 does not affect overall mRNA export, suggesting that DDX3 is not required for general mRNA export but may be involved in export of specific mRNAs (Lai et al. 2008). Since DDX3 has recently been shown to have a role in anti-viral gene expression, it

is possible that DDX3 might also be involved in the export of the above-mentioned immunologically relevant mRNAs via CRM-1.

#### 1.2.5. DDX3's role in Protein Translation

Many DEAD-box proteins have been implicated in translation. The DEAD-box protein eIF4A is thought to be part of the cap binding complex, in which it unwinds or rearranges RNA-duplex structures at the 5' end of mRNA; preparing it for scanning by the small ribosomal subunit. It is also thought that eIF4A may strip RNA of proteins after the RNA has been exported from the nucleus (Svitkin et al. 1996; Rogers et al. 2002). DDX3 homologues Ded1p and Dbp1p from *S. cerevisiae* have also been shown to function in the initiation of translation; with Ded1p being faster and more efficient than eIF4A at scanning long 5'UTRs (Chang & Tarn 2009; Berthelot et al. 2004; Marsden et al. 2006).

Human DDX3 has also been shown to interact with several translation initiation factors (Table 1.3). DDX3 has been implicated in protein translation through its interaction with the multi-component translation initiation factor eIF3 (Lee et al. 2008). DDX3 had been suggested to have a role in translation regulation; inhibiting translation via an interaction with eIF4E (Shih et al. 2008) while promoting  $\beta$ -globin mRNA translation via an interaction with eIF3 (Lee et al. 2008). Knockdown of DDX3 was also shown to negatively affect the translation of mRNAs containing complex secondary structures in their 5'UTRs (Lai et al. 2008), similar to what was found in yeast Ded1p. DDX3 has recently been shown to promote translation of selected mRNA in association with eIF4F (Soto-Rifo et al. 2012). DDX3 has also been shown to have a role in assembly of 80S translation initiation complexes, with DDX3

interacting with components of the 80S ribosome in an RNA independent manner (Geissler et al. 2012).

<b>Translation Initiation Factors that interact with DDX3</b>	
<b>Translational initiation factor</b>	<b>Reference</b>
eIF4e	(Shih et al. 2008; Lai et al. 2008)
eIF4a	(Lai et al. 2008)
eIF4 $\alpha$	(Lai et al. 2008)
eIF3	(Lee et al. 2008)
PABP	(Lai et al. 2008)
eIF4F	(Soto-Rifo et al. 2012)

**Table 1.3: Human DDX3 interacts with translational initiation factors.**

### 1.2.6. Summary of DDX3's nuclear and cytoplasmic functions

DDX3 is involved in a range a cellular processes, which occur in both the nucleus and the cytoplasm. Figure 1.7, describes the various nuclear functions (DDX3's role in transcription and mRNA processing) and also the cytoplasmic functions (translation and innate immune signalling) that DDX3 is implicated in. DDX3's functions in both compartments suggests that transport of DDX3 between the nucleus and cytoplasm ought to be regulated and that its distribution in the cell might affect its participation in these processes.

## Cytoplasm

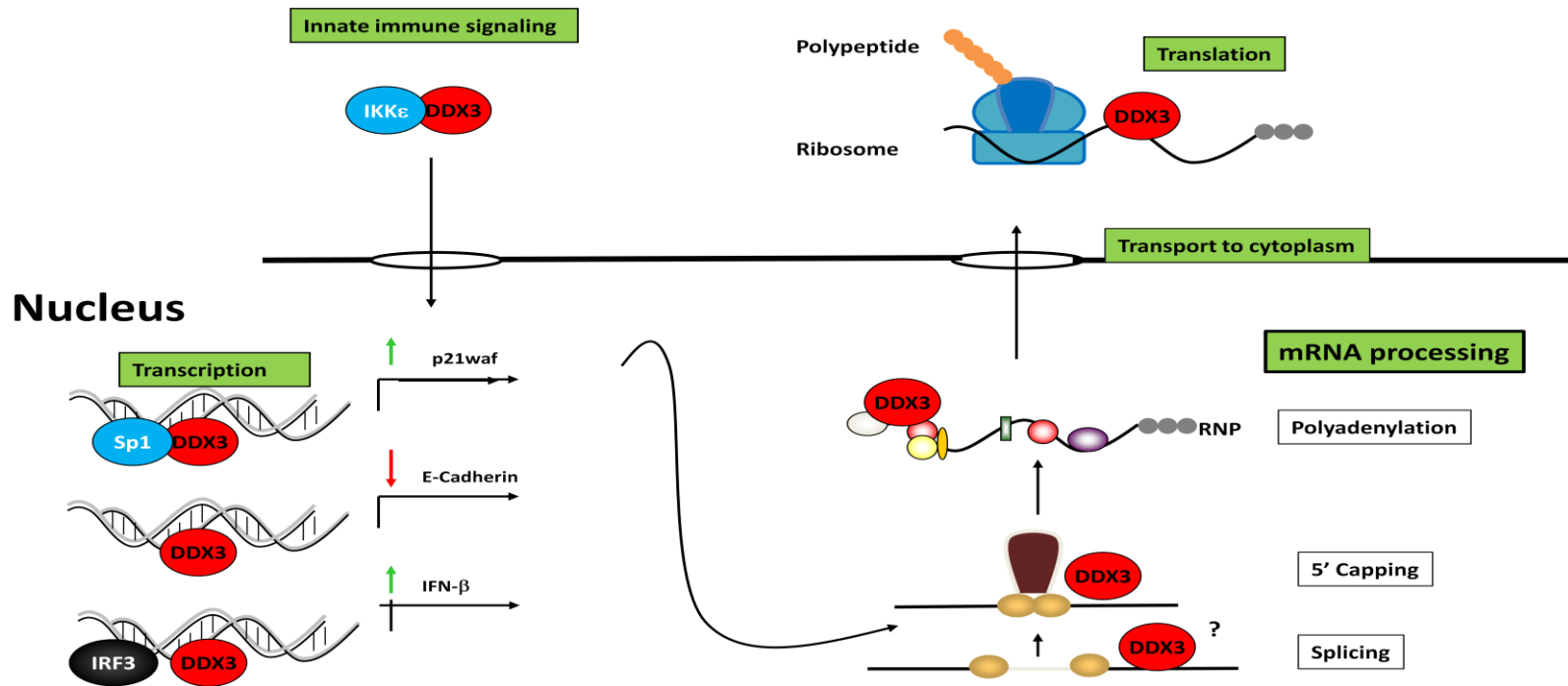


**Figure 1.7: DDX3 is a multifunctional protein with distinct roles in the nucleus and the cytoplasm.**

DDX3 has roles in all aspects of RNA metabolism. Transcription: DDX3 can regulate transcription of genes, increasing activation of the cell cycle regulator p21<sup>waf1/cip1</sup> promoter, decreasing activation of the E-Cadherin promoter and increasing activation of the IFN $\beta$  promoter (Chao et al. 2006; Botlagunta et al. 2008; Soulat et al. 2008). mRNA processing: DDX3 has been implicated in various stages of mRNA processing. Translation: DDX3 has been implicated in translation initiation. Adapted from (Schröder 2010).

### 1.3. Aims of this study

---

As DDX3 has distinct roles in both the nucleus and the cytoplasm, understanding how DDX3 is transported across the nuclear membrane may elucidate how DDX3's participation in nuclear and cytoplasmic processes is regulated and reveal what the role of DDX3 is in regulating these processes.

This study is primarily interested in understanding the factors that influence the cellular localisation of DDX3. Whether DDX3 is a nucleocytoplasmic shuttling protein will be confirmed. We were interested in understanding how DDX3 is exported and imported through the nuclear pore and whether the cellular localisation of DDX3 can change in response to the cellular environment.

As DDX3 has been shown to be a target for various viruses, we also investigated whether viral proteins affect DDX3 localisation in the cell, which may play a role in viral pathogenesis. Viruses have been implicated in disrupting various cellular functions including immune signalling, cell cycle regulation and stress responses (Bowie & Unterholzner 2008; Carrillo-Infante et al. 2007; White & Lloyd 2012).

As we were interested in the localisation of DDX3 in response to cellular stress, we investigated how oxidative stress affects the localisation of DDX3 to cytoplasmic granules.

As DDX3 has been shown to play a role in regulating the cell cycle, we investigated if DDX3 localisation and expression changes during the cell cycle.

## **Chapter 2 : MATERIALS AND METHODS**

---

### **2.1. Standard Laboratory Procedures**

---

Good laboratory practice was employed at all times. A laminar flow hood was used for all tissue culture experiments. All solutions are outlined in Appendix II.

### **2.2. Molecular Biological methods**

---

#### **2.2.1. Preparation of chemically competent cells**

---

Chemically competent cells were prepared from *E.coli* strain Novablue (*Merck*) (endA1) or *E.coli* strain BL21/DE3 (*NEB*) with  $\text{CaCl}_2$  solution, which facilitates transformation of the cells with DNA. 50  $\mu\text{l}$  of Novablue competent cells were added to 5 ml of LB broth, and cultured overnight at 37°C. LB broth (100ml) was inoculated with 1ml of the *E.coli* overnight pre-culture and incubated at 37°C until the  $\text{OD}_{600}$  of the culture reached 0.4-0.8 (after approximately 6 hours). Then, the bacteria were pelleted by centrifugation at 4°C for 20 minutes at 3,000g. The pellet was immediately resuspended in 34ml of ice-cold transformation buffer (TB) and incubated on ice for 10 minutes. The cells were pelleted as before and resuspended in 8ml ice-cold TB. 600  $\mu\text{l}$  of Dimethyl sulphoxide (DMSO, *Sigma-Aldrich*) was added and the cells were incubated on ice for a further 10 minutes. Aliquots of 200-300  $\mu\text{l}$  were snap frozen in liquid nitrogen and stored immediately at - 80°C.

#### **2.2.2. Transformation of chemically competent cells**

---

Competent cells were thawed on ice. 50  $\mu\text{l}$  of cells were transferred into a cold 1.5ml tube containing 50 ng of plasmid DNA or 1-2  $\mu\text{l}$  of ligated DNA from ligation reaction (see section 2.2.7.3.3) and kept on ice for 30 mins before being heat-shocked for 35 seconds at 42°C in a water bath, and then placed on ice for a further 2 minutes. 80  $\mu\text{l}$  of LB broth was then added to the transformed cells and they were

immediately plated onto LB agar plates (LB broth with 1.5 % (w/v) agar) containing 100µg/ml ampicillin antibiotic and incubated at 37°C overnight.

For kanamycin resistant plasmids an additional outgrowth step was required. After heat-shock 100µl of SOC medium or LB broth was added to cells, and the tube was left shaking at 37°C in a bacterial incubator for 1hr. Outgrowth at 37°C for 1 hour is best for cell recovery and maintenance of antibiotic resistance. Transformed cells were then spread onto LB agar plates containing 100µg/ml kanamycin and incubated at 37°C overnight.

## 2.2.2. Isolation of plasmid DNA

### 2.2.2.1. Small-scale DNA amplification

---

Plasmid isolation and purification from bacterial cells was performed using the mi-Plasmid Mini Prep Kit (*Metabion*) according to the manufacturer's protocol. Briefly, 5ml LB broth containing appropriate antibiotic was inoculated with a single transformed *E.coli* colony from an agar plate. The culture was incubated overnight at 37°C with constant shaking. The bacterial cells were centrifuged at 5000 g for 5 mins and subjected to lysis and purification as per the manufacturer's instructions. All plasmids were eluted in molecular grade water.

### 2.2.2.2. Large-scale DNA amplification

---

Plasmid isolation and purification from bacterial cells was performed using the Nucleobond Xtra Midi Kit (*Macherey-Nagel*) according to the manufacturer's protocol. Briefly, a starter culture of LB broth (5ml) containing appropriate antibiotic was inoculated with a single transformed *E.coli* colony and incubated at 37°C with constant shaking for 3-6h. This was then added to LB broth (100ml) containing appropriate antibiotic and incubated over night at 37°C with constant

shaking. The bacterial cells were centrifuged at 3000g for 20mins and subjected to lysis and purification as per the manufacturer's instructions. All plasmids were eluted in molecular grade water.

#### 2.2.2.3. DNA quantification

DNA concentrations and purity were determined using a NanoDrop® ND-1000 Spectrophotometer according to the manufacturer's protocol.

#### 2.2.3. Agarose gel electrophoresis

The principle of agarose gel electrophoresis is to separate nucleic acids according to their molecular size in an electric field. PCR products were electrophoresed on agarose gels in a BRL Horizon 58 Life Technologies electrophoresis unit. Agarose gels were prepared by adding 0.8-2.0% (w/v) agarose (*Thermo Fisher Scientific*) to 100ml 1 X TAE buffer (Appendix II), and heated until the agarose dissolved. Ethidium Bromide (10,000x; *Thermo Fisher Scientific*) or GelRed™ Nucleic acid stain (10,000x; *Biotium*) was added and mixed by swirling gently. The solution was transferred into gel moulds and allowed to set. Agarose gels were transferred to the electrophoresis apparatus and overlaid with 1xTAE. DNA samples were mixed with 10x Loading Dye, and then were loaded into the gel wells. 7 µl 1kb DNA Ladder (*Thermo Fisher Scientific*) was included in each gel as a size reference. Gels were electrophoresed at 120 V for 15-30 minutes. DNA was visualized by a UV Transluminator and imaged using a Syngene G box gel documentation system (*Frederick*).

## 2.2.4. DNA purification

### 2.2.4.1. Gel purification

---

The required DNA fragment was excised from an agarose gel after visualising the DNA on a UV-transilluminator (*Viber Lourmat*). DNA fragments were purified using QIAquick Gel Extraction Kit (*Qiagene*), according to the manufacturer's protocol and eluted in 30µl molecular grade water.

## 2.2.5. Polymerase Chain Reaction (PCR)

### 2.2.5.1. End-point PCR

#### 2.2.5.1.1. Principle

---

The polymerase chain reaction (PCR) is a sensitive and selective *in vitro* method for exponential amplification of a specific DNA fragment of defined length and sequence template DNA.

#### 2.2.5.1.2. Primer design

---

Primer pair design is the largest variable in PCR application and the single most critical factor in determining the specificity of the PCR. Primers were designed based on deposited GenBank sequences. Primer pairs were designed so they were complementary to the 5' and 3' ends of the fragment to be amplified. Primers were designed to incorporate appropriate restriction enzyme sites to allow cloning into chosen plasmid vectors. The following parameters were respected: G/C content of 40-60% and length of 16-30 nt with a melting temperature ( $T_m$ ) of 50°C or higher. Of note, complementary sequences of primer pairs should be avoided, since this often results in primer-dimer formation, which can impair the efficiency of the PCR.

### 2.2.5.1.3. PCR reaction mix

Primers were obtained from Eurofins MWG Operon and resuspended in molecular grade water (*Thermo Fisher Scientific*) to a concentration of 100pmol/ $\mu$ l. Phusion<sup>TM</sup> High Fidelity PCR polymerase (*Finnzymes*) was used according to the manufacturer's protocol for a 20 $\mu$ l reaction, see Table 2.1. PCR amplification was carried out on a MJ research PTC-200 Thermo Cycler.

<b>Components</b>	<b>50 <math>\mu</math>l Volume (<math>\mu</math>l)</b>	<b>20 <math>\mu</math>l Volume (<math>\mu</math>l)</b>	<b>Final Conc.</b>
5xHF Buffer ( <i>Phusion</i> )	10	4	1x
10 mM dNTPs ( <i>Metabion</i> )	1	0.4	200 $\mu$ M
Primer 1	X	X	0.5 $\mu$ M
Primer 2	X	X	0.5 $\mu$ M
Template DNA	X	X	1pg-10ng per 50 $\mu$ l Rxn
Phusion DNA Polymerase	0.5	0.2	0.02 U/ $\mu$ l
Water	Add to 50	Add to 20	

**Table 2.1: PCR Master Mix.**

Table shows the components and their concentrations in each Phusion<sup>TM</sup> PCR Master Mix.

#### 2.2.5.1.4. PCR cycling program

PCR cycling programs were performed using an MJ research PTC-200 Thermo Cycler. The programs are listed in Table 1.2. Cycling conditions were determined as per manufacturer's instructions. Generally, an annealing temperature approximately 5°C below the lowest  $T_m$  of the pair of primers is used. For primers with high  $T_m$ , a two-step cycling program was used which does not have an annealing step.

Cycle step	2-step protocol		3-step protocol		Cycles
	Temp.	Time	Temp.	Time	
<b>Initial denaturation</b>	98°C	30 s	98°C	30 s	1
<b>Denaturation</b>	98°C	5 - 15 s	98°C	5 - 10 s	25-35
<b>Annealing</b>	-	-	X°C	10 - 30 s	
<b>Extension</b>	72°C	15 -30 s/kb	72°C	15 - 30 s/kb	
<b>Final extension</b>	72°C	5-10 min	70°C	5-10 min	1
	4°C	hold	4°C	hold	

Table 2.2: PCR cycling program

#### 2.2.6. Site directed mutagenesis PCR

##### 2.2.6.1. Principle

The aim of site directed mutagenesis PCR is to introduce a specific mutation at a defined site in a DNA sequence. The basic procedure utilizes a supercoiled double-stranded DNA (dsDNA) plasmid containing the insert of interest and two synthetic oligonucleotide primers containing the desired mutation in the middle of their sequence. The oligonucleotide primers, each complementary to opposite strands of the vector, are extended during temperature cycling by the DNA polymerase. Incorporation of the oligonucleotide primers generates a mutated plasmid containing staggered nicks. Following temperature cycling, the PCR product is

treated with *Dpn I* (*New England Biolabs*). The *Dpn I* endonuclease (target sequence: 5'-GM6ATC-3') is specific for methylated and hemimethylated DNA and is used to digest the parental DNA template, and thus to select for mutation-containing synthesized DNA. DNA isolated from almost all *E.coli* strains is dam - methylated and therefore susceptible to *Dpn I* digestion. The nicked vector DNA containing the desired mutations is then transformed into competent cells.

### 2.2.6.1. Primer Design

Primers were designed using the QuickChange primer design tool software (Agilent). Primers are listed in Table 2.3.

<b>Site-Directed mutagenesis primers</b>		
<b>Mutant</b>	<b>Forward Primer</b>	<b>Reverse primer</b>
<b>NES mutant</b>	5'- ctggaccagcagtttgctggcgagacgcgaactcttcagata atcagag-3'	5'- ctctgattatctgaagagttcgcgtctgcgccagcaactgctggtc cag-3'
<b>NSL 1</b>	5'- gcaaaagcatgctattcctattatcgagaggcaagagacttg atggcttgtgc-3'	5'- ttgggcacacatcaagtctcttgctctgcgataataggaatagcat gctt3'
<b>NLS2-1</b>	5'- gctttgagggccatgaaggaaaatggagcggctggcgccg caaac-3'	5'- gtttgcggcggccagccgctccattttccttcatggccctcaaagc- 3'
<b>NLS2-2</b>	5'- gaaaatggagcggctggggcagccaacaataccaatctc- 3'	5'- gagattgggtattgtttggctgccccagccgctccattttc -3'
<b>T204D</b>	5'- agcttactcgttatactgcccagatccagtgcaaaagcat-3'	5'-atgcttttgactggatctggcgagtataacgagtaagct-3'
<b>T323D</b>	5'-atgccattttagtagccgatccaggacgtctagtgat- 3'	5'-atccactagacgtcctggatcggctactaacaatggcat-3'
<b>T204A</b>	5'-ctcgttatactgcccagctccagtgcaaaagcat-3'	5'-atgcttttgactggagctggcgagtataacgag-3'
<b>T323A</b>	5'-gccattttagtagccgctccaggacgtctagtg-3'	5'-cactagacgtcctggagcggctactaacaatggc-3'

**Table 2.3: Site Directed mutagenesis primers.**

### 2.2.6.2. PCR reaction mix

Verbatim High Fidelity PCR Kit (*Thermo Fisher Scientific*) was used for site directed mutagenesis PCR. Primers were obtained from Eurofins MWG Operon and resuspended in molecular grade water (*Thermo Fisher Scientific*) at a concentration of 100 $\mu$ mol/ $\mu$ l. A 50 $\mu$ l reaction was used; with reagents added as per Table 2.4. A negative control with no polymerase was run alongside the positive PCR.

<b>Components</b>	<b>50 <math>\mu</math>l Volume (<math>\mu</math>l)</b>	<b>Final amounts</b>
5xHF Buffer (Verbatim)	10	1x
20 mM dNPTs	1	200 $\mu$ M
Primer 1	X	125ng
Primer 2	X	125ng
Template DNA	X	5-50ng per 50 $\mu$ l Reaction
Verbatim DNA Polymerase	1.0	2.5 U/ $\mu$ l
Water	Add to 50	

**Table 2.4: PCR Master Mix.**

Table shows the components and their volumes in each Verbatim PCR Master Mix.

### 2.2.6.3. PCR cycling conditions

Site directed mutagenesis PCR conditions were as per Table 2.5.

<b>Segment</b>	<b>Cycles</b>	<b>Temperature</b>	<b>Time</b>
Initial Denaturation	1	95°C	30 seconds
Denaturation	25-30	95°C	30 seconds
Annealing		55°C	1min
Extension		68°C	1min/1kb
Final extension	1	68°C	5-10 min
		4°C	Hold

**Table 2.5: PCR Conditions.**

Protocol as per QuikChange Site-Directed Mutagenesis Kit (*Agilent*) instructions.

### 2.2.6.4. *Dpn1* digestion and transformation

*Dpn1* (*New England Biolabs*) was used to digest the parental template DNA. 1µl of *Dpn1* was added to both the positive and negative control PCR tubes. 10µl of product was run on a 0.8% Agarose gel to confirm PCR amplification. *E.coli* was transformed with either positive and negative control PCR product and plated onto LB agar plates. Colonies were picked from positive plate and grown for small scale DNA purification. DNA was sent for sequencing to confirm mutagenesis.

## 2.2.7. Gene cloning technology

### 2.2.7.1. Principle

The aim of recombinant DNA technology is the cloning of DNA fragments into plasmids via the joining of two segments of DNA to generate a single DNA molecule capable of autonomous replication within *E.coli* hosts. There are four major steps in DNA cloning: 1) preparation of vector and insert; 2) ligation of vector and insert; 3) transformation into a host; 4) screening of selected clones. The ultimate purpose was to clone genes of interest and to express their encoded protein in different host cells (bacterial or mammalian cells). When expressed as a non-fusion protein an ATG codon was present at the start of the insert ORF. When

the insert was expressed as a fusion protein, the orientation and reading frame were maintained.

#### 2.2.7.2. Vectors and insert sequences

All bacterial plasmid vectors contain basic features, such as an origin of DNA replication (ori) enabling replication in bacteria; a multiple cloning site (MCS) with an array of unique restriction enzyme sites; selectable markers such as antibiotic resistance genes (Kmy r and Amp r). For expression in bacterial, yeast or mammalian systems, vectors also have to contain specific features recognised by the host cells, including a specific ori, a specific promoter region upstream of the MCS directing the transcription of the insert and selection markers and also features to induce translation, eg. Kozak sequence for bacterial expression. Vector maps of all plasmids used and an outline of their respective uses are listed in Appendix I.

The insert sequences were derived from two different sources. Insert sequences were isolated directly from previously recombinant plasmids containing the inserts via enzymatic digestion of the insert (subcloning) or were amplified by PCR. Whether subcloned from another vector or amplified by PCR, inserts contained compatible restriction sites with the multiple cloning site (MCS) of the chosen expression vector.

### 2.2.7.3. Cloning protocols

#### 2.2.7.3.1. Enzymatic digestion of the vector and the insert

The vector and insert DNA were digested with one or two different restriction enzymes with recognition sites included within the MCS of the vector and at the ends of the insert, generating compatible and cohesive ends. All restriction enzymes were obtained from *New England Biolabs* and used with manufacturer's buffers. Appropriate buffers for double digestions were used, as per manufacturer's instructions. The digestion reaction was performed for 3-16h at 37°C, or overnight at 37°C as per Table 2.6.

<b>Components</b>	<b>35µl reaction</b>
<b>Purified vector or insert DNA</b>	Approx. 1.0µg 15µl PCR product
<b>10x Buffer</b>	3.5
<b>Enzyme I</b>	1.0
<b>Enzyme II</b>	1.0
<b>BSA</b>	0.5
<b>ddH2O</b>	<b>Up to 35</b>

**Table 2.6: Restriction enzyme digestion reaction.**

Table shows the components and their volumes for each restriction enzyme digest of DNA insert or vector.

#### 2.2.7.3.2. Dephosphorylation of vector for one enzyme cloning

Antarctic Phosphatase (*New England Biolabs*) was used to dephosphorylate vector during one enzyme cloning. Antarctic Phosphatase catalyzes the removal of 5' phosphate groups from DNA and RNA. Since phosphatase-treated fragments lack the 5' phosphoryl termini required by ligases, vector cannot self-ligate. After treatment the reaction was carried out for 1h at 37°C (Table 2.7) followed by heat inactivation at 65°C for 5 mins.

<b>Components</b>	<b>Volume (<math>\mu</math>l)</b>	<b>Working Conc.</b>	<b>Final Conc.</b>
10x Buffer	3.0	10x	1x
Antartic Phosphatase enzyme	1.0	NA	4-5U/ $\mu$ g DNA
BSA	0.5	100x	100 $\mu$ g/ml
ddH2O	Up to 30	NA	NA

**Table 2.7: Dephosphorylation reaction.**

Table shows the components and their volumes for dephosphorylation of digested vectors.

#### 2.2.7.3.3. Ligation of the vector and the insert

Following restriction digest, vector and insert were gel-purified and then ligated. Ligations were carried out with 2xLigase Premix (*Clonables, Novagen/Merck Millipore*) as outlined in Table 2.8. An excess of insert is required for successful ligation. A negative control with dH<sub>2</sub>O instead of DNA insert was also included, to control for re-ligation of vector. The ligation reactions were incubated at 16°C for 20mins.

<b>Components</b>	<b>Volume (<math>\mu</math>l)</b>	<b>Conc.</b>
Vector	<b>0.5-1.5</b>	0.0125 pmol
DNA insert	<b>1.0-2.0</b>	0.025-0.7 pmol
2xligase	2.5	

**Table 2.8: Ligation reaction.**

Table shows the components and their volumes for ligation of purified DNA inserts into appropriate vectors.

#### 2.2.7.3.4. Transformation and selection

50µl of competent *E.coli* cells were transformed with 2µl of the ligation reaction mixture. The transformation procedures were described in section 2.2.1.2. Transformants were plated on LB plates containing appropriate antibiotic.

#### 2.2.7.3.5. Screening of the transformants

Colonies on LB plates were used to inoculate small ON cultures for small scale plasmid purification. Restriction digestion was carried out using appropriate restriction enzymes to confirm the presence of insert.

#### 2.2.7.3.6. Sequencing

Positive clones were then sequenced to confirm their correct sequence, orientation and reading frame. Plasmids were sent to either Eurofins MWG Operon (Germany) or SourceBiosource (Ireland) for sequencing.

#### 2.2.7.4. Plasmid construction

DDX3 truncation mutants were generated by cloning relevant sequences into the EcoRI and Sal I site of the vector pCMV-Ha (*Clontech*) (Appendix I). The Ha-tag is to the N-terminus of DDX3. Primers used are listed in Table 2.9.

NES-addition mutants, which re-attached the NES region to N- terminal deletion mutants, were generated as shown in Figure 2.1 by amplifying the first 1-22 amino acids of DDX3 flanked by two EcoR1 site. Constructs for truncation mutants were linearised using the EcoR1 restriction enzyme and dephosphorylated using Antarctic Phosphate (*New England Biolabs*) to prevent religation of the NES 1-22 fragment. The NES 1-22 fragment was ligated into truncation mutants, and transformed into *E.coli*. Positive clones were sent for sequencing to confirm correct orientation of insert.

DDX3-GFP plasmids were generated by using Ha-tagged mutants as template for PCR, and cloning the products into EcoRI and Sall sites of the pEGFP-N1 vector (*Clontech*) (Appendix I).

<i>DDX3 mutants</i>	<i>Forward primer</i>	<i>Reverse primer</i>
<b>DDX3 primers</b>		
<b>22-662</b>	5'-gccgaattcggatgaactcttcagataatcagagt-3'	5'-acgcgtcgactcagttaccccacca-3'
<b>44-662</b>	5'-gccgaattcggatgaggaaccgagaagct-3'	5'-acgcgtcgactcagttaccccacca-3'
<b>66-662</b>	5'-gccgaattcggatgaaggatgcgtatagc-3'	5'-acgcgtcgactcagttaccccacca-3'
<b>80-662</b>	5'-gccgaattcggatggggaagtctagcttc-3'	5'-acgcgtcgactcagttaccccacca-3'
<b>100-662</b>	5'-gccgaattcggatgggacggagtattac-3'	5'-acgcgtcgactcagttaccccacca-3'
<b>110-662</b>	5'-attgaattcggatgggtgacagaagtggc-3'	5'-acgcgtcgactcagttaccccacca-3'
<b>120-662</b>	5'-attgaattcggatgcgtggtgaaacagt-3'	5'-acgcgtcgactcagttaccccacca-3'
<b>130-662</b>	5'-gccgaattcggatgtcagatgaagatgaT-3'	5'-acgcgtcgactcagttaccccacca-3'
<b>DDX3 NES-1-22</b>	5'- agtcgtggacgttctaagagcaga -3'	5'-cgaattccgttcaggtctaggccag-3'
<b>DDX3 GFP</b>	5'-tcttatggccatggaggcccgaattc -3'	5'- aaatgtcgacgggttaccaccagtc -3'

**Table 2.9: Primers used for PCR amplification of DDX3 mutants.**

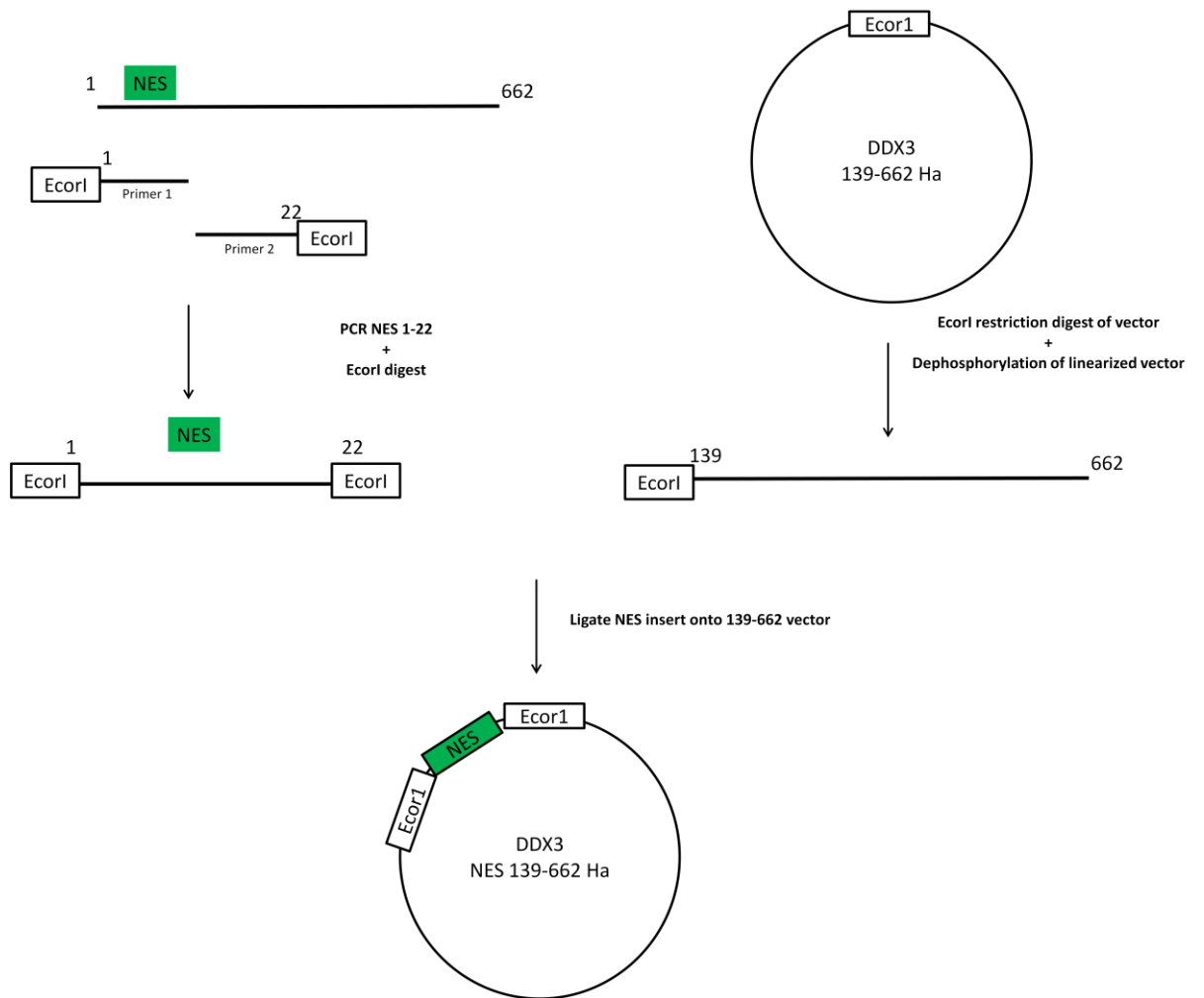


**Figure 2.1: Schematic of NES addition plasmid construction.**  
Not drawn to scale.

## 2.3. Protein methods

---

### 2.3.1. One-Dimensional SDS-PAGE

---

Sodium dodecyl sulphate polyacrylamide gel electrophoresis (SDS-PAGE) migrates and separates proteins according to their molecular weight under denaturing conditions. Solution for resolving gels, 5% stacking gels, and buffers are outlined in Appendix II. Protein samples were mixed with 2x Laemmli sample buffer before being heated at 95°C for 5 minutes. Alongside a protein molecular weight marker (*Fermentas*), the samples were loaded into the wells of the stacking gel. Gels were then run using the BIO-RAD Minigel electrophoresis apparatus in SDS-PAGE running buffer at 100-150 V constant voltage for 50-90 minutes, or until sufficiently resolved.

### 2.3.2. Coomassie Blue staining

---

When required, SDS-PAGE gels were stained with Coomassie Blue Staining Solution (Appendix II) for 20 minutes at 56°C, followed by destaining in Destaining solution (Appendix II) until the background was clear.

### 2.3.3. Western blot analysis

#### 2.3.3.1. Electroblotting procedure

---

Once the proteins had been separated by SDS-PAGE, they were transferred electrophoretically to a polyvinylidene fluoride (PVDF) transfer membrane (*Immobilon, Sigma-Aldrich*) in a semi-dry electrophoretic transfer unit (*Biometra*). Membrane was pre-soaked in methanol (*Sigma-Aldrich*) and cold transfer buffer (Appendix II) for 10 min.

#### 2.3.3.2. Immunoblotting procedure

After transfer, the membrane was incubated by shaking gently in a blocking solution (5% semi-skimmed milk powder in 1×PBS/0.01 % Tween (*Sigma*)) at room temperature for 1 h to prevent non-specific antibody binding. Subsequently, the membrane was incubated with a primary antibody, in 5% Milk PBS/Tween, for 2 hour at room temperature, or 4°C overnight. Antibody concentrations and information is listed in Appendix II. Following 3 x 10min washes in 1 X PBS/Tween, the membrane was then incubated with a horseradish peroxidase conjugated secondary antibody for 2h at room temperature, and then washed again 3 x 10 min in 1 X PBS/Tween.

#### 2.3.3.3. Chemiluminescent detection

Immunoreactive proteins were detected using Enhanced ChemiLuminescence (ECL). ECL was prepared by mixing 1ml of ECL A, 1ml of ECL B and 0.6µl of H<sub>2</sub>O<sub>2</sub> (Appendix II) and then added to the membrane for 30 secs. Commercial ECL was also used (*Millipore*) as per manufactures guidelines. Membranes were placed between two layers of plastic and placed in a film cassette. In the dark room, Autorad film (UltraCruz™ Autoradiography Film, *Santa Cruz Biotechnology*) was placed on top of the membranes in the cassette for 1-30 min. Autorad film was then developed and fixed using a Fuji Medical film processor (*Fuji*).

#### 2.4. Mammalian cell culture methods

All cell culture experiments were performed in a Holten LaminAir laminar flow hood at Biosafety Level II. Cells were maintained at 37°C in a humidified atmosphere of 5% CO<sub>2</sub> in a Thermo Scientific Forma Steri Cycle incubator.

### 2.4.1. Cells culture

---

HEK293T and HeLa adherent cell lines were cultured in Dulbecco's Modified Essential Medium (DMEM) (*Invitrogen*) with 10% fetal calf serum (*Thermo Fisher Scientific*) and antibiotics (10 µg/ml gentamicin (*Sigma*) (Table 2.10). Confluent cultures were passed at 1:10 ratio for HEK293T and HeLa in T 75cm<sup>2</sup> tissue culture flasks (*Corning*) every 2-3 days. Cells were dissociated using 5% (w/v) trypsin-EDTA solution (*Sigma*) and resuspended in DMEM.

<b><i>Cells</i></b>	<b><i>Description</i></b>	<b><i>Morphology</i></b>	<b><i>Maintained in</i></b>
HEK293T	Immortalised Human embryonic kidney cell line, containing the SV40 Large T-antigen	Epithelial	DMEM
HEK 293 R1s	Immortalised Human embryonic kidney cell line, stably transfected with IL-1R1	Epithelial	DMEM
HeLa	Human cervical carcinoma cell line	Epithelial	DMEM
HepG2	Human Liver carcinoma cell line	Epithelial	DMEM

---

**Table 2.10: Cell line information**

## 2.4.2. Transient transfection of mammalian cell lines

Cells were transfected with plasmids using either Calcium Phosphate or GeneJuice™ (*Merck/Novagen*) according to the manufacturer's protocol.

### 2.4.2.1. Calcium Phosphate transfection

For a 10cm TC dish, 500µl (-volume of DNA) 2X HBS (Appendix II) were aliquoted into a sterile 1.5 ml microfuge tubes. 20 µg of plasmid DNA was added to 2xHBS. 30µl 2.5M CaCl<sub>2</sub> (Appendix II) was then added and mixed gently during the addition. After 20min incubation, solution was added dropwise to the cells. Cells were incubated at 37°C for 24-48 hours before harvesting. For a 6-well plate, 12-well plate or 24-well plate, reaction was scaled down appropriately.

### 2.4.2.2. Gene juice transfection

Genejuice™ transfection (*Merck/Novagen*) was carried out as per the manufacturer's instructions. Transfection assays were carried out in flat bottomed 96-well plates. Genejuice was diluted in serum free medium (SFM) at a 1:25 dilution and left for 5min. The DNA/Genejuice mixture was left for 15 min before addition to the cells in the 96 well plate. A total amount of 230ng DNA in 10µl GeneJuice/SFM mixture was added to each well and mixed by pipetting.

### 2.4.2.3. siRNA transfection

Short Interfering RNA (siRNA) can be used to interfere with the expression of specific mRNAs containing complementary nucleotide sequences. Lipofectamine 2000 was used to transfect HEK293Ts and HeLa cells with Stealth™ RNAi oligonucleotides (*Invitrogen*) specific for DDX3 or a control siRNA with matched GC content (

Table 2.11). For a 6-well plate, 100pmole (5 $\mu$ l) of siDDX3-1, siDDX3-2, siDDX3-3 or si medium GC was added to 125 $\mu$ l of Optimem (*Gibco*) in a sterile eppendorf tube. 125 $\mu$ l of Optimem (*Gibco*) was mixed with 5  $\mu$ l Lipofectamine 2000 in a sterile eppendorf, and left for 15 min. The Lipofectamine/Optimem mix was added to the siRNA/Optimem eppendorf tube mixed with pipetting, and incubated for 15 min. 255 $\mu$ l of Lipofectamine/siRNA mix was added to cells. After 24 h, cells from each well were split into two new wells. The following morning a second siRNA transfection was carried out, and 6 h later expression plasmids were transfected into cells using the calcium phosphate method. Cells were harvested 24 h after the calcium phosphate transfection.

<i>siRNA</i>	<i>Sequence</i>	<i>Identifier</i>
<b>DDX3-1</b>	5'-GGGAGAAAUAUCAUGGGAAACAUU-3'	(HSS102712)
<b>DDX3-2</b>	5'-UUCAACAAGAAGAUCCAACAAAUCC-3'	(HSS102713)

**Table 2.11: siRNA sequence and Identifier (*Invitrogen*).**

### 2.4.3. Cell treatments

For Leptomycin B (LMB) treatment, cells were treated with 20 nM LMB (*Sigma*) 3 hours before harvesting.

For Sendai virus (SeV, Charles River Laboratories) stimulation, Sendai virus was added at a 1:200 dilution from original stock (16,000/ml) at required time points.

Etoposide was added to cells at a concentration of 25 $\mu$ M or 50 $\mu$ M for 4 hours.

IL1- $\alpha$  /TNF- $\alpha$  was added at a concentration of 10ng/ $\mu$ l of IL1 and 100ng/ $\mu$ l of TNF for 4 hours.

Importazole was added to cells at a concentration of 40 $\mu$ M for 4/8 h.

Sodium Arsenite was added to cells at a concentration of 1 mM for 20 minutes.

## 2.5. Co-immunoprecipitation (Co-IP) assay

### 2.5.1. Principle

Immunoprecipitation (IP) is the technique of precipitating a protein antigen out of solution using a matrix-bound antibody that specifically binds to that particular protein. Co-immunoprecipitation involves the immunoprecipitation of intact native protein complexes.

### 2.5.2. Co-immunoprecipitation (Co-IP) assay

HEK293T cells were transfected with 4 µg of expression plasmids for Ha-tagged proteins in a 6-well plate; or 20 µg in a 10cm dish. 48 hours post-transfection, cells were lysed in 200µl IP-lysis buffer for 6 well plate; or 850 µl for 10cm dishes (Appendix II). The required antibody was coupled to Protein G Sepharose Beads (*Sigma*), or Protein A/G agarose beads (*Santa Cruz*) in 5% BSA/PBS-Tween (0.05%) overnight at 4°C with constant rotation. Lysates were added to beads for 3 hours at 4°C or overnight at 4°C with constant rotation. Beads were washed three times with 1ml of IP-Lysis Buffer and drained of all wash buffer. Beads were then resuspended in 2x Laemmli sample buffer (Appendix II) and boiled for 10min at 95 °C. Co-immunoprecipitation samples were then analysed for interaction by SDS-PAGE and Western blotting.

## 2.6. In vitro Recombinant protein Pull down Assay

### 2.6.1. Expression and purification of recombinant His-tagged Proteins in E.coli

1 µl plasmid DNA (pHIS-Parallel-2 expression plasmid) was transformed chemically into competent *E. coli* strain BL21/DE3 (*New England Biolabs*) as described in section 2.2.2.1. Overnight pre-culture was performed at 37°C by inoculating with one transformed colony in 12 ml of LB (AMP) overnight.

Alternatively, 5  $\mu$ l of a glycerol stock was used to inoculate the 12ml pre-culture of LB (AMP). 10 ml of the overnight pre-culture was inoculated into a 100 ml LB (AMP) culture and incubated at 37°C up to the logarithmic phase of growth. When  $OD_{600} = 1.2$ , protein expression was induced by the addition of isopropyl  $\beta$ -D-1 thiogalactopyranoside (IPTG) to a final concentration of 100  $\mu$ M at room temperature. The *E.coli* cells were pelleted by centrifugation of 3000g for 45min at 4°C, and then resuspended in 1 ml native lysis buffer (Appendix II). Lysates were snap frozen in liquid nitrogen and thawed using a water bath. Three cycles of freeze-thawing were carried out. Additional sonication (30% power for 10sec x 3) were performed on the lysates to completely lyse the bacteria. The lysates were cleared by centrifugation at 13000g for 30 min. 100  $\mu$ l Ni-NTA bead slurry (*Qiagen*) was washed three times with His-Wash Buffer (Appendix II), then added to the cleared lysates, and incubated at 4°C for overnight with constant rotation. The beads were then washed twice with 1.5 ml of His washing buffer I and II and the proteins were eluted by 100 $\mu$ l of elution buffer (Appendix II). Aliquots of protein were run on SDS-PAGE and stained with Coomassie Blue to assess purity and amount of purified recombinant proteins.

### 2.6.2. *In vitro* Pulldown assay

For pull-downs, equal amounts of the different His- or GST- tagged fusion proteins were used, as estimated by SDS-PAGE and Coomassie Blue staining prior to use. Cell lysates containing Myc-tagged proteins expressed in HEK293T cells or 0.5 $\mu$ g of recombinant protein were incubated with the purified His- or GST-tagged proteins coupled to Nickel-Agarose or Glutathion-Sepharose respectively, with constant rotation for 4h or overnight at 4°C. Beads were washed three times in

1.5ml lysis buffer, and then all the liquid drained. Beads were then resuspended in 2x Laemmli sample buffer (Appendix II) and boiled for 10min at 95 °C. Samples were analysed for interactions by SDS-PAGE and Western blotting.

## 2.7. Intracellular protein Co-localisation Studies

### 2.7.1. Immunofluorescent staining

Cells were cultured on round coverslips (*Lennox*) in a 6 well plate. 24 hours after plating, cells were transfected with 4µg DNA using the Calcium Phosphate method. 1 hour before transfection the medium was replaced. 48 h post-transfection, cells were fixed in 4% paraformaldehyde (Appendix II) for 15min on ice, followed by washing in PBS (Appendix II). Cells were permeabilised with 0.5% Triton X-100 for 30min on ice, followed by washing in PBS (Appendix II). Cells were blocked for 1h with 5% BSA in PBS-Tween (0.05%). Cells transfected with expression plasmids for Ha-tagged proteins were subjected to direct immunofluorescence using anti-Ha-AlexaFluor594 (*Invitrogen*) diluted at 1: 500 in 5% BSA in PBS-Tween (0.05%). The antibody solution was incubated with the cells for 2 h at room temperature in the dark. Indirect immunofluorescence was performed using primary antibodies, details of antibodies used and their concentrations can be found in Appendix II. After primary antibody incubation, cells were washed three times in PBS-Tween (0.05%). Addition of appropriate secondary antibodies followed, either anti-rabbit-AlexaFluor 488 (*Invitrogen*) or anti-mouse-AlexaFluor 488 (*Invitrogen*) diluted 1:1000 in 5% BSA in PBS-Tween (0.05%). After staining cells were mounted in SlowFade Gold Antifade Reagent containing DAPI (*Invitrogen*) on microscope slides and sealed using clear nail varnish.

Cells were viewed using an Olympus Fluoview Confocal Microscope and analysed using Olympus Fluoview FV10-ASW software. Images were captured using a 40x objective lens. Sequential excitation at 405nm, 488nm and 594nm was used. The term co-localisation refers to the coincidence of green and red fluorescence, as detected by the confocal microscope. Olympus Fluoview FV10-ASW software was used to measure the degree of co-localisation by calculating the Pearson's correlation coefficient ( $R(r)$ ). Pearson's correlation coefficient is one of the standard techniques used to quantify the covariance between two signals.

#### 2.7.1.1. Mitochondria staining

Where required, Mitotracker Red (*Invitrogen*) was used to stain mitochondria for immunofluorescence microscopy. 100nM of Mitotracker Red diluted in serum free medium was added to live cells for 1 h before fixation. After staining, cells were prepared as described before.

#### 2.7.1.1. Lipid droplet staining

Staining of lipid droplets required the addition of oleic acid to induce lipid droplet formation. 24 h after transfection, Oleic acid (Sigma) was added to cells at a concentration of 200 $\mu$ M overnight. Cells were fixed and stained as previously described in 2.7.1., with the secondary antibody being conjugated to AlexaFluor-488. SUDAN III (*Sigma*) at 2mg/ml in 70% Ethanol was added to fixed cells for 20 mins at room temperature and in the dark. Cells were washed 3 times with 70 % ethanol, followed by 2 washes with PBS. After staining, cells were prepared as described before.

### 2.7.3. Low content analysis

Cells were stained as described above. Olympus Fluoview Software was used to analyze the nuclear and cytoplasmic intensity of different stains. DAPI stain was used as a reference area for the nucleus and the bright field light image for the cytoplasmic area. A single line through the cell was then analyzed for the intensity of staining in the nucleus and cytoplasm. Intensity of staining in the nucleus divided by intensity of staining in the cytoplasm gave the nuclear/cytoplasmic ratio, see Figure 1.1.

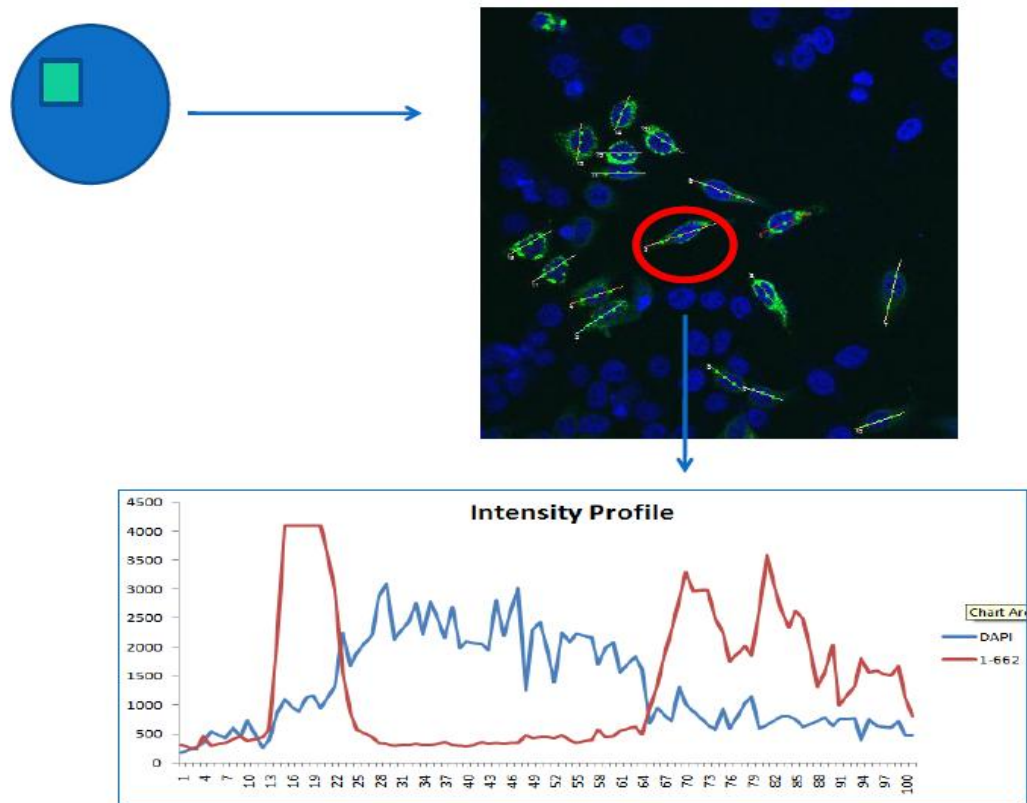


**Figure 2.2: Nuclear/Cytoplasmic intensity was measured using Olympus Fluoview Software.** A straight line was analyzed through each cell; using DAPI and bright field light image to specify nuclear and cytoplasmic areas, respectively. Intensity of staining for nucleus and cytoplasm was then used to determine the nuclear/cytoplasmic ratio.

### 2.7.3. High Content analysis

The GE IN Cell Analyzer 1000 is an automated cellular and sub-cellular imaging system. The IN Cell Analyzer was used for high content analysis of cells.

#### 2.7.3.1. Preparation of cells for IN Cell Analyzer

HeLa cells were grown in a 96 well plate. For experiments requiring overexpression of proteins, cells were transfected with expression plasmids via calcium phosphate transfection. Cells were fixed and stained in 96 well plate as described earlier. Briefly, 100 $\mu$ l 4% PFA was added per well for 15 min while on ice, followed by a wash in PBS. For permeabilization, 100 $\mu$ l of 0.05% Triton-X was added to wells for 30min on ice. Cells were blocked in 100 $\mu$ l of 5% BSA/PBS-Tween. Antibodies were diluted as described in Appendix II, and 100 $\mu$ l of antibody solutions was added to wells. Cells were washed with 300 $\mu$ l of PBS-Tween between antibody incubations. After secondary antibody incubation, DAPI (*Sigma*) was used at a concentration of 0.5 $\mu$ g/ml to stain nucleus and Phalloidin–Tetramethylrhodamine B isothiocyanate (*Sigma*) was used at a concentration of 0.1 $\mu$ M to stain actin filaments. This was followed by further washing in PBS-Tween. After staining, cells were covered with 200 $\mu$ l PBS for analysis.

#### 2.7.3.2. Analyzes of High-Content data

Data was collated by IN cell Software (GE). DAPI and Phalloidin–Tetramethylrhodamine B isothiocyanate staining were used to define nuclear and cytoplasmic regions, respectively, which were used as a mask for detection of changes in DDX3 staining (Figure 2.3 A). To exclude non-transfected cells; data was parsed by setting a minimum threshold fluorescence intensity score using a non-transfected negative control. Data was parsed using Python programming language.

For experiments looking at endogenous proteins all cells were analysed. Nuclear/cytoplasmic ratio was determined using an equation which took into account background intensity and area of nuclear and cytoplasm (Figure 2.3 B).

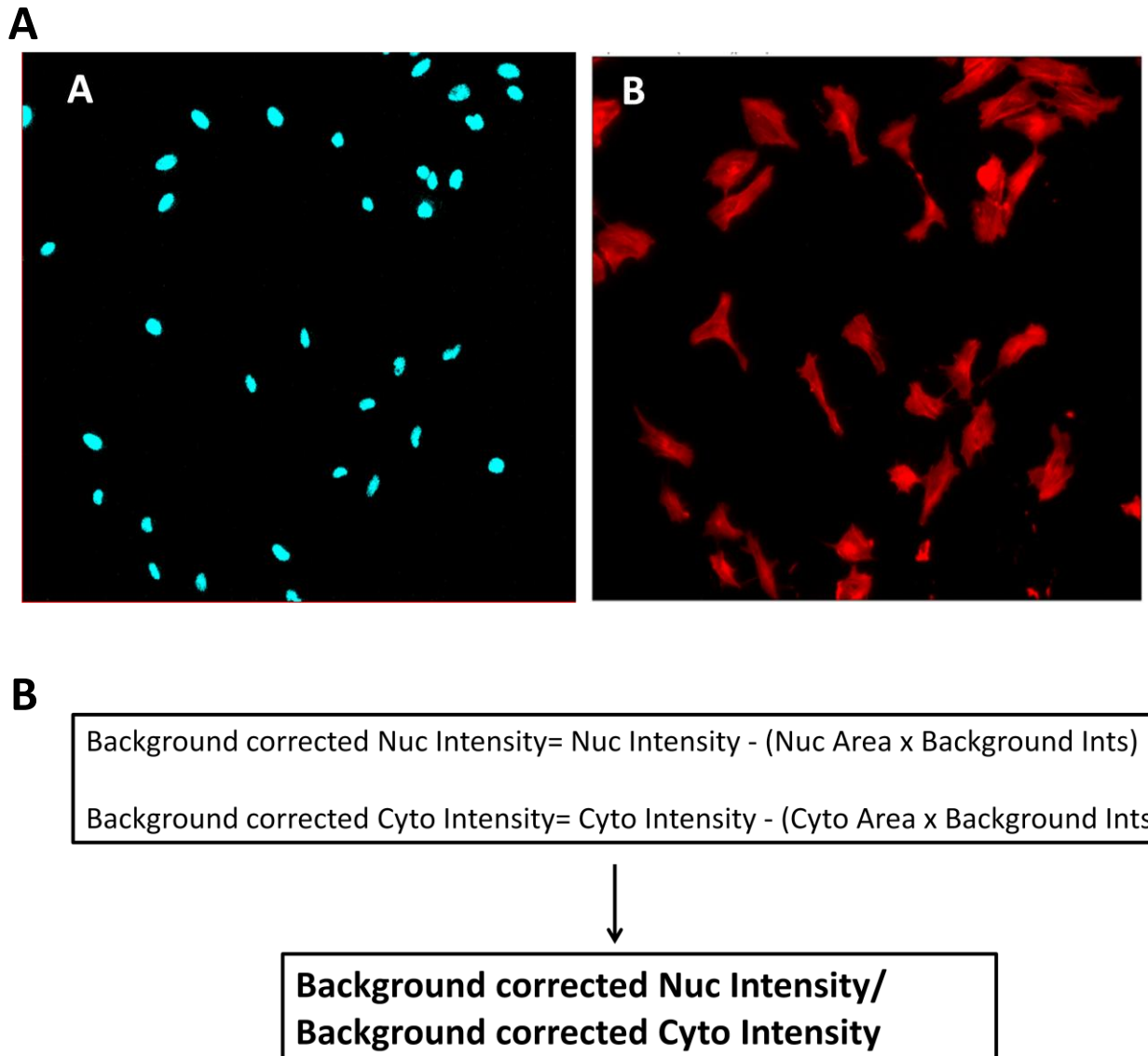


**Figure 2.3: High Content microscopy workflow.**

**A:** HeLa cells are stained with a primary  $\alpha$ -DDX3 and secondary  $\alpha$ -rabbit Alexa Fluor-488, and with Rhodamine Phalloidin which binds F-actin. **Key:** A (DAPI), B (Rhodamine-Phalloidin). **B:** Nuclear/cytoplasmic ratio equation. Background corrected intensities are calculated, and then used to calculate nuclear/cytoplasmic ratio.

## 2.8. Nuclear Cytoplasmic fractionation

---

### 2.8.1. Principle

---

Cells were fractionated into their cytoplasmic and nuclear components. A hypotonic buffer swells cells to allow for lysis of the cytoplasmic membrane without disruption of the nuclear membrane. A stronger lysis buffer is then used to lyse the nuclear membrane.

### 2.8.2. Method

---

HeLa cells were lysed on 10 cm plates for 5 mins using 500 $\mu$ l of Subcellular fractionation buffer (Appendix II). Cells were scraped from plate and placed in 1.5 ml eppendorf tube. Lysates were passed through a 25 G needle 10 times using a 1 ml syringe. The nuclear pellet was centrifuged out at 720g for 5 min, supernatant was retained as the cytosolic fraction. The nuclear pellet was washed once by adding 500 $\mu$ l of fractionation buffer. The nuclear pellet was pelleted by centrifugation at 720g for 10 min. Wash buffer was removed and the nuclear pellet was resuspended in standard lysis buffer (containing 10% glycerol, 1% NP-40), and incubated for 30mins on ice, with vortexing intermittently. The cytosolic fraction (supernatant) was centrifuged at 10,000g to clear any remaining fragments. The supernatant is the cytosolic fraction, pellet is the mitochondrial fraction. If the mitochondrial fraction is desired, pellet is washed like the nuclear pellet and resuspended in the same buffer as above.

## 2.9. Cell cycle arrest and synchronization

### 2.9.1. Principle

Cell cycle synchronization is the process of growing cells in culture to be at the same stage of the cell cycle. Synchronization of cells at specific stages of the cell cycle can be achieved by using inhibitors that block cells at specific stages of the cell cycle.

### 2.9.2. Double thymidine block (G1/S block)

HeLa cells were plated at 25-30% confluency and grown in complete DMEM (*Invitrogen*) supplemented with 2mM thymidine (*Sigma*) for 18h. After this initial thymidine block, cells were washed in PBS twice and released into fresh complete DMEM for 9h. Cells were then added to complete DMEM supplemented with 2mM thymidine for 17h for the second block. Cells are blocked at G1/S boundary by this treatment. If required, cells were released into complete DMEM and harvested at specific time points to monitor cell cycle progression.

### 2.9.3. Thymidine/Nocodazole block (G2/M block)

HeLa cells were plated at 40% confluency and grown in complete DMEM supplemented with 2mM thymidine for 24h. After initial thymidine block, cell were released into fresh complete DMEM for 3h. After release, 100ng/ml nocodazole (*Sigma*) was added to cell for 12h. Cells are blocked at mitotic (G2/M) boundary by this treatment. If required, cells were released into complete DMEM and harvested at specific time points to monitor cell cycle progression.

### 2.9.4. Serum starvation (G0/G1 block)

HeLa cells at 30-40% confluency were washed twice with PBS and grown in serum-free medium for 72 h. Cells are blocked at G0/G1 stage by this treatment.

Cells were released into complete DMEM and harvested at specific time points to monitor cell cycle progression.

## Chapter 3 : Nuclear export of DDX3

---

### 3.1. Introduction

---

DDX3 has been shown to affect cellular processes in both the nucleus and the cytoplasm; therefore how DDX3 is exported from the nucleus is important. The nuclear export of DDX3 has not been studied in much detail, but it has been addressed in the context of its interaction with HIV-Rev protein. Furthermore it has been shown that DDX3 might be exported through both CRM-1 and Tap (Yedavalli et al. 2004; Lai et al. 2008).

In the following passages, the current knowledge on how DDX3 is exported from the nucleus will be discussed.

#### 3.1.1. DDX3 export via Tip Associated Protein (TAP)

---

Tip-associated protein (TAP), a member of the NXF family, is considered as the major receptor for bulk mRNA export (Herold et al. 2000; Stutz 2003). DDX3 has been shown to interact with TAP in an RNA independent manner, and to associate with mRNPs (Lai et al. 2008). One study showed that knockdown of TAP resulted in a reduced nuclear export of DDX3; suggesting that DDX3 can at least partly be exported via TAP (Lai et al. 2008). However, the functional relevance of the DDX3-TAP interaction is unclear, as DDX3 does not seem to be required for bulk mRNA export.

#### 3.1.2. DDX3 export via CRM-1

---

The *Xenopus laevis* DDX3 homologue An3 has been shown to be exported from the nucleus in a CRM-1-dependent manner (Askjaer et al. 1999). An3 export is mediated by a leucine-rich NES in its N-terminus. This NES is tightly conserved in DDX3 homologues including human DDX3 (X- and Y-linked), with the NES matching

the PKI-class NES consensus (Figure 3.1). Removal of the NES resulted in nuclear accumulation of An3 and reduced binding to CRM-1. Mutation of the NES through substitution of Leu-19 and Leu-21 with alanine residues also resulted in nuclear accumulation (Askjaer et al. 1999). An3 nuclear export was also shown to be coupled to An3 helicase activity. An An3 DEAD-box mutant (DEAD->DQAD) displayed reduced export from the nucleus; while binding to CRM-1 was not affected and neither was RNA binding capacity (Askjaer et al. 2000). The NES of An3 has been described as a high affinity NES; meaning that it binds strongly to the hydrophobic cleft of CRM-1 (Güttler et al. 2010). The interaction between An3 and CRM-1 was dependent on Ran-GTP as expected for CRM-1 cargo (Askjaer et al. 1999; Güttler et al. 2010).

Human DDX3 has been shown to be retained in the nucleus upon treatment with Leptomycin B (LMB) (Sekiguchi et al. 2004; Yedavalli et al. 2004). LMB is a powerful inhibitor of CRM-1 mediated nuclear export, binding covalently and irreversibly to cysteine 528 in the NES-binding region of CRM-1 and thus preventing nuclear export of CRM-1 cargo (Yashiroda & Yoshida 2003; Kudo et al. 1999). Interestingly, Sekiguchi *et al.* showed that disruption of the NES through substitution of Leu-19 and Leu-21 to alanine did not affect export of hamster DDX3; however export of this mutant was still sensitive to LMB treatment (Sekiguchi et al. 2004). The authors suggested the existence of another NES-region within the DDX3 protein or that CRM-1 may not be the only form of export utilized by DDX3.

Another group investigated the role DDX3 played in the export of un-spliced/partially spliced HIV-1 transcripts via the Rev-RRE/CRM1 pathway (Yedavalli et al. 2004). They demonstrated that DDX3 interacts with CRM-1 independently of

its N-terminus, which contains its putative NES. Instead, the C-terminus of DDX3 was required for CRM-1 binding and this binding occurred in a Ran-GTP independent manner (Yedavalli et al. 2004). DDX3 was shown to co-localise with nucleoporins along the outer nuclear rim, and was suggested to play a role in processing of RNAs to permit their nuclear export through the NPC. A subsequent molecular modelling study, showed that the region between residues 420-560 of DDX3 might be responsible for binding to CRM-1. The authors also suggested that DDX3 could unwind viral RNA during nuclear transport due to the proximity of the DDX3 binding groove to the HIV-Rev binding groove of CRM-1 (Sharma & Bhattacharya 2010).

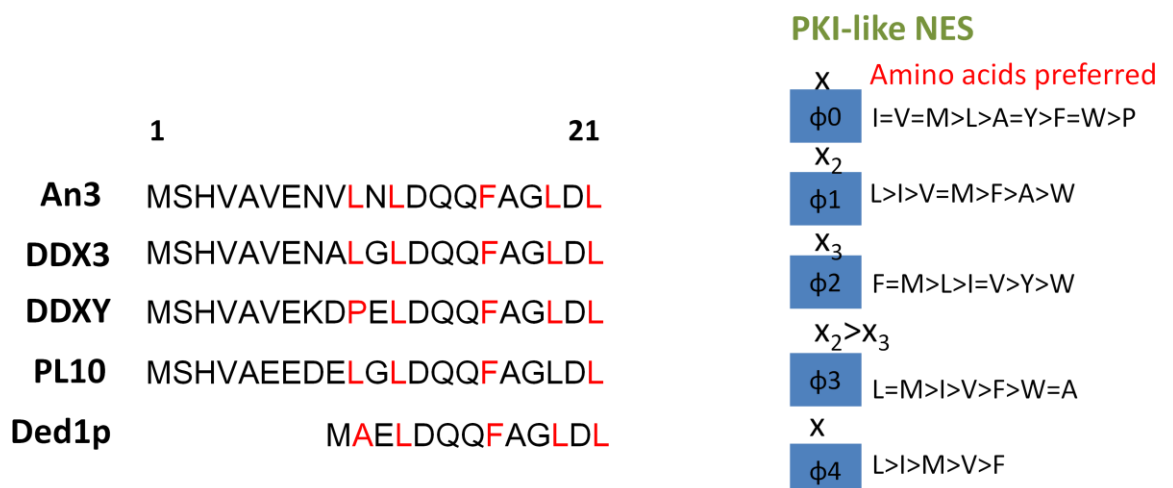


**Figure 3.1: Leucine rich NES is conserved in the DDX3 homologues and corresponds to a PKI-like NES.**

Alignment of *Xenopus* An3 NES sequence with DDX3X (X-homologue) and DDXY (Y-homologue) (human), PL10 (mouse), Ded1p (yeast).

### 3.1.3. Conclusion

---

The literature on DDX3 nuclear export is complicated by conflicting results. The export of DDX3 has been suggested to occur mainly via CRM-1 however involvement of the putative highly conserved N-terminal NES is unclear (Yedavalli et al. 2004; Sharma & Bhattacharya 2010). The *Xenopus* DDX3 homologue An3 has been shown to be exported via CRM-1; with the an NES in its N-terminus being required for its export (Askjaer et al. 1999). The interaction of NES-containing proteins with CRM-1 is well understood; with NESs binding at 5 specific hydrophobic ( $\phi$ ) pockets in CRM-1. The An3 NES has been described as having high affinity for CRM-1 (Askjaer et al. 2000). Due to the near perfect conservation of this NES sequence between An3 and DDX3, it would be expected that the NES of human DDX3 should also mediate CRM-1 binding and DDX3 export.

### 3.2. Aims

---

In this chapter, I investigated the nuclear export of DDX3. I aimed to confirm that DDX3 is exported via CRM-1, and test whether DDX3's helicase activity is required for export. Using different truncation mutants we aimed to characterise the regions required for nuclear export, and to test the functionality of the putative N-terminal NES in human DDX3.

### 3.3. Results

---

#### 3.3.1. DDX3 localises predominantly in the cytoplasm in a range of transformed cells Lines

---

Within the literature the localisation of DDX3 is unclear, with most reports suggesting a predominantly cytoplasmic localisation (Yedavalli et al. 2004; Sekiguchi et al. 2004) and others suggesting a nuclear localisation (Owsianka & Patel 1999). Owsianka *et al.* showed DDX3 localised to the nucleus in a speckled manner with only low levels of DDX3 in the cytoplasm (Owsianka & Patel 1999). Others have suggested that DDX3 has a nuclear localisation in primary skin cells compared to a cytoplasmic localisation in transformed squamous cell carcinoma (SCC) (Chao et al. 2006). However, most of the literature would suggest DDX3 localises predominantly to the cytoplasm.

I first tested the localisation of DDX3 in HeLa cells using immunofluorescence confocal microscopy, staining for endogenous DDX3 and F-actin. DDX3 localised predominantly in the cytoplasm in HeLa cells (Figure 3.2).

I then decided to test the localisation of DDX3 in a range of transformed cell lines. HEK293ts, a kidney cell line; HeLa, a cervical cell line; MC7F, a breast cancer cell line; and A549, cell a human alveolar basal epithelium cell line, were stained for endogenous DDX3. DDX3 has a predominantly cytoplasmic localisation in all of these cell lines (Figure 3.3).

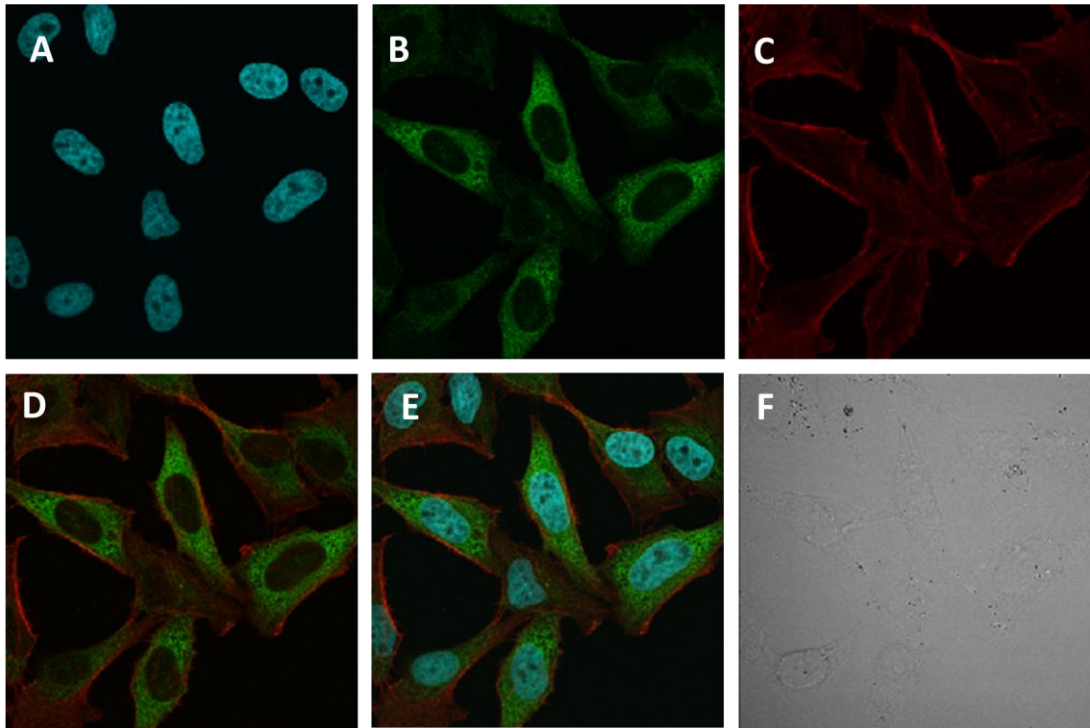


**Figure 3.2: Endogenous DDX3 localises in the cytoplasm.**

HeLa cells were stained with a primary  $\alpha$ -DDX3 and secondary  $\alpha$ -rabbit Alexa Fluor-488 and also with tetramethylrhodamine isothiocyanate-phalloidin which binds F-actin. **Key:** A (DAPI), B ( $\alpha$ -DDX3), C (Rhodamine-Phalloidin), D (Merge B and C), E (Merge A,B and C) and F (Contrast).

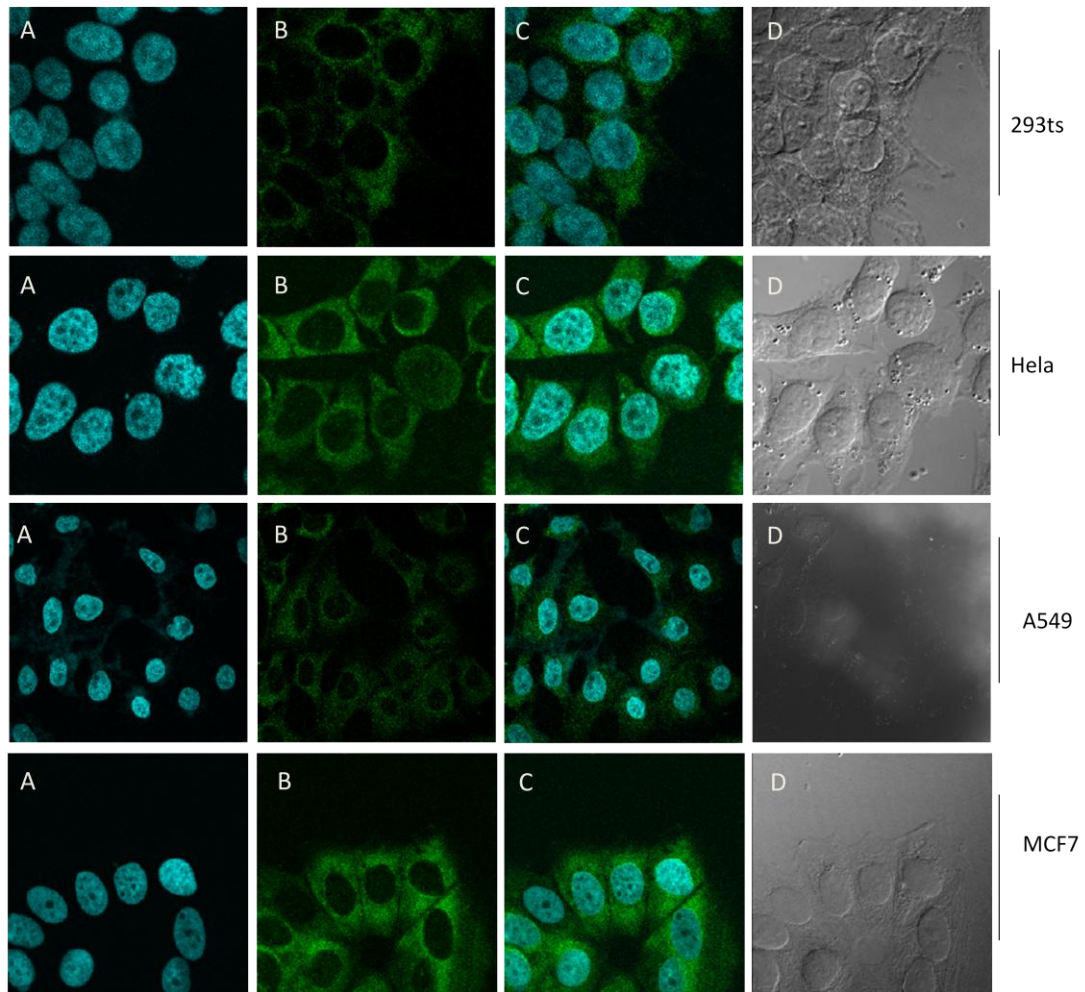


**Figure 3.3: DDX3 has a cytoplasmic localisation in a range of human cell lines.**

HEK 293Ts, HeLa, MCF7 and A549 cells were stained with a primary  $\alpha$ -DDX3 and secondary  $\alpha$ -rabbit Alexa Fluor-488 as described in Chapter 2. **Key:** A (DAPI), B ( $\alpha$ -DDX3), C (Merge A+B), D (Contrast).

### 3.3.2. DDX3 is exported from the nucleus in a CRM-1 dependent manner

DDX3 has been described as a nucleocytoplasmic shuttling protein. It has been described to be exported from the nucleus in a CRM-1 dependent manner (Sekiguchi et al. 2004; Askjaer et al. 1999; Askjaer et al. 2000); and also through TAP (Lai et al. 2008). Confocal microscopy was used to confirm whether DDX3 export occurs via the protein exportin CRM-1. To this end, HeLa cells were transfected with expression plasmids for Ha-tagged DDX3 (Ha-DDX3), and were subsequently treated with the CRM-1 inhibitor Leptomycin B (LMB). Treatment with LMB resulted in nuclear accumulation of overexpressed Ha-DDX3; whereas in untreated control

cells, overexpressed Ha-DDX3 localised to the cytoplasm (Figure 3.4). I next tested whether endogenous DDX3 localised to the nucleus in HeLa cells after treatment with LMB, staining with an antibody against endogenous DDX3 and fluorochrome-conjugated secondary antibody. Treatment with LMB resulted in nuclear accumulation of endogenous DDX3; whereas in untreated control cells DDX3 had cytoplasmic localisation (Figure 3.4). To confirm this result, Nuclear/Cytoplasmic fractionation was used to separate cells into their nuclear and cytoplasmic fractions. Western blot analysis of the nuclear and cytoplasmic fractions showed that there was more DDX3 in the nuclear fractions after treatment with LMB compared to untreated controls, confirming that treatment with LMB causes an accumulation of DDX3 in the nucleus (Figure 3.4).

In conclusion, DDX3 is exported predominantly via CRM-1. Treatment with LMB resulted in the nuclear accumulation of both overexpressed and endogenous DDX3; with the majority of DDX3 being retained in the nucleus after treatment.

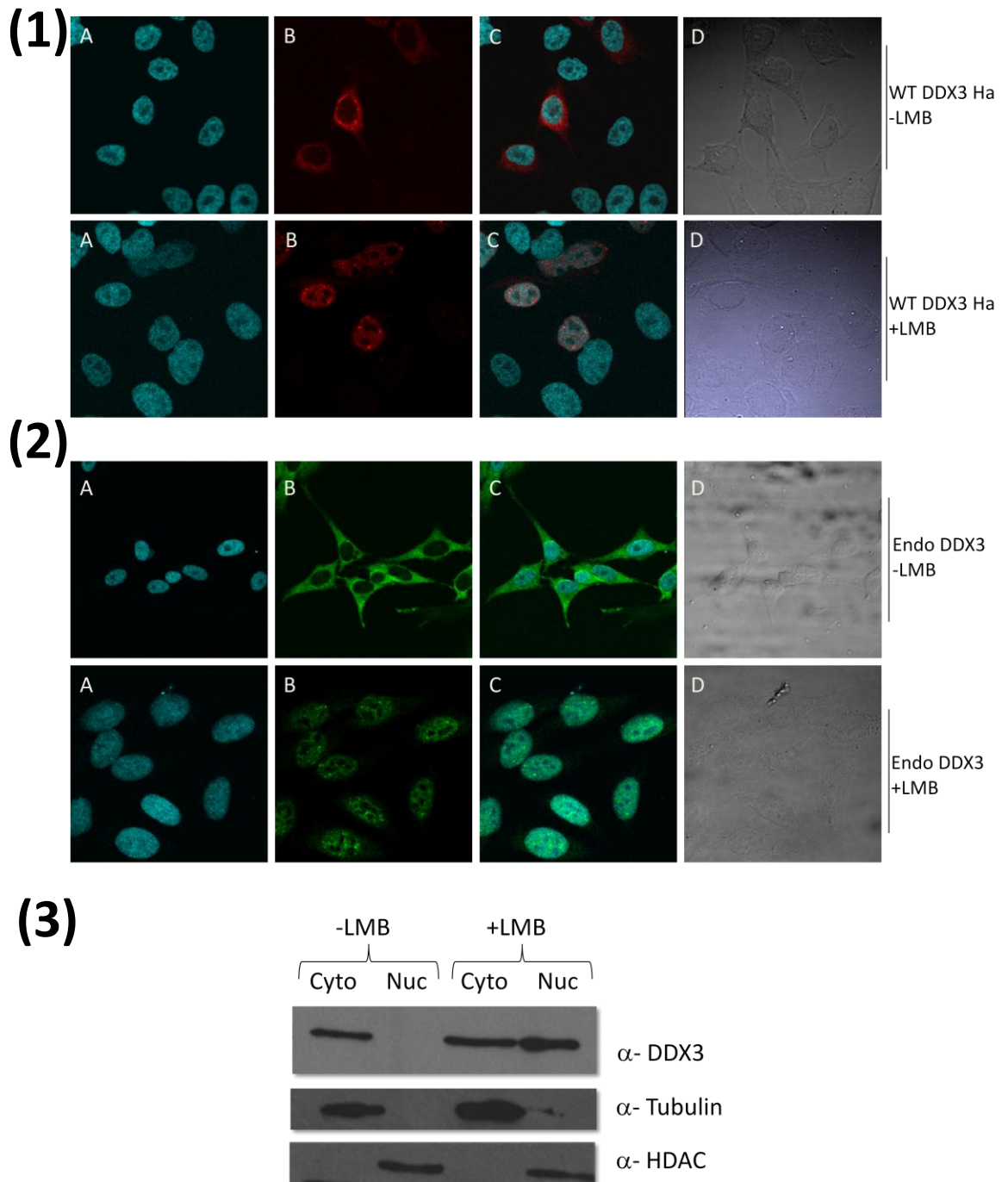


**Figure 3.4: CRM-1 is required for the export of DDX3. DDX3 accumulated in the nucleus when treated with 20mM Leptomycin B (LMB) for 2 hours.**

**(1):** HeLa cells were transfected with expression plasmids for WT Ha-DDX3, and stained with  $\alpha$ -Ha Alexa Fluor-594. **Key:** A (DAPI), B (Ha-DDX3), C (Merge A+B), D (Contrast). **(2):** HeLa cells were stained with a primary  $\alpha$ -DDX3 and secondary  $\alpha$ -rabbit Alexa Fluor-488. **Key:** A (DAPI), B ( $\alpha$ -DDX3), C (Merge A+B), D (Contrast). **(3):** HeLa Cells were fractionated into the nuclear and cytoplasmic fractions and immunoblotted as described in Chapter 2. Blots were probed with  $\alpha$ -DDX3,  $\alpha$ -Tubulin and  $\alpha$ -HDAC. Representative blot of three experiments.

### 3.3.3. DDX3 helicase activity is not required for nuclear export

Askjaer et al. showed that the nuclear export of An3 was coupled to its helicase activity (Askjaer et al. 2000). The single point mutant K230E, bearing a substitution in motif I (Walker A), has been previously characterized as having lost both its RNA unwinding activity and its ability to hydrolyse ATP (Yedavalli et al. 2004). When the K230E mutant was overexpressed in HeLa cells, it localised predominantly in the cytoplasm in untreated cells, and became sequestered in the nucleus upon treatment with LMB (Figure 3.5). Therefore, unlike DDX3's *Xenopus* homologue An3, human DDX3 does not require its helicase activity for nucleocytoplasmic shuttling.

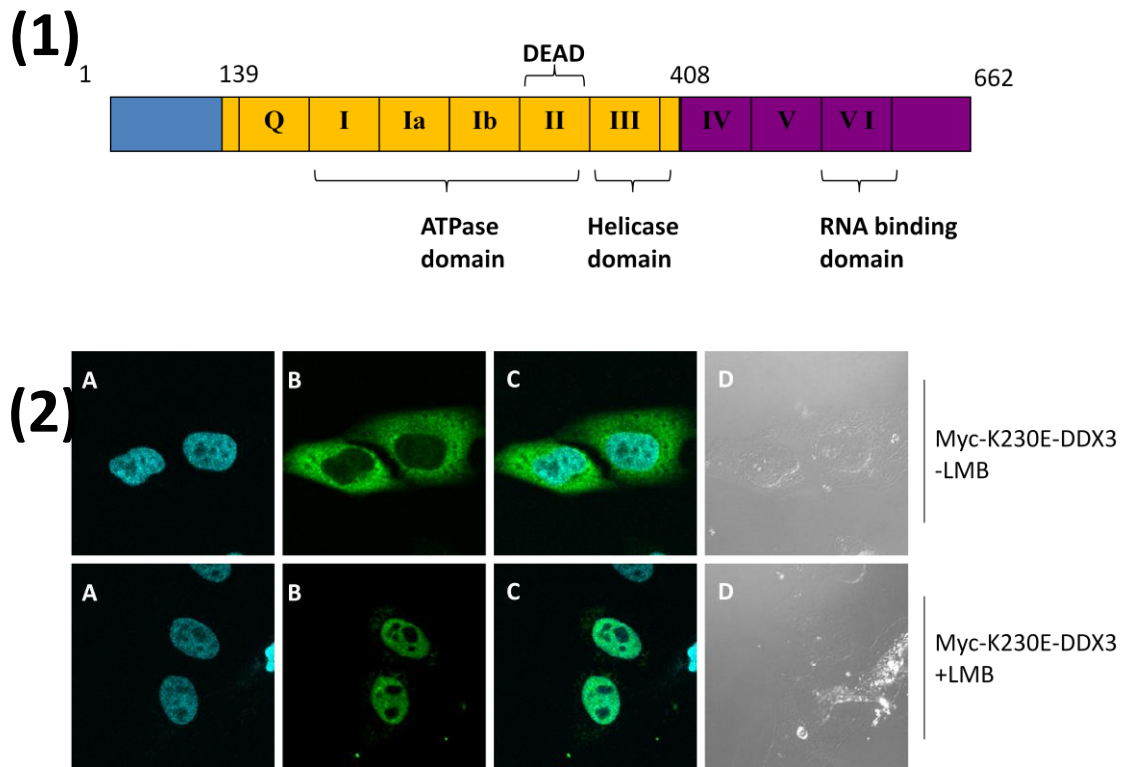


**Figure 3.5: Helicase activity of DDX3 is not required for nuclear export.**

**(1):** A schematic representation of protein structure of DDX3. **(2):** HeLa cells were transfected with expression plasmids for K230E mutant which has lost its ability to hydrolyse ATP and unwind RNA. Cells were treated with 20mM LMB for 2 hours or left untreated. Cells were stained with primary  $\alpha$ -myc antibody and secondary  $\alpha$ -mouse Alexa Fluor-488. **Key:** A (DAPI), B (Myc-DDX3), C (Merge A+B), D (Contrast).

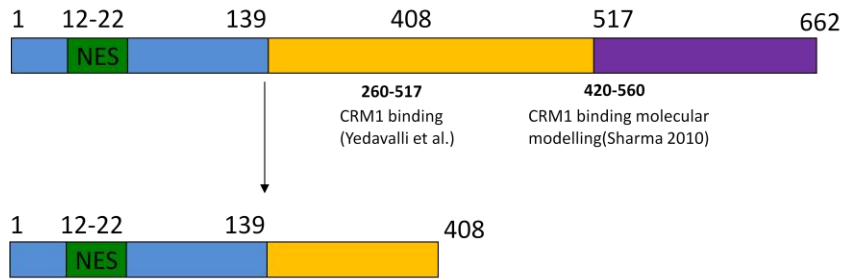
### 3.3.4. Mapping the region of DDX3 required for nuclear export

The region of DDX3 required for nuclear export is unknown, with roles for both the N-terminus and C-terminus being described in the literature (Sekiguchi et al. 2004; Yedavalli et al. 2004).

#### 3.3.4.1 The C-terminus of DDX3 is not required for nuclear export

Since the C-terminus of human DDX3 had previously been described as the region in which CRM-1 binding occurs (Yedavalli et al. 2004; Sharma & Bhattacharya 2010) (Figure 3.6); removal of the C-terminus would be expected to result in nuclear accumulation. However; overexpression of a C-terminal deletion mutant (1-408) in HeLa cells resulted in cytoplasmic localisation; suggesting that nuclear export had not been affected (Figure 3.6). Since the region of DDX3 responsible for import is unknown; we also treated the cells with LMB to ensure import was not being affected by removal of the C-terminus. Treatment with LMB resulted in nuclear accumulation of the 1-408 mutant (Figure 3.6). Therefore, these results show that the C-terminus of DDX3 is not required for CRM-1 mediated export. If CRM-1 binding to DDX3 does occur via the C-terminus as described in the literature, this interaction is not required for the export of the protein.

(1)



(2)

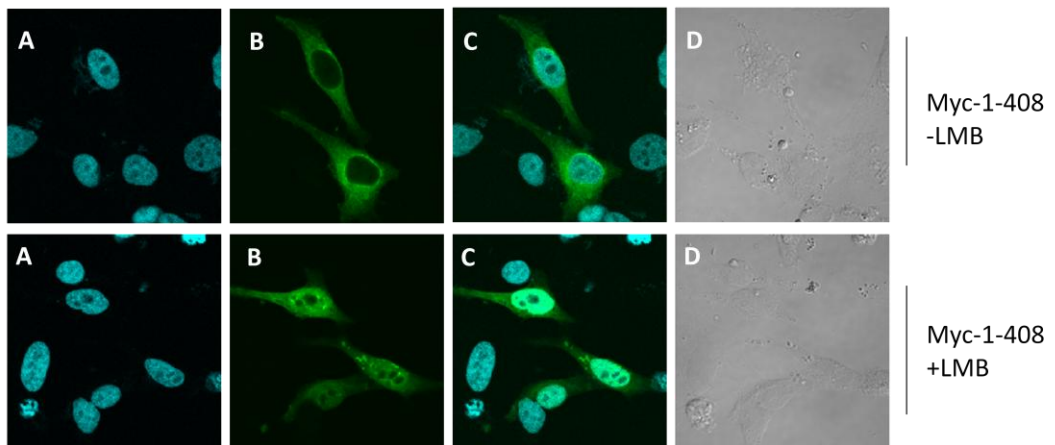


**Figure 3.6: The C-terminus of DDX3 is not required for export or import of DDX3.**

(1): A schematic showing CRM-1 binding sites as described in the literature and the C-terminal truncation mutant 1-408, (not drawn to scale). (2): HeLa cells were transfected with expression plasmids for myc-tagged 1-408 truncation mutant of DDX3. Cells were treated with 20mM LMB for 2 hours or left untreated. Cells were stained with primary  $\alpha$ -myc antibody and secondary  $\alpha$ -mouse Alexa Fluor-488. **Key:**A (DAPI), B (Myc-DDX3),C (Merge A+B), D (Contrast).

#### 3.3.4.2. The N-terminus of DDX3 is required for nuclear export

As the C-terminus of DDX3 is not required for nuclear export, I next investigated an N-terminal deletion mutant 139-662, which has the first 139 amino acids removed. I was very interested in the localisation of this N-terminal mutant, since it had previously been shown to lack the ability to induce IFN- $\beta$  promoter activation (Schröder et al. 2008), and also contains the binding sites for IKK $\epsilon$  and IRF3 (Gu et al. 2012). NetNES software ([www.expasy.org](http://www.expasy.org)) is an online bioinformatic tool which predicts classical NES, and NetNES predicted a putative classical NES in the N-terminus of DDX3 (Figure 3.7). This NES corresponds to the highly conserved putative NES that has been characterised in the *Xenopus* DDX3 homologue An3 (Askjaer et al. 2000). Removal of the N-terminus removes this putative NES at amino acids 12-22, and also a described binding site for the translation initiation factor eIF4E (Shih et al. 2008).

I tested the localisation of the N-terminal deletion mutant 139-662 using immunofluorescent staining and nuclear cytoplasmic fractionation. HeLa cells were transfected with expression plasmids for Ha-DDX3 and Ha-139-662, followed by immunofluorescent staining and confocal microscopy. I found that Ha-DDX3 had a clear cytoplasmic localisation and Ha-139-662 had a clear nuclear localisation (Figure 3.8). Nuclear/Cytoplasmic fractionation was used to separate cells into their cytoplasmic and nuclear fractions. Western blot analysis of the cytoplasmic and nuclear fractions showed that there was more Ha-139-662 in the nuclear fractions compared to Ha-DDX3 (Figure 3.8). Thus, the 139-662 mutant had a distinct nuclear localisation in HeLa cells, showing that the N-terminus of DDX3 is required for nuclear export.

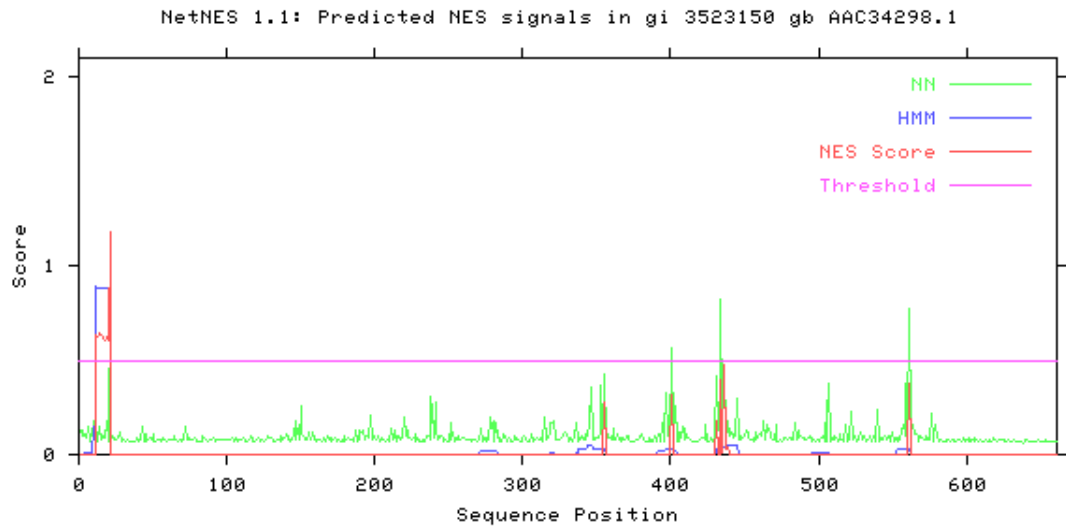


**Figure 3.7: DDX3 has a putative NES at residues 12-22.**

Graphical plot of the values (NES score) calculated by the NetNES software from the Markov Model (HMM), and Artificial Neural Network (NN) scores. If the calculated NES score exceeds the threshold, then the residue concerned is predicted to be involved in a nuclear export signal.

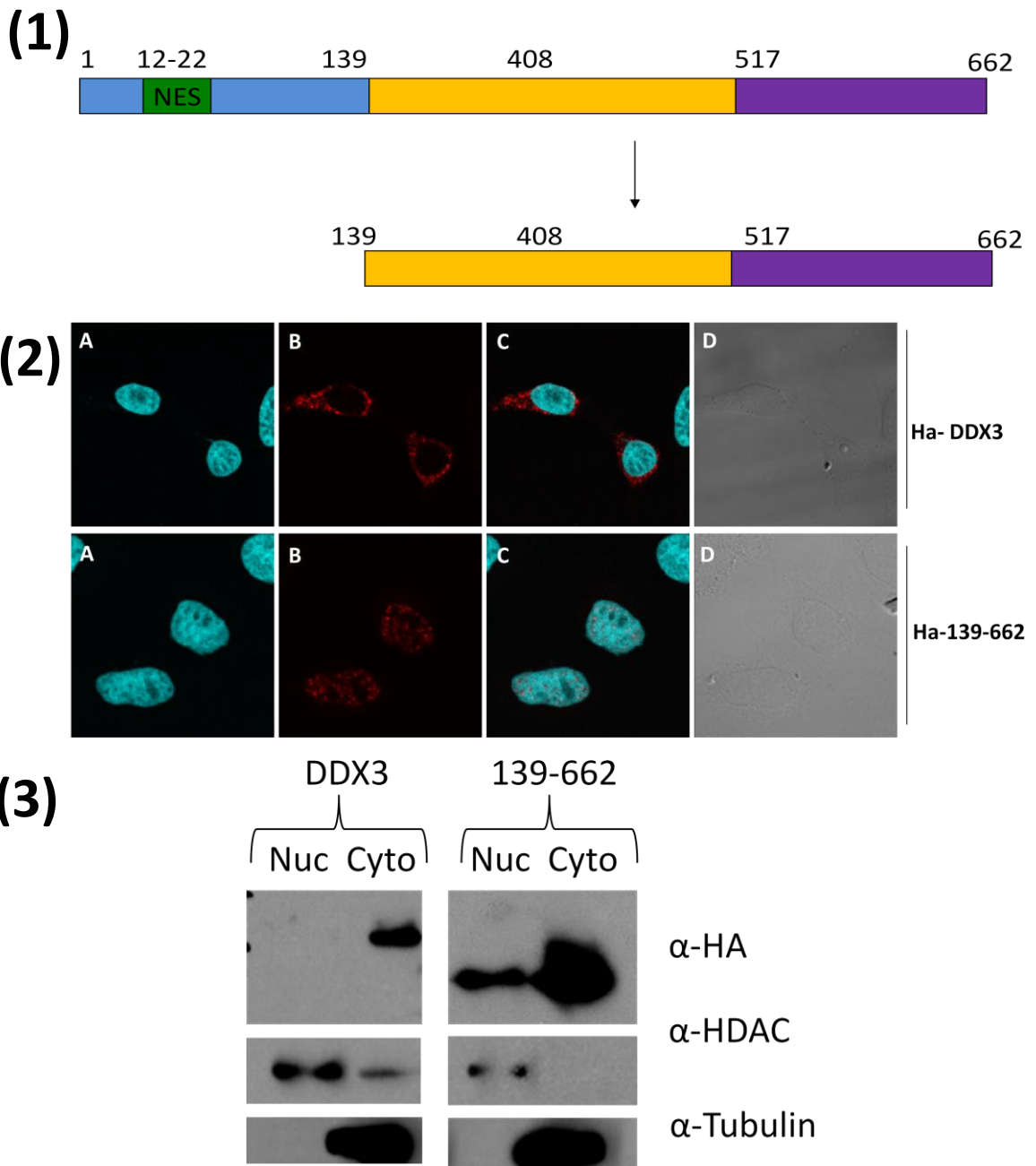


**Figure 3.8: WT DDX3 localises predominantly in the cytoplasm; whereas N-terminal deletion mutant 139-662 localises predominantly in the nucleus.**

**(1):** A schematic depicting the N-terminal truncation mutant 139-622 (not drawn to scale). **(2):** HeLa cells were transfected with expression plasmids for Ha-tagged constructs for WT DDX3 and 139-662 truncation mutant. Cells were stained with  $\alpha$ -Ha Alexa Fluor-594. **Key:** A (DAPI), B (Ha-DDX3), C (Merge A+B), D (Contrast). **(3):** HeLa Cells were fractionated into the nuclear and cytoplasmic fractions and immunoblotted as described in Chapter 2. Blots were probed with  $\alpha$ -Ha,  $\alpha$ -Tubulin and  $\alpha$ -HDAC. Representative blot of three experiments.

### 3.3.5. The NES in the N-terminus of DDX3 is required for nuclear export

I hypothesized that the nuclear localisation of the 139-662 mutant, was due to the removal of the putative NES at amino acids 12-22. Therefore, I designed and generated additional truncation mutants which truncated the N-terminus stepwise, removing the NES and eIF4E binding site.

HeLa cells were transfected with expression plasmids for Ha-tagged 22-662 and 44-662, followed by immunofluorescent staining and confocal microscopy. Removal of the putative NES and eIF4E binding site resulted in clear nuclear accumulation of DDX3 (Figure 3.9).

(1)



(2)

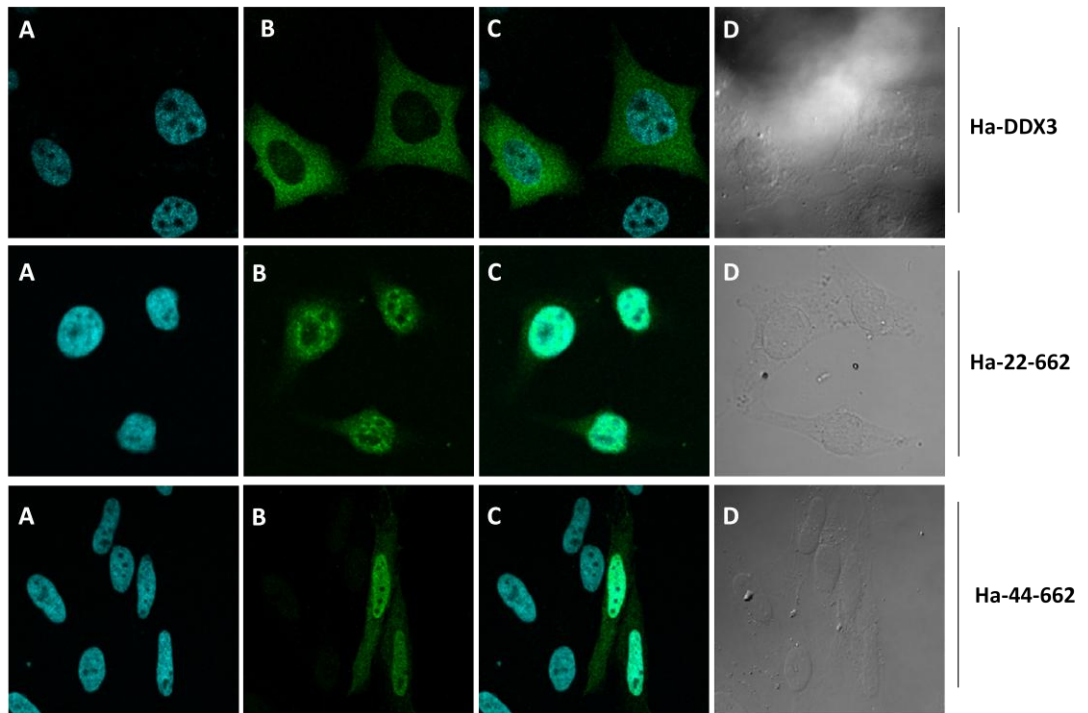


**Figure 3.9: Removal of putative NES results in nuclear accumulation of DDX3.**

(1): A schematic depicting the N-terminal truncation mutants 22-622 and 44-662 (not drawn to scale). (2): HeLa cells were transfected with expression plasmids for Ha-tagged WT DDX3, 22-662 or 44-662 truncation mutants. Cells were stained with primary  $\alpha$ -Ha antibody and secondary  $\alpha$ -mouse Alexa Fluor-488. **Key:**A (DAPI), B (Ha-DDX3), C (Merge A+B), D (Contrast).

To further validate the nuclear localisation of these truncation mutants; I decided to quantify the nuclear/cytoplasmic intensity of staining for DDX3 and its mutants. I used the nuclear DAPI stain and the light image to define the nucleus and cytoplasm of the cell, respectively. Using the Olympus Fluoview 1000 software the intensity of the fluorochrome of interest can be defined as nuclear intensity and cytoplasmic intensity using the nuclear stain (DAPI) and light image to define the boundaries. With this "Low content analysis", I measured the nuclear/cytoplasmic ratio of over-expressed Ha-DDX3; Ha-139-662 mutant and Ha-22-662 mutant. Results showed that wild type Ha-DDX3 localised predominantly in the cytoplasm, while the 22-662 and 139-662 mutants localised predominantly in the nucleus. Interestingly the 22-662 mutant had a reduced nuclear/cytoplasmic ratio compared to the 139-662 mutant (Figure 3.10); suggesting that residues downstream of the NES might also contribute to nuclear export.

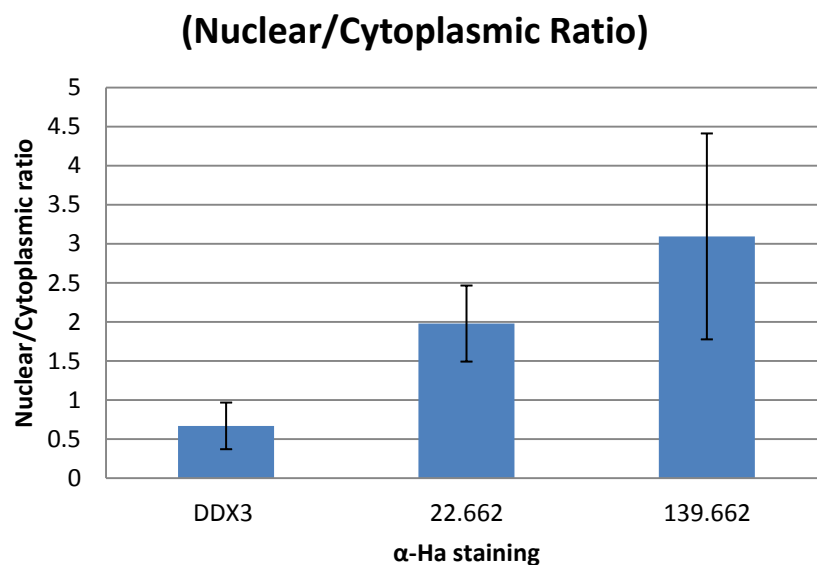


**Figure 3.10: N-terminal deletion mutants 22-662 and 139-662 are predominantly nuclear, compared to WT DDX3 which is predominantly cytoplasmic.**

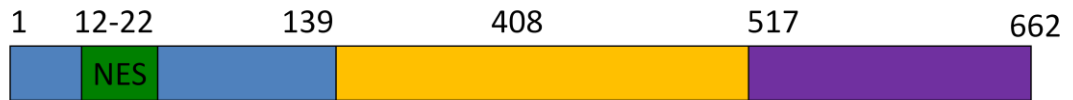
HeLa cells were transfected with expression plasmids for Ha-tagged DDX3 1-662, 22-662 or 139-662. Cells were stained with  $\alpha$ -Ha antibody and secondary  $\alpha$ -mouse Alexa Fluor-488. Cells were analyzed for nuclear/cytoplasmic intensity using Olympus Fluoview Software, as described in Chapter 2. A predominantly cytoplasmic stain is  $<1$ ; Nuclear stain is  $>1$ .  $n=30$  ( $n=15$  cells analysed from two independent experiments). Standard deviation error bars.

#### 3.3.5.1. Disrupting the NES of DDX3 results in impaired nuclear export

To further confirm the requirement of the N-terminal NES region for export of DDX3, an NES point mutant was designed. The NES-CRM-1 binding site can be disrupted by changing the hydrophobic leucines within the NES to inert amino acids; such as alanine. Askjaer et al. showed that disrupting the NES of the DDX3 *Xenopus* homologue An3 by substituting the leucines at residues 19 and 21 with alanine disrupted nuclear export of An3 (Askjaer et al. 1999). An equivalent mutant was constructed for human DDX3, which substituted the leucines at residues 19 and 21 with alanine as previously described. Site directed mutagenesis was carried out as described in Chapter 2.

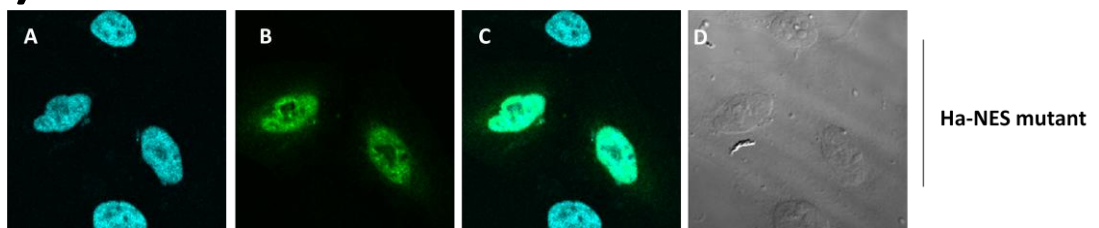
HeLa cells were transfected with expression plasmids for the Ha-NES mutant, followed by immunofluorescent staining and confocal microscopy. As expected, the NES mutant localised predominantly in the nucleus; therefore confirming that the NES sequence of human DDX3 is required for CRM-1 mediated nuclear export (Figure 3.11).

(1)



1 21  
DDX3 MSHVAVENALGLDQQFAGLDL  
NES mutant MSHVAVENVNLNDQQFAGADA

(2)



(3)

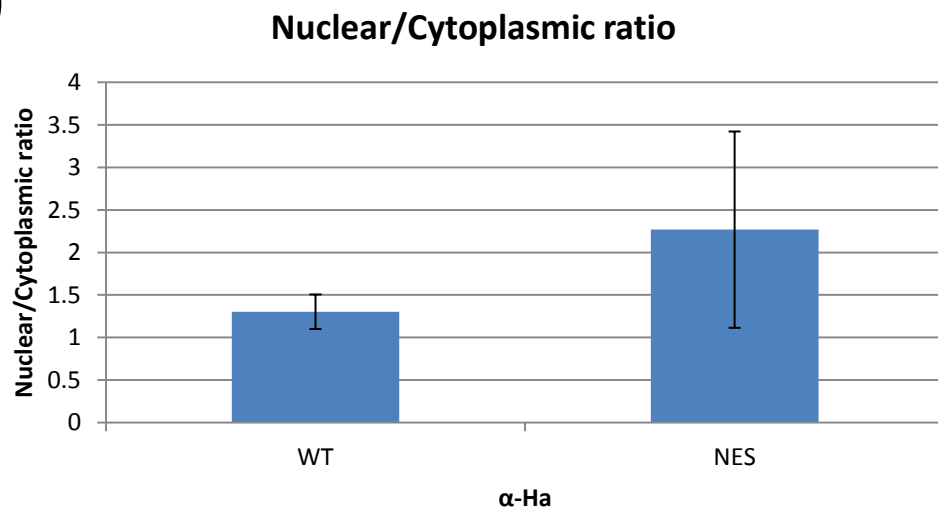


**Figure 3.11: DDX3 NES mutant localises predominantly in the nucleus.**

(1): Schematic representation of NES mutant. (2): HeLa cells were transfected with expression plasmid for Ha-tagged NES mutant, cells were stained with primary  $\alpha$ -Ha and secondary  $\alpha$ -mouse Alexa Fluor-488; as described in Chapter 2. **Key:** A (DAPI), B (Ha-DDX3), C (Merge A+B), D (Contrast).

(3): HeLa cells were transfected with expression plasmids for Ha-tagged DDX3 1-662 and NES mutant. Cells were stained with  $\alpha$ -Ha antibody and  $\alpha$ -mouse Alexa Fluor-488. High content analysis of nuclear/cytoplasmic ratio was carried out using the GE IN Cell analyser as described in Chapter 2.

Mutagenesis of NES regions by substituting the leucines to alanines is reported to disrupt the binding of CRM-1 to the NES (Askjaer 1998; Güttler et al. 2010). A semi-endogenous immunoprecipitation was carried out, to test if Ha-tagged DDX3 WT or mutants interacted with endogenous CRM-1. Briefly, HEK 293Ts cells were transfected with expression plasmids for Ha-tagged constructs, namely for wild type DDX3, the N-terminal deletion mutant 139-662 and the NES mutant, and immunoprecipitation was performed using an  $\alpha$ -CRM-1 antibody (*Novus Biologicals*). Cell lysates were incubated with  $\alpha$ -CRM-1 bound sepharose beads supplemented with recombinant non-hydrolysable RanQ69L-GTP. The RanQ69L-GTP was added to the binding reaction to increase the affinity of CRM-1 for the NES (Güttler et al. 2010). In Figure 3.12, Ha-WT interacted with CRM-1, however the Ha-NES mutant and Ha-139-662 did not interact with CRM-1, suggesting DDX3 can interact with CRM-1 and that the NES region is required for this interaction.

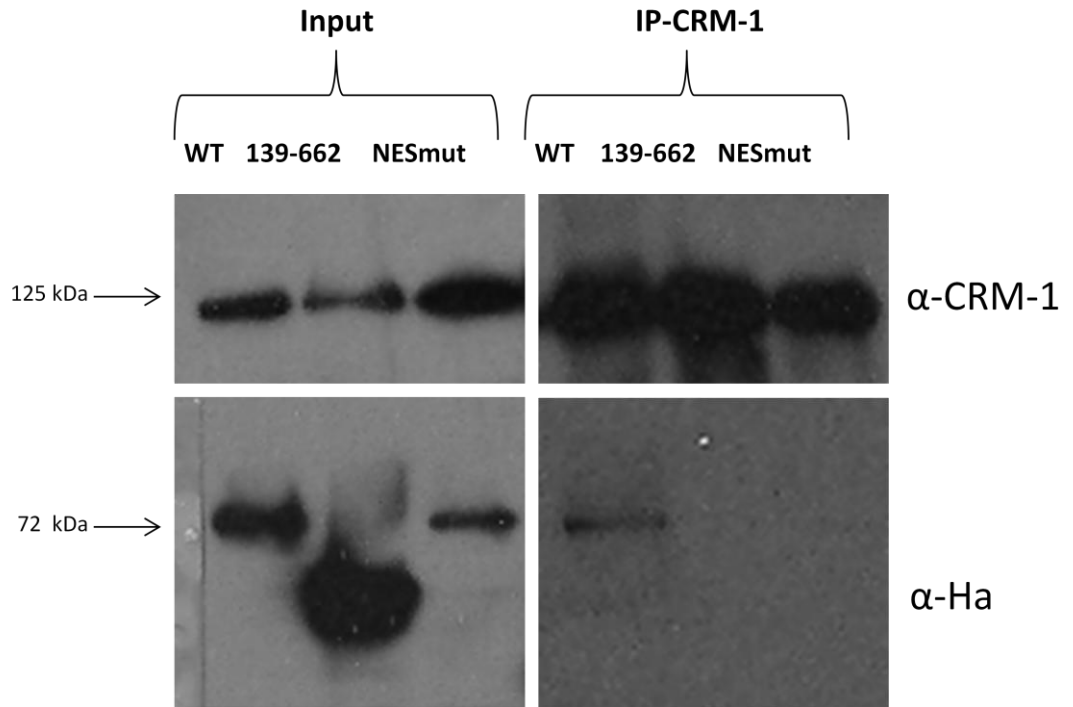


**Figure 3.12: WT DDX3 co-IPs with endogenous CRM-1 stronger than NES mutant and 139-662.** 233ts were transfected with Ha-tagged WT DDX3, NES mutant and 139-662. Protein G sepharose beads (*Sigma*) were incubated with  $\alpha$ -CRM-1 antibody, and blocked with 5% BSA in PBS-tween. Cell lysates were added to beads alongside non-hydrolysable His-RanQ69L-GTP and washed three times in PBS-tween. SDS-PAGE gel electrophoresis and semi-dry transfer was carried out as per materials and methods. Blots were probed with  $\alpha$ -CRM-1 (*NovusBiologicals*) and  $\alpha$ -Ha (*Covance*). Representative blot of two experiments.

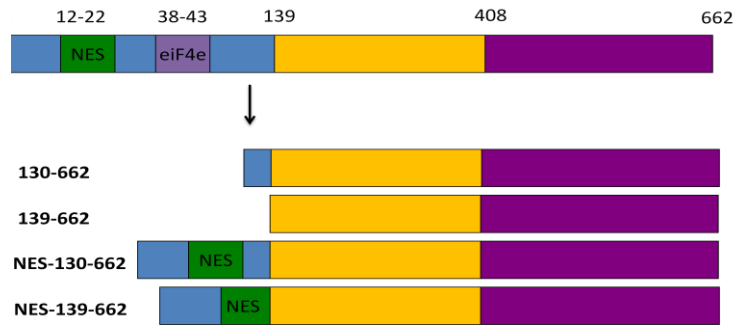
### 3.3.5.2. The NES of DDX3 is sufficient to restore nuclear export of export deficient mutants

---

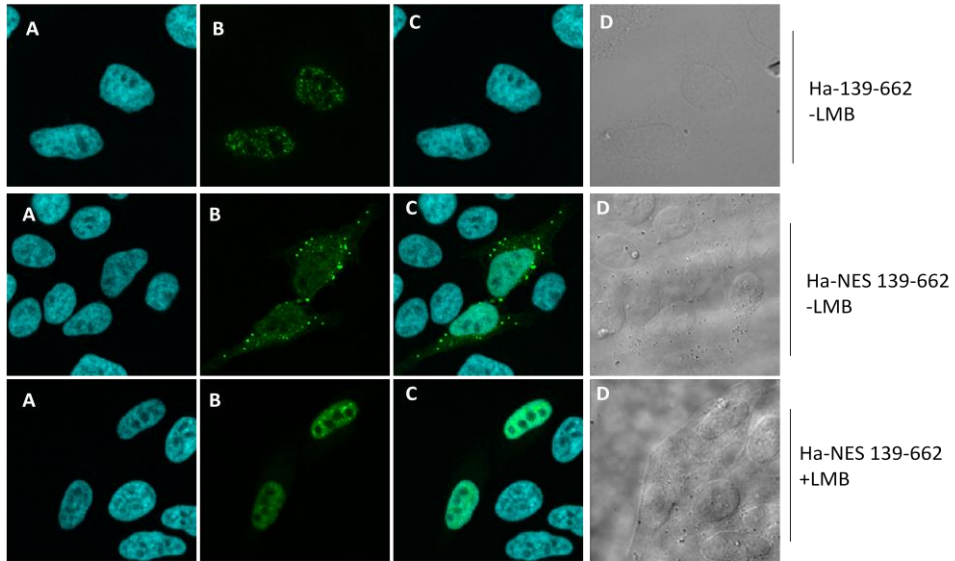
I next investigated whether the NES sequence (12-22 aa) was sufficient to facilitate the export of DDX3 from the nucleus to the cytoplasm, using an approach previously used to characterize the NES of other proteins (Chevalier et al. 2005). To this end, I affixed the 1–22 amino-acid region of DDX3 to the N-terminus of the export- deficient mutants 130-663 and 139-662. The NES-130-662 and NES-139-662 mutants were then overexpressed in HeLa cells, and treated with LMB to test if the NES conferred CRM-1 dependent export (Figure 3.13). The NES-130-662 and NES-139-662 had a cytoplasmic localisation in untreated cells and a nuclear localisation in LMB treated cells.

Therefore, the NES region restored cytoplasmic localisation of the nuclear N-terminal truncation mutants 130-662 and 139-662. This demonstrated that the NES of DDX3 is functional and sufficient to export DDX3, and mediates export of DDX3 in a CRM-1 dependent manner.

(1)



(2)



(3)

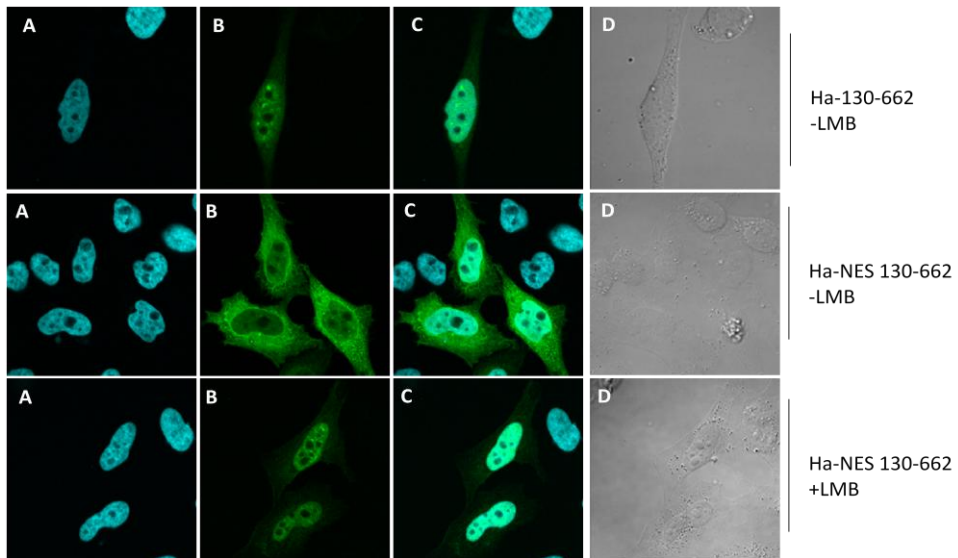


**Figure 3.13: The N-terminal NES (1-22) is sufficient to mediate export of DDX3.**

(1): Schematic depicting NES- N-terminal mutants which were constructed by adding the NES containing region (1-22) onto N-terminal mutants 130-662 and 139-662. (2): HeLa cells were transfected with expression plasmids for Ha-tagged 139-662 or NES 139-662. (3): HeLa cells were transfected with expression plasmids for Ha-tagged 130-662 and NES 130-662 mutants. Cells were treated with 20mM LMB for 2 hours or left untreated. Cells were stained with primary  $\alpha$ -Ha antibody and secondary  $\alpha$ -mouse Alexa Fluor-488. **Key:** A (DAPI), B (Myc-DDX3), C (Merge A+B), D(Contrast).

### 3.4. Discussion

---

DDX3 is known to shuttle between the nucleus and the cytoplasm, with a predominantly cytoplasmic localisation usually being reported (Yedavalli et al. 2004; Sekiguchi et al. 2004). Within the literature there is some confusion as to how DDX3 is exported from the nucleus, with studies concerning human DDX3, hamster DDX3 and *Xenopus* An3 showing conflicting results.

I first tested where DDX3 localised in a range of cell lines, and found that DDX3 had a predominantly cytoplasmic localisation in all cell lines. Human DDX3 has been shown to be exported via two proteins, the main mammalian exportin CRM-1 and the major nuclear mRNA exporter TAP (Yedavalli et al. 2004; Lai et al. 2008). My results showed that DDX3 is exported from the nucleus in a predominantly CRM-1 mediated manner. Treatment of HeLa cells with the CRM-1 inhibitor LMB resulted in nuclear accumulation of both overexpressed and endogenous DDX3 in HeLa cells, shown by confocal microscopy and nuclear cytoplasmic fractionation. The DDX3 *Xenopus laevis* homologue An3 was shown to be exported via CRM-1, with export coupled to helicase activity (Askjaer et al. 2000), hence I investigated if DDX3 export was reduced when helicase activity was abrogated. Using the DDX3 helicase mutant K320E, I found that DDX3 shuttled as normal between the nucleus and the cytoplasm, suggesting that nuclear trafficking of DDX3 was not coupled to helicase activity. The An3 paper showed that the helicase inactive mutant interacted as normal with CRM-1, and they suggested that DDX3 may be involved in RNA processing during the nuclear export process (Askjaer et al. 2000). Why DDX3's export was not affected when helicase activity was abrogated is unclear, maybe there are differences in the ways DDX3 processes RNA compared to An3. To my

knowledge, helicase activity has not been coupled to nuclear export of any other proteins.

I next wanted to narrow down which regions of DDX3 are required for its nuclear export. *Xenopus laevis* An3 and hamster DDX3 have both been shown to export in a CRM-1 dependent manner. Conversely, the highly conserved N-terminal NES was critical for nuclear export in An3, but not in hamster DDX3 (Askjaer et al. 2000; Sekiguchi et al. 2004). A study using human DDX3 showed that the N-terminal NES was not required for CRM-1 binding, and in fact the C-terminus of DDX3 was required for binding (Yedavalli et al. 2004). My study found that the N-terminus NES of DDX3 is required for nuclear export. Mutagenesis of DDX3's NES resulted in nuclear accumulation of DDX3. The NES was also capable of restoring nuclear export to previously export deficient mutants. I also showed that DDX3's N-terminal NES was required for binding to CRM-1. NES-like sequences occur quite often in proteins, however in order to be functional NESs usually occur within N-terminal, C-terminal or unstructured regions of the cargo, as otherwise they are unable to bind to the CRM-1 docking site (Güttler et al. 2010). Since the DDX3's NES is in the N-terminus, interaction with CRM-1 would be feasible. Yedavalli et al., showed that HIV-Rev and CRM-1 utilised DDX3 helicase activity to export partially spliced and unspliced HIV mRNAs, and that the C-terminus of DDX3 directly interacted with CRM-1 in a Ran-independent manner, suggesting that DDX3 was an effector of CRM-1 transport rather than a cargo (Yedavalli et al. 2004). Since HIV-Rev protein and DDX3 both contain functional NESs, how and whether they both simultaneously interact with CRM-1 is unclear. Yedavalli et al. also showed that DDX3 localised to the cytoplasmic side of the NPC, so maybe DDX3 plays a role in

restructuring HIV-1 RNA for nuclear export, or plays a role in disassembly of the REV-RNA-CRM-1 complex.

DDX3 has also been shown to be exported via TAP (Lai et al. 2008). Since there are no commercial inhibitors for TAP, I did not investigate a role for TAP in DDX3 export. My results with the CRM-1 inhibitor LMB would suggest that TAP can only play a minor role in DDX3 export. Also the NES mutant had a strong nuclear localisation confirming that CRM-1 is likely the predominant player in DDX3 export. There might be a role for DDX3 in the export of specific mRNAs through CRM-1 or TAP. It is tempting to think that since CRM-1 has been shown to play a role in the export of immunologically relevant mRNAs (IFN  $\alpha$ -1 mRNA) (Kimura et al. 2004), maybe DDX3 is involved in this process.

In conclusion, DDX3 is exported from the nucleus via CRM-1, and DDX3's N-terminal NES is required and sufficient for CRM-1 mediated nuclear export.

## **Chapter 4 : Investigating the Nuclear import of DDX3**

---

### **4.1. Nuclear import of DEAD box helicases**

---

There is little known about how members of the DEAD-box family of proteins are imported into the nucleus. Since DDX3 must be imported into the nucleus to partake in some of its functions such as regulation of gene promoters, we wanted to understand how DDX3 is mediated. DDX3 is involved in the transcription of proteins involved in a variety of cellular functions, including cell cycle regulation and innate immune signalling (Chao et al. 2006; Botlagunta et al. 2008; Schröder et al. 2008; Soulat et al. 2008).

In the following passages, the current knowledge on how DEAD box family members and DDX3 are imported into the nucleus will be discussed.

#### **4.1.1 RAN Dependent- Importins**

---

The nuclear import of the DEAD-box RNA helicase A/nuclear DNA helicase II (RHA) (also known as DHX9) has been investigated. RHA is a nucleocytoplasmic shuttling protein which is involved in multiple steps of gene expression, having an established role in the transcription of a range of genes (Aratani et al. 2001; Fujii et al. 2001; Myöhänen & Baylin 2001). It has also been found to be part of the spliceosome and is involved in processing of transcripts (Zhou et al. 2002). RHA has also been shown to be involved in viral gene expression, promoting nuclear export of CTE- containing RNA and also HIV-1 RRE-containing RNA (Tang et al. 1997; Li et al. 1999).

A study investigating the nuclear import of RHA showed that the C-terminus contained a nuclear transport domain (Nichols et al. 2000). A further study characterised a 19 amino acid NLS within the C-terminus, which had no consensus

with other known NLSs such as the classical monopartite NLS, bipartite NLS or M9 of hnRNP A1. The RHA NLS was nonetheless imported via the classical Importin- $\alpha/\beta$  nuclear import pathway, interacting with Importin-  $\alpha$  1 and importin-  $\alpha$  3 (Aratani et al. 2006).

The nuclear import of another member of the DEAD-Box family member, DDX5 (also known as p68), has also been investigated. DDX5 is involved in various stages of gene expression, and is highly related to DDX17 (also known as p72), sharing 92% sequence similarity over their central helicase domains (Lamm 1996). DDX5 has been reported to regulate transcription of a range of genes, in particular oestrogen receptor- $\alpha$  (ER- $\alpha$ ) and p53-dependent genes (Fuller-Pace & Ali 2008; Endoh et al. 1999; Bates et al. 2005). DDX5 is a nucleocytoplasmic shuttling protein, with a predominately nuclear localisation. DDX5 has been shown to shuttle between the nucleus and the cytoplasm in a Ran dependent manner, and two functional classical NLSs and two functional NESs were characterised (Wang, Gao, et al. 2009). The two functional NLSs were found within the helicase core domain and the C-terminus, and the two NESs were also found within the helicase core domain and the C-terminus.

There has been no research published on how DDX3 is imported into the nucleus.

#### 4.1.2 RAN Dependent-Transportins

As stated previously, Transportin has been associated with the nuclear import of a range of mRNA processing proteins (Güttinger et al. 2004; Truant 1999). DDX3 was found to interact with Transportin by tandem Mass Spectrometry (MS) (Güttinger et al. 2004). However, another research group could not show direct

binding of DDX3 to Transportin, and analysis of the DDX3 protein sequence showed that DDX3 does not contain the PY-NLS motif which is required for transportin binding (Lee et al. 2006).

#### 4.1.3. RAN Independent-Calmodulin

The Calmodulin import pathway has been suggested to be an evolutionary conserved pathway, involved in nuclear transport of a small set of proteins in a  $\text{Ca}^{2+}$ -dependent manner (Sweitzer & Hanover 1996; Hanover et al. 2009). DEAD-box family members have been identified as calmodulin binding proteins, such as DDX3, DDX1, DDX5, DDX11, DDX21, DDX47, DDX49 and DDX57 (Shen et al. 2005; Jang et al. 2007). DDX1 was shown to interact with calmodulin in a  $\text{Ca}^{2+}$  dependent but phosphorylation independent manner, whereas DDX5 interacted in a  $\text{Ca}^{2+}$ -independent and phosphorylation-independent manner (Jang et al. 2007). DDX3 has been shown to bind to calmodulin in a  $\text{Ca}^{2+}$ -independent but phosphorylation-dependent manner (Jang et al. 2007), however whether DDX3 or other DEAD-box proteins can be imported via the Calmodulin pathway has not been investigated.

#### 4.1.4. Inhibitors of nuclear import

Recently nuclear inhibitor proteins became available, which will be discussed in the following sections.

##### 4.1.4.1. Importin $\alpha/\beta$ inhibitors

Recently Kosugi *et al.* described peptide inhibitors that inhibited nuclear import. These peptide inhibitors called Bimax 1 and Bimax 2 bind to importin- $\alpha$  in the absence of importin- $\beta$  and prevent cargo release into nucleus (Kosugi et al. 2008). Structural interaction analysis also confirmed their interaction with importin- $\alpha$  (Marfori et al. 2012). Bimax 1/2 inhibited the importin- $\alpha/\beta$  pathway specifically,

with the importin- $\beta$  cargo Snail being imported normally in the presence of Bimax 1/2.

Bimax 1/2 caused an increased nuclear localisation of importin- $\alpha$ , suggested to occur due to their inhibition of cargo release, thus preventing importin- $\alpha$  from recycling to the nucleus. This prevents further import of cNLS containing proteins because of the unavailability of importin- $\alpha$  in the cytoplasm.

#### 4.1.4.2. Importazole (IPZ) small molecule inhibitor

Also recently, a small molecule inhibitor of nuclear import was described, called Importazole (IPZ). IPZ bound importin  $\beta$  *in vitro* and disrupted importin- $\beta$ /RanGTP mediated nuclear import (Soderholm et al. 2011). IPZ reversibly blocked importin- $\beta$  mediated nuclear import, and had no effect on transportin mediated nuclear import. IPZ did not have any effect on CRM-1 mediated export showing that IPZ does not inhibit all karyopherins, and also that RanGTP levels were not affected, because CRM-1 requires Ran-GTP to export proteins (Soderholm et al. 2011).

#### 4.1.4.3. Calmodulin Inhibitors

Calmodulin inhibitors have been described to inhibit the nuclear import of proteins which are imported via the calmodulin/ $\text{Ca}^{2+}$  pathway. Calmodulin inhibitors, such as W13, have been shown to alter the cellular localisation of various proteins, including the cell cycle regulators p21<sup>Cip1</sup> (Taulés et al. 1999) , Cdk4 and Cyclin D1 (Taulés et al. 1998).

## 4.2. Aims

---

In this chapter, I investigated how DDX3 is imported into the nucleus. We characterised the regions of DDX3 required for nuclear import and investigated the functionality of putative NLSs found within DDX3. I used nuclear import inhibitors to attempt to specify what nuclear import factors DDX3 utilises to be imported into the nucleus.

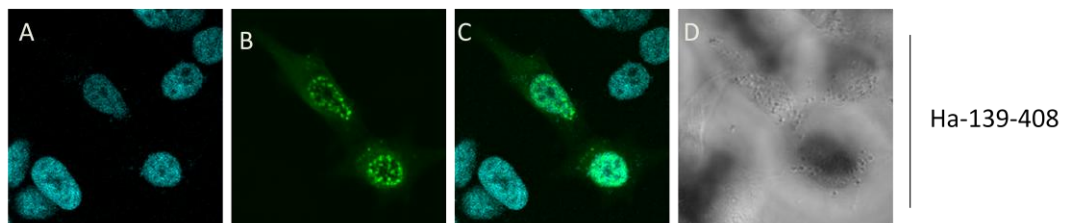
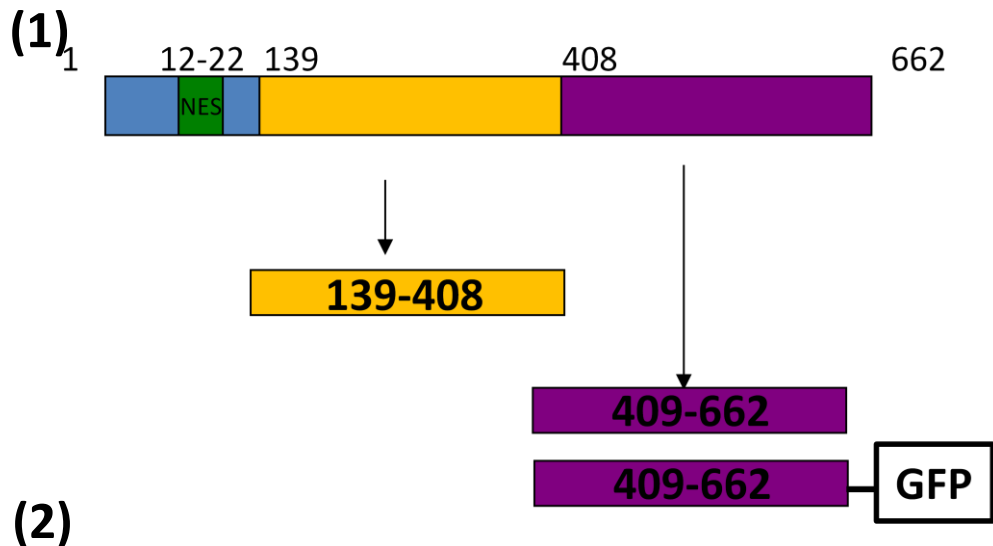
## 4.3. Results

---

### 4.3.1. DDX3 contains two globular RecA-like domains which are imported into the nucleus independently

---

To define the regions of DDX3 that contribute to nuclear import, I first tested N-terminal and C-terminal truncation mutants of DDX3. N-terminal truncations lack the functional NES and therefore have lost the ability to export from the nucleus, (Chapter 3). HeLa cells were transfected with expression plasmids for Ha-tagged 139-408 and 409-662 DDX3, followed by immunofluorescent staining and confocal microscopy. The 139-408 and 409-662 both accumulated in the nucleus, suggesting that nuclear import was facilitated by these two independent regions (Figure 3. A and B). Since these mutants are quite small, approximately 27 kDa, I wondered if the overexpressed protein was passively diffusing into the nucleus. I decided to increase the size of the truncation mutants by sub-cloning them into a vector generating fusion protein with Green Fluorescent Protein (GFP). GFP is approximately 27 kDa, therefore the 409-662-DDX3-GFP is approximately 50kDa. Proteins greater than 40kDa cannot passively diffuse through the nuclear pore (La Cour et al. 2004). I found that the 409-662 GFP mutant also localised to the nucleus, showing that import was indeed facilitated independently by the C-terminus of DDX3 (Figure 4.1). I also cloned other GFP-tagged truncation mutants however even though sequencing showed cloning was successful no GFP protein was detected when plasmids were transfected into HeLa cells suggesting a problem with plasmid expression.



**(3)**

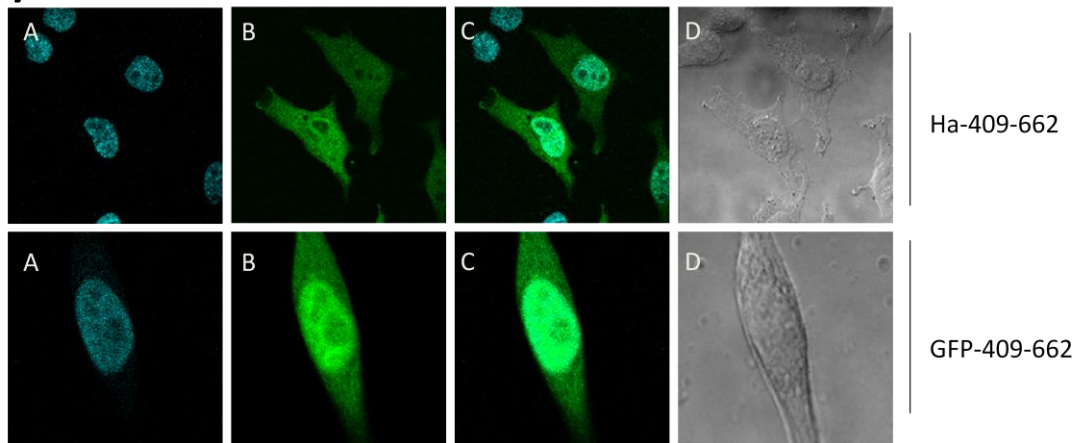


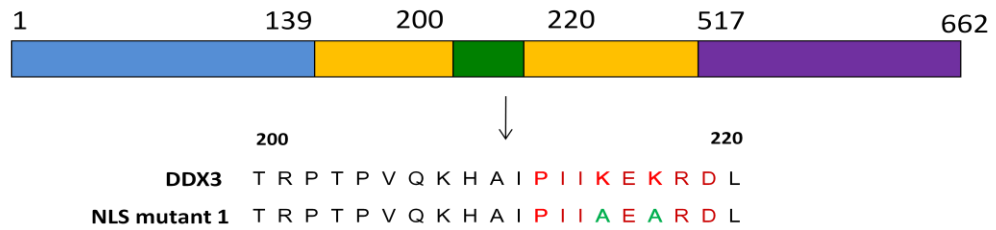
**Figure 4.1: The DDX3 truncation mutants 139-408 and 409-662 are imported independently into the nucleus, suggesting two distinct regions facilitate nuclear import of DDX3.**

**(1):** A schematic depicting 139-408 and 409-662 truncation mutants (not drawn to scale). **(2):** HeLa cells were transfected with expression plasmid for Ha-tagged 139-408. **(3):** HeLa cells were transfected with expression plasmids for Ha-tagged 409-662 or GFP-tagged 409-662. HeLa cells expressing Ha-tagged constructs were stained with a primary  $\alpha$ -Ha and secondary  $\alpha$ -mouse Alexa Fluor-488 antibody. HeLa cells expressing GFP tagged constructs were not stained. **Key:**A (DAPI), B ( $\alpha$ -Ha or GFP), C (Merge A+B), D (Contrast).

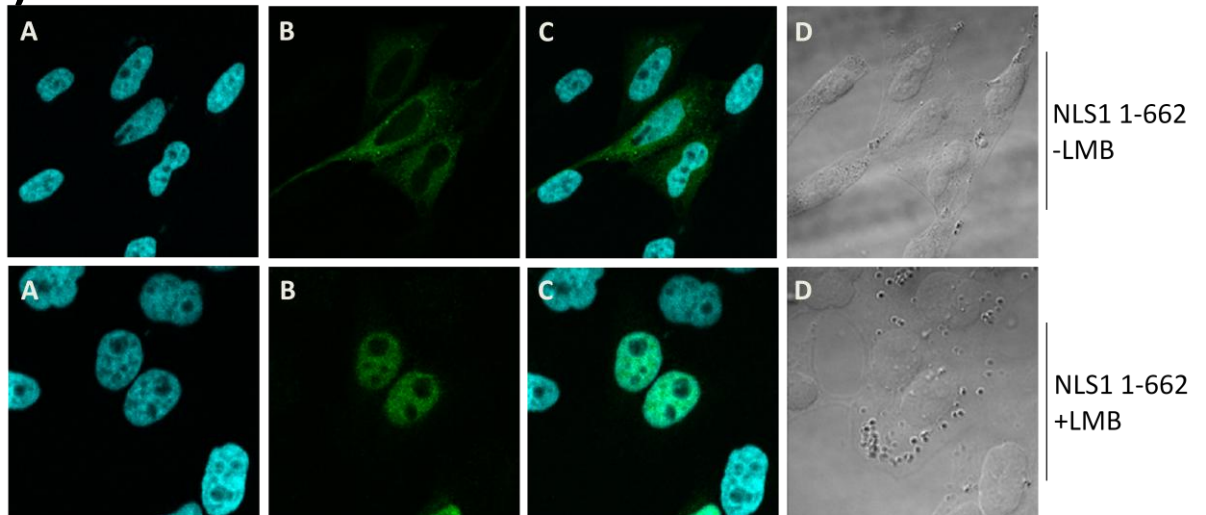
#### 4.3.2. Putative NLS found using predication software

I decided to use available software to identify putative NLS regions in DDX3. The software PSORT II can be used to identify classical NLS sequences in proteins (Horton & Nakai 1997). PSORT II identified a putative NLS between amino acids 211 and 219 of DDX3, which was within the region 139-408 that can import independently. Using site directed mutagenesis we mutated two hydrophobic residues to alanines, namely the lysines at positions 215 and 217. This "NLS-1" mutation was in generated in full length DDX3 (NLS1- 1-662) and C-terminal truncation 1-408 (NLS1-1-408). HeLa cells were transfected with expression plasmids for Ha-tagged NLS1-1-662 and NLS1-1-408 mutant, and treated with LMB or left untreated. HeLa cells were stained for immunofluorescence followed by confocal microscopy. The NLS1-1-662 and NLS1-1-408 were cytoplasmic in untreated cells and nuclear in LMB treated cells, suggesting that nuclear import was not affected by the mutation (Figure 4.2).

(1)



(2)



(3)

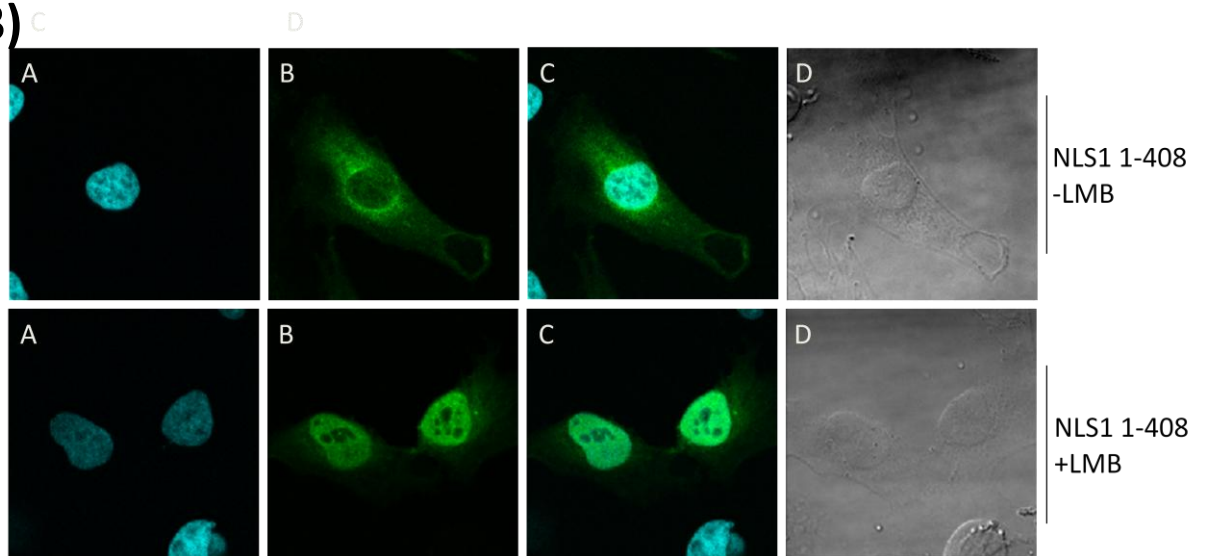


**Figure 4.2: Mutation of putative NLS predicted by PSORTII did not disrupt nuclear import.**

(1): A schematic depicting the NLS-1 mutation in both full length and C-terminal DDX3 (not drawn to scale). (2): HeLa cells were transfected with an expression plasmid for Ha-tagged NSL 1-662 and treated with 20mM LMB for 2 hours or left untreated. (3): HeLa cells were transfected with an expression plasmid for Ha-tagged NSL 1-408 and treated with 20mm LMB for 2 hours or left untreated. HeLa cells were stained with a primary  $\alpha$ -Ha and secondary  $\alpha$ -mouse Alexa Fluor-488. Key: A (DAPI), B (Ha-DDX3 ),C (Merge A+B), D (Contrast).

I next used a new software, Nuclmport which was suggested to identify NLS better than previously published software (Mehdi et al. 2011). Nuclmport identified a putative NLS at amino acids 259-264, which is located in an exposed loop in the protein structure of DDX3 (Figure 4.3).

(1)

Nuclmport Results on DDX3X		Comments
Probability of Import	0.98	
Probability of NLS	0.18	
Predicted Class1	255- KENGRY <b>GRRK</b> QYPISLVLAP	Probability being Class1 =0.16
Predicted Class2	89- GSGSRG <b>RFDDRGR</b> SDYDGIG	Probability being Class2 =0.47
Predicted Class4	253- AMKENGRY <b>GRRK</b> QYPISLVL	Probability being Class4=0.03
Predicted Class6	64- <b>KDK</b> DAYSSFGSRSDSR <b>GKSS</b>	Probability being Class6 =0.02
Interaction with Imp-alpha	Yes	Indirect Interaction
Interaction with Imp-beta	Yes	Indirect Interaction
Interaction with Ran	Yes	Indirect Interaction

(2)



**Figure 4.3: Nuclmport was used to identify other putative NLS regions in DDX3.**

(1): Another putative NLS sequence in DDX3 was found using Nuclmport, which applies a different algorithm to test for NLS sequence in proteins than PSORTII. (2): The predicted class 1 NLS at aa 259-263 of DDX3 is in an exposed loop, shown here using Pymol.

I first mutated two arginine residues 259 and 260 to alanines in the C-terminal truncation mutant 1-408 (NLS2-1). Further mutagenesis to the putative NLS was carried out with a total of four amino acids changed to alanines (NLS2-2), (Figure 4.4). HeLa cells overexpressing expression plasmids for Ha-tagged NLS2-1 and NLS2-2 were treated with LMB. NLS2-1 and NLS2-2 were cytoplasmic in untreated cells and nuclear in cells treated with LMB (Figure 4.4).

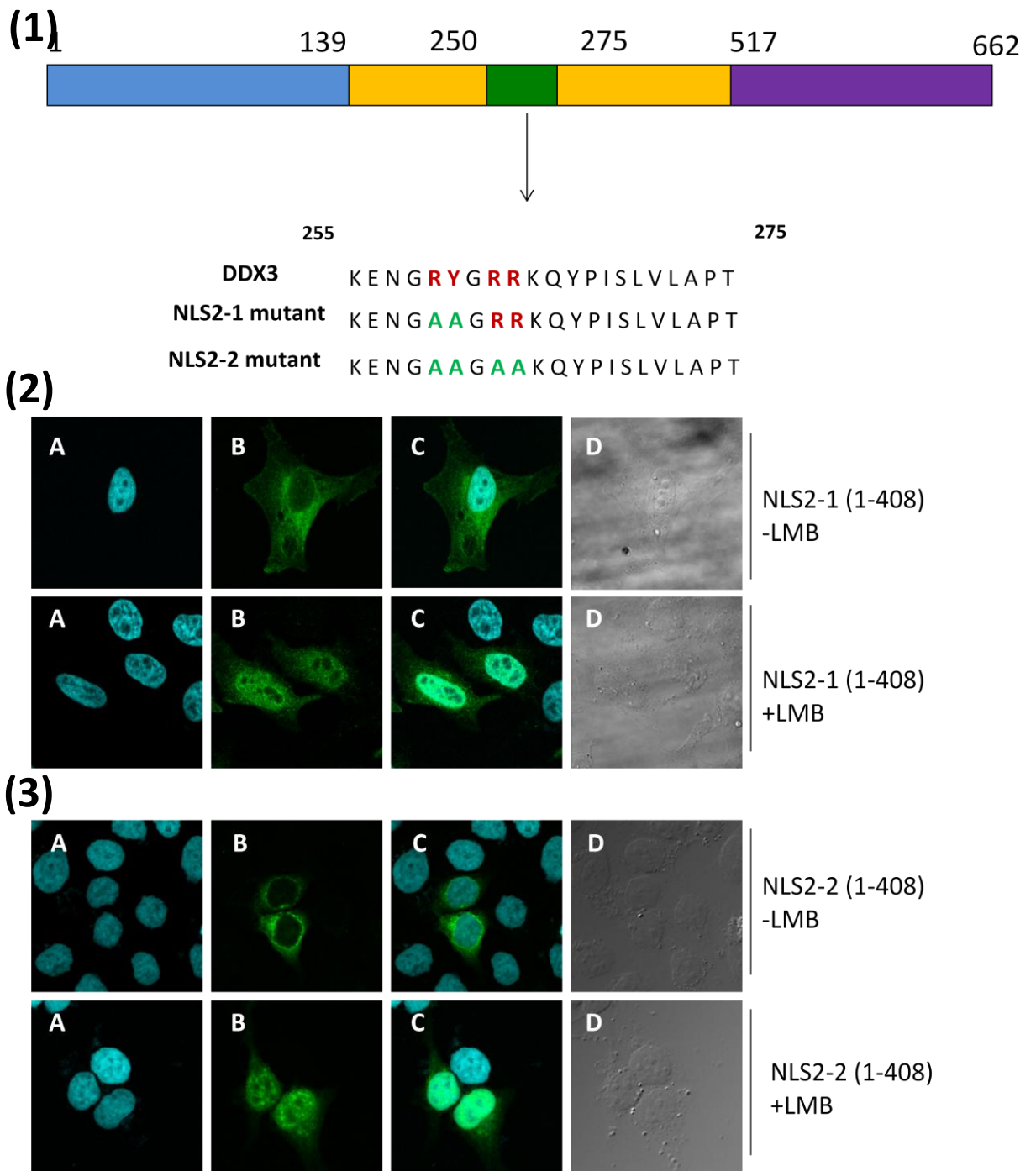
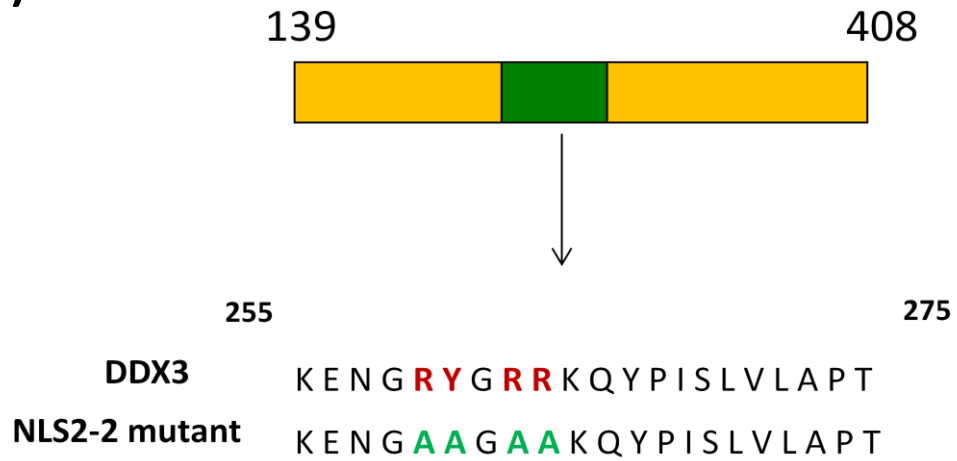


**Figure 4.4: Mutation to putative NLS predicted by NuclImport did not disrupt nuclear import of DDX3.**

**(1):** A putative NLS sequence was found using NuclImport; two mutants were designed to mutate two and four key residues to alanine in C-terminal truncation (1-408). **(2):** HeLa cells were transfected with expression plasmids for Ha-tagged NLS2-1 (1-408) and treated with 20mM LMB for 2 hours or left untreated. **(3):** HeLa cells were transfected with expression plasmids for Ha-tagged NLS2-2 (1-408) and treated with 20mM LMB for 2 hours or left untreated. HeLa cells were stained with a primary  $\alpha$ -Ha and secondary  $\alpha$ -mouse Alexa Fluor-488. **Key:** A (DAPI), B (Ha-DDX3), C (Merge A+B), D (Contrast).

I then thought that the N-terminus might have some role in nuclear import since the NLS predictor software NuclImport predicted a putative NLS in the N-terminus of DDX3 (Figure 4.5). I decided to create an NLS2-2 mutant which had both the N-terminus and C-terminus truncated, NLS2-2 139-408. As earlier stated, truncation of the N-terminus prevents nuclear export of DDX3 from the nucleus. The 139-408 mutant localised to the nucleus and cytoplasm, as did the NLS2-2 139-408 mutant in HeLa cells (Figure 4.5). However NLS2-2 139-408 mutant localised less to the nucleus, suggesting that nuclear import was impaired but not completely hindered. This would suggest that the NLS identified by NuclImport software plays a role in nuclear import of DDX3, however DDX3's N-terminus also plays a role in nuclear import. All together, evidence would suggest that the putative NLSs identified by NuclImport software are not critical for DDX3's nuclear import.

(1)



(2)

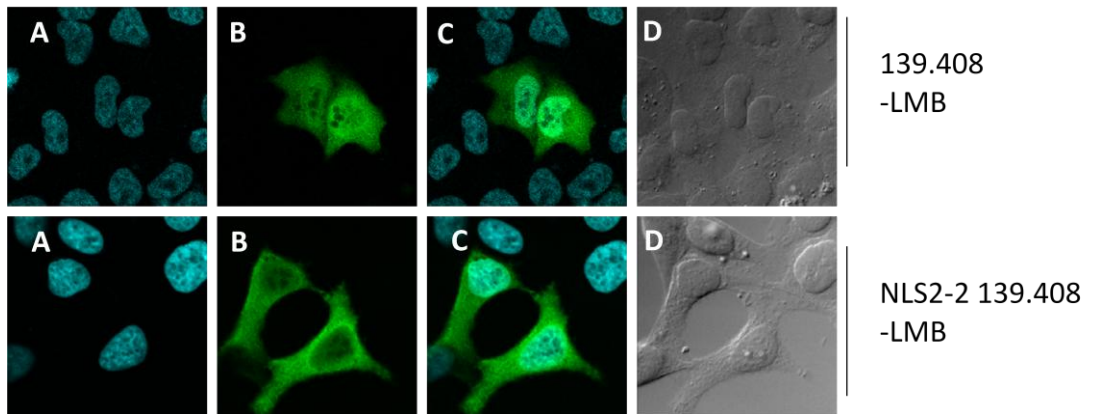


**Figure 4.5: Mutation to putative NLS predicted by NuclImport did disrupt nuclear import of 139-408 mutant.**

(1): A putative NLS sequence was found using NuclImport; site mutants of four key residues to alanine in a N-terminal and C-terminal truncation (139-408). (2): HeLa cells were transfected with expression plasmids for Ha-tagged 139-408 and NSL2.2 139-408. HeLa cells were stained with a primary  $\alpha$ -ha and secondary  $\alpha$ -mouse Alexa Fluor-488. **Key:** A (DAPI), B (Ha-DDX3), C (Merge A+B), D (Contrast).

### 3.3.3. Investigating the nuclear import of DDX3 using import inhibitors

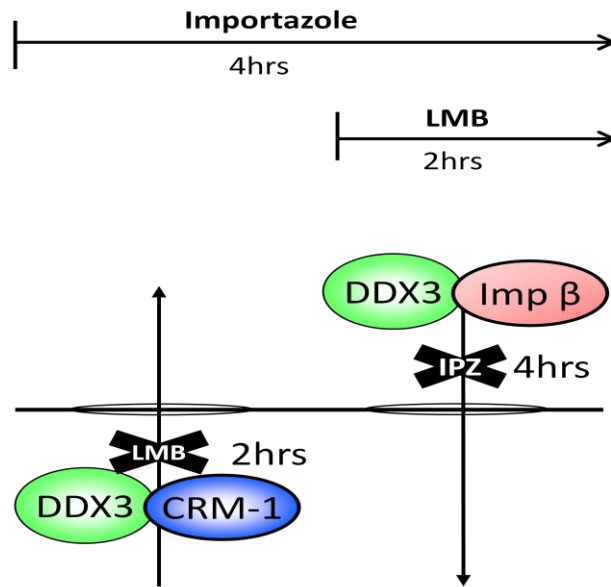
Since mutagenesis of the putative NLSs of DDX3 failed to inhibit import, I decided to try a different approach to investigate the nuclear import of DDX3. A range of nuclear import inhibitors have been described in the literature (Taulés et al. 1999; Soderholm et al. 2011; Kosugi et al. 2008), so I decided to test whether these inhibitors could affect DDX3 import.

#### 4.3.3.1. Importazole does not inhibit the import of DDX3

Importazole (IPZ) is a cell-permeable diaminoquinazoline compound that has been shown to specifically target the transport receptor importin- $\beta$  and disrupt its interaction with RanGTP. IPZ reversibly blocks importin- $\beta$  (NLS)-mediated nuclear import without affecting transportin M9-mediated nuclear import and CRM1-mediated nuclear export (Soderholm et al. 2011).

First, I tested whether IPZ inhibited the import of endogenous DDX3. Since DDX3 has a predominantly cytoplasmic localisation, it is difficult to test if import is being inhibited. Treating the cells with nuclear export inhibitor LMB and IPZ, allowed us to test if import has been affected. IPZ was added to cells for 4 hours, followed by LMB treatment for 2 hours (Figure 4.6). If DDX3 was prevented from being imported into the nucleus, LMB treatment would not result in nuclear accumulation of DDX3. I found that IPZ did not inhibit the import of endogenous DDX3, as DDX3 accumulated in the nucleus in cells treated with IPZ and LMB (Figure 4.6).

(1)



(2)

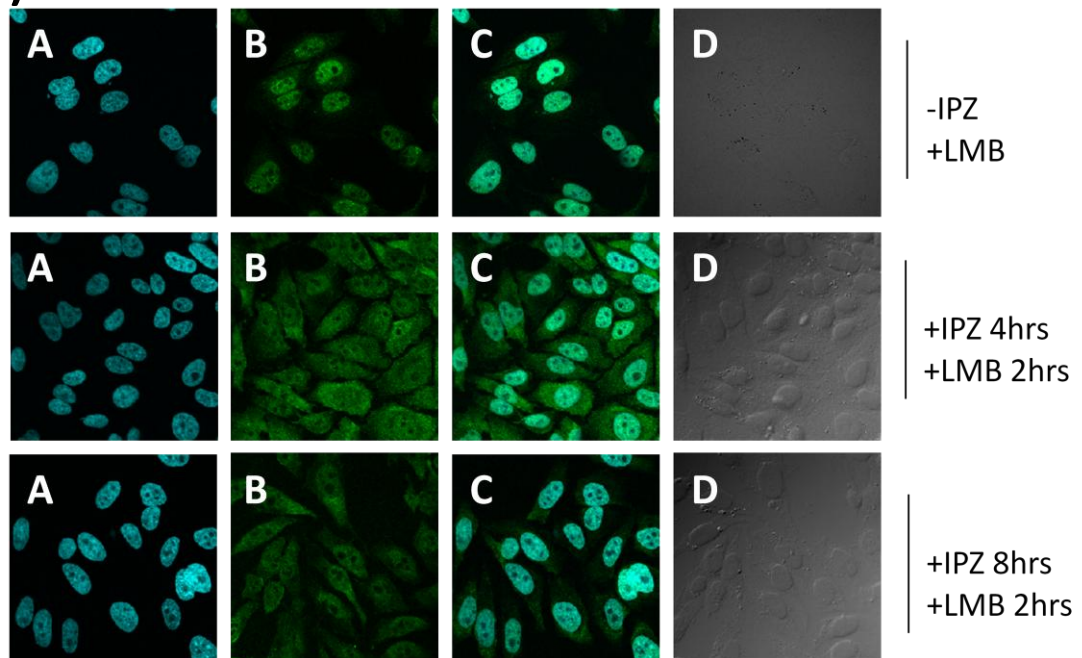


**Figure 4.6: Nuclear import of endogenous DDX3 is not affected by the Importin  $\beta$  inhibitor Importazole (IPZ).**

(1): Schematic showing that if DDX3 imports via Importin  $\beta$ , IPZ treatment for 4 Hrs followed by 2 hrs LMB treatment would result in nuclear accumulation of DDX3. (2): HeLa cells were treated with 40 $\mu$ M IPZ for 4/8 hours and treated with 20mM LMB for 2 hours Cells were stained with a primary  $\alpha$ -DDX3 and secondary  $\alpha$ -rabbit Alexa Fluor-488. **Key:** A (DAPI), B ( $\alpha$ -DDX3), C (Merge A+B), D (Contrast).

Since I have shown that the different domains of DDX3 can be imported independently, I then tested these domains separately with IPZ treatment. HeLa cells were transfected with expression plasmids for Ha-tagged 139-408, 409-662 or 1-408 and treated with IPZ for 4 hours. The 1-408 mutant was also treated with LMB to inhibit export, while the export-deficient 139-408 and 409-662 mutants did not require LMB treatment. HIV-Rev protein was used as a positive control for IPZ, since HIV-rev can be imported via importin- $\beta$  (Henderson & Percipalle 1997). As shown in Figure 4.7, IPZ treatment did not inhibit import of 139-408 and 409-662, with both mutants having a nuclear localisation despite IPZ treatment. The 1-408 mutant had a nuclear localisation after treatment with IPZ and LMB, meaning that its import also was not blocked by IPZ. The control protein HIV-rev was more cytoplasmic in cell treated with IPZ, showing that the IPZ treatment was able to inhibit Importin- $\beta$  mediated import under the conditions used.

In conclusion, I found that IPZ failed to inhibit import of DDX3, suggesting that DDX3 is imported in an importin- $\beta$  independent manner.

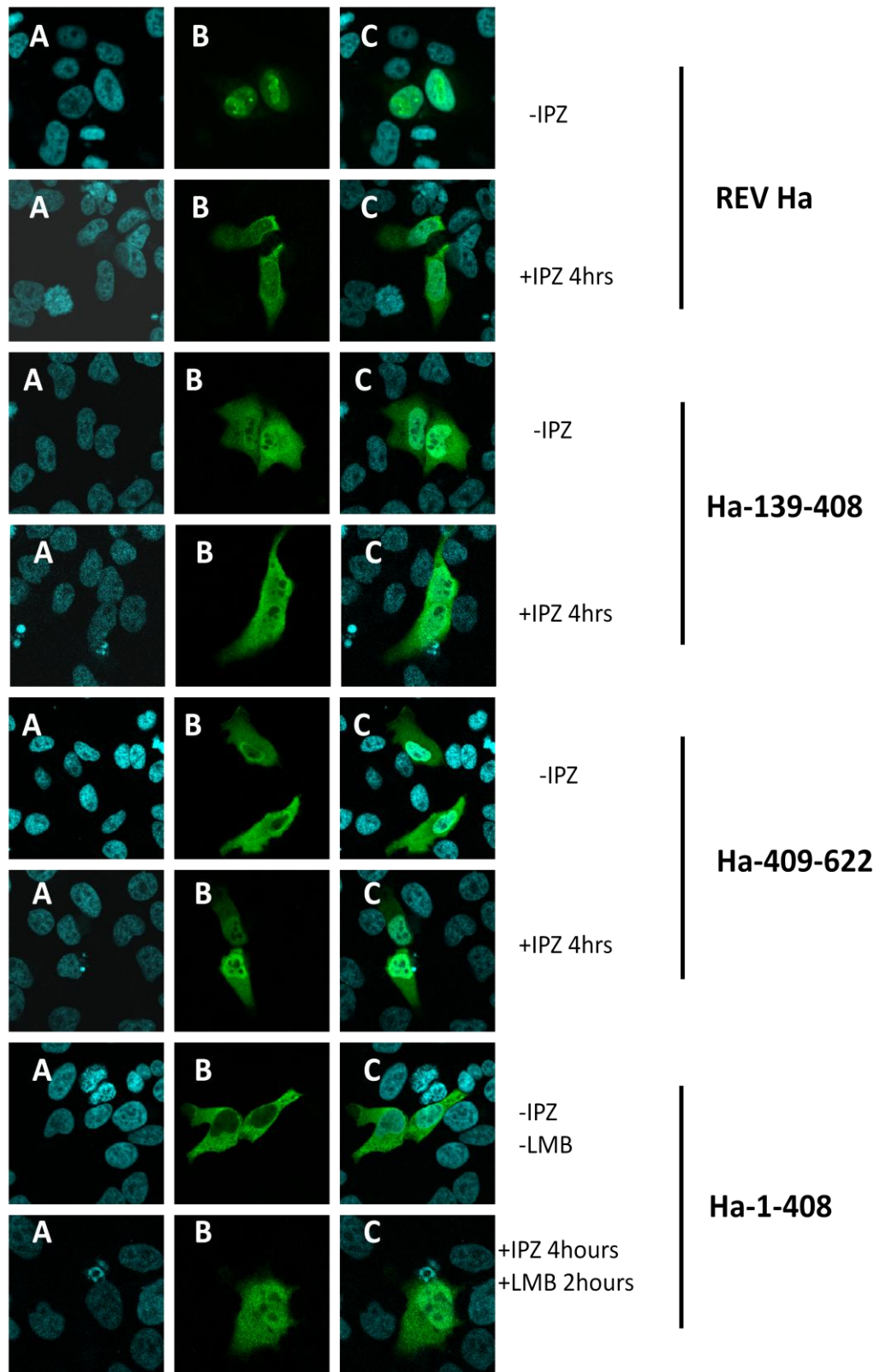


**Figure 4.7: Nuclear import of DDX3 truncations is not affected by the Importin- $\beta$  inhibitor Importazole (IPZ).**

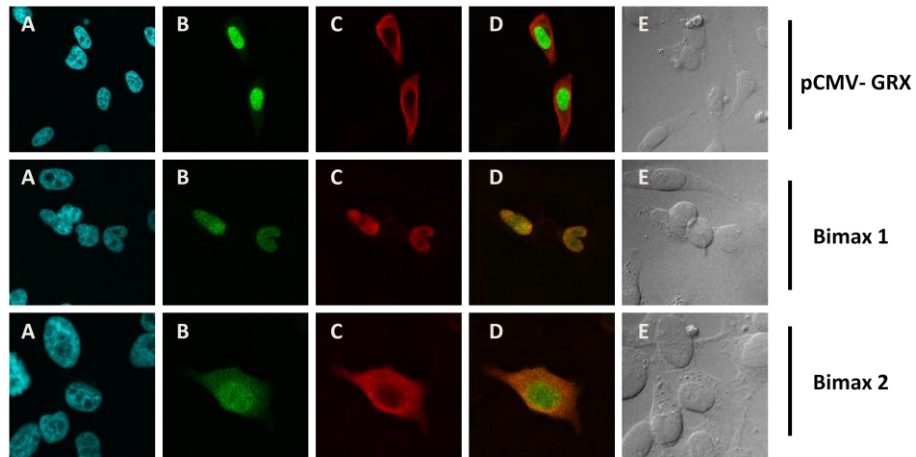
HeLa cells were transfected with expression plasmids for Ha-tagged Rev, or DDX3 truncation mutants. HeLa cells expressing Rev, 139-408, 409-662 were treated with 40 $\mu$ M IPZ for 4 hours. HeLa cells expressing plasmids for 1-408 were treated with 40 $\mu$ M IPZ for 4 hours and with 20mM LMB for 2 hours. Cells were stained with a primary  $\alpha$ -Ha and secondary  $\alpha$ -mouse Alexa Fluor-488. **Key:** A (DAPI), B ( $\alpha$ -Ha), C (Merge A+B), D (Contrast).

#### 4.3.3.2. Bimax inhibitors do not inhibit nuclear import of DDX3

Bimax inhibitors are peptide inhibitors designed to bind importin- $\alpha$ . Overexpression of Bimax inhibitors antagonizes the importin- $\alpha$  cargo release mechanism, resulting in nuclear accumulation of importin- $\alpha$  and importin- $\beta$ . The exclusion of importin- $\beta$  from the cytoplasm results in inhibited importin- $\beta$  mediated nuclear import (Kosugi et al. 2008).

I tested if nuclear import of DDX3 could be inhibited by Bimax inhibitors. To this end, HeLa cells were transfected with expression plasmids for flag-tagged Bimax 1, Bimax 2 or Control vector PCV-GRX, alongside the SV40NLS-GFP as a control. As before, since DDX3 is normally localised in the cytoplasm, to assess if import was inhibited we treated the cells with LMB, blocking the nuclear export of DDX3. If import has been inhibited, treatment with LMB should not result in nuclear accumulation of DDX3. HeLa cells were fixed and stained for immunofluorescent confocal microscopy. As shown in Figure 4.8, overexpression of Bimax-2 resulted in an increase of cytoplasmic SV40NLS-GFP, suggesting that the inhibitor was working. After treatment with LMB, DDX3 localised to the nucleus in cells expressing plasmids for Bimax 1, Bimax2 and pCMV-GRX. In conclusion, Bimax inhibitors did not inhibit the import of DDX3.

(1)



(2)

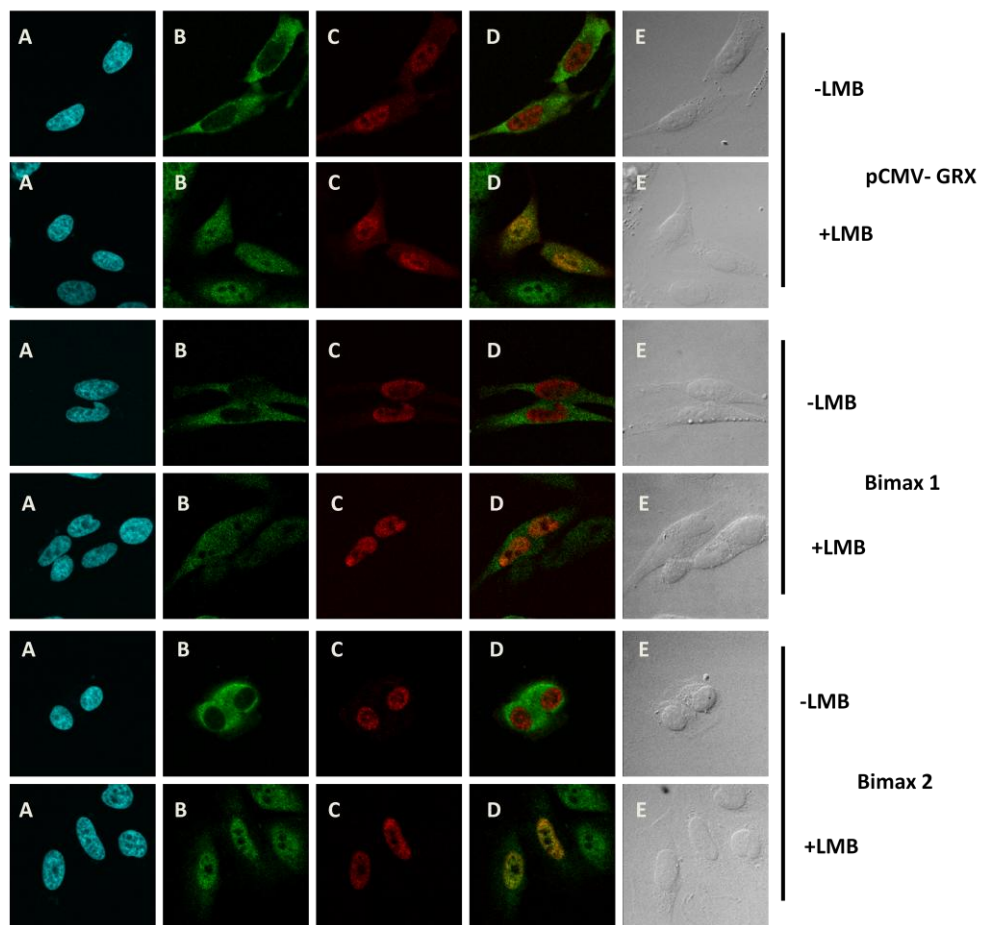


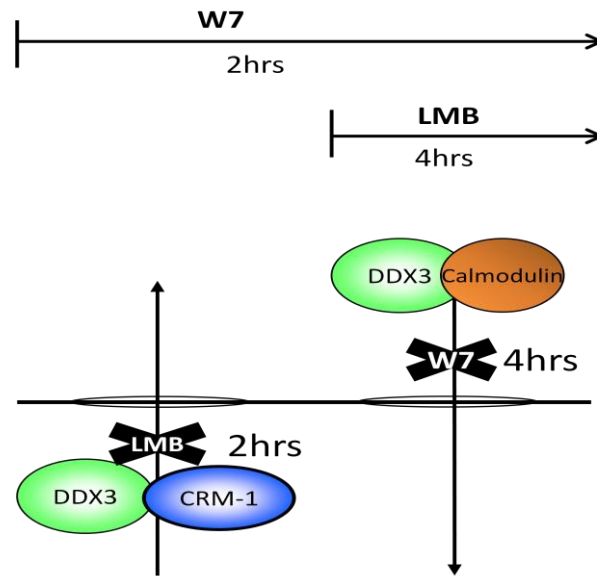
**Figure 4.8: Nuclear import of DDX3 is not inhibited by the Importin  $\beta$  inhibitors Bimax 1 or Bimax 2.**

**(1):** HeLa cells were transfected with expression plasmids for flag-tagged pCMV-GRX, Bimax 1 and Bimax 2, and gfp-tagged SV40-NLS. Cells were stained with a primary  $\alpha$ -flag and secondary  $\alpha$ -mouse Alexa Fluor-594. **(2):** HeLa cells were transfected with expression plasmids for flag-tagged pCMV-GRX, Bimax 1 and Bimax 2. Cells were stained with a primary  $\alpha$ -DDX3 and secondary  $\alpha$ -rabbit Alexa Fluor-488, and a primary  $\alpha$ -flag and secondary  $\alpha$ -mouse Alexa Fluor-594. **Key:** A (DAPI), B ( $\alpha$ -DDX3), C (Merge A+B), D (Contrast).

#### 4.3.3.3. Calmodulin inhibitors do not inhibit nuclear import of DDX3

Since my results suggested DDX3 is imported into the nucleus in an importin- $\beta$  independent manner, I next decided to investigate the Calmodulin/ $\text{Ca}^{2+}$  nuclear import pathway. Calmodulin inhibitor W7 (*Sigma*) has been shown to inhibit nuclear import of proteins that utilise the calmodulin/ $\text{Ca}^{2+}$  nuclear import pathway, such as P21 (Taulés et al. 1999). Here I used P21 as a control. HeLa cells were transfected with expression plasmids for Ha-tagged DDX3 and P21, followed by treatment with W7. As before, LMB was also added to prevent export of DDX3. If import was inhibited, treatment with LMB should not result in nuclear accumulation of DDX3. As shown in Figure 4.9, DDX3 localised to the nucleus after treatment with W7 and LMB, suggesting that the inhibitor had no effect on DDX3 nuclear import.

(1)



(2)

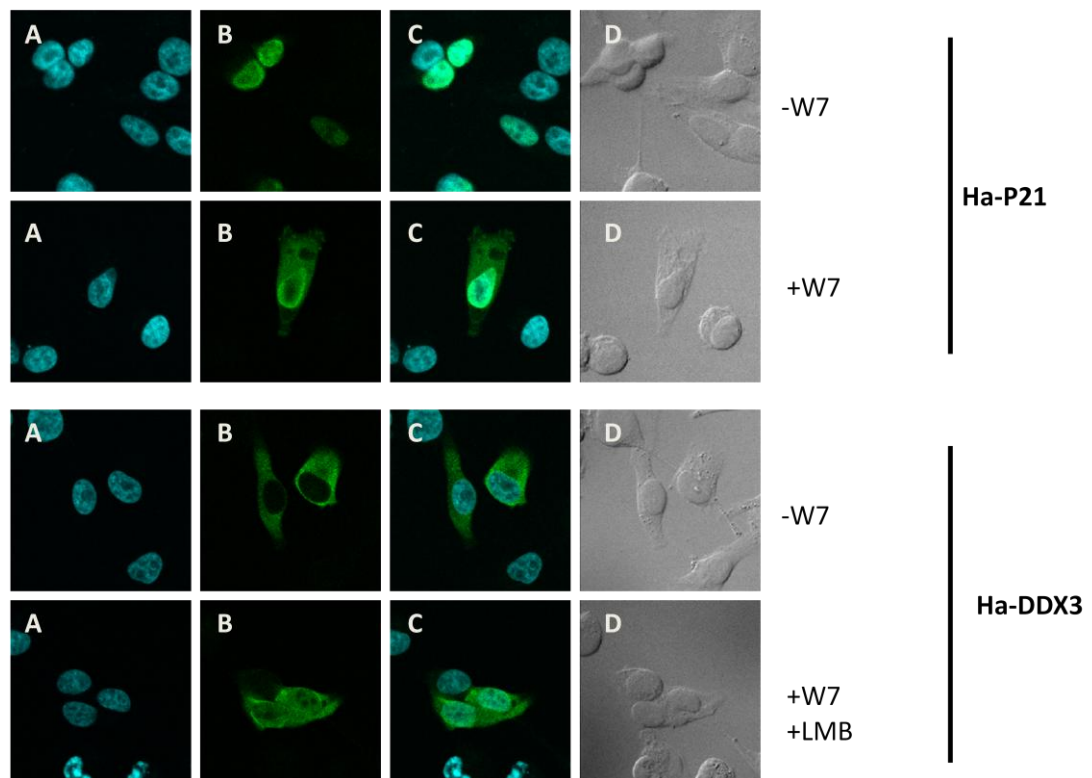


**Figure 4.9: Nuclear import of DDX3 is not affected by the Calmodulin inhibitor W7.**

(1): Schematic showing that if DDX3 imports via calmodulin, W7 treatment for 4 Hrs followed by 2 hrs LMB treatment would result in nuclear accumulation of DDX3. (2): HeLa cells were transfected with Ha-tagged DDX3 and P21 followed by treatment with 30 $\mu$ g/ml W7 for 4 hours. Cells transfected with Ha-DDX3 were also treated with 20mM LMB for 2 hours. Cells were stained with a primary  $\alpha$ -Ha and secondary  $\alpha$ -mouse Alexa Fluor-488. **Key:** A (DAPI), B (Ha-DDX3), C (Merge A+B), D (Contrast).

### 4.3. Discussion

---

DDX3 normally has a cytoplasmic localisation, however it is constantly shuttling in and out of the nucleus. There have been no studies published about the regulation of DDX3s nuclear import, hence we decided to investigate how DDX3 is imported into the nucleus.

I found that the two globular RecA-like domains of DDX3 are imported into the nucleus independently. The 139-408 and 409-662 mutants were localised to the nucleus in HeLa cells, showing that DDX3 has more than one region responsible for nuclear import. Within the region 139-408 two separate NLS prediction software (PSORTII and NuclImport) predicted class I NLSs at different regions. However, when key basic residues were mutated to inert alanine, import of DDX3 was not clearly affected, suggesting that these putative NLSs are not critical for nuclear import. There can be many reasons why the putative NLSs within 139-408 were not critical for nuclear import, for example importin- $\alpha$  may not be able to bind these NLS due to their localisation within a structured region of DDX3, this would not be the case for the NLSs situated at an exposed loop. Of note, there was no putative NLS found within the 409-662 region, suggesting that a non-classical NLS must occur within this region as it was imported sufficiently on its own.

Recently, inhibitors of nuclear import were described. Using two different inhibitors for importin- $\beta$  mediated pathways, I was able to test whether DDX3 is imported via importin- $\alpha/\beta$  or importin- $\beta$ . My results suggest that DDX3 is imported independently of importin- $\beta$ , with DDX3 being imported as normal after using both the importin- $\beta$  inhibitor IPZ or the the importin- $\alpha/\beta$  Bimax inhibitors. I found that DDX3 could be imported independently via two separate regions, however import

of truncation mutants was also not sensitive to IPZ. My results suggest that neither region of DDX3 is imported via importin- $\beta$ , suggesting that DDX3 is imported independently of importin- $\beta$ .

After my exhaustive search for NLSs and testing various importin- $\alpha/\beta$  inhibitors, I then decided to look at other import pathways. DDX3 has previously been shown to interact with calmodulin, which has been suggested to play a role in import of a small set of proteins (Jang et al. 2007; Sweitzer & Hanover 1996; Hanover et al. 2009). The calmodulin inhibitor W7 did not affect nuclear import of DDX3 in our assays. A previous paper showed that p21<sup>waf1/cip1</sup> was imported in a calmodulin dependent manner, with a calmodulin inhibitor causing cytoplasmic re-localisation of p21<sup>waf1/cip1</sup> (Taulés et al. 1999). Therefore it was used as a positive control in assay. However another paper suggested that binding of calmodulin to p21<sup>waf1/cip1</sup> inhibits phosphorylation of p21<sup>waf1/cip1</sup> at Ser153 within its bipartite NLS by protein kinase C (PKC), resulting in inhibition of nuclear import (Rodríguez-Vilarrupla et al. 2005; Rousseau et al. 1999). A search for the highly conserved SOX protein family Calmodulin-NLS (Kaur et al. 2010) in DDX3 using PROSITE resulted in no hits, suggesting DDX3 does not contain this Calmodulin-NLS.

My data suggests that DDX3 is imported in a manner independent of importin- $\alpha/\beta$  and calmodulin. DDX3 could potentially use the nuclear import protein transportin, which has been reported to facilitate the import of a range of mRNA processing proteins (Lee et al. 2006). DDX3 was shown to interact with transportin 1/2 by tandem MS in one study, however another research group was unable to show direct binding of DDX3 to transportin or identify a PY-NLS in DDX3's protein sequence (Güttinger et al. 2004; Lee et al. 2006). Using PROSITE, I also searched for

a PY-NLS in DDX3, obtaining no hits. DDX3 could still potentially be imported via transportin, maybe through a different NLS. The basic residue enriched  $\beta$ -like import receptor binding (BIB) motif characterised in RL23A has been described to interact with transportin and importin- $\beta$ , and recently has been suggested to represent a distinct NLS sequence (Jäkel & Görlich 1998; Kimura et al. 2012). However, DDX3 was not shown to contain a BIB like NLS in this study (Kimura et al. 2012). Perhaps DDX3 can interact with transportin but only after specific post-translational modification. For example, STAT1 contains no classical NLS however after tyrosine phosphorylation STAT1 dimerises resulting in a functional arginine/lysine rich NLS (Melen et al. 2001; Fagerlund et al. 2002). As there are no inhibitors of transportin presently available, we were unable to investigate whether DDX3 is imported in this manner. The role for transportin in importing DDX3 could be investigated using knockdown experiments of transportin, this however would inhibit both direct and indirect transport via transportin.

It is possible that DDX3 does not directly interact with nuclear import factors. Perhaps DDX3 can "piggy back" into the nucleus in complex with another protein which contains an NLS. On the other hand, nuclear import of some proteins has been shown to occur independently of nuclear import factors, through direct interactions with components of the NPC (Sachdev et al. 2000). As DDX3 has been shown to localise to nucleoporins at the cytoplasmic side of the NPC, it is not implausible that DDX3 could be imported through direct interactions with the NPC. This could be investigated in import assays with digitonin permeabilised cells in the absence of cytoplasmic factors.

In conclusion, how DDX3 is imported into the nucleus is still unclear. Here I have shown DDX3 imports independently of the classical import pathway and the calmodulin pathway.

## **Chapter 5 : Regulation of DDX3 localisation by viral infection**

---

### **5.1. Introduction**

---

DDX3 has a range of distinct functions in the nucleus and the cytoplasm. In chapter one we introduced DDX3 functions in mRNA processing in the nucleus and the cytoplasm. In addition to that, DDX3 has been shown to play a critical role in innate immune signalling and also to be a target for various viruses. In this chapter the role of DDX3 in innate immune signalling and the viral targeting of DDX3 will be discussed.

#### **5.1.1. The role of DDX3 in the immune system**

---

The immune system allows organisms to fight pathogens and is comprised of the innate and adaptive systems. The innate immune system is the first line of defence. Innate immune cells express Pattern Recognition Receptors (PRRs), which recognise Pathogen-Associated Molecular Patterns (PAMPs) and endogenous Danger-Associated Molecular Patterns (DAMPs) and initiate an appropriate immune response (Medzhitov 2001). PAMPs are molecules associated with pathogens, which alert an organism to intruding pathogens. DAMPS are molecules released by stressed cells which act as endogenous danger signals to promote a non-infectious inflammatory response. Different PRRs recognise specific PAMPs, allowing the organism to mount a response to a broad range of pathogens.

Currently, six different families of PRRs have been identified, with the ability to recognise a large range of different PAMPs.

- Membrane bound PRRs
  - Toll like receptors (TLRs)
  - C-type Lectin receptors (CLRs)
- Cytoplasmic PRRs
  - Retinoic-acid inducible genes (RIG-I) receptors (RLRs)
  - NOD-like receptors (NLRs)
  - Aim2-like receptors (ALRs)
  - other cytosolic DNA receptors

Recognition of viruses by the innate immune system is mediated mainly by a specialised groups of TLRs, the RLRs, and DNA receptors. The anti-viral Toll-like receptors include TLR3, TLR7, TLR8 and TLR9, which recognise viral nucleic acids within the lumen of the endosome. The RLR family recognises viral RNAs in the cytoplasm of cells. Recently many new PRRs for cytoplasmic DNA recognition have been described, including DNA-dependent activator of interferon (IFN)-regulatory factors (DAI) (Takaoka et al. 2007), absent in melanoma 2 (AIM2) (Bürckstümmer et al. 2009), RNA polymerase III (Pol III), leucine-rich repeat (in Flightless I) interacting protein-1 (Lrrfip1) (Yang et al. 2010), DExD/H box helicases (DHX9, DHX36, DDX41) (Kim et al. 2010; Zhang et al. 2011), and the IFN-inducible protein IFI16 (Unterholzner et al. 2010). The sensing of PAMPs or DAMPs by PRRs results in the expression of genes encoding pro-inflammatory cytokines, type I Interferons, chemokines and anti-microbial proteins. Activation of most PRRs leads to the activation of the transcription factor NF- $\kappa$ B and pro-inflammatory cytokines. In addition, anti-viral PRRs also activate IFN-regulatory factor (IRF) 3 and IRF7, leading to induction type I IFNS, potent anti-viral cytokines.

Type I interferons are produced in response to anti-viral signalling, with TLR3, TLR4, the RLRs and cytoplasmic DNA receptors all utilising the kinases TBK1 (TANK-

associated NF- $\kappa$ B) and IKK $\epsilon$  [I $\kappa$ B (inhibitor of NF- $\kappa$ B) kinase  $\epsilon$ ] to phosphorylate and activate IRF3/7, as depicted in Figure 5.1.

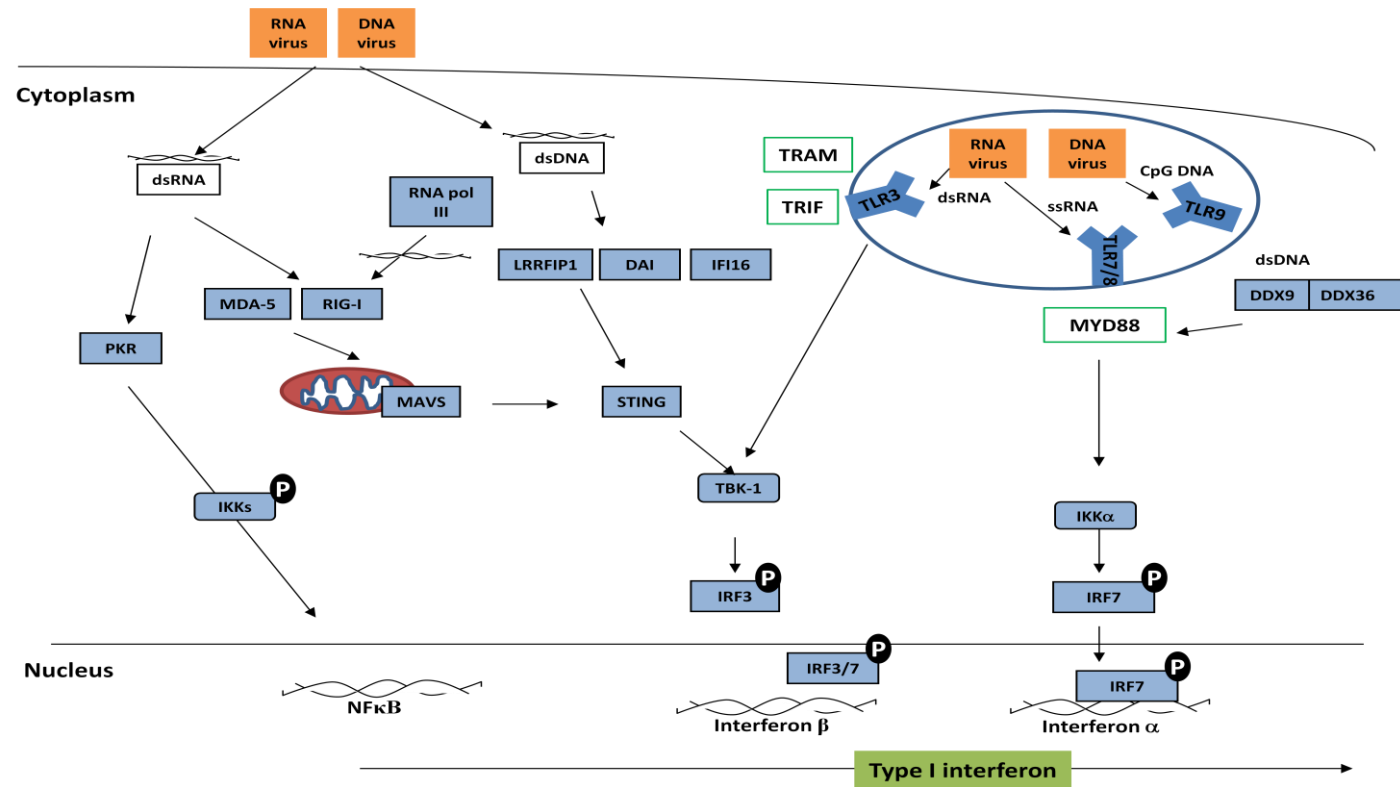


**Figure 5.1: Antiviral signalling leading to type I IFN production.**

Recognition of viral and bacterial components by host pattern recognition receptors (PRRs) triggers signalling pathways that induce production of type I IFN. Viruses enter cells either by fusion at the plasma membrane or by endocytosis followed by fusion with the endosomal membrane, and entry into the cytoplasm. Viruses that reach the cytoplasmic compartment produce dsRNA during replication, which is recognised by the RLRs (RIG-I and MDA-5) and dsRNA-dependent protein kinase (PKR). RIG-I signals via the adaptor MAVS, subsequently activating TBK1/IKK $\epsilon$  and IRF3. Viruses that enter endocytic compartments are recognised by Toll-like receptors, TLR3, TLR7, TLR8, and TLR9. TLR9 recognises unmethylated CpG motifs of viral and bacterial DNA. TLR7 and TLR8 recognise ssRNA from RNA viruses. TLR3 recognises dsRNA motifs of both types of viruses. Cytosolic DNA sensors, such as Lrrfip1, recognise viral DNA to induce IFN $\beta$  via IRF3 transactivation. DAI can bind double-stranded viral DNA to induce TBK1-IRF3-dependent IFN $\beta$  production. IFI16 can directly bind viral DNA via its HIN200 domains and initiate IFN $\beta$  induction in a STING-TBK1- and IRF3-dependent manner. RNA polymerase III (Pol III) generates dsRNA intermediate that are ligands for RIG-I. All of these PRRs can activate production of type I IFNs.

There are three members of the RLR family: Retinoic acid-inducible gene I (RIG-I), melanoma differentiation-associated antigen 5 (MDA5), and laboratory of genetics and physiology 2 (LGP2) (Yoneyama & Fujita 2007; Akira et al. 2006). RLRs contain a central DExD/H-box helicase domain and a C-terminal regulatory domain, and RIG-I and MDA5 also contain two N-terminal caspase recruitment domains (CARDs), whereas LGP2 does not. RIG-I recognises 5'-triphosphate ends of RNA followed by a short ds region (up to 1 kb), whereas MDA5 detects long dsRNAs (more than 2 kb), such as polyinosinic polycytidylic acid (poly I:C) (Kato et al. 2008). Upon dsRNA recognition, RIG-I or MDA-5 localise to the outer membrane of the mitochondria where their N-terminal CARD domains interact with the CARD domain of MAVS (also known as IPS-1, VISA and Cardiff). Activated MAVS recruits the I $\kappa$ B kinase IKK- $\epsilon$  and TANK-binding kinase 1 (TBK1), which phosphorylate IFN-regulatory factor (IRF) 3 and IRF7, resulting in type I IFN induction (Caillaud et al. 2005; Sharma et al. 2003).

The cytoplasmic DNA PRRs utilise adaptor molecules to signal to members of the IRF family to promote type I interferon induction. DHX9 and DHX36 recruit MyD88 to activate IKK- $\alpha$  mediated phosphorylation of IRF7 and type I IFN induction (Kim et al. 2010). On the other hand, during RNA-pol III DNA recognition, RNA-pol III produces a dsRNA intermediate which then activates RIG-I and MAVS (Ablasser et al. 2009). IFI16 utilises the endoplasmic reticulum-resident protein Stimulator of interferon genes (STING), which then signals downstream to TBK1 to induce type I interferons (Unterholzner et al. 2010).

The role of DDX3 in innate immune signalling was exposed in studies investigating how vaccinia virus evades innate immune response. Vaccinia virus (VACV) protein K7 was shown to interact with DDX3 and that this interaction had a potent inhibitory effect on Toll-like receptor (TLR)-dependent and -independent IRF3/7 activation and IFN $\beta$  induction (Schröder et al. 2008). DDX3 was shown to interact with IKK $\epsilon$  in Sendai virus-infected cells and to enhance IRF3/7 activation and induction of IFN $\beta$  (Schröder et al. 2008). An N-terminal DDX3 deletion mutant (aa 139-662) lost the ability to enhance activation of the IFN $\beta$  promoter (Schröder et al. 2008). Interestingly, K7 binds to the N-terminus of DDX3 between residues 81-90 (Figure 5.2) (Oda et al. 2009), and binding of K7 to DDX3 inhibits its antiviral function. Site-directed mutagenesis showed that the residues Phe84 and Phe85 in DDX3 were required to induce IFN $\beta$  promoter activation. Phe84 and Phe85 also mediate binding to the vaccinia protein K7. Therefore, it seems that the residues Phe 84 and Phe 85 are targeted by VACV protein K7 to inhibit DDX3's function in the induction of type I Interferons (Oda et al. 2009). Recently, we have shown that DDX3 acts as a downstream scaffold adaptor during RIG-I signalling, mediating IKK $\epsilon$  activation and coupling the activated kinase to IRF3 (Gu et al. 2013).

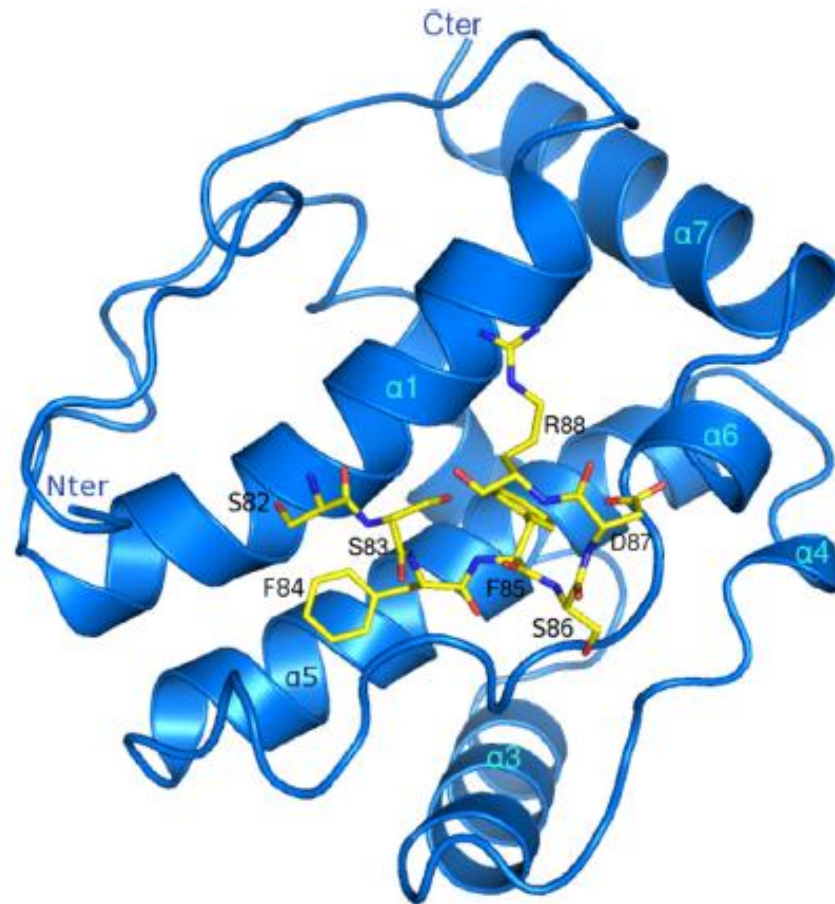


**Figure 5.2: Structure of K7-DDX3 complex.**

K7 is shown in blue ribbons, and the DDX3 peptide (aa82-88) in the yellow stick model. Taken from Oda et al. 2009.

DDX3 has also been identified as a TBK1-substrate and transcriptional regulator of the IFN $\beta$  promoter. Soulat *et al.* identified several serine/threonine residues within the two recA-like domains of DDX3 as TBK1 phosphorylation sites (Soulat et al. 2008). They also showed that these phosphorylation sites were required for IFN $\beta$  induction, as site directed mutagenesis of these sites resulted in reduced IFN $\beta$  induction. Using chromatin immunoprecipitation, the authors also showed that DDX3 was able to bind directly to the IFN $\beta$  enhancer region upon infection with *Listeria monocytogenes*, in an IRF3 independent manner (Soulat et al. 2008).

DDX3 has also been shown to be a component of the MAVS complex through Yeast-2-Hybrid studies. It was shown to be a positive regulator of MAVS mediated IFN $\beta$  induction and the interaction site with MAVS was mapped to the C-terminus of DDX3 (Oshiumi, Ikeda, et al. 2010). DDX3 was also shown to bind Poly I:C and viral RNA in solution; and the authors suggested that DDX3 may be an initial sensor of viral RNA, intensifying MAVS signalling before sufficient levels of RIG-I are induced in an IFN-dependent manner (Oshiumi, Ikeda, et al. 2010).

In summary, DDX3 has been shown to regulate type I interferon production with potential effects in both the nucleus and the cytoplasm. DDX3 has been implicated at three stages of the IFN $\beta$  activation pathway. **1.** After viral RNA sensing by RIG-I/MDA-5, DDX3 has been shown to be a component of the IPS-1 complex (Oshiumi, Ikeda, et al. 2010). **2.** Downstream of the MAVS complex DDX3 has been shown to interact with IKK $\epsilon$  (Schröder et al. 2008) and TBK1 (Soulat et al. 2008), with these interactions presumably taking place in the cytoplasm. **3.** Downstream of TBK1 and IKK $\epsilon$ , in the nucleus, DDX3 has been shown to bind directly to the IFN $\beta$  promoter, potentially after being phosphorylated by TBK1 at residues within the two recA-like domains of DDX3 (Soulat et al. 2008). Figure 5.3, depicts the various stages of the IFN induction pathway that DDX3 has been implicated in, with roles both in the cytoplasm and the nucleus. Oshiumi et al. suggested that DDX3 interacts with the MAVS complex constitutively, however this was shown in cells overexpressing DDX3 (Oshiumi, Ikeda, et al. 2010); whereas its interaction with IKK $\epsilon$  occurred after viral infection (Schröder et al. 2008) and it interacted directly with the IFN $\beta$  promoter enhancer region upon infection with *Listeria monocytogenes* (Soulat et al. 2008). It is not implausible that DDX3 could interact with IPS-1 at the

mitochondria following MAVS activation and also with IKK $\epsilon$  following viral infection, since IKK $\epsilon$  has been shown to be recruited to the mitochondria after MAVS activation (Meylan et al. 2005). It might thus be a possibility that DDX3 is responsible for the recruitment of IKK $\epsilon$  to the mitochondria.

It is also possible that DDX3 participates in signalling events in the cytoplasm before it translocates to the nucleus to bind to the IFN $\beta$  promoter. Investigating the subcellular localisation of DDX3 in uninfected and infected cells might thus help to elucidate what role DDX3 is playing in the induction of type I interferons at different stages of viral and bacterial infections.

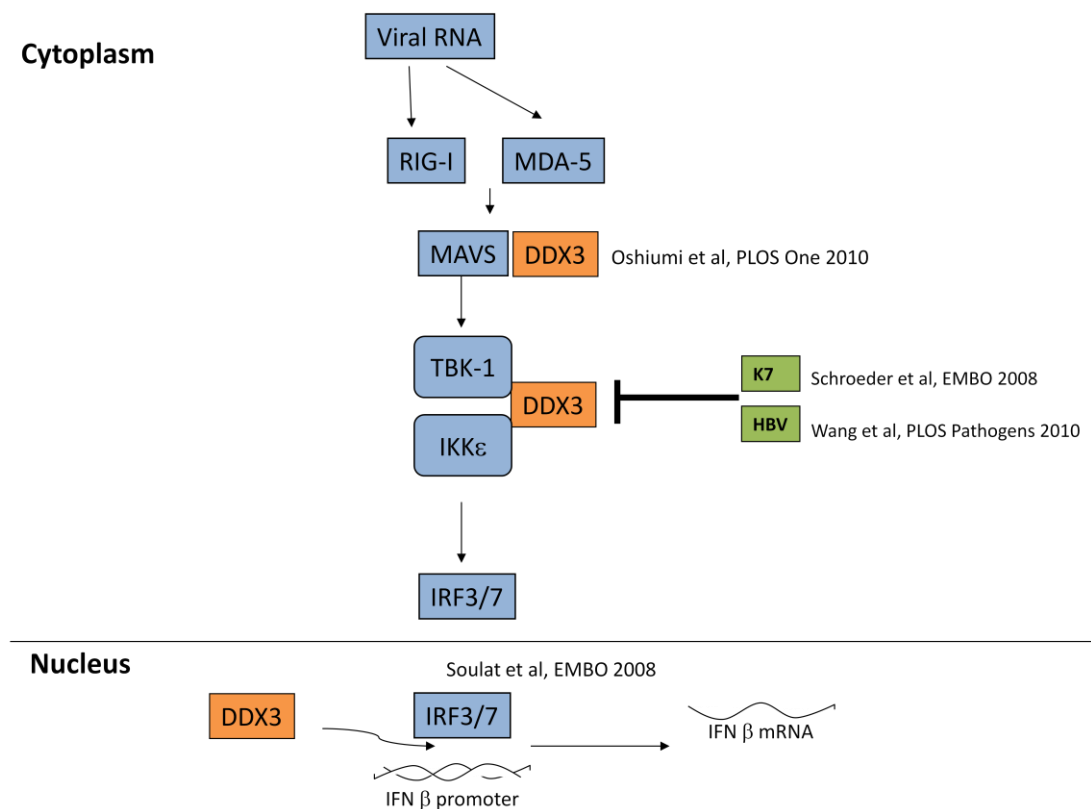


**Figure 5.3: DDX3 is required for IFN $\beta$  induction and is a target for viral immune evasion.**

Viral RNA binds to either RIG-I or MDA-5 leading to recruitment of MAVS and downstream activation of the kinases TBK-1 and IKK $\epsilon$ ; which are required for the phosphorylation and activation of IRF3. IRF3 stimulates IFN $\beta$  induction. DDX3 has been shown to interact at the level of TBK1/IKK $\epsilon$  (Schröder et al. 2008), with the MAVS complex (Oshiumi, Ikeda, et al. 2010) and also to directly bind to the IFN $\beta$  promoter (Soulat et al. 2008). DDX3 has also been shown to enhance MAVS function through regions in its C-terminus (Oshiumi, Ikeda, et al. 2010). Vaccinia protein K7 inhibits DDX3 role in inducing IFN $\beta$  (Schröder et al. 2008). HBV pol also inhibits IFN $\beta$  induction via interaction with DDX3 (Wang & Ryu 2010).

### 5.1.2. DDX3 is targeted by viruses

DDX3 has been shown to be targeted by various viruses, including Vaccinia Virus, HCV, HBV, and HIV. Viruses have been suggested to both inhibit and subvert DDX3 functions to block IFN induction and allow the replication of their genome, respectively.

#### 5.1.2.1. DDX3 is a target for Vaccinia virus

VACV is a complex enveloped virus belonging to the genus *Orthopoxvirus*, which is a member of the poxvirus family. It has a linear double-stranded DNA genome, which encodes for approximately 250 genes. The central portion of orthopoxvirus genomes (~100 kb) is highly conserved and contains genes essential for virus replication, whereas the termini encodes for non-essential proteins which are important virulence factor and immune evasion proteins (Smith et al. 1997).

VACV protein K7 evades the host immune system by targeting DDX3. As earlier stated DDX3 is targeted by VACV protein K7 to inhibit type I interferon induction (Schröder et al. 2008; Oda et al. 2009).

#### 5.1.2.2. DDX3 is a target for HBV

Hepatitis B virus (HBV) is a complex, enveloped virus belonging to the genus *Orthohepadnavirus*, which is a member of the *Hepadnaviridae* family. HBV encodes various proteins which allow it to evade detection by the innate immune system (Wieland & Chisari 2005). The genome can be found in two different forms, a partially double stranded relaxed circular DNA in the virions and a covalently closed DNA molecule in the nucleus of infected cells (Kay & Zoulim 2007). The covalently closed DNA molecule is transcribed into pregenomic RNA (pgRNA) in the nucleus,

which is then exported to the cytoplasm and reverse transcribed into single stranded DNA.

DDX3 is also targeted by HBV. First, overexpression of DDX3 was shown to inhibit replication of HBV through an interaction with HBV pol. The authors suggested that DDX3 inhibits viral DNA reverse transcription (Wang, Kim, et al. 2009). Later it was shown that HBV pol targets DDX3 in an immune evasion strategy. HBV inhibited DDX3's interaction with IKK $\epsilon$ , which resulted in inhibition of IRF3 activation and IFN $\beta$  induction in a manner similar to K7 (Wang & Ryu 2010; Yu et al. 2010).

#### 5.1.2.3. Introduction to HIV

Human Immunodeficiency Virus (HIV) is a single-stranded positive-sense RNA virus, belonging to the genus *lentivirus* which is a member of the *Retroviridae* family. The HIV genome consists of a single-stranded RNA that contains 9 open reading frames, which can produce 15 proteins (Figure 5.4) (Frankel & Young 1998).

During viral infection, HIV-1 enters the cell through binding of the Env glycoprotein to the CD4 receptor along with the chemokine receptor CXCR4 or CCR5. Once in the cytoplasm, the viral RNA is reverse transcribed into proviral DNA by the viral Reverse Transcriptase (RT) and then enters the nucleus as a pre-integration complex (PIC). In addition to the structural proteins Gag, Pol and Env, HIV-1 also encodes the important regulatory proteins Tat and Rev. Tat (Transcriptional transactivator) is responsible for activating transcription of the HIV Long Terminal Repeat (LTR) promoter, while Rev (Regulator of virion expression) is involved in transporting unspliced and partially spliced viral mRNAs from the nucleus to the cytoplasm (Emerman & Malim 1998; Frankel & Young 1998; Freed

2004). Alongside the structural and regulatory proteins, HIV also encodes accessory protein Nef (negative effector), Vif (viral infectivity factor), Vpr (viral protein r) and Vpu (viral protein u). The accessory proteins are not required for HIV gene expression, however they play important roles in immune evasion and pathogenesis (Chinnasamy et al. 2000; Freed 2004).

Rev facilitates nuclear export of unspliced and incompletely spliced mRNAs by binding to the rev response element (RRE), a 350-nt structured RNA found in the introns of unspliced viral mRNAs (Pollard & Malim 1998; Malim et al. 1989). It is a 18kDa protein which has been shown to localise to the nucleolus of HIV-1 infected cells and Rev-expressing cells (Dundr et al. 1995). Rev is exported from the nucleus via the CRM-1 pathway and interacts with CRM-1 via its N-terminal leucine-rich NES (Askjaer 1998). HIV-1 transcription yields 3 different sized transcripts, ~2 kb, ~4 kb, and ~9 kb RNAs. In the early phase of the viral life cycle, the ~2 kb pre-RNA (which encodes rev) is exported from the nucleus via TAP, the standard mRNA nuclear export pathway. Upon translation and maturation in the cytoplasm, Rev is imported into the nucleus where it helps to export partially spliced ~4 kb RNA and ~9 kb via the CRM-1 pathway. Once in the cytoplasm translation of the ~4 kb and ~9 kb RNA can occur, and also packaging of the genomic ~9 kb RNA into virions (Blissenbach et al. 2010).

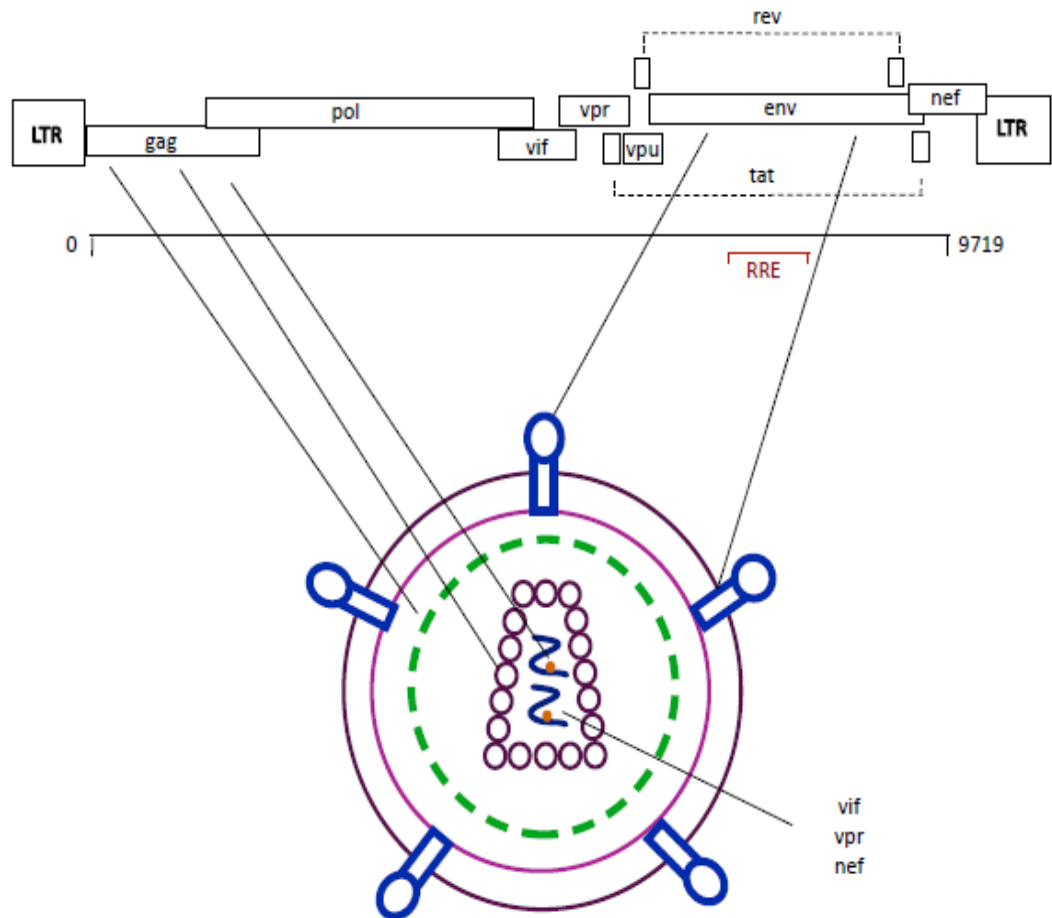


**Figure 5.4: Organization of the HIV-1 genome.**

The location of the long terminal repeats (LTRs) and the genes encoded by HIV-1 are indicated. Gag, Pol and Env proteins are initially synthesised as polyprotein precursors. The Gag precursor is cleaved by the viral protease (PR) into the proteins: matrix (MA), capsid (CA), nucleocapsid (NC) and p6. The GagPol precursor undergoes PR-mediated processing to generate the Gag proteins and the Pol enzymes: PR, reverse transcriptase (RT) and integrase (IN). The Env glycoprotein precursor gp160 is cleaved by a cellular protease during transport to the cell surface, generating the mature surface glycoprotein gp120 and the trans-membrane glycoprotein gp41. The sizes of the genes and encoded proteins are not to scale. Adapted from (Frankel & Young 1998).

DDX3 is an essential cofactor for HIV replication. DDX3 was first linked to HIV when cells expressing HIV-Tat were shown to have increased levels of DDX3 (Yedavalli et al. 2004), and a role for DDX3 as a cofactor for the CRM-1/HIV Rev mediated export of HIV RNA was suggested. HIV-Rev has its own functional NES which has been shown to interact with CRM-1, so that it can export unspliced viral RNA via CRM-1. (Askjaer 1998; Güttler et al. 2010). Knockdown of DDX3 was shown to reduce the nuclear export of unspliced HIV-RNA, and consequently to decrease

viral replication (Yedavalli et al. 2004; Ishaq et al. 2008). Yedavalli *et al.* showed that DDX3's helicase activity was essential for the nuclear export of HIV-mRNA. They also showed that DDX3 interacted with CRM-1 via its C-terminus, independent of its putative N-terminal NES. They suggested that DDX3 might play a role in restructuring cargo RNAs to allow their transport through the nuclear pore (Yedavalli et al. 2004).

Another study suggested a role for DDX3 in unwinding of DNA/RNA through a unique helicase motif (Garbelli et al. 2011). They showed that DDX3 has a unique motif which can bind nucleic acids, and is important for RNA/DNA helicase activity. Targeting of this motif with a specific peptide resulted in decreased binding of HIV RNA to DDX3 and a decrease in HIV replication (Garbelli et al. 2011). DDX3 has also been shown to play a role in translation of HIV-RNA independently of its role in HIV-RNA nuclear export (Liu et al. 2011).

It is undisputed that DDX3 is an important cofactor for HIV replication, however the exact role of DDX3 in HIV-RNA nuclear export and translational regulation is unclear. DDX3 could facilitate HIV-RNA export through an interaction with CRM-1 and/or HIV rev, or it could play a role in packaging viral RNA for export through its helicase activity.

#### 5.1.2.4. DDX3 is a target of HCV

HCV is a single-positive strand RNA virus, belonging to the genus *Hepacivirus*, which is a part of the *Flaviviridae* family. HCV infection is a major cause for chronic hepatitis, liver cirrhosis and hepatocellular carcinoma. The genome consists of a 5'-non-coding region (NCR), which includes an Internal Ribosomal Entry Site (IRES), a single open reading frame that encodes a large polyprotein and a 3' NCR (Kato

2000). The polyprotein is processed by cellular and virally encoded proteases to produce the structural and non-structural proteins. The structural proteins consist of the core, envelope glycoproteins and P7; and the non-structural proteins consist of NS2, NS3, NS4A, NS4B, NS5A and NS5B (Figure 5.5).

There are six major genotypes of HCV, which are defined by nucleotide variation. These genotypes can be further divided into more than 80 subgroups. There is large diversity within HCV, with a 30-59% variation among viral genotypes and 15-30% variation among subgroups and within a single patients 1-5% variation in nucleotide sequence (Simmonds et al. 1993; Bukh et al. 1994). The highest sequence variation is found within the hypervariable region of the envelope glycoproteins E1 and E2. There is little sequence variation found within the 5'UTR which contain specific sequences and RNA secondary structure that are required for replication and translation.

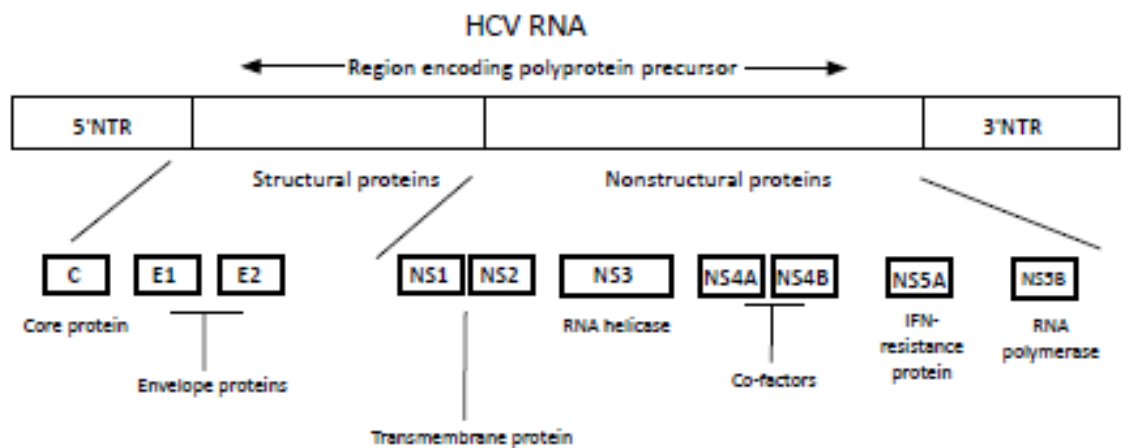
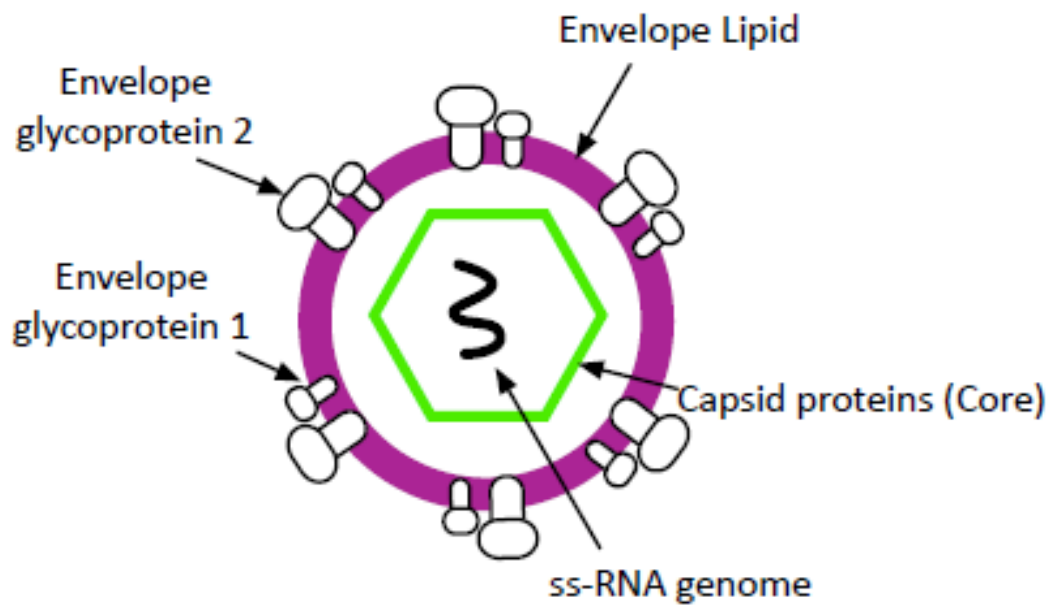


**Figure 5.5: Schematic of HCV virion structure and genome organisation.**

HCV is formed by an enveloped particle harbouring a plus-strand RNA of 9.6 kb. The genome consists of a long open-reading frame (ORF) encoding a 3010 amino acid polyprotein. Translation of the HCV ORF is directed by an IRES within the 5' UTR. The HCV polyprotein is cleaved co- and post-translationally by cellular and viral proteases into ten different products, with the structural proteins (Core (C), E1 and E2) located in the N-terminal third and the nonstructural (NS2-5) replicative proteins in the remainder. Putative functions of the cleavage products are shown. Adapted from (Ashfaq et al. 2011).

DDX3 has been shown to interact with HCV Core protein and is required for HCV replication (Owsianka & Patel 1999; Mamiya & Worman 1999; You et al. 1999; Ariumi et al. 2007). HCV Core is a highly conserved basic, RNA-binding protein that forms the viral nucleocapsid and might also regulate viral and cellular gene expression (McLauchlan 2000; Nguyen et al. 2006). Core protein is a dimeric, alpha-helical protein that can be separated into three domains, D1 (a basic hydrophilic region covering two-thirds of the N-terminus (aa 1–118)), D2 (a hydrophobic domain of the central domain (aa 119-173)) and D3 (the hydrophobic signal sequence containing aa 174–191) (Angus et al. 2010; McLauchlan 2000; Boulant et al. 2005). The D1 region of HCV Core is important for RNA binding and Core oligomerisation and D2 is required for HCV Core association with membranes (Boulant et al. 2005; Boulant et al. 2006). HCV Core protein plays an important role in recruiting non-structural proteins and replication complexes to lipid droplets which is required for virus production (Miyazari et al. 2007; Boulant et al. 2007). HCV Core protein has also been suggested to play a role in the development of HCC, as it has been shown to alter the expression of genes involved in tumour surveillance (Nguyen et al. 2006).

The function of the HCV Core protein interaction with DDX3 is unclear, with some reports suggesting HCV enhances DDX3 transcriptional functions (You et al. 1999) and others suggesting HCV Core allows the virus to evade clearance through inhibiting DDX3's anti-viral response (Oshiumi, Ikeda, et al. 2010). HCV Core protein has been shown co-localise with DDX3 in both the cytoplasm (You et al. 1999; Mamiya & Worman 1999) and nucleus (Owsianka & Patel 1999), though more studies have shown a cytoplasmic co-localisation. HCV Core protein has been

suggested to target the cytoplasmic function of DDX3; as HCV Core protein co-localises with DDX3 in the cytoplasm in distinct speckles (Owsianka & Patel 1999). Recently, these distinct HCV Core protein speckles have been shown to occur around lipid droplets, and to be rich in mRNA associated proteins such as DDX3 (Ariumi, Kuroki, Kushima, et al. 2011; Pérez-Vilaró et al. 2012). The interaction of DDX3 with the D1 domain of HCV Core protein has been shown to occur via DDX3's C-terminus, with one group suggesting aa 473–611 and another aa 553–622 (Owsianka & Patel 1999; Mamiya & Worman 1999).

HCV Core protein has been shown to enhance the ATPase activity of DDX3 and the ability of DDX3 to induce pCMV-Luc, indicating that DDX3 has a role in transcriptional regulation and that this role is targeted by HCV Core protein (You et al. 1999). Core protein has also been shown to interfere with the DDX3-substituted *ded1*-deletion yeast, inhibiting growth and translational initiation of capped mRNAs (Mamiya & Worman 1999). Two studies have shown that HCV replication requires DDX3 (Ariumi et al. 2007; Angus et al. 2010). However, this effect of DDX3 was found to be independent of its interaction with HCV Core protein (Angus et al. 2010).

Another study investigating the functional relevance of the HCV Core-DDX3 interaction found that HCV Core protein abrogated DDX3's effect on IPS-1-mediated IFN $\beta$  induction (Oshiumi, Ikeda, et al. 2010). They suggested that the Core protein switches DDX3's role in IFN $\beta$  induction to a HCV-replication mode. However, DDX3's interaction with HCV Core protein has been shown to result in enhanced IFN $\beta$  and ISRE induction (Kang et al. 2012). In this study it was shown that the interaction of

DDX3 and HCV Core could be lost through antigenic variation of the Core protein in cultured adapted viruses (Kang et al. 2012).

As stated above, HCV Core protein has been shown to alter expression of proteins involved in cell cycle regulation. DDX3 expression has been shown to be down-regulated in HCC patients with HCV infection (Chang et al. 2006), and DDX3 has been shown to promote transcription of the tumour suppressor p21<sup>waf1/cip1</sup> (Chang et al. 2006; Chao et al. 2006; Wu, Liu, et al. 2011). DDX3 has been suggested to have roles as both a tumours suppressor and oncogene, so it is possible that the HCV Core protein interaction with DDX3 could alter DDX3's role in cell cycle regulation.

In summary, the functional relevance of the HCV Core protein-DDX3 interaction and co-localisation is unclear. The requirement of DDX3 for HCV replication is potentially independent of its interaction with HCV Core, and the effect of HCV Core protein on the transcriptional and translation functions of DDX3 are unclear. Possibly some functions of DDX3 are required for HCV replication (for example its RNA helicase activity), and other functions, such as its role in the induction of type I IFNs are inhibited by HCV.

### 5.1.3. Conclusion

During innate immune signalling, signalling events occur within specific location in the cytoplasm and in the nucleus of the cell. DDX3 plays a critical role in innate immune signalling, with DDX3 potentially having roles in both cytoplasmic and nuclear innate immune signalling events (Schröder et al. 2008; Soulat et al. 2008). Mis-localisation of DDX3 could affect DDX3's role in innate immune signalling, and pathogens might have evolved the ability to alter DDX3's cellular localisation,

allowing the pathogen to evade the immune system and possibly utilise DDX3's RNA helicase activity to promote viral replication.

## 5.2. Aims

---

In this chapter I investigated the cellular localisation of DDX3 in response to immunological signalling pathways. I also wanted to investigate the interaction of DDX3 with viral proteins. Since DDX3 has been shown to be required for HIV and HCV replication, I decided to focus on viral proteins from HIV and HCV, and examine if DDX3 cellular localisation was altered by viral proteins.

## 5.3. Results

---

### 5.3.1. High content analysis to investigate change in localisation after a range of stimuli

---

Due to DDX3's role in innate immune signalling and IFN $\beta$  induction, I was interested in whether stimulation of cells could cause a change in DDX3 localisation. High content analysis (HCA) microscopy is a useful tool for quantifying changes in the nuclear/cytoplasmic localisation of a protein in cells. Using HCA one can image hundreds of cells simultaneously and objectively quantify the localisation of proteins of interest in these cells.

To investigate whether stimulation of cells could change DDX3's cellular localisation, HeLa cells were plated in a 96-well plate and treated with various stimuli. I wanted to investigate whether stimulation of immunological signalling pathways changes DDX3's localisation, so I treated cells with Sendai virus (SeV), Interferon- $\alpha$  (IFN), Tumor Necrosis Factor (TNF) and Interleukin-1 (IL-1). As a positive control for a nuclear localisation of DDX3, cells were treated with LMB. In Figure 5.6, I show that there was no significant increase in the level of nuclear localised DDX3 after the treatments. There was a possible slight increase at 1hr SeV stimulation, however other treatment did not seem to change the localisation of DDX3.

## High Content Analysis

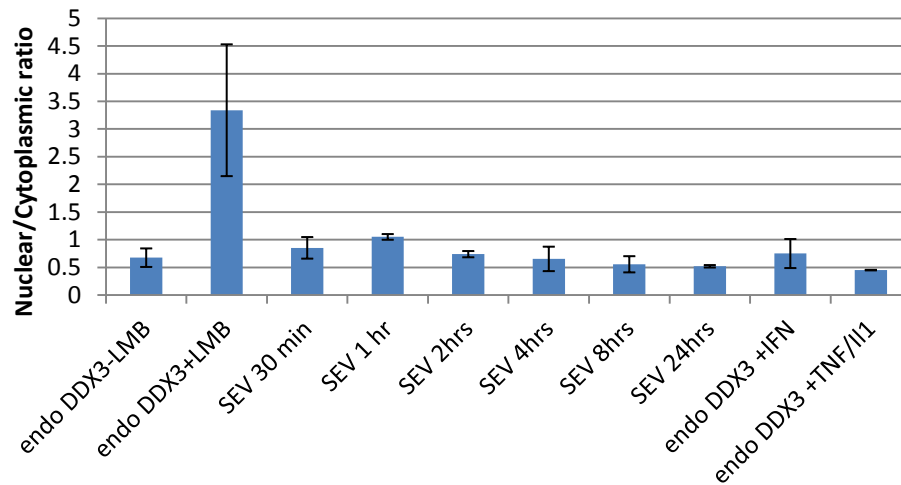


**Figure 5.6: Endogenous DDX3 does not change localisation after treatment with various stimuli.** HeLa cells were treated with 20mM LMB for 4 hrs, SeV for time points indicated, IFN- $\alpha$  for 24 hrs, TNF- $\alpha$  and IL-1. Cells were stained with  $\alpha$ -DDX3 antibody, followed by  $\alpha$ -rabbit Alexa Fluor-488, Rhodamine-Phalloidin and DAPI. High content analysis of the nuclear/cytoplasmic ratio was carried out using the GE IN Cell analyser as described in Chapter 2.

### 5.3.2. Does DDX3 localisation change after overexpression of IKK $\epsilon$ ?

Since DDX3 has been found to interact with IKK $\epsilon$  following activation of the RIG-I pathway, I decided to test if overexpression of IKK $\epsilon$  would affect its cellular localisation. HeLa cells were transfected with an expression plasmid for flag-tagged IKK $\epsilon$  and treated with SeV for 24 hrs or left untreated. The cellular localisation of DDX3 did not change in response to overexpression of IKK $\epsilon$  nor treatment with SeV (Figure 5.7).

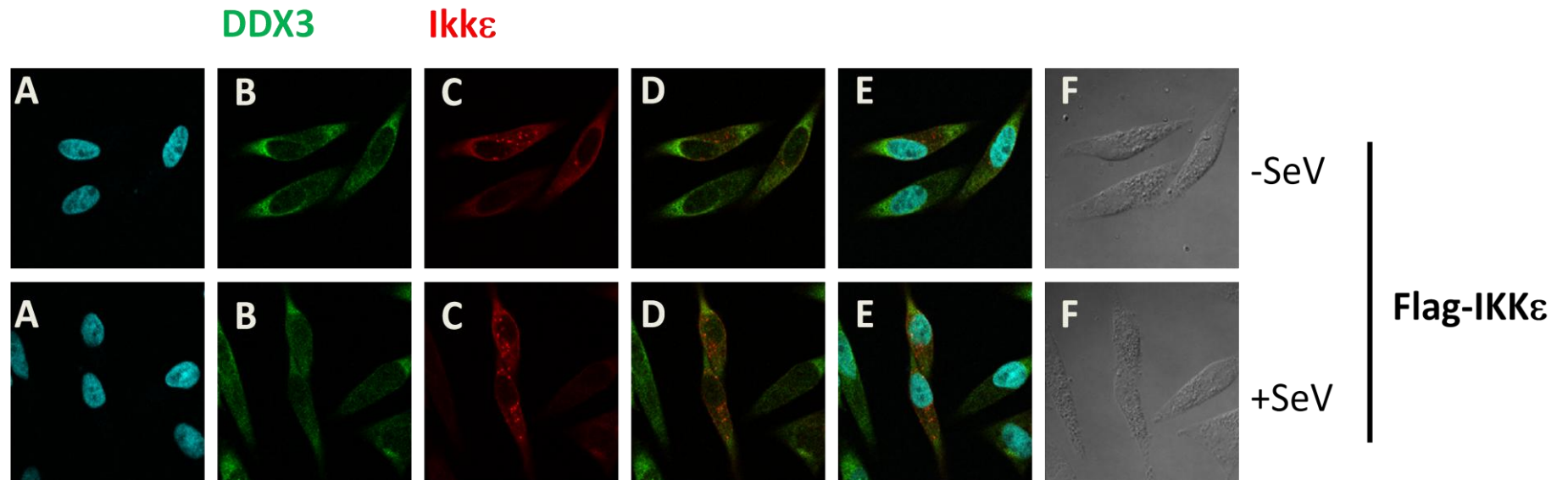


**Figure 5.7: Overexpression of IKK $\epsilon$  does not change the cellular localisation of endogenous DDX3.**

HeLa cells were transfected with expression plasmid for flag-tagged IKK $\epsilon$  and then treated with SeV for 24 hrs. Cells were stained with  $\alpha$ -DDX3 (*Bethyl*) and secondary  $\alpha$ -rabbit Alexa Fluor-488 and  $\alpha$ -flag and secondary  $\alpha$ -mouse Alexa Fluor-594. **Key:** A (DAPI), B (DDX3), C (Flag-IKK $\epsilon$ ), D (merge B and C), E (merge A,B and C) and F (Contrast).

### 5.3.3. Investigating the relationship between HIV-Rev protein and DDX3

#### 5.3.3.1. HIV-Rev changes the localisation of DDX3

DDX3 has been shown to be required for HIV-Rev mediated viral mRNA nuclear export. I decided to test if HIV-Rev and DDX3 co-localised in HeLa cells after overexpression of Ha-Rev. To this end, HeLa cells were transfected with expression plasmids for Ha-Rev, and stained for endogenous DDX3 and Ha-Rev. Interestingly, DDX3 co-localised with Ha-Rev in the nucleolus of the HeLa cells (Figure 5.8). DDX3 usually has a predominantly cytoplasmic localisation. Here, DDX3 still had a predominantly cytoplasmic localisation, however a small amount of DDX3 co-localised with Ha-Rev protein in the nucleolus. Z-stack analysis confirmed that Ha-Rev and endogenous DDX3 co-localised in the nucleolus of HeLa cells after overexpression of Ha-Rev protein (Figure 5.9). Since overexpression of Ha-Rev resulted in endogenous DDX3 being enriched in the nucleolus, this suggests that HIV Rev protein required DDX3 in the nucleolus.

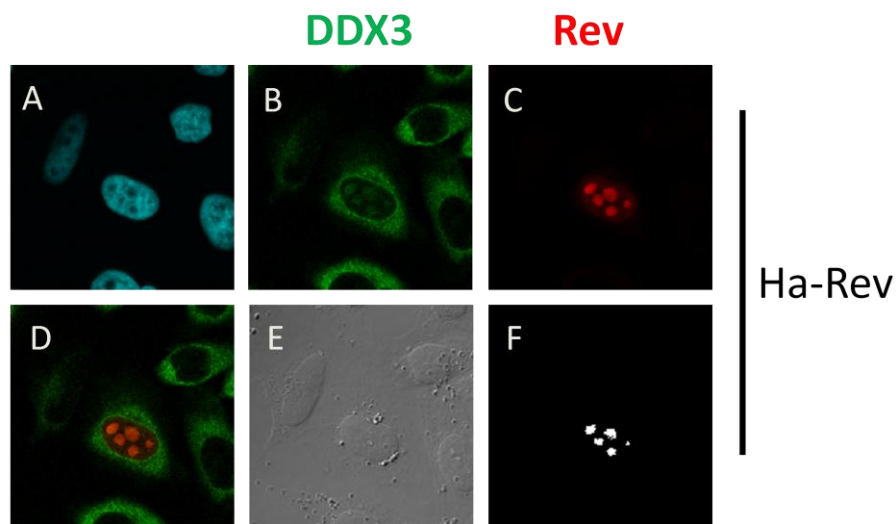


**Figure 5.8: Endogenous DDX3 co-localises with HIV-Rev protein in the nucleolus.**

Overexpression of HIV-Rev protein recruits DDX3 to the nucleolus, with endogenous DDX3 co-localising with HIV-Rev in the nucleolus. Co-localisation points highlight the positions of overlapping signals, generated using Olympus Fluoview Co-localisation Software. HeLa cells were transfected with expression plasmids for Ha-Rev. Cells were stained with  $\alpha$ -DDX3 (*Bethyl*) and secondary  $\alpha$ -rabbit Alexa Fluor-488 and  $\alpha$ -Ha Alexa Fluor-594. **Key:** A (DAPI), B (DDX3), C (Ha-Rev), D (merge A,B and C), E (Contrast) and F (Co-localisation Points).

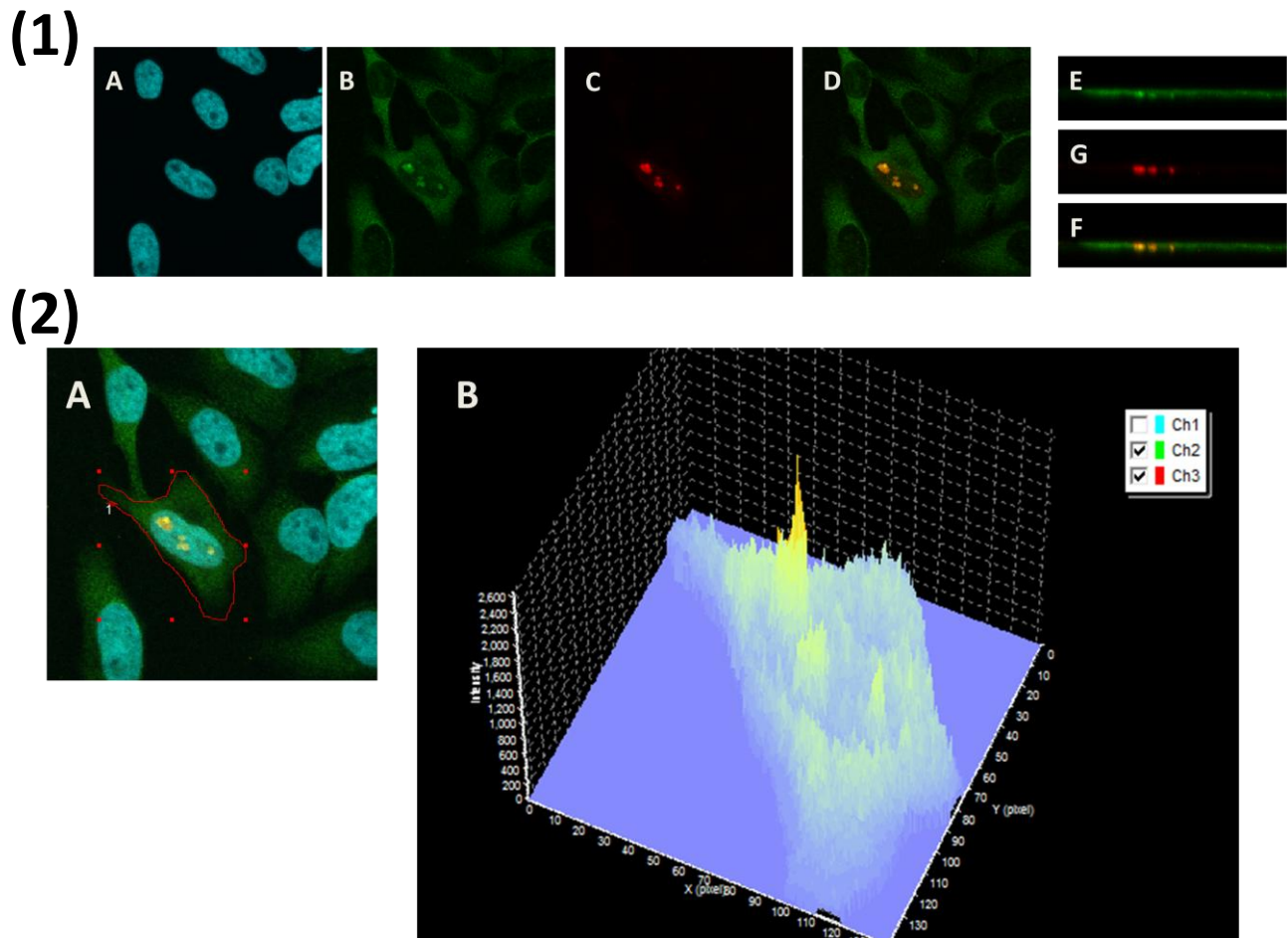


**Figure 5.9: Endogenous DDX3 co-localises with HIV-Rev protein in the nucleus.**

**(1):** Z-stack image analysis of the effect overexpression of HIV-Rev protein has on DDX3's localisation, with endogenous DDX3 co-localising with HIV-Rev in the nucleolus. HeLa cells were transfected with expression plasmids for Ha-Rev. Cells were stained with  $\alpha$ -DDX3(*Bethyl*) and secondary  $\alpha$ -rabbit Alexa Fluor-488 and  $\alpha$ -Ha Alexa Fluor-594. Shown are X-Y projections and X-Z projections. **Key:** **X-Y projections:** A (DAPI), B (DDX3), C (Ha-Rev), D (merge B and C) and **X-Z projections:** E (DDX3), G (Ha-Rev) and H (merge B and C).

**(2):** Fluorescence intensity profile is presented also as a landscape plot. (A) Red line represents Region of Interest (ROI) analysed by (B) intensity profile.

HIV-Rev has been shown to require DDX3 and the exportin CRM-1 to export unspliced and partially spliced viral RNAs from the nucleus. Since overexpression of HIV-Rev enriches endogenous DDX3 in the nucleolus, I speculated that endogenous CRM-1 might also be enriched in the nucleolus. As before, HeLa cells were transfected with expression plasmids for Ha-tagged Rev, and stained for endogenous CRM-1 and Ha-Rev. In Figure 5.10, in HeLa cells not expressing Ha-Rev, endogenous CRM-1 had a diffuse localisation in the nucleus. However, in cells expressing Ha-Rev protein, endogenous CRM-1 was enriched in the nucleolus and co-localised with Ha-Rev. Both DDX3 and CRM-1 have been shown to be required for efficient HIV-Rev mediated mRNA export, our results suggest that HIV-Rev draws proteins required for mRNA nuclear export into the nucleolus of cells.

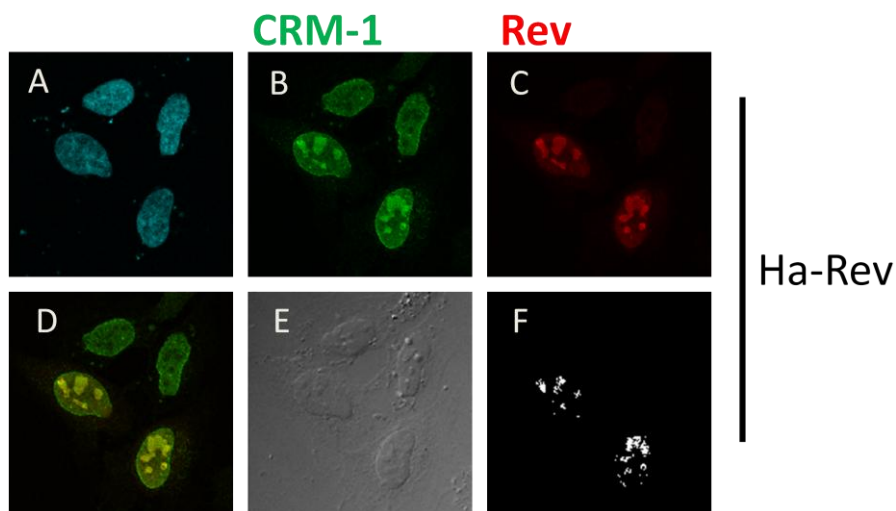


**Figure 5.10: Endogenous CRM-1 co-localises with HIV-Rev protein in the nucleus.**

Overexpression of HIV-Rev protein recruits CRM-1 to the nucleus, with endogenous CRM-1 co-localising with HIV-Rev in the nucleolus. Co-localisation points highlight the positions of overlapping signals, generated using Olympus Fluoview Co-localisation Software. HeLa cells were transfected with expression plasmids for Ha-Rev. Cells were stained with  $\alpha$ -CRM1 (*Novus Biologicals*) and secondary  $\alpha$ -rabbit Alexa Fluor-488 and  $\alpha$ -Ha Alexa Fluor-594. **Key:** A (DAPI), B (CRM-1), C (Ha-Rev), D (merge B and C), E (Contrast) and F (Co-localisation Points).

### 5.3.3.2. DDX3 interacts with HIV-Rev protein

Since overexpression of HIV-Rev protein caused endogenous DDX3 to change cellular localisation, I investigated if DDX3 and HIV-Rev protein directly interacted. I initially investigated if DDX3 interacted with HIV-Rev using co-immunoprecipitation. To this end, 293Ts were transfected with expression plasmids for Myc-tagged DDX3 and Ha-tagged HIV-Rev protein. Cell lysates were prepared and immunoprecipitated using an anti-Ha antibody and probed for the presence of myc-tagged protein. Myc-tagged DDX3 was detected in immunoprecipitates containing HA-Rev and not in control immunoprecipitates (Figure 5.11). Also, Ha-Rev was detected in the immunoprecipitates indicating that the immunoprecipitation process was successful.

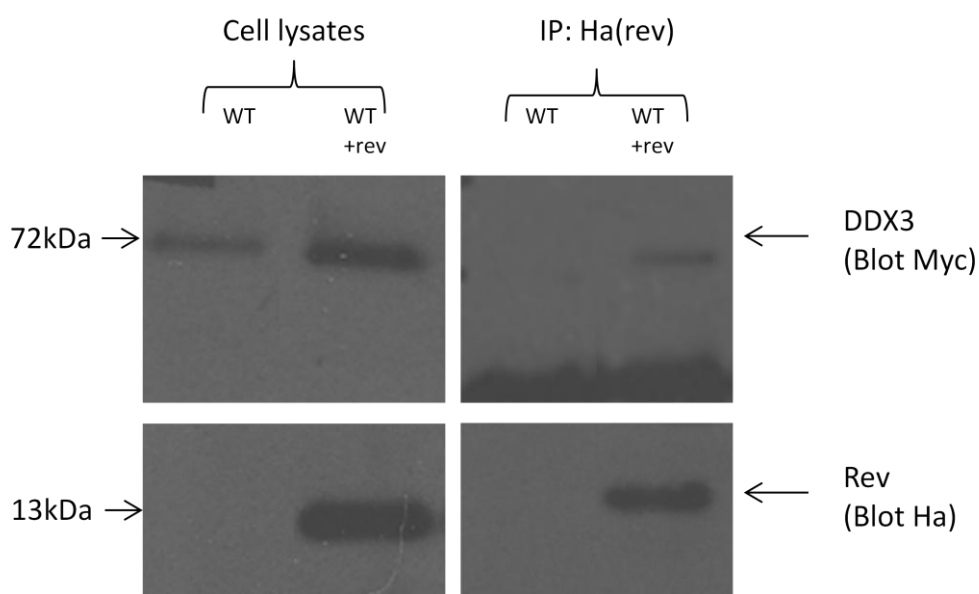


**Figure 5.11: Myc-tagged DDX3 co-immunoprecipitates with Ha-tagged HIV-Rev.**

HEK 293ts were transfected with Ha-tagged HIV-Rev and myc-tagged WT-DDX3. Protein G sepharose beads (*Sigma*) were incubated with anti-Ha antibody, and blocked with 5% BSA in PBS-tween. Cell lysates were added to beads and washed three times in IP-lysis buffer. SDS-PAGE gel electrophoresis and semi-dry transfer was and blots were probed with  $\alpha$ -Myc (*Sigma*) and  $\alpha$ -Ha (*Covance*). Representative blot of three experiments.

I next carried out co-immunoprecipitations assays to map the interaction of Ha-Rev with DDX3. To this end, HEK 293Ts were co-transfected with expression plasmids for Ha-Rev and Myc-tagged DDX3 or DDX3 truncation mutants. Full length DDX3, 1-139, 1-408 and 139-408 were expressed with or without Ha-Rev. Cell lysates were prepared and immunoprecipitated using an anti-Ha antibody and probed for the presence of myc-tagged protein. Myc-tagged DDX3, 139-408 and 1-408 were detected in immunoprecipitates containing HA-Rev and not in control immunoprecipitates (Figure 5.12). Also, Ha-Rev was detected in the immunoprecipitates, indicating that the immunoprecipitation process was successful.

I also confirmed these results by carrying out GST-pulldown assays with recombinant His-tagged DDX3 and recombinant GST-YFP-tagged Rev. Briefly, recombinant GST-YFP-Rev and His-Tagged DDX3 1-408, 139-408 and 409-662 were expressed in *E.coli*. GST-YFP-Rev was then immobilised on glutathione-sepharose beads and His-tagged DDX3 proteins were eluted. Recombinant His-Tagged DDX3 protein was incubated with GST-YFP-Rev beads or control empty glutathione-sepharose beads. Non-bound protein was washed off using lysis buffer, and subsequently the proteins bound were eluted into sample buffer. Recombinant HIV-Rev pulled down recombinant N-terminal domain (1-408) His-DDX3, confirming that this is a direct interaction (Figure 5.13). Interestingly, neither the 139-408 truncation nor the 409-622 truncation did interact with Rev-GST-YFP.

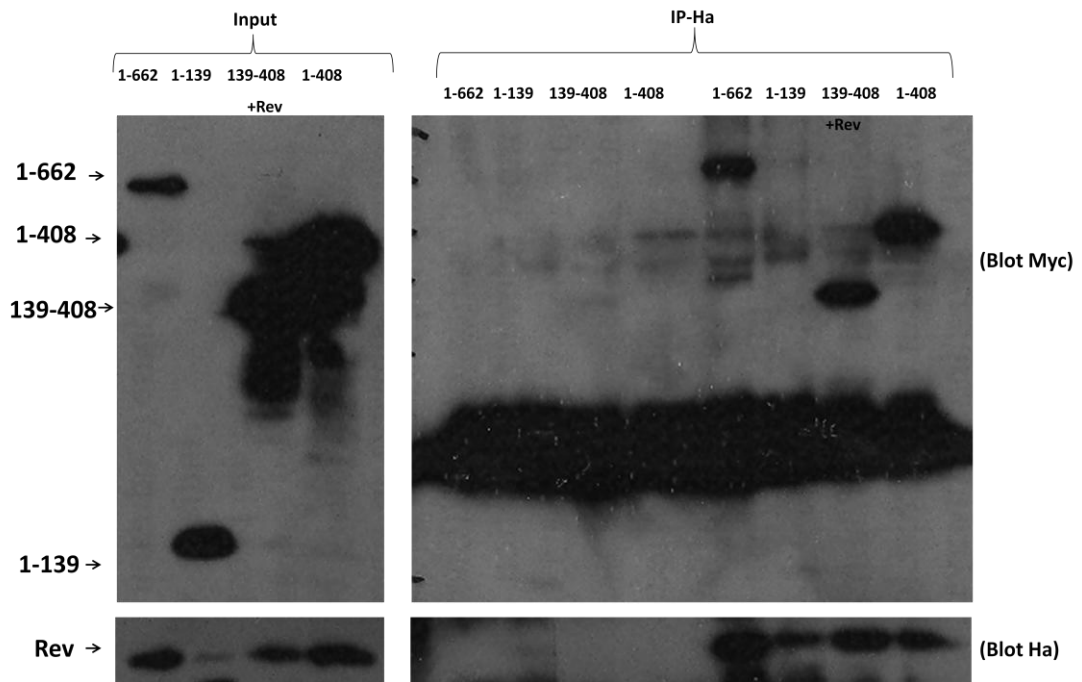


**Figure 5.12: DDX3 interacts with HIV-Rev through residues between aa 139-408.**

HEK 233ts were transfected with Myc-tagged WT DDX3, 1-408, 139-408 and 1-139; with or without Ha-Rev. Protein G sepharose beads (*Sigma*) were incubated with  $\alpha$ -Ha antibody, and blocked with 5% BSA in PBS-tween. Cell lysates were added to beads and washed three times in PBS-tween. SDS-PAGE gel electrophoresis and semi-dry transfer was carried out as per materials and methods. Blots were probed with  $\alpha$ -myc (*Sigma*) and  $\alpha$ -Ha (*Covance*). Representative blot of three experiments.

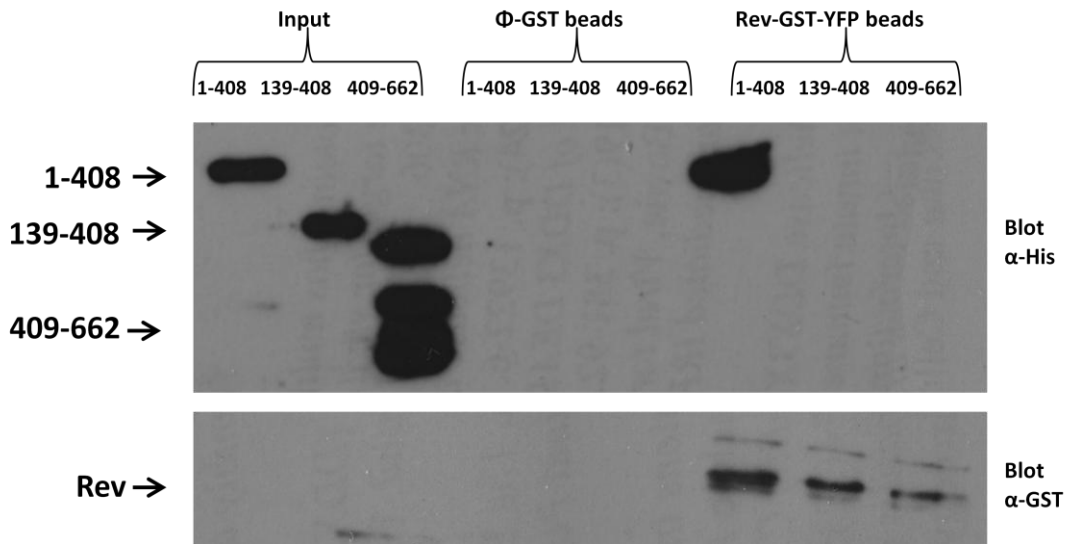


**Figure 5.13: DDX3 interacts directly with HIV-Rev.**

Purified recombinant full-length His-DDX3 or the indicated His-DDX3 truncation mutants were incubated with recombinant GST-. Following pull-down with Glutathione beads, interacting proteins were subjected to SDS-PAGE and western blot analysis with  $\alpha$ -His and  $\alpha$ -GST. Representative of three experiments.

### 5.3.3.3. Overexpression of DDX3 does not affect HIV-Rev mediated expression of Gag protein

Since DDX3 has been shown to be required for HIV-replication I decided to investigate the effects of DDX3 expression of HIV-Rev mediated protein expression. HIV-Rev is required for the nuclear export of RRE-containing mRNA. Here an expression plasmid pGag-RRE was used to monitor Rev-dependent expression, as the binding of Rev to the RRE is required for export of Gag mRNA and hence Gag protein expression. The expression plasmid pGag-CTE was used as a control, since Gag-CTE can export its mRNA independently of Rev. In Figure 5.14, Gag-RRE expression only occurred in the presence of Rev as expected. DDX3 over-expression did not change Rev mediated expression of Gag protein (Gag-RRE) nor Rev independent Gag protein (Gag-CTE ).

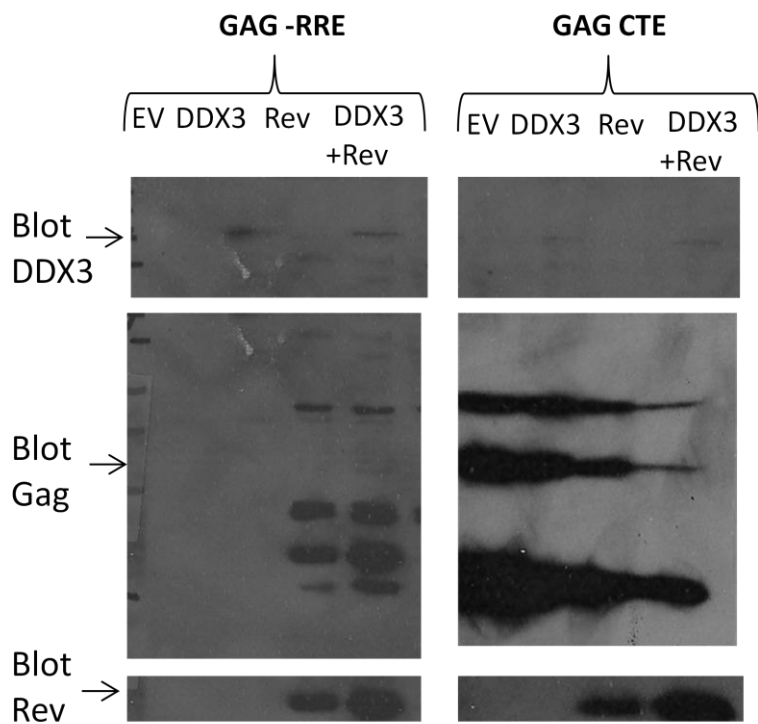


**Figure 5.14: Overexpression of DDX3 does not change HIV-Rev mediated expression of Gag.** HEK 293T cells were transfected with expression plasmids for Gag-RRE, and/or Ha-tagged WT DDX3 and/or HIV-Rev. Cells were lysed and subjected to SDS-PAGE gel electrophoresis and semi-dry transfer was carried out as per materials and methods. Blots were probed with  $\alpha$ -Gag (Centre for Aids Research) and  $\alpha$ -Ha (Covance). Representative blot of three experiments.

### 5.3.4. Investigating the relationship of DDX3 and HCV Core protein

#### 5.3.4.1. HCV Core protein co-localises with endogenous DDX3 in distinct cytoplasmic speckles

DDX3 has been suggested to interact with HCV Core protein. I decided to investigate whether HCV-Core protein affected the cellular localisation of DDX3. HeLa cells were transfected with expression plasmids for Ha-tagged Con1 genotype Core protein, and stained for Ha-Con1 and endogenous DDX3. In Figure 5.15, overexpression of Ha-Con1 caused a dramatic redistribution of DDX3, changing from a normally diffuse cytoplasmic localisation to a distinct cytoplasmic speckle localisation. Endogenous DDX3 co-localised with Ha-Con1 in these cytoplasmic speckles.

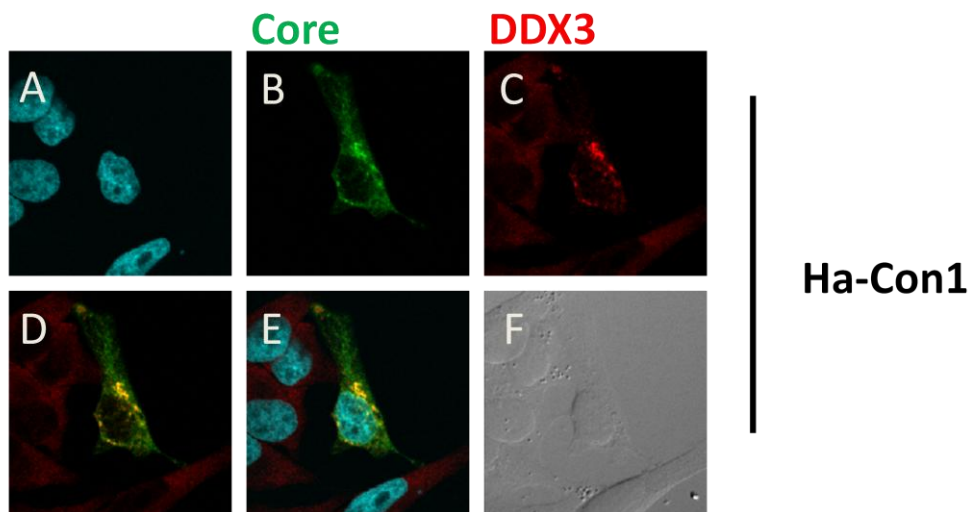


**Figure 5.15: HCV Core protein co-localises with endogenous DDX3 in cytoplasmic speckles in HeLa cells.**

HeLa cells were transfected with Ha-tagged Con1 and stained with  $\alpha$ -Ha (*Covance*) and secondary  $\alpha$ -mouse Alexa Fluor-488, and  $\alpha$ -DDX3 (*Bethyl*) and secondary  $\alpha$ -rabbit Alexa Fluor-594. **Key:** A (DAPI), B (Ha-Con1), C (DDX3), D (merge B and C), E (merge A, B and C), and F (contrast).

#### 5.3.4.2. HCV Core protein prevents the nucleocytoplasmic shuttling

DDX3 interacted with HCV Core protein in cytoplasmic speckles in HeLa cells. I wondered if the recruitment of DDX3 to these cytoplasmic speckles by HCV Core protein could prevent DDX3 from shuttling as normal between the cytoplasm and the nucleus. To this end, I transfected HeLa cells with expression plasmid for Ha-tagged Core protein from a range of HCV isolates, referred to as Con1-Ha, H77-Ha, and JFH1-Ha. Con1 is derived from genotype 1b, H77 is derived from genotype 1a and JFH1 is derived from genotype 2a. Cells were subsequently treated with the CRM-1 inhibitor Leptomycin B (LMB), and stained for Ha-Core protein and endogenous DDX3. Ha-Core protein from all genotypes co-localised with endogenous DDX3 in the cytoplasm of cells, in cells left untreated and in cells treated with LMB (Figure 5.16, Figure 5.17, Figure 5.18). The expression of Ha-Core recruited endogenous DDX3 into distinct cytoplasmic speckles in both the treated and untreated cells, and the Core protein from all genotypes had the same effect. Importantly, endogenous DDX3 had a nuclear localisation in cells not expressing the HCV-Core protein after treatment with LMB, suggesting that HCV-Core protein is affecting the nuclear shuttling of DDX3.

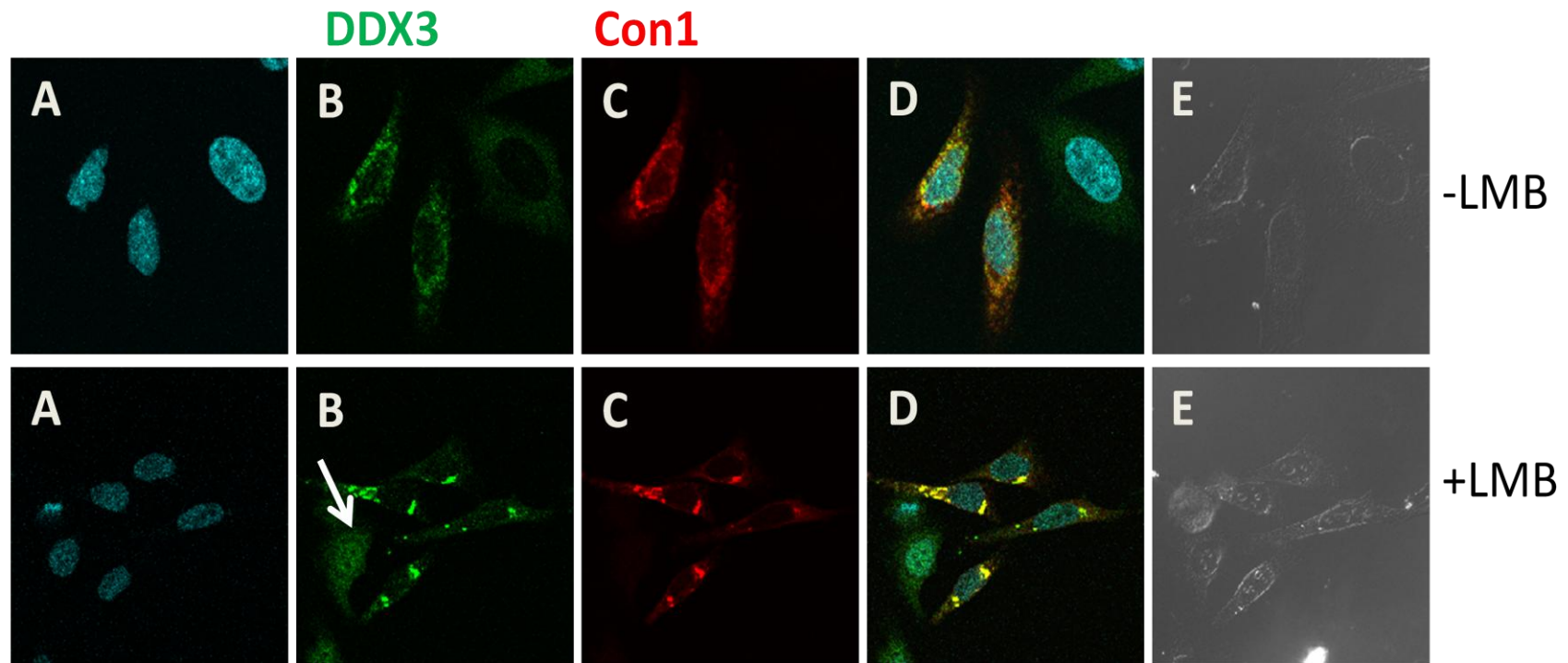


**Figure 5.16: HCV Core protein from different genotypes Con1 of HCV virus prevents shuttling of DDX3 into the nucleus.**

HeLa cells were transfected with expression plasmids for HCV Core protein from different genotype Ha-Con1 and treated with 20mM Leptomycin B (LMB) for 2 hours or left untreated. Cells were stained with  $\alpha$ -DDX3 (*Bethyl*) and  $\alpha$ -rabbit Alexa Fluor-488 and  $\alpha$ -Ha Alexa Fluor-594. Arrows indicate cells not expressing Core protein with nuclear DDX3 after treatment with LMB. **Key:** A (DAPI), B (DDX3), C (Ha-tagged Core), D (merge A,B and C) and E (Contrast).

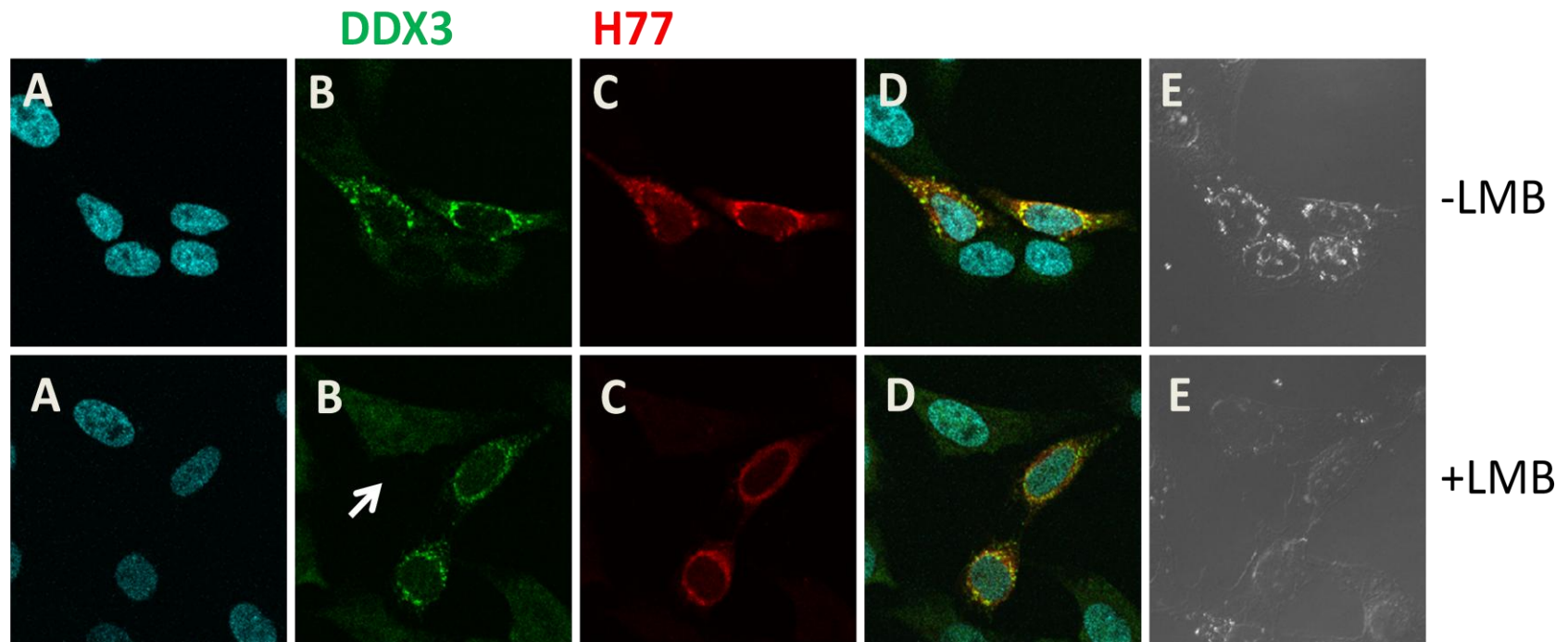


**Figure 5.17: HCV Core protein from different genotypes H77 of HCV virus prevents shuttling of DDX3 into the nucleus.**

HeLa cells were transfected with expression plasmids for HCV Core protein from different genotypes, Ha-Con1, Ha-H77 or Ha-Jc1 and treated with 20mM Leptomycin B (LMB) for 2 hours or left untreated. Cells were stained with  $\alpha$ -DDX3 (*Bethyl*) and  $\alpha$ -rabbit Alexa Fluor-488 and  $\alpha$ -Ha Alexa Fluor-594. Arrows indicate cells not expressing Core protein with nuclear DDX3 after treatment with LMB. **Key:** A (DAPI), B (DDX3), C (Ha-tagged), D (merge A, B and C) and E (Contrast).

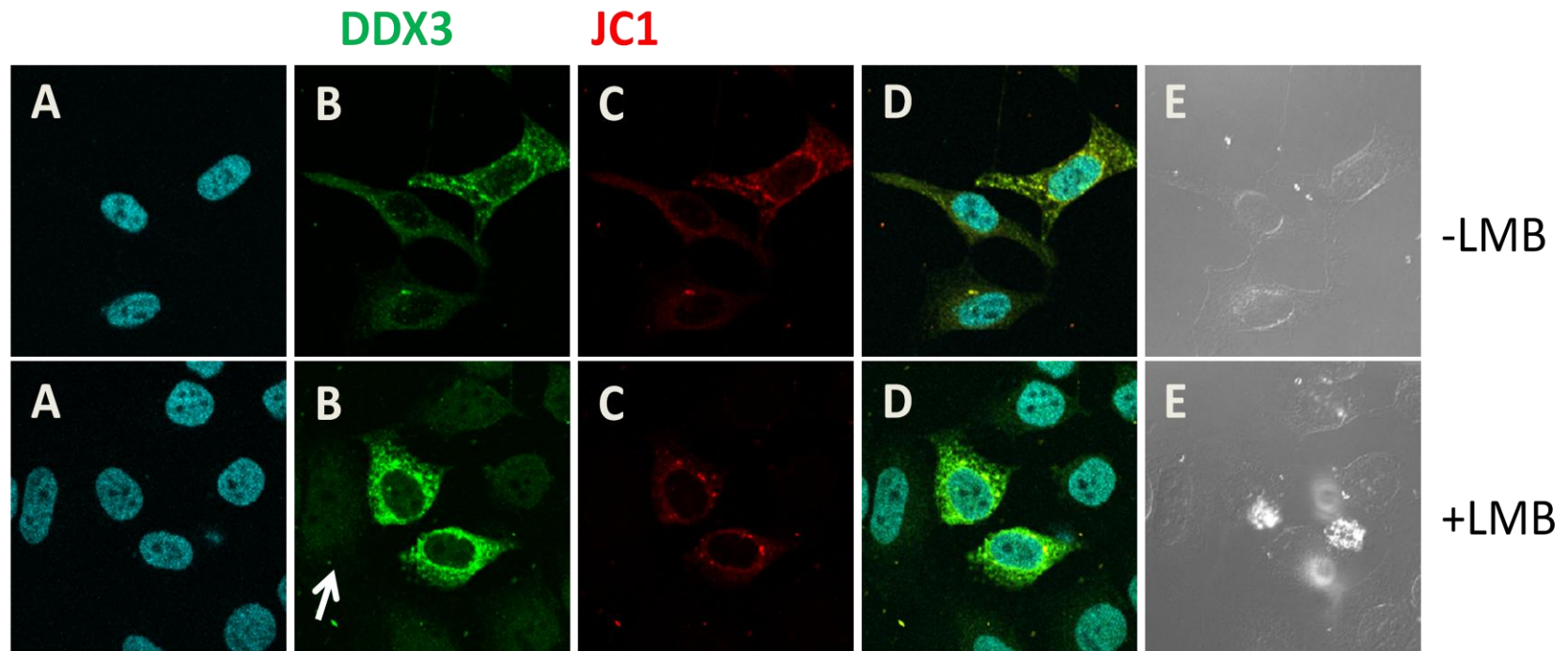


**Figure 5.18: HCV Core protein from different genotypes JC1 of HCV virus prevents shuttling of DDX3 into the nucleus.**

HeLa cells were transfected with expression plasmids for HCV Core protein from genotypes Ha-Jc1 and treated with 20mM Leptomycin B (LMB) for 2 hours or left untreated. Cells were stained with  $\alpha$ -DDX3 (*Bethyl*) and  $\alpha$ -rabbit Alexa Fluor-488 and  $\alpha$ -Ha Alexa Fluor-594. Arrows indicate cells not expressing Core protein with nuclear DDX3 after treatment with LMB. **Key:** A (DAPI), B (DDX3), C (Ha-tagged HCV Core), D (merge A, B and C) and E (Contrast).

As stated earlier, overexpressed HCV Core protein redistributed endogenous DDX3 protein in HeLa cells, changing DDX3 from a diffuse cytoplasmic localisation to a cytoplasmic speckle localisation. HCV Core protein has been previously been reported to localise to lipid droplets in hepatocytes during HCV infection. To this end, I used HepG2 cells (a hepatocyte cell line) to test if DDX3 was recruited to lipid droplets by HCV Core protein. HepG2 cells were transfected with expression plasmids for Ha-tagged Con1 and treated with oleic acid (Sigma) overnight to induce lipid droplets. HepG2 cells were then stained for Ha-Con1 and endogenous DDX3 (Figure 5.19 A). I also stained lipid droplets using the lysochrome dye SUDAN III and stained for endogenous DDX3. Since overexpressed Con1 caused a strong redistribution of endogenous DDX3, I could identify the cells overexpressing HCV Core protein. In (Figure 5.19 B), Ha-Con1 overexpression caused endogenous DDX3 to localise around lipid droplets.

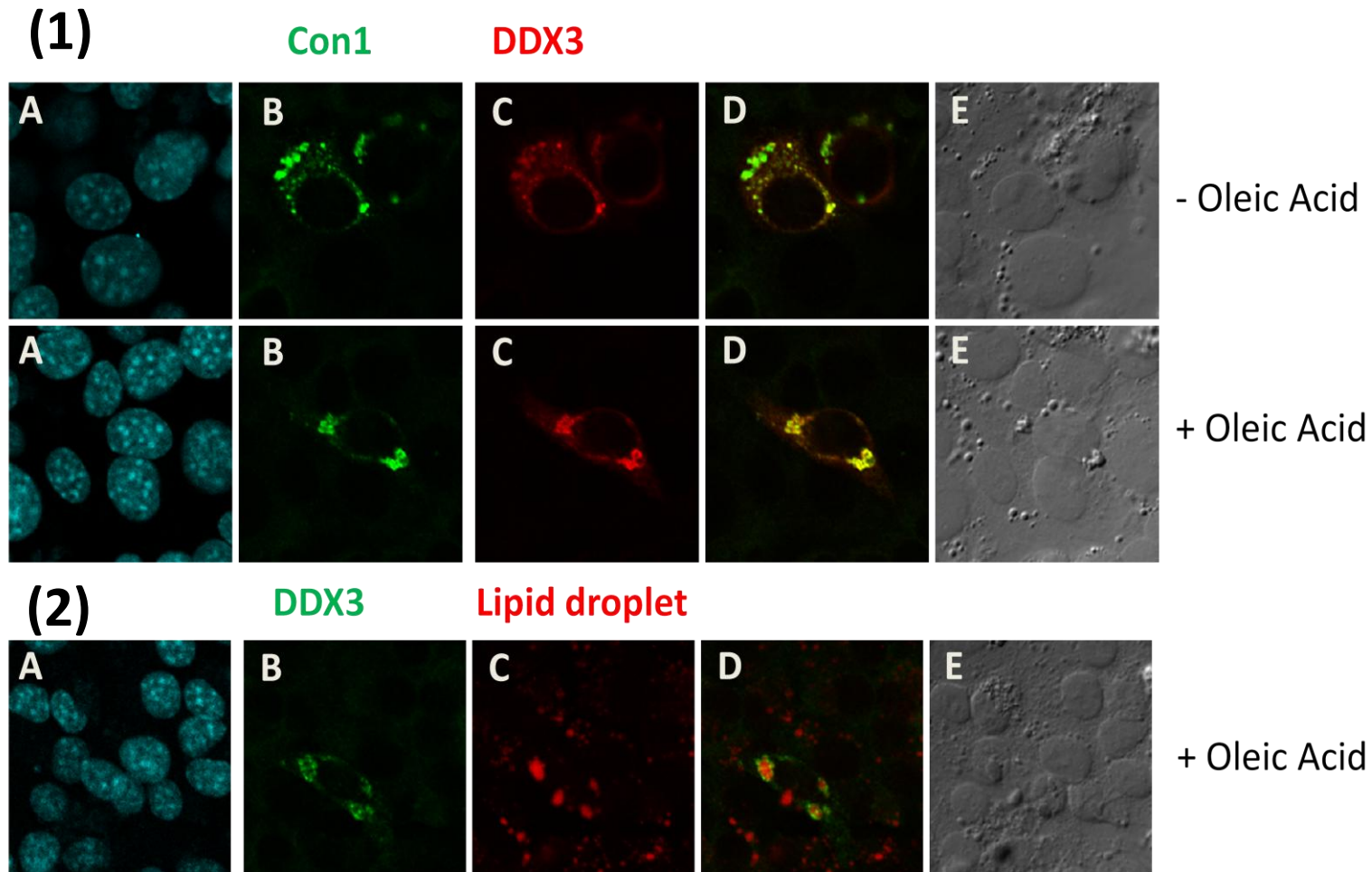


**Figure 5.19: HCV-Con1 and endogenous DDX3 co-localise around lipid droplets in HepG2 hepatocyte cells line.**

**(1):** HepG2 cells were transfected with Ha-Con1 and treated with oleic acid or left untreated. B: Cells were stained with  $\alpha$ -DDX3 (Bethyl) and  $\alpha$ -rabbit Alexa Fluor-488 and  $\alpha$ -Ha Alexa Fluor-594. Key: A (DAPI), B (DDX3), C (Ha-tagged Core), D (merge B and C) and E (Contrast). **(2):** HepG2 cells were transfected with Ha-Con1 and treated with oleic acid. Cells were stained with  $\alpha$ -DDX3(Bethyl) and  $\alpha$ -rabbit Alexa Fluor-488 and lipid droplets were stained with Sudan III dye. Key: A (DAPI), B (DDX3), C (Lipid droplet), D (merge B and C) and E (Contrast).

#### 5.3.4.3. Core protein inhibits DDX3 shuttling through a direct interaction.

Since HCV Core protein causes a re-distribution of DDX3 to cytoplasmic granules we wondered if a HCV Core mutant lacking the ability to interact with DDX3 would also cause the re-distribution. A Con1 Y35A mutant has been reported to lack the ability to interact with DDX3 (Angus et al. 2010). Here, HepG2 cells were transfected with expression plasmids for Ha-tagged Con-1 and a Con-1 Y35A mutant. In Figure 5.20, overexpression of the Ha-Con1 caused endogenous DDX3 to localise to cytoplasmic granules, however the Con1 Y35A mutant did not change DDX3 localisation. The degree of co-localisation of the mutant HCV Core protein with DDX3 was significantly less than wild type HCV Core, suggesting that DDX3 is recruited to lipid droplets via a direct interaction with HCV Core.

DDX3's interaction with HCV Con1 protein prevented DDX3 from shuttling between the cytoplasm and nucleus. Since HCV Con1 Y35A did not change DDX3 localisation, we wondered if DDX3 shuttled as normal in cells overexpression HCV Con1 Y35A. To this end, we transfected HepG2 cells with expression plasmid for Ha-tagged Con1 Y35A protein and subsequently treated cells with the CRM-1 inhibitor Leptomycin B (LMB), and stained for Ha-Core protein and endogenous DDX3. Ha-Con1 Y35A protein did not inhibit the nuclear import of DDX3, as DDX3 localised to the nucleus in cells expressing Ha-Con1 Y35A after treatment with LMB (Figure 5.21).

(1)

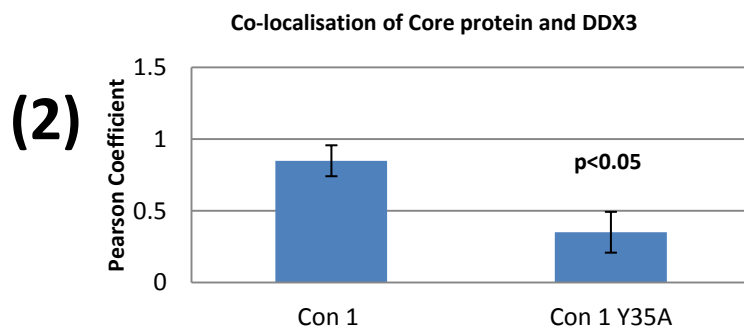
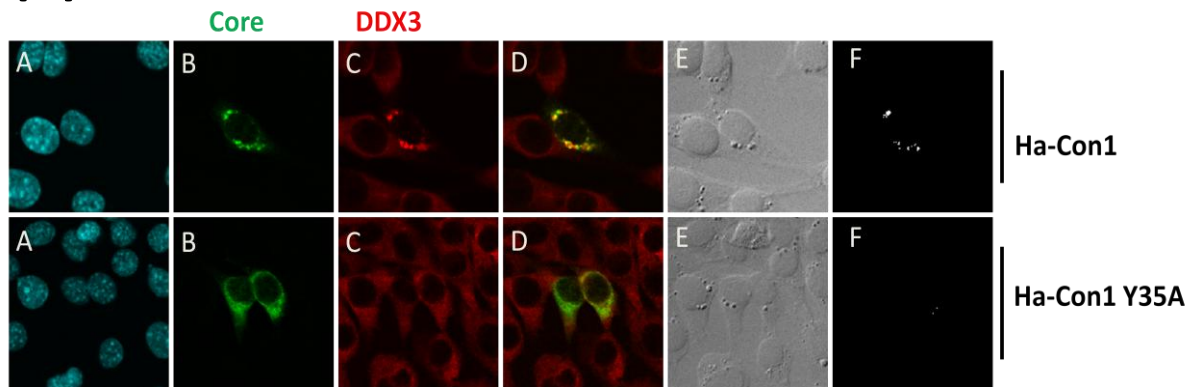


**Figure 5.20: Con1 Y35A mutant does not cause change in DDX3 localisation.**

(1): HepG2 cells were transfected with Ha-Con1 and Ha-Con1 Y35A mutant and stained with  $\alpha$ -Ha (Covance) secondary and  $\alpha$ -mouse Alexa Fluor-488, and  $\alpha$ -DDX3 (Bethyl) and  $\alpha$ -rabbit Alexa Fluor-594. Co-localisation points highlight the positions of overlapping signals, generated using Olympus Fluoview Co-localisation Software. **Key:** A (DAPI), B (Ha-Core), C (DDX3), D (merge B and C), E (contrast) and F (Co-localisation points). (2): Pearson's coefficient was calculated for the degree of co-localisation between HCV Core protein and DDX3. Results represent >10 cells from  $n=2$  independent experiments.

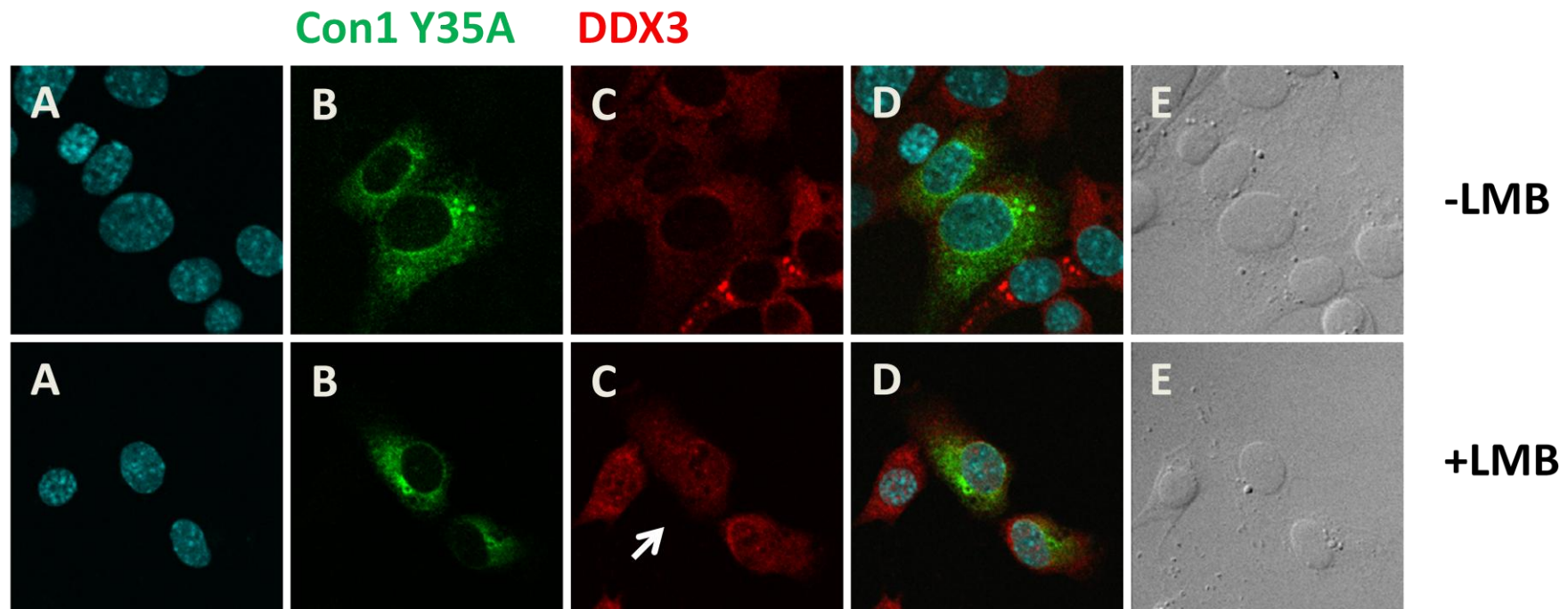


**Figure 5.21: HCV Con1 Y35A Core protein does not prevent shuttling of DDX3 into the nucleus.**

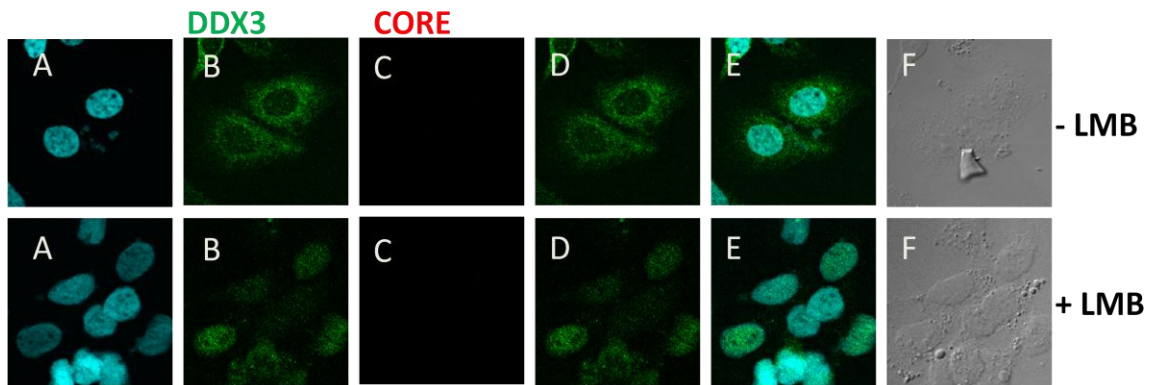
HeLa cells were transfected with expression plasmids for HCV Con1 Y35A Core protein and treated with 20mM Leptomycin B (LMB) for 2 hours or left untreated. Cells were stained with  $\alpha$ -DDX3 (*Bethyl*) and  $\alpha$ -rabbit Alexa Fluor-488, and  $\alpha$ -Ha Alexa Fluor-594. Arrows indicate cells not expressing Core protein with nuclear DDX3 after treatment with LMB. **Key:** A (DAPI), B (Ha-tagged Con Y35A), C (DDX3), D (merge A, B and C) and E (Contrast).

#### 5.3.4.4. DDX3 nuclear shuttling is inhibited in Huh7 cells expressing non-replicating full length HCV genome

---

I was interested in investigating whether HCV Core protein changes the localisation of DDX3 in cells expressing all the viral proteins associated with HCV. The non-replicating pBRTM/HCV1-3011 DNA construct (Grakoui et al. 1993) contains the entire HCV H77 genotype 1a open reading frame under the control of the T7 promoter, but lacks the 3' and 5' untranslated regions. Huh7 cells expressing T7 polymerase were transfected for 12h using Lipofectamine2000 with the T7-driven pBRTM/HCV1-3011 DNA construct and control EV (Stevenson et al. 2011). I was also interested in confirming whether HCV Core protein prevented the shuttling of DDX3. Therefore, cells were treated with Leptomycin B (LMB) or left untreated, and stained for HCV Core protein (*Abcam*) and endogenous DDX3 (*Bethyl*). As shown in Figure 5.22, Huh7 cells transfected with the pBRTM/HCV1-3011 DNA construct expressed HCV Core protein, whereas cells transfected with EV did not. DDX3 protein co-localised with HCV Core in cytoplasmic speckles in cells expressing HCV Core protein, and treatment with LMB failed to cause DDX3 to localise to the nucleus. Treatment with LMB caused DDX3 to localise to the nucleus in control cells transfected with EV, confirming that LMB treatment worked in this experiment. These results confirm that expression of HCV Core protein causes DDX3 to localise to cytoplasmic speckles and also prevents the nuclear shuttling of DDX3.

## Control



## HCV DNA construct

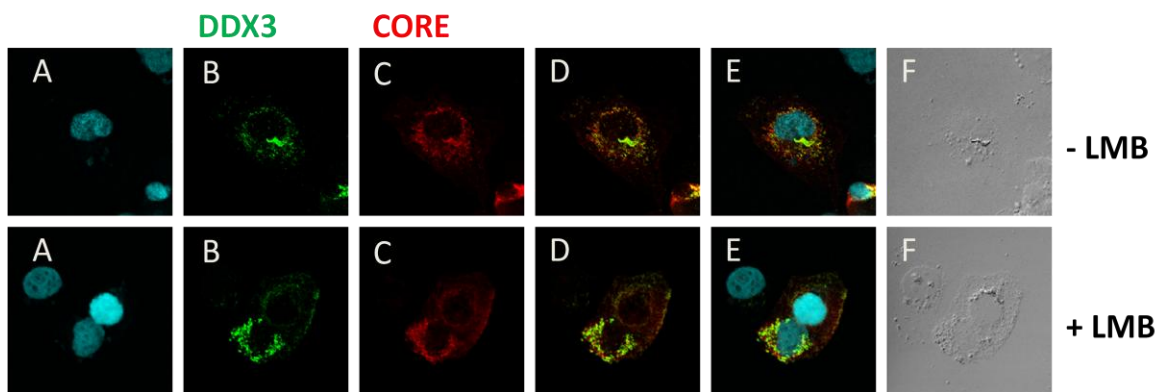


**Figure 5.22: HCV Core protein prevents shuttling of DDX3 into the nucleus.**

Huh7 cells were transfected with expression plasmids for pBRTM/HCV1-3011 construct and control EV, and treated with 20mM Leptomycin B (LMB) for 2 hours or left untreated. Cells were stained with  $\alpha$ -DDX3 (*Bethyl*) and  $\alpha$ -rabbit Alexa Fluor-488, and  $\alpha$ -HCV Core (*Abcam*) and  $\alpha$ -Alexa Fluor-594. **Key:** A (DAPI), B (DDX3), C (HCV Core), D (merge B and C), E (merge A,B and C) and F (contrast). n=1.

#### 5.3.4.5. HCV infection causes cellular redistribution of endogenous DDX3 in a hepatocyte cell lines

---

Using a HCV infection system, we confirmed whether DDX3's localisation changed during HCV infection. Huh7 cells (a hepatocyte cell line) were infected with HCV virus (J6/JFH genotype 2a) at MOI=0.5 (ie. one viral particle for every two cells seeded) for 72 hours (Lindenbach et al. 2005). I was also interested in confirming whether HCV infection prevented the shuttling of DDX3, therefore cells were also treated with LMB or left untreated, and subsequently stained for HCV Core protein (*Abcam*) and endogenous DDX3 (*Bethyl*). As shown in Figure 5.23, in Huh7 cells infected with HCV DDX3 changed from a diffuse cytoplasmic localisation to a cytoplasmic speckle localisation, co-localising with the HCV-Core protein in these cytoplasmic speckles. LMB treatment failed to sequester DDX3 in the nucleus in cells infected with HCV and expressing HCV Core protein. Since DDX3 localised to the nucleus in cells treated with LMB and not infected with HCV (indicated by white arrow in Figure 5.23), this confirmed that LMB treatment worked. These results confirmed that HCV infection causes DDX3 to co-localise with HCV Core at cytoplasmic speckles, and also that HCV infection prevents the nuclear shuttling of DDX3.

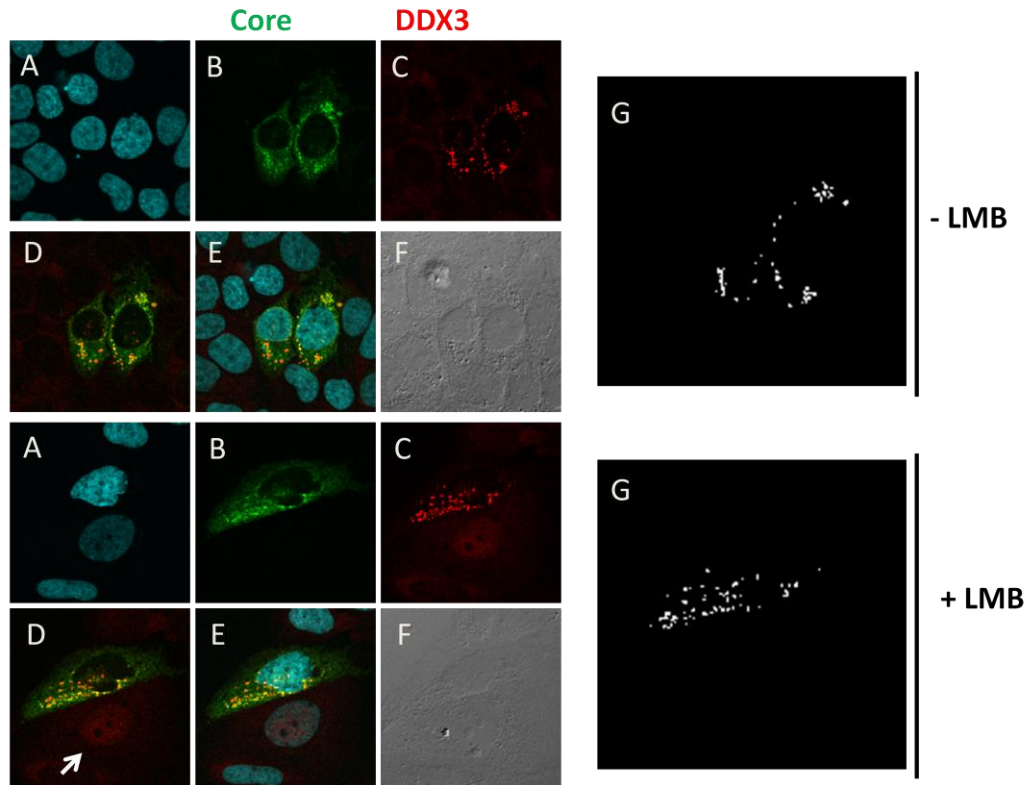


**Figure 5.23: HCV infection causes DDX3 to co-localise with HCV Core protein in cytoplasmic speckles in Huh7 cells.**

Huh7 cells were infected with HCV virus at an MOI=0.5 for 72h and treated with 20mM Leptomycin B (LMB) for 2 hours or left untreated. Cells were stained with  $\alpha$ -HCV Core (*Abcam*) and secondary and  $\alpha$ -mouse Alexa Fluor-488 and  $\alpha$ -DDX3 (*Bethyl*) and  $\alpha$ -rabbit Alexa Fluor-594. Co-localisation points highlight the positions of overlapping signals, generated using Olympus Fluoview Co-localisation Software. **Key:** A (DAPI), B (HCV Core), C (DDX3), D (merge B and C), E (merge A, B and C), F (contrast) and G (Co-localisation points). n=2.

#### 5.3.4.6. Does HCV Core expression change protein expression of DDX3?

Our previous results showed overexpression of HCV Core protein and HCV infection changed the localisation of endogenous DDX3. We also observed that the staining intensity for DDX3 was increased in cells overexpressing Core protein. This observation suggested that there might be an increase in DDX3 protein after overexpression of HCV Core protein and HCV infection. To investigate whether expression of HCV Core affects the amounts of DDX3 protein, we transfected HEK293Ts cells with varying amounts of a construct for Ha-tagged Con-1. As shown in Figure 5.24, endogenous DDX3 expression mirrored that of overexpressed Ha-Con1. In general, there was more DDX3 protein in cells; overexpressing Ha-Con1 compared to cells transfected with EV. There was less Ha-Con1 protein and less endogenous DDX3 in cells transfected with the highest amount of HCV Core protein, however this could be due to cell death.

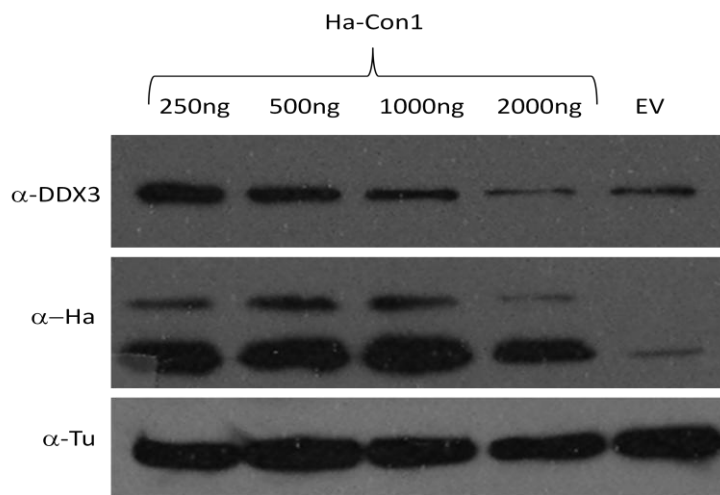


**Figure 5.24: Expression of Ha-tagged Core protein increased endogenous DDX3 protein expression.** HEK293ts were transfected with varied amounts of an expression plasmid for Ha-tagged HCV Core Con1. Cells were lysed and subjected to SDS-PAGE gel electrophoresis and semi-dry transfer. Blots were probed with  $\alpha$ -DDX3 (*Bethyl*),  $\alpha$ -Ha (*Covance*) and  $\alpha$ -Tubulin (*Abcam*). Representative blot of three experiments.

#### 5.3.4.7. HCV causes redistribution of eIF4E

Since HCV Core protein caused DDX3 to localise to cytoplasmic speckles, we wondered if the localisation of other RNA associated proteins was sensitive to HCV Core expression. We decided to examine the localisation of the RNA helicase eIF4E after overexpression of HCV Core protein. DDX3 has been shown to repress cap-dependent translation but to promote HCV IRES-mediated translation, through an interaction with eIF4E (Shih et al. 2008). HeLa cells were transfected with constructs Ha-tagged HCV Core protein and stained for endogenous eIF4E. As shown in Figure 5.25, overexpression of Ha-tagged HCV Core protein resulted in a small amount of eIF4E co-localising with Ha-Con1 in cytoplasmic speckles. The majority of eIF4E had a predominantly cytoplasmic localisation, suggesting that only a small amount of eIF4E protein is recruited to cytoplasmic granules compared to DDX3.

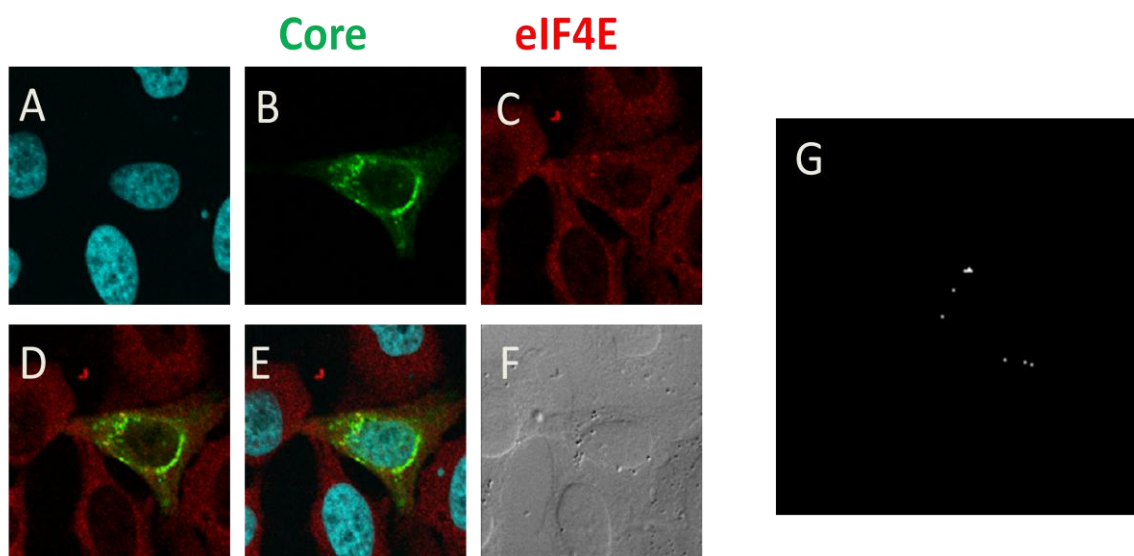


**Figure 5.25: Overexpression of HCV Core protein Con1 causes some eIF4E to co-localise in cytoplasmic speckles with Core protein.**

HeLa cells were transfected with Ha-tagged HCV Core Con1. Cells were stained for  $\alpha$ -eIF4E (*Abcam*) and  $\alpha$ -rabbit alexa Fluor-594 and  $\alpha$ -Ha (*Covance*) and  $\alpha$ -mouse Alexa Fluor-488. Co-localisation points highlight the positions of overlapping signals, generated using Olympus Fluoview Co-localisation Software. **Key:** A (DAPI), B (Ha-tagged Core), C (DDX3), D (merge B and C), E (merge A,B and C) and F (Co-localisation points).

#### 5.3.4.7. Does DDX3 localise differently in primary cells compared to transformed cells?

---

As stated earlier, DDX3 has been suggested to have a nuclear localisation in non-transformed cells, and a cytoplasmic localisation in transformed cells (Chao et al. 2006). I decided to test DDX3 localisation in primary hepatocytes versus a hepatocyte cell line. HepG2 cells and primary hepatocytes were grown on coverslips and prepared for immunofluorescence. DDX3 had a stronger nuclear localisation in primary hepatocytes compared to transformed HepG2 cells (Figure 5.26).

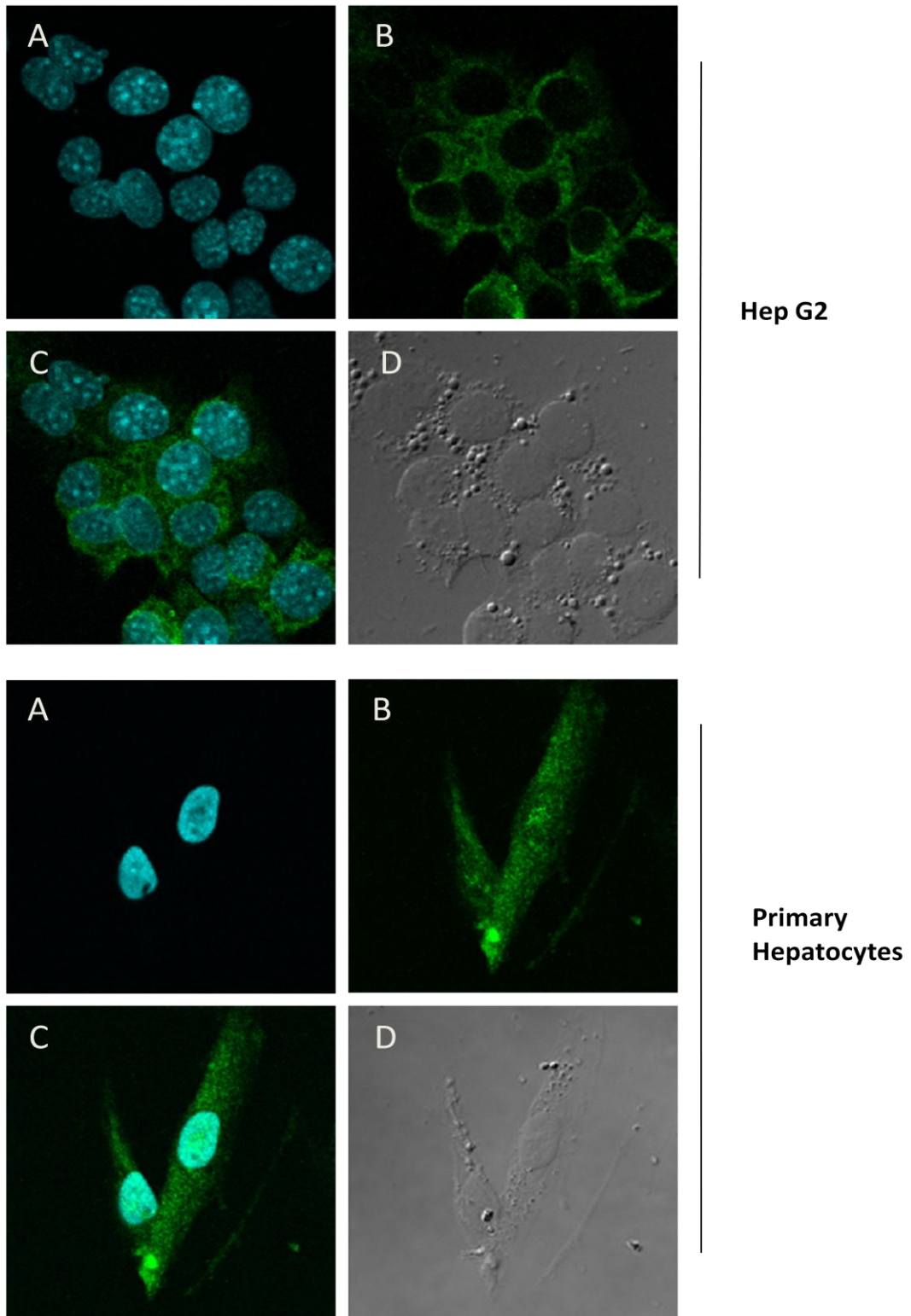


**Figure 5.26: DDX3 has a more nuclear localisation in primary cells compared to transformed cells.** HepG2 cells and Primary Hepatocytes cells were grown on coverslips and stained with a primary  $\alpha$ -DDX3 (*Bethyl*) and secondary  $\alpha$ -rabbit Alexa Fluor-488 as described in Chapter 2. **Key:** A (DAPI), B ( $\alpha$ -DDX3), C (Merge A+B), D (Contrast).

#### 5.4. Discussion

---

Here I have investigated the cellular localisation of DDX3 in response to viral infection. Since DDX3 has been suggested to play a role in nuclear signalling events, for example DDX3 has been shown to bind to the IFN $\beta$  promoter upon infection with *Listeria monocytogenes* (Soulat et al. 2008), I speculated that DDX3 would translocate to the nucleus in response to immunological stimulation. I found that DDX3 localisation did not change drastically in response to a range of stimuli, namely SeV, IFN, and Il-1 $\alpha$ /TNF- $\alpha$ . A small portion of DDX3 could still be translocating to the nucleus in response to SeV, as it possible that only small amounts of DDX3 are needed in the nucleus for IFN $\beta$  induction. Life cell imaging could be used to give further insight into the real time translocation of DDX3 in response to various stimuli. I also found no change in DDX3 cellular localisation in response to overexpression of IKK $\epsilon$  and after SeV stimulation. In the future, it would be interesting to examine the localisation of DDX3 in response to these stimuli in more immunologically relevant cells, such as primary macrophages and dendritic cells.

Here I have also examined the relationship between viral proteins and DDX3. I have shown that overexpression of HIV-Rev protein can cause DDX3 to accumulate in the nucleolus of HeLa cells. I have also shown that the N-terminus (1-408) of DDX3 directly interacts with HIV-Rev protein. Interestingly, HIV-Rev also re-localised the exportin CRM-1 to the nucleolus, suggesting that HIV-Rev recruits proteins required for the nuclear export of HIV-mRNA into the nucleolus. The re-localisation of CRM-1 by overexpression of HIV-Rev had been described previously, however to my knowledge the re-localisation of DDX3 has not been reported before

(Zolotukhin & Felber 1999; Daelemans et al. 2002). DDX3 has been shown to be part of the T cell nucleolar proteome (Jarboui et al. 2011), and HIV Tat expression has been shown to enrich DDX3 in the nucleolus of Jurkat T cells also (Jarboui et al. 2012). Many proteins from RNA viruses localise to the nucleolus, utilising the nucleolus to promote viral replication (Hiscox 2007). Studies have shown that HIV-Tat and HIV transcripts must associate with the nucleolus for HIV replication (Michienzi et al. 2002; Michienzi et al. 2000), to maybe DDX3 plays a role in viral RNA processing in the nucleolus of HIV infected cells.

Previous studies have shown that overexpression of DDX3 promoted Rev mediated gene expression through its role in HIV RNA nuclear export (Yedavalli et al. 2004), while other studies have shown that DDX3 promotes both Rev-dependent and independent HIV gene expression, by being involved in HIV-1 RNA translation (Liu et al. 2011). DDX3 has also been shown to be required for translation initiation of complex RNAs which contain secondary structures within 5'UTR, such as HIV RNAs which contain the TAR hairpin motif within its 5'UTR (Soto-Rifo et al. 2012). In our hands, overexpression of DDX3 did not affect Rev-dependent expression of HIV-Gag protein. Since there was already endogenous DDX3 in these cells, it would be interesting to investigate whether knockdown of DDX3 affects Rev-mediated expression of HIV Gag protein. HIV-Rev is known to interact with CRM-1 via its leucine rich NES, however recruitment of CRM-1 to the nucleolus does not necessarily occur due to this interaction. It would be interesting to examine the HIV-Rev protein recruitment of CRM-1 in the absence of DDX3, using knockdown cells. In Chapter Three, I have shown that DDX3 has a functional NES, which can interact with CRM-1. Since HIV-Rev protein and DDX3 both have functional NESs it

is difficult to see how both proteins would interact with CRM-1 at the same time to export RRE-containing RNA. Since DDX3 is a multifunctional protein, it is not surprising that HIV utilises the different functions of DDX3 to promote viral replication. Future work is needed to further characterise the various roles DDX3 might play in HIV replication.

Here I have also examined the relationship between DDX3 and HCV Core protein. We found that HCV Core protein changed the cellular localisation of DDX3, and that HCV Core protein prevented the nucleocytoplasmic shuttling of DDX3. HCV Core protein has been reported to recruit DDX3 to lipid droplets by various groups (Angus et al. 2010; Ariumi, Kuroki, Kushima, et al. 2011; Sato et al. 2006), however I am the first to show that HCV prevents the nucleocytoplasmic shuttling of DDX3. Angus et. al showed that DDX3 co-localised to lipid droplets in cells infected with HCV, however they suggested that DDX3's interaction with HCV was not required for HCV replication (Angus et al. 2010). HCV infection has also been shown to utilise Processing Body (PB) and Stress Granule (SG) components to promote HCV replication, shutting down translation of cellular mRNAs while promoting translation of viral RNA (Ariumi, Kuroki, Kushima, et al. 2011; Garaigorta et al. 2012; Ruggieri et al. 2012). Here I found that two SG components, DDX3 and to a lesser extent eIF4E, were recruited to cytoplasmic speckles by HCV Core protein. Since the interaction of DDX3 with Core has been suggested not to be required for HCV infection, it is possible that in the absence of a Core-DDX3 interaction other SG components can still be recruited to cytoplasmic granules. As earlier stated, mis-localisation of DDX3 could potentially inhibit many of DDX3 nuclear and cytoplasmic functions. Mis-localisation of DDX3 has been found in some cancers, with DDX3

switching from a nuclear to cytoplasmic localisation to in transformed cells (Chang et al. 2006). It is appealing to think that the change from a nuclear to a cytoplasmic localisation in HCC is caused by DDX3's interaction with HCV Core protein. I have shown that in primary hepatocytes DDX3 has a nuclear and cytoplasmic localisation, and changes to a predominantly cytoplasmic localisation in transformed cells. Is it possible that mis-localisation of DDX3 by HCV Core protein might be a causative factor in HCV associated cancers? Several studies have implicated inactivation of p21<sup>waf1/cip1</sup> in HCV associated cancers (Fukushima et al. 2001; Feitelson et al. 2002). Since DDX3 has been shown to promote induction of the tumour suppressor p21<sup>waf1/cip1</sup>, sequestering DDX3 in the cytoplasm would likely inhibit expression of this tumour suppressor.

It is remarkable that two different viruses have the abilities to change the cellular localisation of DDX3 in distinct ways. The fact that it is advantageous for DDX3 to be nuclear for HIV and cytoplasmic for HCV shows that both the nuclear and cytoplasmic functions of DDX3 can be targeted by viruses to promote viral replication.

## Chapter 6 : Regulation of DDX3 localisation by cellular stress

During our initial investigations of DDX3's cellular localisation, we noticed that over-expressed DDX3, and even truncations lacking the NES, sometimes localised in distinct cytoplasmic speckles. We hypothesised that these cytoplasmic speckles were stress granules. During our investigations into HCV, we showed that DDX3 could also localise to distinct cytoplasmic speckles after HCV infection. HCV infection has been found to utilise SGs, both promoting and inhibiting the formation of SG to promote HCV replication (Ariumi, Kuroki, Kushima, et al. 2011; Ruggieri et al. 2012; Garaigorta et al. 2012). The following sections introduce RNA granules and the role DDX3 may play in SG formation.

### 6.1. Introduction to RNA granules

Gene expression can be controlled post-transcriptionally by regulating the level of protein synthesized from its mRNA. During the mRNA life cycle, nascent mRNA can be packaged into distinct granules which regulate the translation and decay of mRNA, including Processing Bodies (PBs) and Stress Granules (SGs). PBs are usually comprised of 5'-3' mRNA decay components and occur constitutively, increasing in size and number in response to cellular stresses (Anderson & Kedersha 2009). In general, PBs are involved in the decay of mRNAs, whereas SGs protect mRNA and allow re-initiation of translation as soon as cellular stress has been resolved. SGs are assembled after various cellular stresses, including oxidative, genotoxic or osmotic stress, heat shock or viral infection. Several different RNA-associated proteins are found in SGs and PBs, including RNA helicases, RNA binding proteins, transcription factors and translational regulators (Anderson & Kedersha 2008). Some known components of SGs are listed in Table 6.1. SGs are produced after phosphorylation

of translation initiation factor eIF2 $\alpha$  by stress inducible kinases (such as PKR), resulting in accumulation of stalled pre-initiation complexes containing 40s ribosome subunits (Srivastava 1998). SGs can contain mRNA transcripts of various proteins, including housekeeping genes. Interestingly, the mRNA of stress-induced proteins, such as HSP70 and HSP90, are not recruited to SG suggesting that SGs allow cells to preferentially translate mRNA required to resolve the cellular stress while protecting stalled mRNA (Anderson & Kedersha 2008). SGs allow rapid reactivation of translation upon stress recovery since ribosome pre-initiation complexes are retained in an assembled state. They are also suggested to promote cell survival, since they sequester components of apoptotic signal transduction pathways such as RACK1 (Arimoto et al. 2008).

<b>Protein Name</b>	<b>Protein function</b>	<b>Ref</b>
TIA-1 and TIAR	mRNA silencing	(Kedersha et al. 2002)
eIF4E	Translation	(Kedersha et al. 2005)
eIF4G	Translation	(Kedersha et al. 2005)
eIF3	Translation	(Kedersha et al. 2005)
Traf2	Signalling	(Kim et al. 2005)
G3BP	Ras signalling	(Tourrière et al. 2003)
PABP1	Translation, stabilisation	(Fraser et al. 1999)
Rpb4	Transcription	(Lotan et al. 2005)
DDX3	Transcription, signalling	(Shih et al. 2012)
DDX6	Transcription	(Nonhoff et al. 2007)
Caprin	Cell growth	(Solomon et al. 2007)

**Table 6.1 : Known stress granule components and their protein function.**

Studies have shown that SGs are induced rapidly after stress and disassemble slowly. Time lapse microscopy has shown that SGs are typically large structures with a fixed position in the cytoplasm, however their shape is constantly changing with components of SGs rapidly moving in and out of these granules, whereas PBs are small and move throughout the cytoplasm (Kedersha et al. 2005). SGs and PBs share many components, and have been shown to interact closely with each other,

with studies suggesting that mRNPs can be transferred between PBs and SGs, targeting some mRNA for decay (PBs) and others for protection (SGs).

Viruses have evolved a multitude mechanisms to interfere with cellular processes to facilitate the replication of viruses. Since SGs have been implicated in cell survival through sequestering of apoptotic mediators (Arimoto et al. 2008), it could be advantageous for viruses to induce SG to keep the host cell alive while allowing for viral replication. It can also be advantageous for viruses to induce the formation of SG, as shutting down of host protein translation prevents the production of pro-inflammatory mediators, and also promote IRES-dependent translation (Spriggs et al. 2008). Also many viruses have been suggested to both promote and inhibit SG formation throughout the viral life cycle (White & Lloyd 2012). For example, mammalian orthoreovirus (MRV) infection induces SG in the early stages of infection while inhibiting SG during the mid-phase (Smith et al. 2006; Lin et al. 2007).

Recently two groups have shown that during influenza virus A, the Non-Structural protein 1 (NS1) prevents the induction of SGs by PKR in response to viral double stranded RNA, thereby promoting translation of host mRNA (Onomoto et al. 2012; Khapersky et al. 2012). Virus induced SGs were shown to contain SG components, viral proteins, and RLRs namely MDA5, LGP2, and PKR. These SGs were suggested to be a distinct subset of anti-viral SG (avSGs), as they played a critical role in RIG-I mediated type I Interferon induction in response to virus (Onomoto et al. 2012).

HCV has also been shown to regulate formation of RNA granules, both inhibiting and inducing SG during viral replication (Ruggieri et al. 2012). One study showed

that HCV Core protein promotes translation of viral RNA by hijacking components of SG around lipid droplets, while inhibiting SG induction in response to oxidative stress (Ariumi, Kuroki, Kushima, et al. 2011). Another study involving HCV infection showed that during HCV infection there is fluctuation in SG formation, resulting in phases of active and stalled translation (Ruggieri et al. 2012).

#### 6.1.1. DDX3's association with stress granules

DDX3 could be placed at multiple stages of the mRNA life cycle, with DDX3 potentially having roles in translation initiation, transcription, mRNP remodelling and stress-induced RNA granule formation (Figure 6.1). The *S.cerevisiae* DDX3 homologue Ded1p has been shown to accumulate in PBs, with Ded1p playing a role in both translation and PB formation (Beckham et al. 2008). Human DDX3 has been shown to localise to cytoplasmic SGs in response to stress, interacting with SG components eIF4E, eIF4A and PABP1 (Lai et al. 2008). DDX3 has also been suggested to be a critical component of SG assembly, with knock-down of DDX3 repressing the formation of sodium arsenite-induced SGs in one study (Shih et al. 2012).

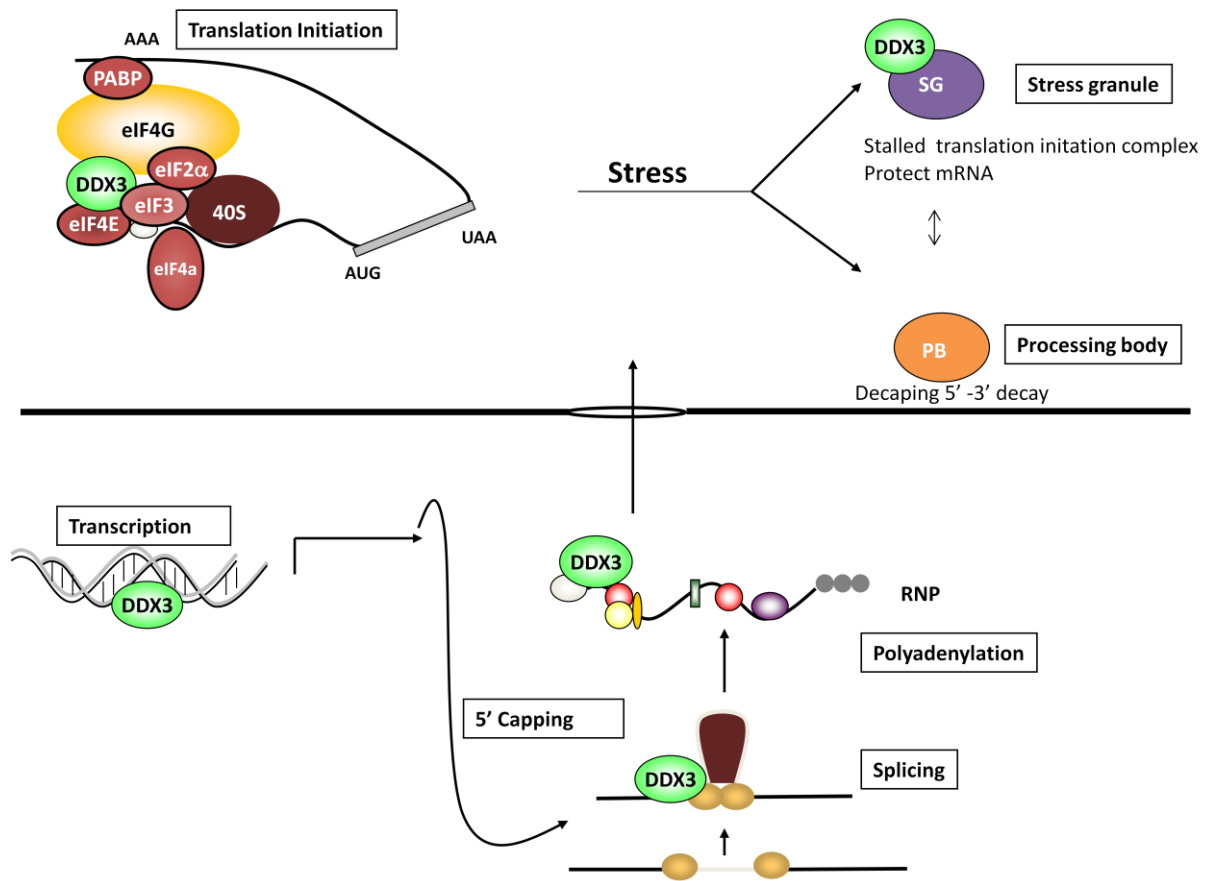


Figure 6.1: DDX3 can be placed at multiple levels of the mRNA life cycle.

### 6.1.2. Conclusion

---

The role of DDX3 in SG formation is unclear. Since viruses have evolved ways to subvert the mRNA life cycle to favour translation of viral mRNA, it is appealing to say that viruses might target DDX3's role in the mRNA life cycle for their benefit. It would be interesting to investigate whether DDX3 plays a role in assembly of avSG, since it has been shown that avSG assembly is required for IFN induction in response to viral infection (Onomoto et al. 2012).

### 6.2. Aims

---

I observed that over-expressed DDX3 and NES-deficient mutants localised to cytoplasmic granules on occasion. In this chapter I aimed to examine if these cytoplasmic granules were SG and whether DDX3 was recruited to SG in response to cellular stresses. I also aimed to determine if SG prevented the nucleocytoplasmic shuttling of DDX3 and also to identify the regions of DDX3 required for recruitment to stress granules.

## 6.3. Results

### 6.3.1. DDX3 localises to cytoplasmic granules in response to stress

Occasionally, I observed a distinct cytoplasmic speckle appearance of Ha-tagged DDX3 and DDX3 truncation mutants that normally had a nuclear localisation in HeLa cells (Figure 6.2). I hypothesized that these speckles could be stress granules, induced by overexpression of DDX3.

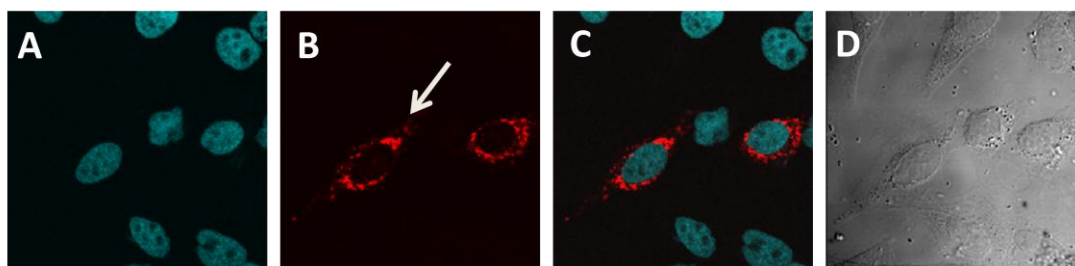


**Figure 6.2: Overexpressed DDX3 has a distinct cytoplasmic speckle localisation.**

HeLa cells were transfected with expression plasmids for WT Ha-DDX3, and stained with  $\alpha$ -Ha Alexa Fluor-594. **Key:** A (DAPI), B (Ha-DDX3), C (Merge A+B), D (Contrast).

First, I tested whether endogenous DDX3 could localise to stress granules after being treated with a stress granule inducing chemical. HeLa cells were treated with 1mM sodium arsenite (SA) for 20mins, and stained for endogenous DDX3 and endogenous eIF4E. SA causes oxidative stress, which results in formation of cytoplasmic SG. As shown in Figure 6.3, DDX3 and eIF4E had a diffuse cytoplasmic localisation in untreated cells, but in HeLa cells treated with 1 mM SA for 20 mins DDX3 and eIF4E co-localised in distinct cytoplasmic speckles. Co-localisation points show the position of overlapping signals between DDX3 and eIF4E staining generated using the Olympus Fluoview Co-localisation software, after treatment with SA there was a large increase in co-localisation. I also tested if overexpressed Ha-DDX3 behaved as endogenous. As shown Figure 6.3, Ha-DDX3 co-localised with

endogenous eIF4E in cytoplasmic speckles upon treatment with SA, suggesting that overexpressed DDX3 is also recruited to SG upon oxidative stress.

Cycloheximide has been reported to inhibit formation of SG. Cycloheximide traps mRNAs in polysomes by blocking translational elongation preventing translation but also induction of SG (Dang et al. 2009). I investigated if cycloheximide would prevent DDX3 speckling following cellular stress. HeLa cells were treated with cycloheximide at 10 $\mu$ g/ml for 4 hours followed by treatment with 1mM SA for 20 min or left untreated. Cells were stained for endogenous DDX3 and endogenous eIF4E. As shown in Figure 6.4, cycloheximide prevented induction of eIF4E and DDX3 containing speckles in response to SA. This suggests that the DDX3/eIF4E containing granules we observed are bona fide SGs.

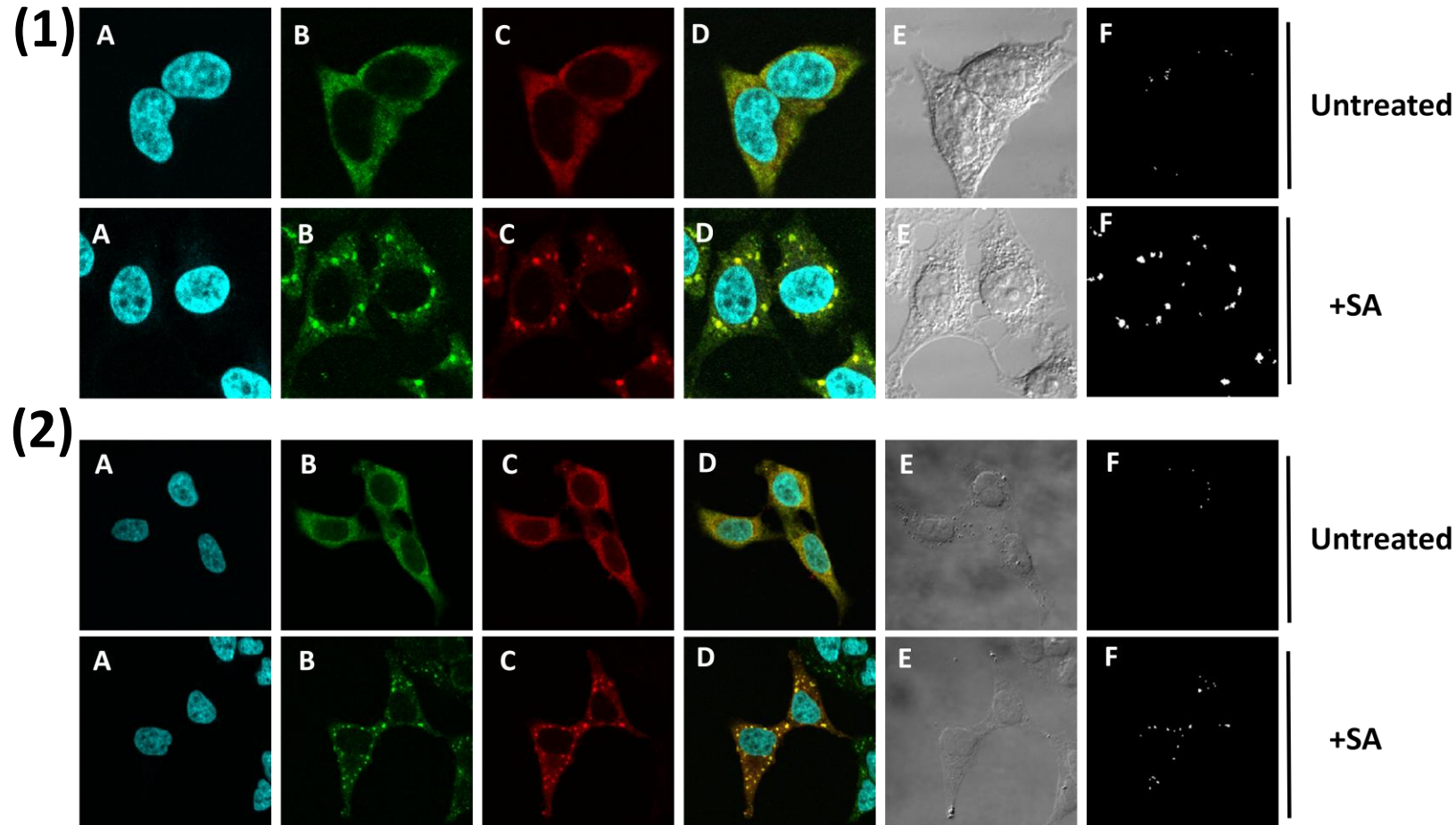


**Figure 6.3: DDX3 co-localises with stress granules component eIF4E after Sodium Arsenite induced oxidative stress.**

HeLa cells were treated with 1mM SA for 20mins or left untreated. Co-localisation points highlight the positions of overlapping signals, generated using Olympus Fluoview Co-localisation Software. **(1):** HeLa cells were stained with  $\alpha$ -eIF4E (*Abcam*) and secondary  $\alpha$ -rabbit Alexa Fluor-488, and  $\alpha$ -DDX3 (*Santa Cruz*) and secondary  $\alpha$ -mouse Alexa Fluor-594. **Key:** A (DAPI), B (DDX3), C (Merge A,B and C), D (Contrast) and F (Co-localisation Points). **(2):** HeLa cells were transfected with expression plasmids for Ha-DDX3. Cells were stained with  $\alpha$ - eIF4E (*Abcam*) and secondary  $\alpha$ -rabbit Alexa Fluor-488 and  $\alpha$ -Ha Alexa Fluor-594. **Key:** A (DAPI), B (eIF4E), C (DDX3), D (merge A,B and C), E (Contrast) and F (Co-localisation Points).

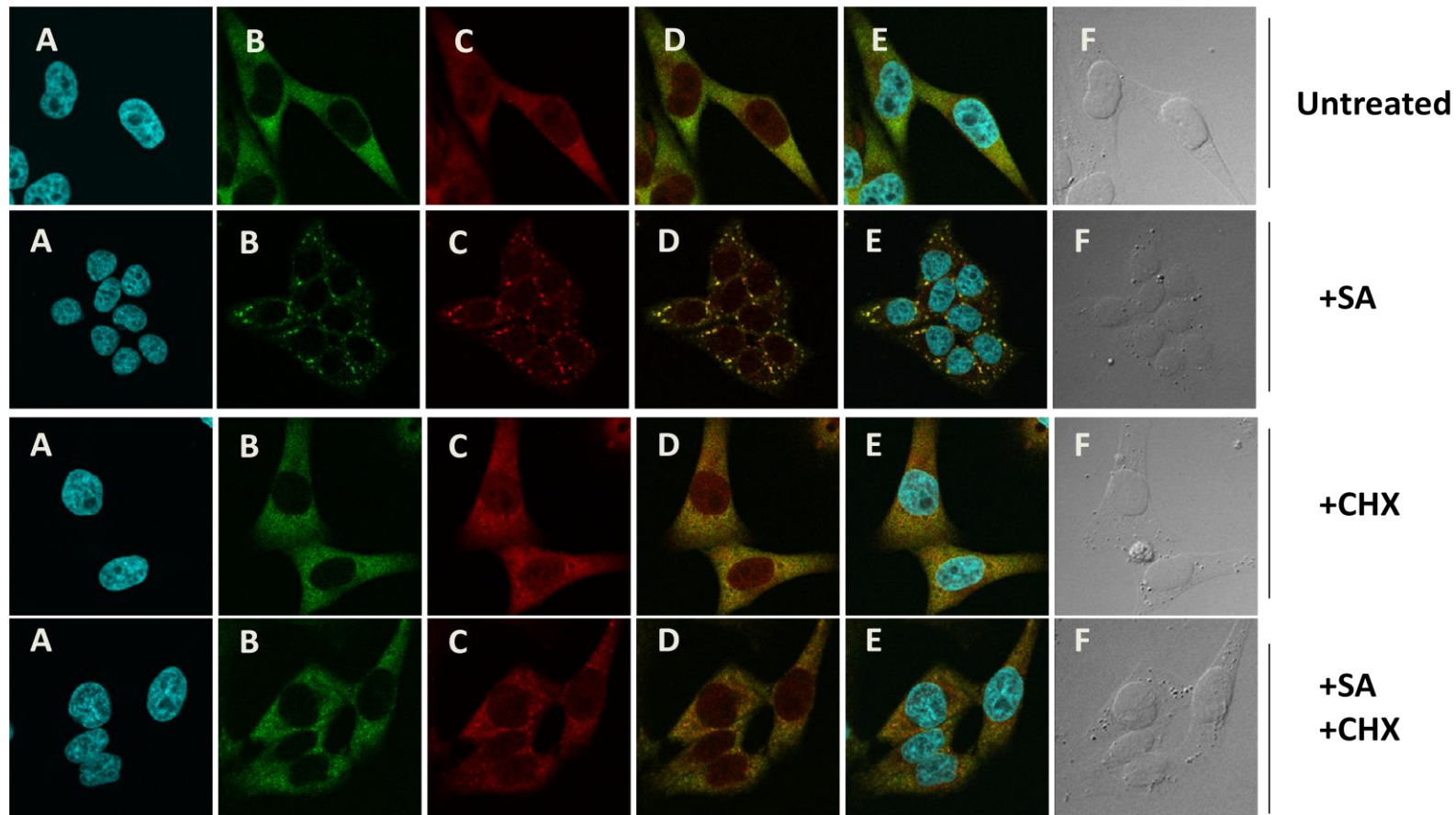


**Figure 6.4: Cycloheximide inhibits formation of DDX3 and eIF4E-containing granules.**

HeLa were treated with 10 $\mu$ g/ml CHX for 4h and treated with 1mM SA for 20mins or left untreated. HeLa cells were stained with  $\alpha$ -eIF4E (*Abcam*) and secondary  $\alpha$ -rabbit Alexa Fluor-488 and secondary, and  $\alpha$ -DDX3 (*Santa Cruz*) and secondary  $\alpha$ -mouse Alexa Fluor-594. **Key:** A (DAPI), B (eIF4E), C (DDX3), D (merge B and C), E (merge A, B and C) and F (Contrast).

### 6.3.2. Helicase activity not required for DDX3 to be recruited to stress granules

Stress granules can contain many RNA helicases, but whether helicase activity is required for recruitment of RNA helicases to SGs is unclear. The DDX3 K230E mutant lacks RNA helicase activity, therefore it could be used to test if helicase activity is required for recruitment to SGs. HeLa cells were transfected with an expression plasmid for a Myc-tagged K230E DDX3 mutant, and treated with 1mM SA for 20 minutes. As shown in Figure 6.5, Myc-K230E DDX3 had a diffuse cytoplasmic localisation in untreated cells, and co-localised in distinct cytoplasmic speckles with eIF4E upon treatment with SA. This suggests that helicase activity is not required for recruitment of DDX3 into stress granules.

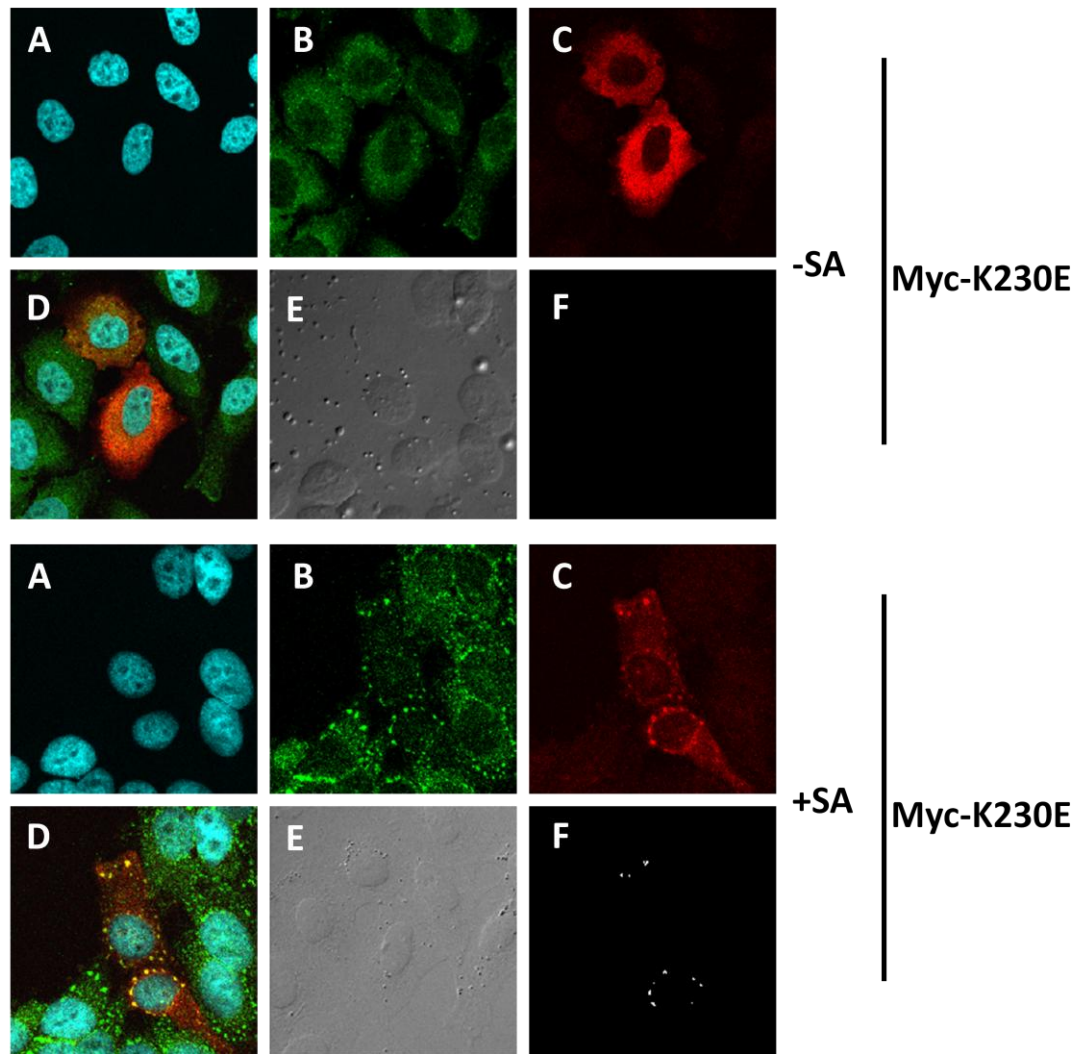


**Figure 6.5: DDX3 helicase mutant K230E co-localises with stress granule component eIF4E after Sodium Arsenite induced oxidative stress.**

HeLa cells were transfected with expression plasmids for myc-K230E DDX3 and treated with 1mM SA for 20 min. Cells were stained with  $\alpha$ -eIF4E (*Abcam*) and secondary  $\alpha$ -rabbit Alexa Fluor-488, and  $\alpha$ -myc (*Sigma*) and  $\alpha$ -Alexa Fluor-594. Co-localisation points highlight the positions of overlapping signals, generated using Olympus Fluoview Co-localisation Software. **Key:** A (DAPI), B (eIF4E), C (Myc-DDX3), D (merge A,B and C), E (Contrast) and F (Co-localisation Points).

### 6.3.3. Stress granules inhibit the nuclear import of DDX3

I had observed that DDX3 nuclear export defective mutants were sometimes found in cytoplasmic speckles in cells overexpressing DDX3 proteins. This suggested that stress granules might be affecting the nuclear shuttling of DDX3. To test if nuclear import was being affected, I transfected HeLa cells with expression plasmids for Ha-tagged DDX3, or the nuclear export defective mutants 22-662 and NES mutant. 14 hours after transfection, cells were treated with 1mM SA for 20 min, and stained as previously described. In Figure 6.6, untreated HeLa cells Ha-22-662 and the Ha-NES mutant had a nuclear localisation, and eIF4E had a predominately diffuse cytoplasmic localisation. After treatment with 1mM SA for 20min, the Ha-22-662 and the Ha-NES mutant were recruited to cytoplasmic speckles, along with endogenous eIF4E.

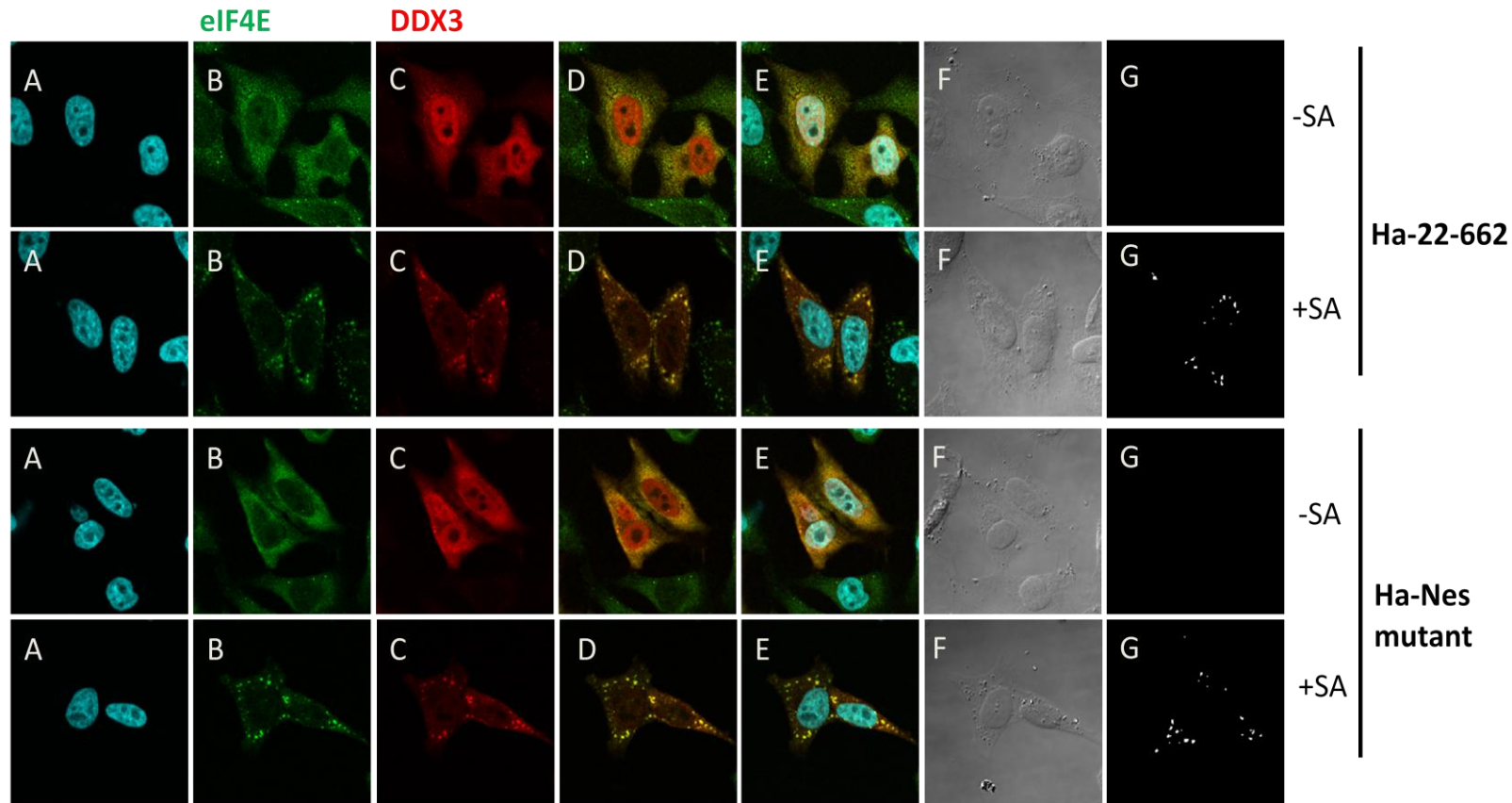


**Figure 6.6: Nuclear export deficient mutants are recruited to stress granules after Sodium Arsenite treatment.**

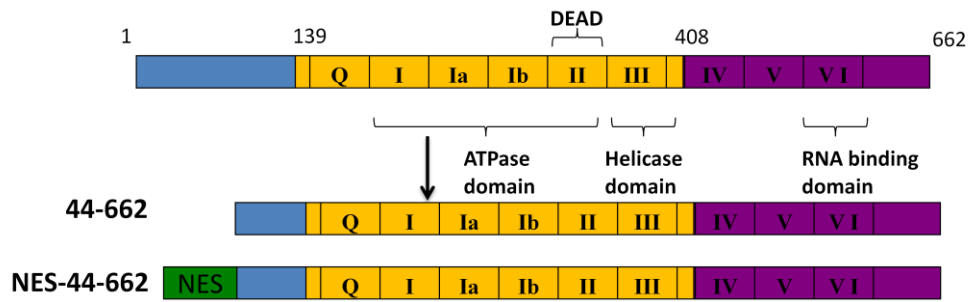
DDX3 truncation mutant and NES mutant interact with eIF4E upon treatment with 1mM Sodium Arsenite for 20 minutes. HeLa cells were transfected with a construct for Ha-22-662 DDX3 and Ha-NES DDX3 mutant, and stained with  $\alpha$ -Ha Alexa Fluor-594, and  $\alpha$ -eIF4E (*Abcam*) and secondary  $\alpha$ -rabbit Alexa Fluor-488. Co-localisation points highlight the positions of overlapping signals, generated using Olympus Fluoview Co-localisation Software. **Key:** A (DAPI), B (eIF4E), C (Ha-DDX3), D (merge B and C), E (merge A, B and C), F (Contrast), and G (Co-localisation points).

#### 6.3.4. The eIF4E binding site is not required for recruitment of DDX3 to stress granules

---

The translation initiation factor eIF4E is a known component of stress granules. DDX3 contains a described eIF4E binding site at amino acids 38-44 "YIPPHLR" (Shih et al. 2008). The N-terminal deletion mutant 44-662 is missing this eIF4E binding site. However, it is also missing the NES at amino acids 12-22, as described in section 3.2.4.3. In order to have an eIF4E binding site deletion mutant which had the ability to export from the nucleus, I created a 44-662 mutant which had the NES (1-22) reattached, referred to as NES-44-662. HeLa cells were transfected with expression plasmids for Ha-44-662 and Ha-NES-44-662 and treated with 1mM SA for 20 min or left untreated. Both eIF4E binding site deletion mutants co-localised with eIF4E after treatment with SA, a large amount of the 44-662 mutant remained nuclear after SA treatment, even though cytoplasmic 44-662 was localised to SGs. The NES-44-662 mutant was predominantly cytoplasmic in both untreated and treated cell as expected, and co-localised with eIF4E after SA treatment (Figure 6.7). Suggesting the described eIF4E binding domain in DDX3 is not required for recruitment into eIF4E-containing SGs.

(1)



(2)

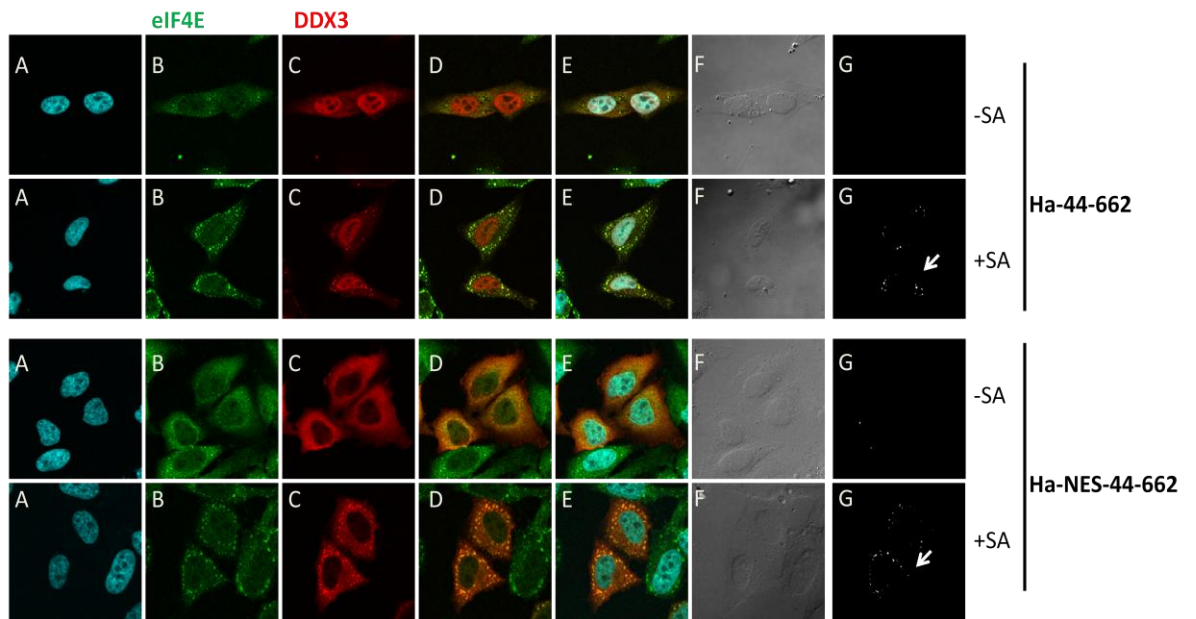


**Figure 6.7: The eIF4E binding site is not required for recruiting DDX3 to stress granules.**

(1): Schematic depicting the eIF4E binding site deletion mutant and the NES-eIF4E binding site deletion mutant which was constructed by adding the NES containing region (1-22) onto eIF4E binding site deletion mutant 44-662. (2): HeLa cells were transfected with Ha-44-662 or Ha-NES-44-662 mutant, and treated with 1mM SA for 20 min or left untreated. Cells were stained with  $\alpha$ -Ha Alexa Fluor-594, and  $\alpha$ -eIF4E (*Abcam*) and secondary  $\alpha$ -rabbit Alexa Fluor-488. Co-localisation points highlight the positions of overlapping signals, generated using Olympus Fluoview Co-localisation Software. **Key:** A (DAPI), B (eIF4E), C (Ha-DDX3), D (merge B and C), E (merge A, B and C), F (contrast) and G (Co-localisation points).

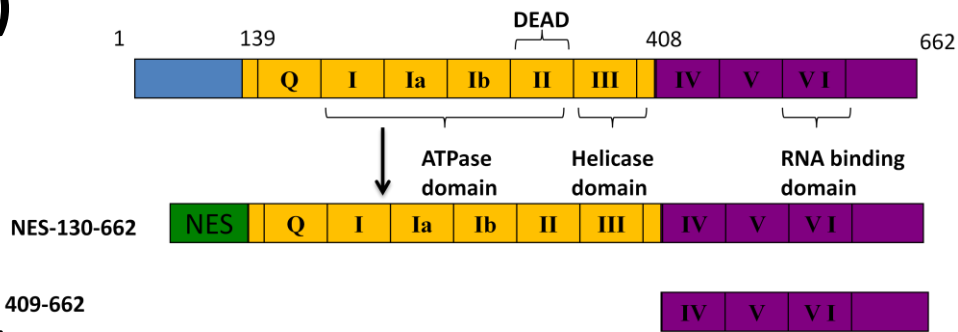
### 6.3.5. The C-terminus and the N-terminus of DDX3 play a role in recruitment to SG

---

Since the eIF4E binding site was not required for recruitment to SG, I decided to map the region of DDX3 required, using a series of N- and C-terminal truncation mutants. The Ha-tagged NES-130-662 plasmid contains the main RNA-binding site and the central ATPase and helicase domains, whereas the 409-662 plasmid is missing the central ATPase and helicase domains while containing part of the RNA-binding domain. HeLa cells were transfected with expression plasmids for Ha-NES-130-662 or Ha-409-662 and treated with 1mM SA for 20 mins or left untreated. The Ha-409-662 mutant also lacks the NES, and localises predominately to the nucleus, with a small portion in the cytoplasmic. Both N-terminal deletion mutants co-localised with the SG marker eIF4E after treatment with SA (Figure 6.8). Interestingly, not all of the 409-662 mutant is recruited to SGs, suggesting that the residues within the central 130-408 domain play a role in SG recruitment.

I next tested if the C-terminus was required for recruitment to SGs, since it has an RNA binding domain. HeLa cells were transfected with expression plasmids for Ha-tagged 1-572 and 1-408 DDX3 mutant, and treated with 1mM SA for 20 min or left untreated. Both C-terminal truncation mutants (1-572 and 1-408) localised with eIF4E after SA treatment, however 1-408 was not recruited to SG to the same extent as 1-572 (Figure 6.9). Overall this suggests that the C-terminus is not absolutely required for DDX3's recruitment to SG.

(1)



(2)

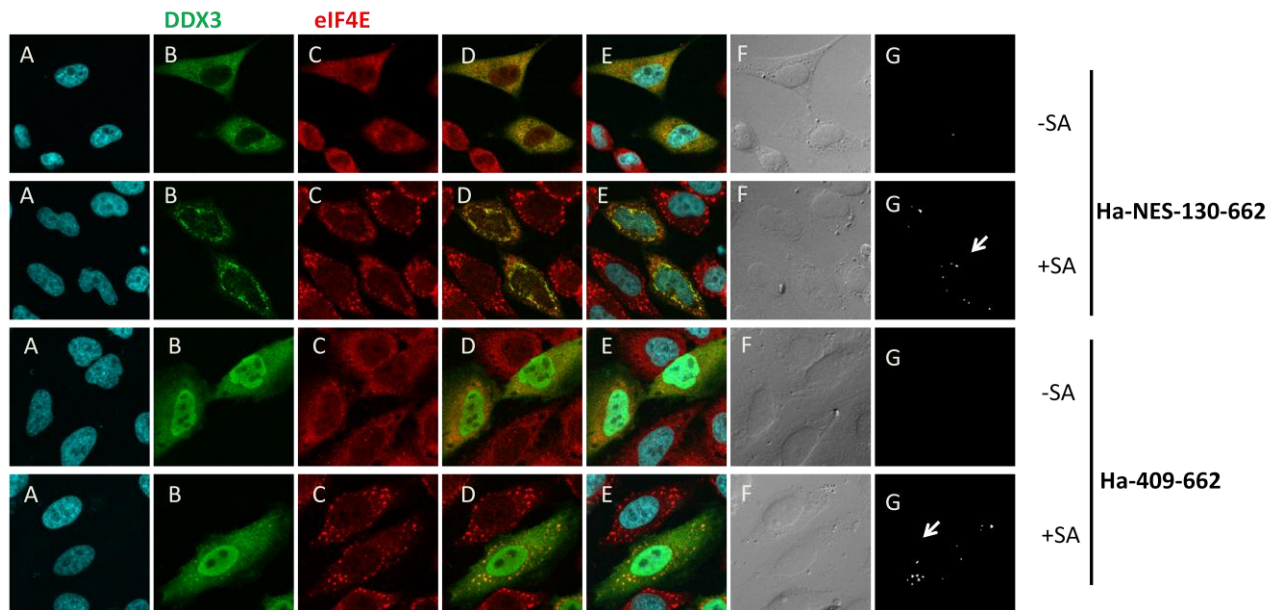


**Figure 6.8: The N-terminus is not critical for recruiting DDX3 to stress granules.**

(1): Schematic depicting the N-terminal deletion mutant. (2): HeLa cells were transfected with Ha-NES-130-662 and Ha-409-662 mutant, treated with 1mM SA for 20 min or left untreated. Cells were stained with  $\alpha$ -Ha (Covance) and secondary  $\alpha$ -mouse Alexa Fluor-488, and  $\alpha$ -eIF4E (Abcam) and secondary  $\alpha$ -rabbit Alexa Fluor-594. Co-localisation points highlight the positions of overlapping signals, generated using Olympus Fluoview Co-localisation Software. **Key:** A (DAPI), B (Ha-DDX3), C (eIF4E), D (merge B and C), E (merge A, B and C), F (contrast) and G (Co-localisation points).

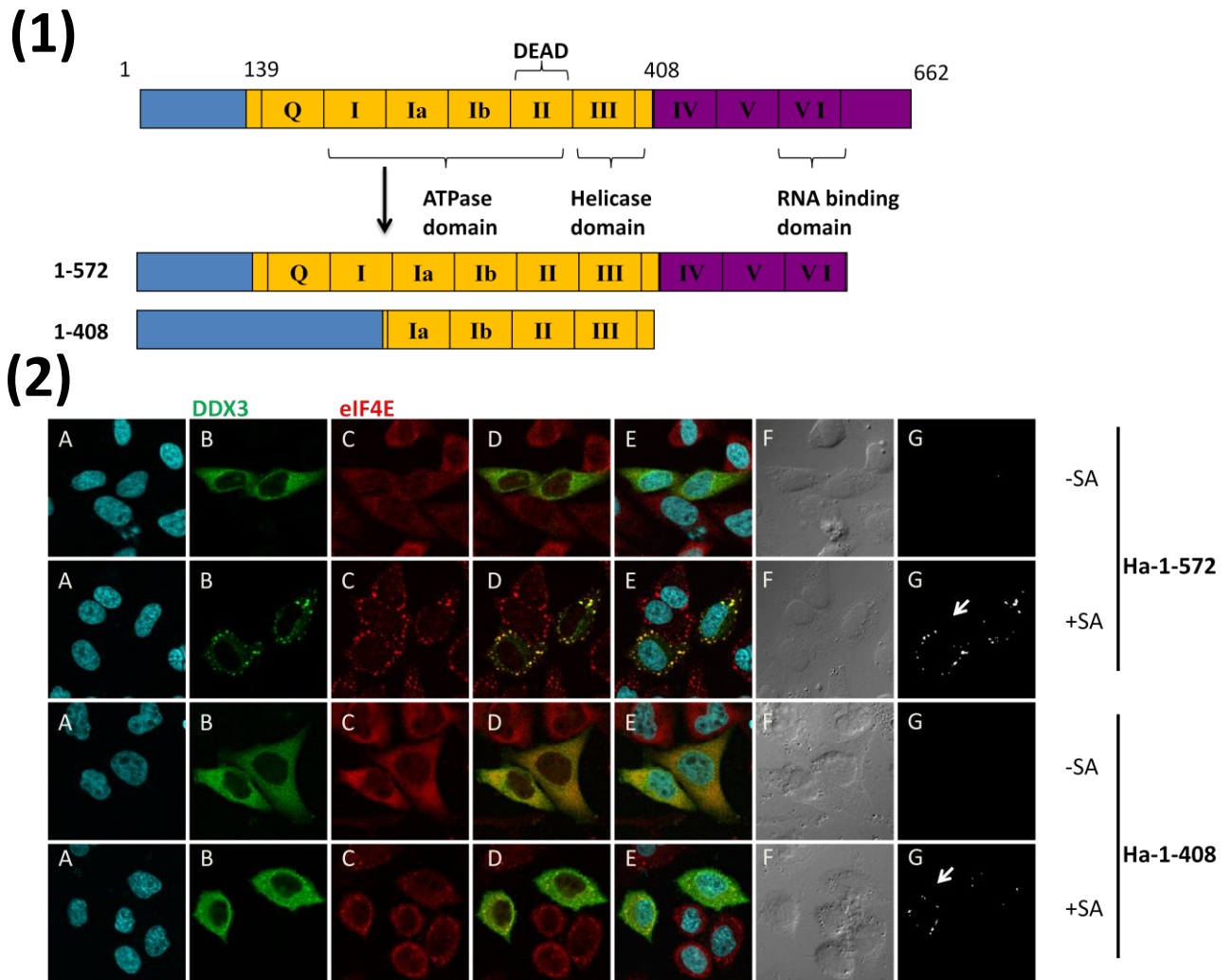
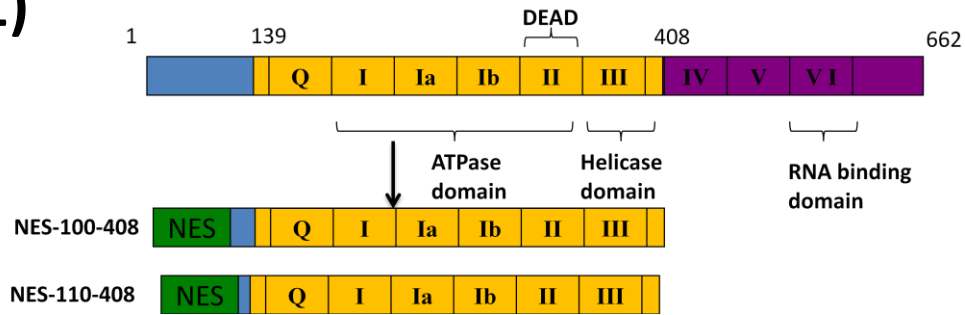


**Figure 6.9: The C-terminus is not critical for recruiting DDX3 to stress granules.**

**(1):** Schematic depicting the C-terminal deletion mutant. **(2):** HeLa cells were transfected with Ha-1-572 and Ha-1-408 mutant, treated with 1mM SA for 20 min or left untreated. Cells were stained with  $\alpha$ -Ha and secondary  $\alpha$ -mouse Alexa Fluor-488., and  $\alpha$ -eIF4E (*Abcam*) and secondary  $\alpha$ -rabbit Alexa Fluor-594. Co-localisation points highlight the positions of overlapping signals, generated using Olympus Fluoview Co-localisation Software. **Key:** A (DAPI), B (Ha-DDX3),C (eIF4E),D (merge B and C), E (merge A, B and C), F (contrast) and G (Co-localisation points).

Since both the N- and C-terminal mutants localised as normal to SG, I decided to test mutants missing both the N- and C-terminus. HeLa cells were transfected with expression plasmids for Ha-tagged NES-100-408 or NES-110-408 and treated with 1mM SA for 20 min or left untreated. Neither the NES-100-408 nor the NES-110-408 co-localised with eIF4E after treatment with SA (Figure 6.10). The C-terminal mutant 1-408 was recruited to SG (Figure 6.9), as did the N-terminal mutants NES-130-662 and 409-662 (Figure 6.8). Here, mutants missing both the N- terminus and C-terminus failed to be recruited to SGs, which suggests that in the absence of the RNA binding domain, the N-terminus (1-110) is required for SG recruitment.

(1)



(2)

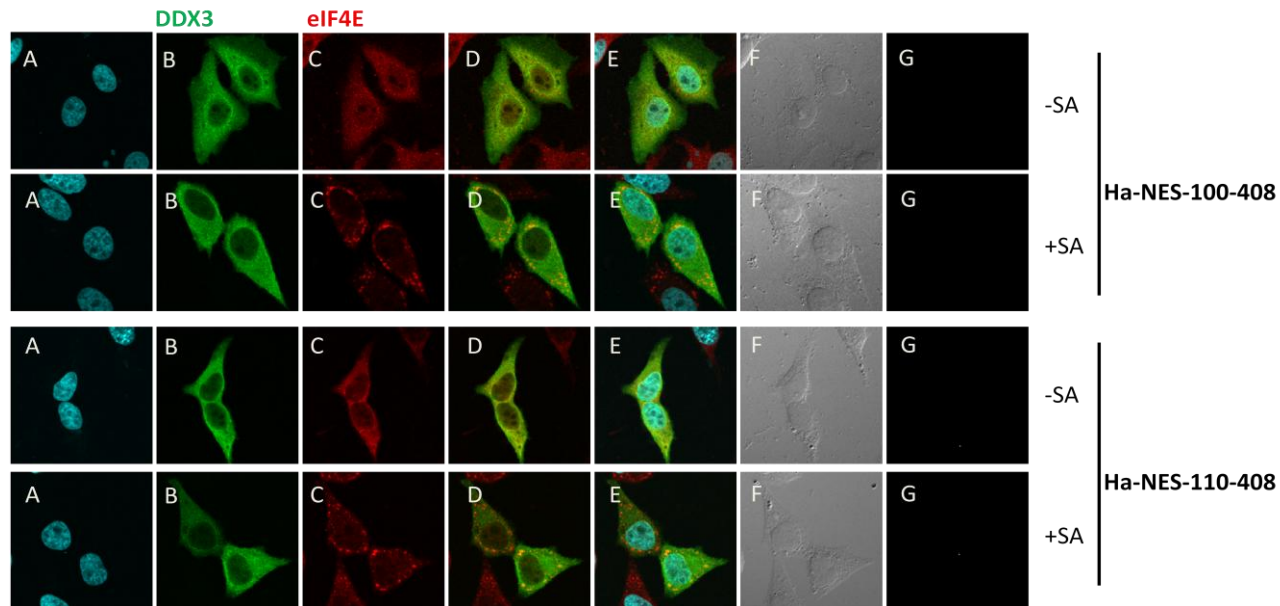


**Figure 6.10: Residues within the N-terminus are critical for recruitment of DDX3 to stress granules in the absence of the C-terminus.**

(1): Schematic depicting the N/C-terminal deletion mutants. (2): HeLa cells were transfected with Ha-NES-100-408 or Ha-NES-110-408 mutant, and treated with 1mM SA for 20 min or left untreated. Cells were stained with  $\alpha$ -Ha and secondary  $\alpha$ -mouse Alexa Fluor-488, and  $\alpha$ -eIF4E (*Abcam*) and secondary  $\alpha$ -rabbit Alexa Fluor-594. Co-localisation points highlight the positions of overlapping signals, generated using Olympus Fluoview Co-localisation Software. **Key:** A (DAPI), B (Ha-DDX3), C (eIF4E), D (merge B and C), E (merge A, B and C), F (contrast) and G (Co-localisation points).

#### 6.4. Discussion

---

Previously, there have been studies linking DDX3 to SGs. DDX3 has been suggested to localise to cytoplasmic SG in response to cellular stresses (Lai et al. 2008) and, recently, to play a critical role in SG assemble (Shih et al. 2012). Here I have confirmed that overexpressed DDX3 can be recruited to SG spontaneously, and also that DDX3 localises to SG in response to cellular stress. Interestingly, SG recruitment prevented the nucleocytoplasmic shuttling of DDX3, as nuclear export deficient mutants had a cytoplasmic speckle localisation after SG assembly. DDX3's helicase activity was not required for SG recruitment, nor was the eIF4E binding site. A recent study found that DDX3 was a critical for SG induction, as knockdown of DDX3 inhibited SG assembly, and overexpression of DDX3 promoted SGs independently of helicase activity (Shih et al. 2012). Shih et al. showed that DDX3 interacted with SG components eIF4E and PABP1, and also that interaction with eIF4E was required for SG assembly as an eIF4E binding mutant (L42A) did not promote SG assembly. They also showed that PABP1 interaction was not required for SG assembly, but they did suggest a role for DDX3 in PABP1 nuclear export as knock-down of DDX3 resulted in nuclear accumulation of PABP1 (Shih et al. 2012).

I found that both the N- and C-terminus of DDX3 contribute to SG recruitment, however truncation mutants NES-110-408 and NES-100-408 are not recruited. It is not surprising that the C-terminus can be recruited to SGs in the absence of the N-terminus, as the C-terminal RNA binding domains can still interact with RNA (Linder & Jankowsky 2011). In the absence of the C-terminus, we found that residues in the N-terminus (1-110) can also mediate recruitment to SGs. Since PABP1 has been shown to interact with the C-terminus and eIF4E with the N-terminus of DDX3 (Shih

et al. 2012; Shih et al. 2008), maybe DDX3 needs to interact with either RNA, PABP1 (C-terminus) or eIF4E (N-terminus) to be recruited to SGs. It would be interesting to investigate if a C-terminal and eIF4E binding site mutant 44-408 would be recruited to SG, to confirm if the eIF4E binding site is important for SG interaction. Also the results here suggest that there are subtle differences in the recruitment of some of the N- and C- terminal mutants to SGs, with the 1-408 and 409-662 mutant seemingly being recruited less to SGs compared to WT-DDX3. This is something that will need to be quantified in the future, possibly using a HCA setting.

As previously described, DDX3 is targeted by a range of viruses to promote replication of the viral genome. Also viruses have been shown to interact with SG components and regulate SG assembly (White & Lloyd 2012). Recently, a role for specialised avSGs in induction of type I interferon in response to influenza A virus has been described (Onomoto et al. 2012). HCV infection has been shown to regulate SGs throughout its life cycle, with phases of stalled and active translation (Garaigorta et al. 2012; Ruggieri et al. 2012). HCV induction of SGs was also shown to be dependent on PKR, and increased in the presence of IFN- $\alpha$ . While one study suggested that HCV promoted SGs at early and late stages of infection (Garaigorta et al. 2012), another study showed that throughout HCV infection there was a highly dynamic oscillation of SGs (Ruggieri et al. 2012). HCV induction of SG was associated with reduced cell division and host protein translation (eg. anti-viral mediators), whereas disassembly of SGs promoted cell survival by preventing long phases of translational shut off (Ruggieri et al. 2012). In Chapter 6, I showed that HCV Core protein confined DDX3 to cytoplasmic speckles after overexpression of HCV Core protein and also during HCV infection. I showed that the SG marker eIF4E

was also recruited into HCV-Core-containing cytoplasmic speckles, however the redistribution of eIF4E was not as noteworthy as DDX3's. Since I have shown here that DDX3 and eIF4E are recruited to SGs, there may be a link between these two observations. Other studies have shown that HCV Core protein hijacks P-bodies and SG components to promote viral RNA translation at lipid droplets (Ariumi, Kuroki, Kushima, et al. 2011). Maybe HCV RNA induces SGs to stall Cap-dependent translation, while HCV Core protein utilises DDX3's function in IRES-mediated translation at lipid droplets (Geissler et al. 2012). Lipid droplets play a critical role in HCV replication, and HCV Core proteins interaction with lipid droplets has been shown to be critical for efficient viral assembly (Miyanari et al. 2007). HCV virus has been suggested to utilise the endosomal sorting complex required for transport (ESCRT) components assembly and budding of viral particles (Ariumi, Kuroki, Maki, et al. 2011), and in the absence of HCV Core protein HCV RNA is not found at lipid droplets (Targett-Adams et al. 2008; Miyanari et al. 2007). Maybe HCV-Core uses DDX3 to recruit HCV RNA and translate the RNA at lipid droplets promoting efficient assembly of viral particles and infection.

In conclusion, DDX3 is a component of eIF4E-containing SGs. Here I have found that both the N-terminus and C-terminus of DDX3 are recruited independently to SGs upon oxidative stress, however an N- and C-terminal truncation mutant (100-408) DDX3 was not recruited to SGs.

## **Chapter 7 : Investigating the role of DDX3 in the cell cycle**

---

### **7.1. Introduction**

---

DDX3 has been implicated in various aspects of cell cycle and cell growth control. The cell cycle is a series of events which result in the replication of genomic DNA and the division of the cell. It consists of four distinct phases: G1 phase, S phase, G2 phase, and M phase (Figure 7.1). The cell cycle is highly regulated in order to prevent uncontrolled cell division and to allow for the detection and repair of DNA damage in cells. Cell cycle progression of eukaryotic cells is controlled by Cyclin, Cyclin dependent kinases (cdk) and cdk inhibitors. One way in which the cell cycle is regulated is through regulation of transport across the nuclear membrane. The localisation of many proteins involved in regulation of the cell cycle changes during the stages of the cell cycle. For example, during mitosis Cyclin B is activated and is rapidly imported into the nucleus just before the nuclear membrane disassembles (Pines & Hunter 1994; Hagting et al. 1999; Takizawa et al. 1999; Gavet & Pines 2010).

DDX3's role in the cell cycle and cell growth control is unclear, as it has been suggested to be both a tumour suppressor (Chao et al. 2006; Chang et al. 2006) and an oncogene (Botlagunta et al. 2008). In the literature, DDX3 has frequently been reported to have a cytoplasmic localisation, however this has usually been observed in transformed cell lines (Yedavalli et al. 2004; Schröder et al. 2008; Owsianka & Patel 1999; Sekiguchi et al. 2004; Lai et al. 2008; Lee et al. 2008). One study reported that DDX3 expression and cellular localisation changed from nuclear to cytoplasmic in human hepatocellular carcinoma (HCC) cancers and squamous cell carcinoma (SCC) (Chao et al. 2006). It is appealing to think that mis-localisation of

DDX3 could contribute to cancer development, since it has been suggested to act as both a tumour suppressor and oncogene.

DDX3's role in cell cycle control and cell growth control will be briefly described in the following sections.

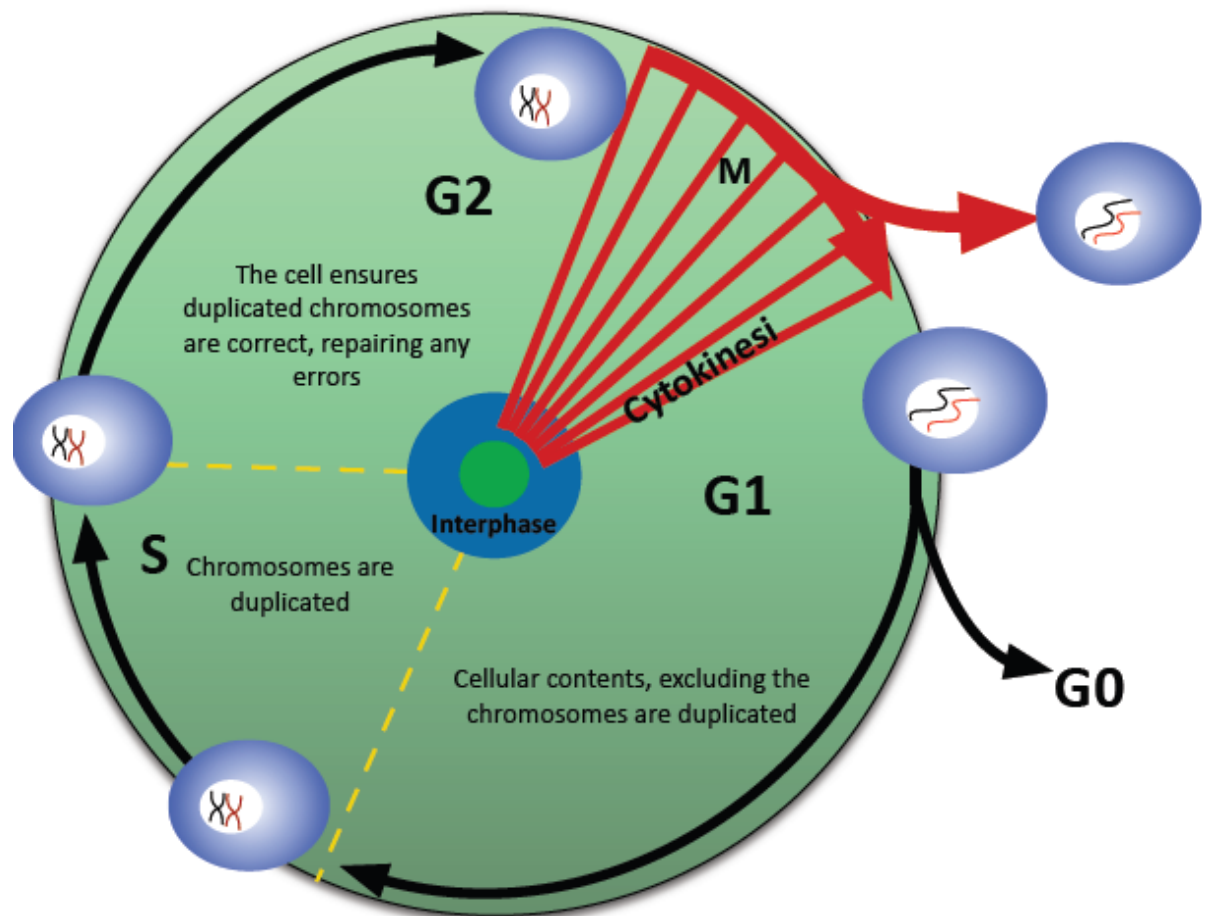


**Figure 7.1: Schematic of cell cycle.**

The cell cycle consists of five distinct phases: G1 phase, S phase, G2 phase, M phase and G0 phase. Adapted from <http://www2.le.ac.uk/departments/genetics/vgec/diagrams/22-Cell-cycle.gif/image>.

### 7.1.1. DDX3's role in cycle control

DDX3 has been suggested to have a role in cell cycle control. Hamster DDX3 has been shown to be required for cyclin A expression in the hamster tsET24 model (Fukumura 2003). Cyclin A is required for progression into the S-phase of the cell cycle. The hamster tsET24 model, which is a temperature-sensitive (ts) mutant cell

line with a DDX3 gene mutation (P267S), exhibit normal cell growth at the permissive temperature of 33.5°C, but arrests in G1 at the non-permissive temperature of 39.5°C. Cells grown at the non-permissive temperature and arrested at G1 had a reduction in Cyclin A and Cyclin B expression levels. There was also a nuclear accumulation of poly-A mRNAs, suggesting a potential role for DDX3 in nuclear export of mRNA.

A later study showed that DDX3 is phosphorylated by Cyclin B/cdc2 kinases during mitosis at residues Thr204 and Thr323, which are in the highly conserved Q and Ib motifs of the DEAD box family. Cyclin B/cdc2 kinases are key regulators of cell cycle progression in and out of mitosis. Transfection of hamster DDX3 mutant Glu204 (Thr→Glu) did not rescue the tsET24 cell line at the non-permissive temperature, whereas transfection of wild type DDX3, Ala204 and Leu204 did rescue the cell line (Sekiguchi et al. 2007). The Glu204 mutant mimics the phosphorylated Thr204, therefore suggesting that phosphorylation of hamster DDX3 at Thr204 renders DDX3 inactive (Sekiguchi et al. 2007). Thr323 was shown to be critical to DDX3 function, with modification to either alanine or glutamine resulting in a loss of function (Sekiguchi et al. 2007). The authors suggested that phosphorylation of DDX3 at Thr204 by Cyclin B/cdc2 might have a role in repressing Cyclin A expression in early mitosis, when Cyclin A decreases just as Cyclin B increase (Sekiguchi et al. 2007).

DDX3 has also been shown to regulate cell growth through translational control of Cyclin E1 (Lai et al. 2010). Cyclin D and E are specific for cell cycle progression from G1 to S phase. Deregulation of Cyclin E results in perturbed cell cycle progression but also genomic instability and centrosome amplification (Loeb et al.

2005; Spruck 1999). Knockdown of DDX3 in HeLa cells resulted in delayed G1/S transition, due to reduced translation initiation of Cyclin E1 mRNA. They also showed that in the DDX3 loss of function tsET24 cell line, Cyclin E mRNA translation was reduced. Cells grown at the non-permissive temperature has reduced Cyclin E protein but normal Cyclin E mRNA. This translational regulation of Cyclin E mRNA was dependent on DDX3's RNA helicase activity (Lai et al. 2010).

### 7.1.2. DDX3 as a tumour suppressor

---

The tumour-suppressor role of DDX3 has been suggested to be mediated by its effects on the promoter of the tumour-suppressor p21<sup>waf1/cip1</sup>. p21<sup>waf1/cip1</sup> is a critical cdk inhibitor: it interacts with cyclin/cdk complexes and modulates their kinase activity (Harper et al. 1993). p21<sup>waf1/cip1</sup> has also been shown to interact with Proliferating Cell Nuclear Antigen (PCNA) to inhibit DNA synthesis and regulate DNA replication. Induction of p21<sup>waf1/cip1</sup> can occur in a p53-dependent or -independent manner. DDX3 has been shown to transactivate the p21<sup>waf1/cip1</sup> promoter through an interaction with Sp1; where Sp1 has previously been shown to activate the p21<sup>waf1/cip1</sup> promoter (Gartel et al. 2000).

DDX3 has been found to have a growth-suppressive effect in the context of human hepatocellular carcinoma (HCC) and it has been suggested that this is due to its effects on p21<sup>waf1/cip1</sup> promoter activity (Chao et al. 2006). Expression of DDX3 was also shown to be down-regulated in human HCC samples, mainly in male patients with HBV infection (Chang et al. 2005), further supporting DDX3's role as a tumour suppressor. In contrast, DDX3 levels have also been reported to be elevated in HCC cancers (Huang et al. 2004). The discrepancies have been suggested to be

based on differences in regulation at protein and mRNA level (Chang et al. 2006), but it is unclear whether this is a satisfactory explanation for these results.

Chao *et al.* also showed that DDX3 cellular localisation changed in transformed cells. In normal human squamous epithelial cells, DDX3 had a predominately nuclear localisation, while in transformed squamous epithelial cells the nuclear staining for DDX3 was lost or significantly decreased (Chao et al. 2006). DDX3 has also been implicated in Human Papillomavirus (HPV)-associated lung cancer, with reduced levels of DDX3 protein in lung tumours. HPV protein E6 was shown to affect DDX3 levels through inactivation of p53. p21<sup>waf1/cap1</sup> transcription was also suppressed by the E6 alteration to the DDX3/p53 pathway (Wu, Liu, et al. 2011). Reduction in p21<sup>waf1/cap1</sup> expression, caused by suppression of DDX3 and p53 in tumours correlated with poor relapse-free survival rates in lung cancer patients. A recent study has also linked DDX3 to cancer, showing that aggressive Oral Squamous Cell Carcinoma (OSCC) in males has reduced DDX3 expression and also that DDX3 localisation became more cytoplasmic in transformed oral epithelium (Lee et al. 2013).

### 7.1.3. DDX3 as an oncogene

Studies on breast cancer have suggested a role for DDX3 as an oncogene (Botlagunta et al. 2008). Benzo[a]pyrene diol epoxide (BPDE), the active metabolite in tobacco smoke, was shown to induce DDX3 expression in mammary epithelial cells. In the MCF 10A cell line, over-expressed DDX3 induced epithelial-mesenchymal-like transition (EMT) and promoted aggressive properties such as an increase in motility and invasion (Botlagunta et al. 2008). DDX3 also reduced E-Cadherin promoter activity. Loss of E-Cadherin has been shown to result in (EMT),

increased migration and proliferation of cells leading to metastasis (Onder et al. 2008).

DDX3 has also been shown to regulate the transcription factor Snail (Sun et al. 2011). Snail is a transcription factor that is an important regulator for the development and progression of cancer (Nieto 2002). Snail was shown to repress expression of cellular adhesion molecules such as E-Cadherin, resulting in an increase in EMT (Batlle et al. 2000). Sun et al. showed that DDX3 was required for HDAC inhibitor- and Topoisomerase inhibitor (Camptothecin)-induced expression of Snail. They also showed that knockdown of DDX3 resulted in decreased Snail protein, and consequently in increased expression of E-Cadherin, validating the results of Botlagunta *et al.* 2008. The authors also showed a significant correlation between Snail levels and DDX3 levels in samples from patients with Glioblastoma Multiforme (GBM). They suggested that DDX3 did not regulate Snail at a transcriptional level, but that DDX3 acted on Snail by promoting its retention in the nucleus (Sun et al. 2011). Interestingly, DDX3 was found in both the nuclear and cytoplasmic fractions of MCF-7 cells in this study, rather than its usual cytoplasmic localisation in transformed cell lines.

DDX3 expression has also been shown to be regulated by Hypoxia Inducible Factors (HIFs) in a study in breast cancer cells (Botlagunta et al. 2011). Hypoxia is a major characteristic of solid tumours and causes genome wide changes in gene expression. HIFs regulate the expression of hypoxia responsive genes. HIF-1 $\alpha$  has been shown to activate expression of DDX3 by binding to Hypoxia Responsive Elements (HREs) in the promoter region of DDX3 (Botlagunta et al. 2011). Whether DDX3 promotes cancer progression was not examined in this study.

A recent study on Gall Bladder cancer also supported the notion of DDX3 as an oncogene. This authors showed that increased DDX3 expression was associated with increased tumour size and metastasis (Miao et al. 2013). They also showed that DDX3 was expressed predominantly in the cytoplasm of squamous cell/adenosquamous carcinoma samples.

#### 5.1.4. Conclusion

---

DDX3 role in cell cycle regulation is unclear and whether DDX3 acts primarily as a tumour suppressor or oncogene is controversial. Dis-regulation of cell cycle progression may lead to tumour formation, and since DDX3 has been shown to regulate and be regulated by components of the cell cycle it is possible that DDX3 could play a role in tumorigenesis. The expression levels of DDX3 and the cellular localisation of DDX3 might affect its functional roles. For example, nuclear DDX3 might be required for the nuclear export of Cyclin A mRNA, but on the other hand DDX3 needs to be cytoplasmic to aid in the translation of Cyclin E mRNA. DDX3 phosphorylation by Cyclin B seems to result in loss of function, probably due to a loss of enzymatic activity due to the proximity of the Thr323 to ATP-binding site. However, Cyclin B phosphorylation could affect the localisation of DDX3.

If DDX3 is required to promote induction of the p21<sup>waf1/cap1</sup> tumour suppressor through binding to the promoter, inhibition of DDX3 import could potentially inhibit p21<sup>waf1/cap1</sup> induction. Likewise, DDX3's role in oncogenesis could also be affected by mis-localisation. Nuclear DDX3 has also been suggested to regulate Snail's role in E-Cadherin transcription (Sun et al. 2011), in addition to nuclear DDX3 being required for binding to the E-cadherin promoter (Botlagunta et al. 2008). Since viruses have been implicated in tumorigenesis (Carrillo-Infante et al. 2007), viral targeting of DD3

might influence its oncogenic or tumour suppressor effects, possibly also by affecting DDX3's cellular localisation.

## 7.2. Aims

DDX3 has been shown to have roles in cell cycle control and cell growth control. In this chapter I investigated whether DDX3's cellular localisation changed in response to DNA damage. I also investigated if its cellular localisation and expression levels changed during cell cycle progression.

## 7.3. Results

---

### 7.3.1. High content analysis to investigate change in localisation in response to DNA damage

---

High content analysis (HCA) microscopy is a useful tool for determining the nuclear/cytoplasmic localisation of a protein in cells. Using HCA one can image hundreds of cells and objectively quantify the localisation of proteins of interest in cells.

I was interested in whether DNA damage could change the cellular localisation of DDX3. HeLa cells were plated and treated with etoposide (ETO), a known inducer of strand breaks in cellular DNA by inhibiting topoisomerase II (topoII) religation of cleaved DNA molecules (Burden & Osheroff 1998). As a positive control for a nuclear localisation of DDX3, cells were treated with LMB.

As shown in Figure 7.2, there was no increase in the level of nuclear DDX3 after the treatment with ETO.

## High Content Analysis

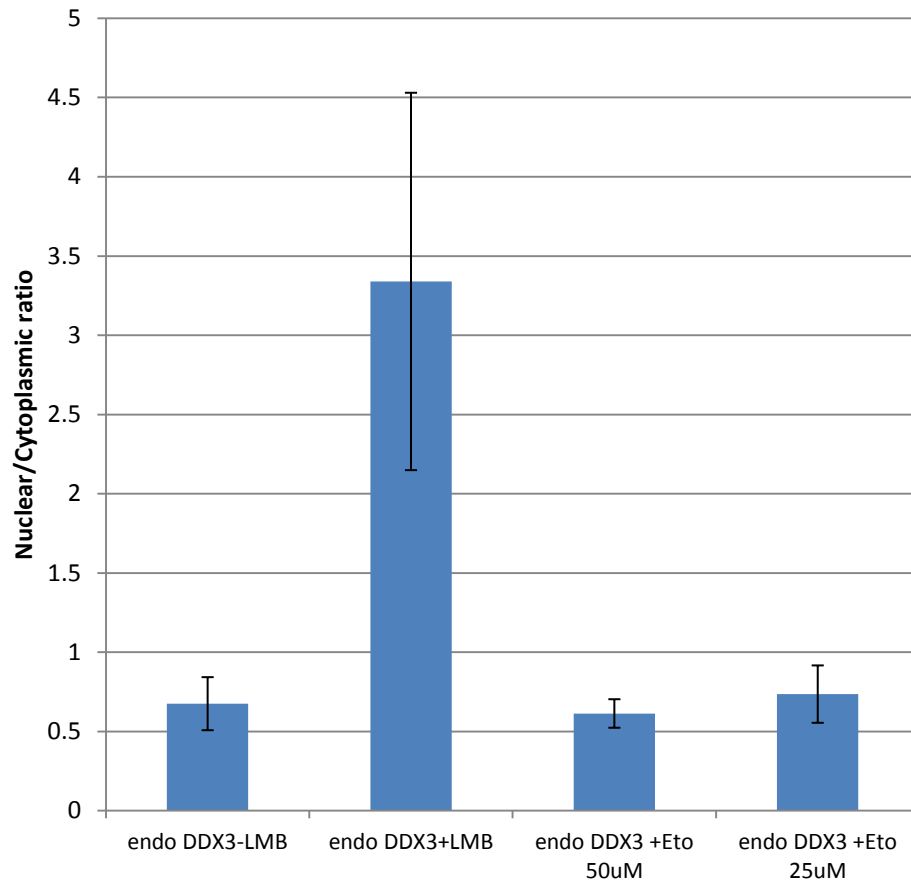


**Figure 7.2: Endogenous DDX3 does not change localisation after treatment with Etoposide.** HeLa cells were treated with 20mM LMB for 4 hrs, or 50 $\mu$ M or 25  $\mu$ M Etoposide for 24 hrs or left untreated. Cells were stained with  $\alpha$ -DDX3 antibody, followed by  $\alpha$ -rabbit Alexa Fluor-488, Rhodamine-Phalloidin and DAPI. High content analysis of the nuclear/cytoplasmic ratio was carried out using the GE IN Cell analyser as described in Chapter 2.

### 7.3.2. Localisation of endogenous DDX3 changes during cell cycle

During the high content analysis, I observed that wild type DDX3 clearly localised to the nucleus in a small percentage of cells, Figure 7.3. I hypothesised that human DDX3's localisation might change depending on different stages of the cell cycle. Changes in nuclear/cytoplasmic localisation could be the result of phosphorylation by cell cycle kinases, such as Cyclin B, as DDX3 has been described as a phosphorylation target of this kinase (Sekiguchi et al. 2007).

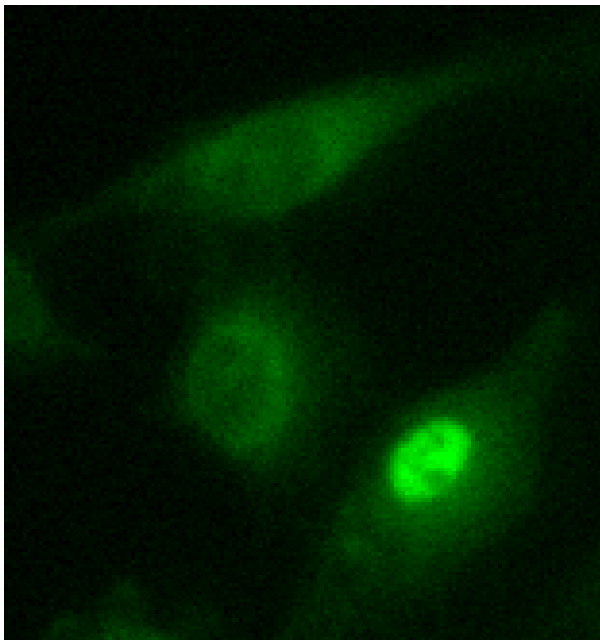


**Figure 7.3: WT DDX3 localised to the nucleus in a small percentage of untreated cells.** Image taken from High Content analysis. HeLa cells overexpressing Ha-tagged DDX3. Cells were stained with primary  $\alpha$ -Ha and secondary  $\alpha$ -mouse Alexa Fluor-488.

Therefore, I decided to investigate the cellular localisation of DDX3 at different stages of the cell cycle. To this end, HeLa cells were grown on coverslips and prepared for immunofluorescence staining and confocal microscopy. Mitotic cells were identified based on the shape of the cell and chromatin condensation level, and by co-staining with  $\alpha$ -Tubulin and phospho-Histone H3 antibody (*Cell Signalling Technologies*). Mitotic cells become rounded during mitosis and the nuclear envelope breaks down resulting in chromatin condensation. The phospho-Histone H3 (Ser28) antibody detects endogenous levels of histone H3 only when phosphorylated at Ser28. Phosphorylation at Ser10, Ser28, and Thr11 of histone H3 is tightly correlated with chromosome condensation during both mitosis and meiosis, and therefore can be used as a marker for mitotic cells (Preuss et al. 2003; Hendzel et al. 1997; Goto et al. 1999).

DDX3 localisation and expression levels were examined in mitotic cells vs non-mitotic cells. Levels of nuclear endogenous DDX3 seemed to increase slightly in seemingly mitotic cells, with an increase in nuclear DDX3 seen at prophase (Figure 7.4).

Hamster DDX3 has been shown to be phosphorylated by Cyclin B during mitosis at Thr204 and Thr323. I thus decided to investigate the localisation of phosphorylated human DDX3 using a phospho-Thr323 DDX3 antibody (*Abcam*) to stain HeLa cells. Phospho-Thr323 DDX3 localised predominantly in the nucleus of untreated HeLa cells. Interestingly, strong cytoplasmic staining occurred in cells in metaphase, with a marked overall reduction in levels of Phospho-Thr323 DDX3 after cytokinesis (Figure 7.5).

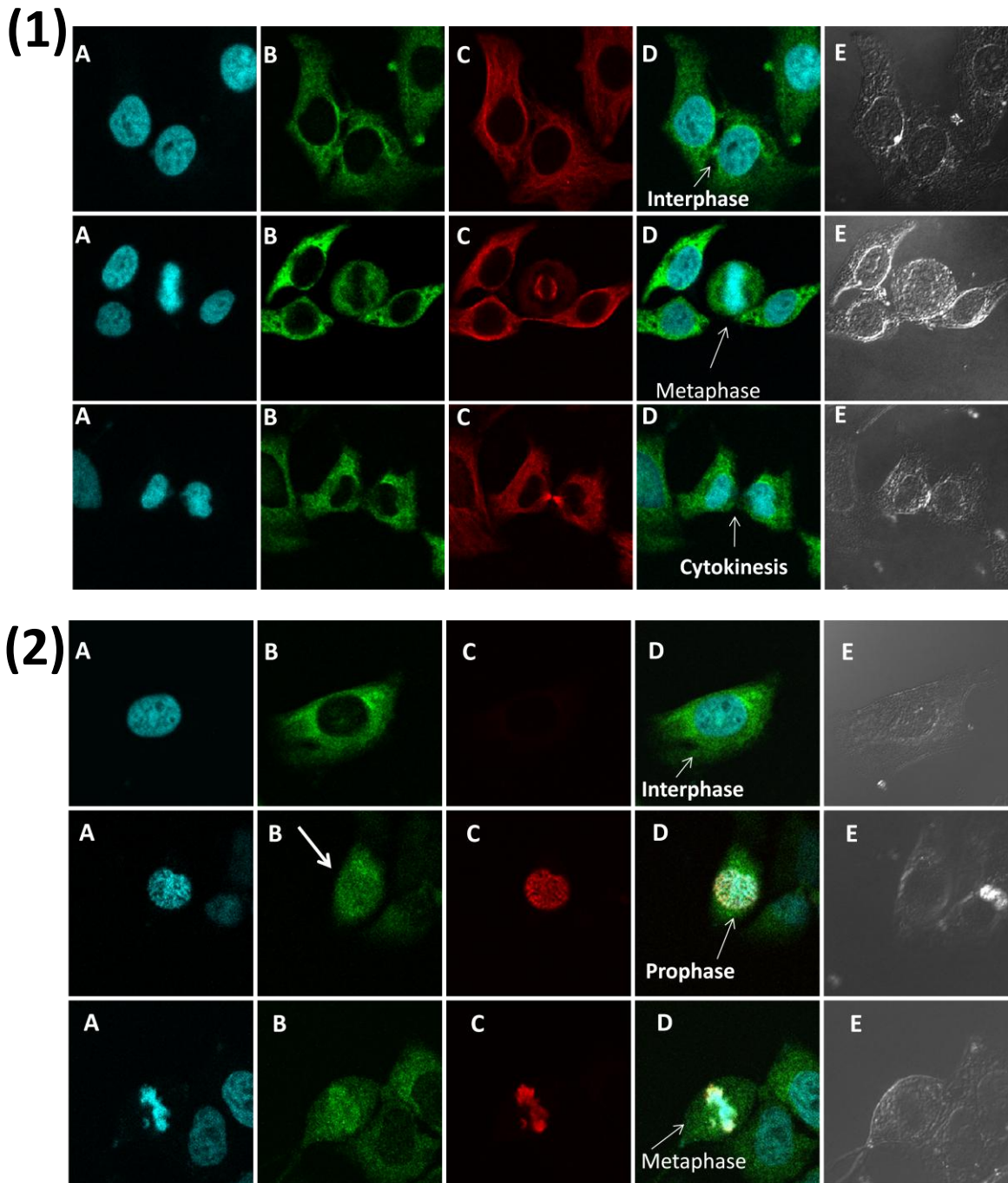
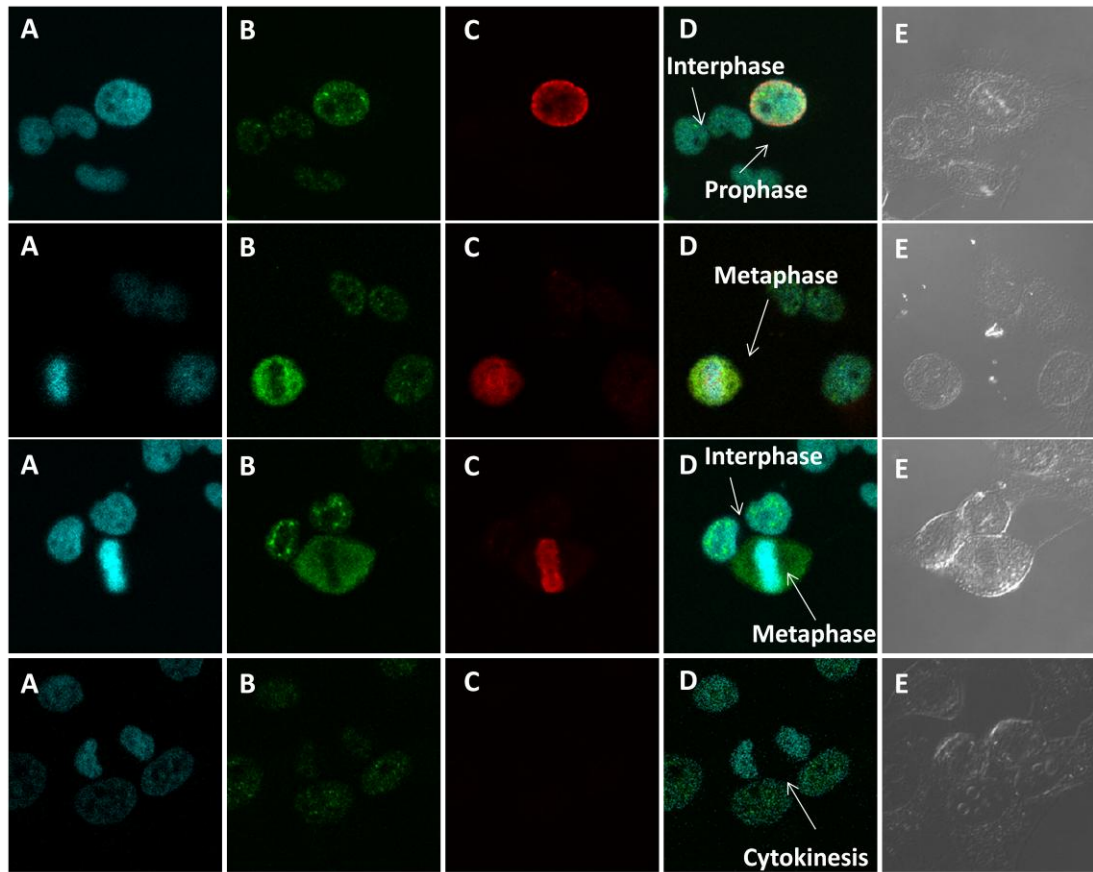


**Figure 7.4:** There is no clear change in the localisation and expression of DDX3 during the cell cycle.

**(1):** HeLa cells were stained for  $\alpha$ -DDX3 (*Bethyl*) and  $\alpha$ -tubulin (*Abcam*). **Key:** A (DAPI), B ( $\alpha$ -DDX3), C ( $\alpha$ -tubulin), D (Merge A, B and C), E (Contrast). **(2):** HeLa cells stained for  $\alpha$ -DDX3 (*Bethyl*) and mitotic marker PhosphoHistone H3 (*Cell signalling Technologies*). **Key:** A (DAPI), B ( $\alpha$ -DDX3), C ( $\alpha$ -PhosphoHistone H3), D (Merge A,B and C), E (Contrast).

(1)



(2)

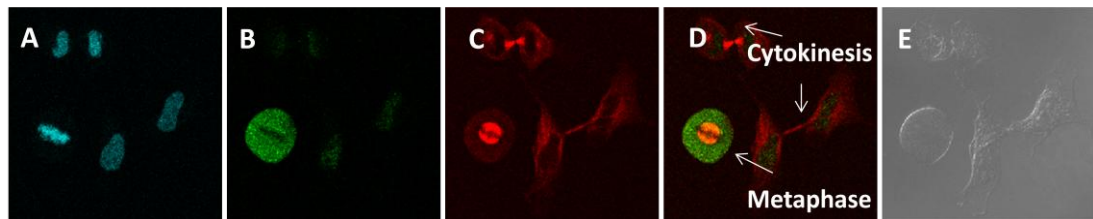


**Figure 7.5: Localisation and level of Phospho-Thr323 DDX3 changes throughout the cell cycle.**

Cells were grown on coverslips and stained with an antibody against Phospho-Thr 323 DDX3 (*Abcam*). **(1):** HeLa cells stained for PhosThr323 DDX3 (*Abcam*) and mitotic marker PhosphoHistone H3 (*Cell Signalling Technologies*). **Key:** A (DAPI), B ( $\alpha$ -PhosThr323 DDX3), C ( $\alpha$ -Phospho Histone H3), D (Merge A, B and C), E (Contrast). **(2):** Cells were grown on coverslips and stained with an antibody against Phospho-Thr 323 DDX3 (*Abcam*) and  $\alpha$ -tubulin (*Abcam*). **Key:** A (DAPI), B ( $\alpha$ -PhosThr323 DDX3), C ( $\alpha$ -tubulin), D (Merge A, B and C), E (Contrast).

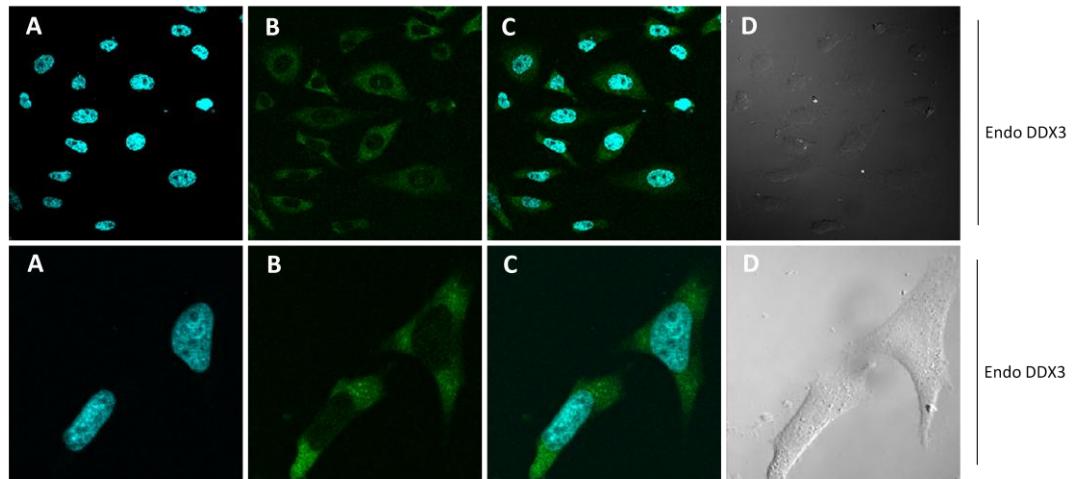
To further investigate the localisation of endogenous DDX3 and phosphorylated DDX3 (Thr323) at different stages of the cell cycle, HeLa cells were treated with cell cycle inhibitors as described in Chapter 2. Cells blocked at G1/S, G2/M and G0/G1 were stained for endogenous DDX3 and Phospho-Thr323.

HeLa cells blocked at the G0/G1 boundary with serum starvation showed cytoplasmic DDX3 and nuclear phospho-Thr323 DDX3 (Figure 7.8).

HeLa cells were blocked at the G1/S boundary with a double thymidine block. DDX3 had a predominantly cytoplasmic localisation and nuclear localisation of Phospho-Thr323 DDX3 in cells blocked at G1/S (Figure 7.6).

HeLa cells blocked at the G2/M boundary with nocodazole showed increased nuclear endogenous DDX3, and phospho-Thr323 DDX3 also localised predominantly in the nucleus (Figure 7.7). Nocodazole causes cells to arrest in prometaphase, suggesting that DDX3 becomes more nuclear at prometaphase.

(1)



(2)

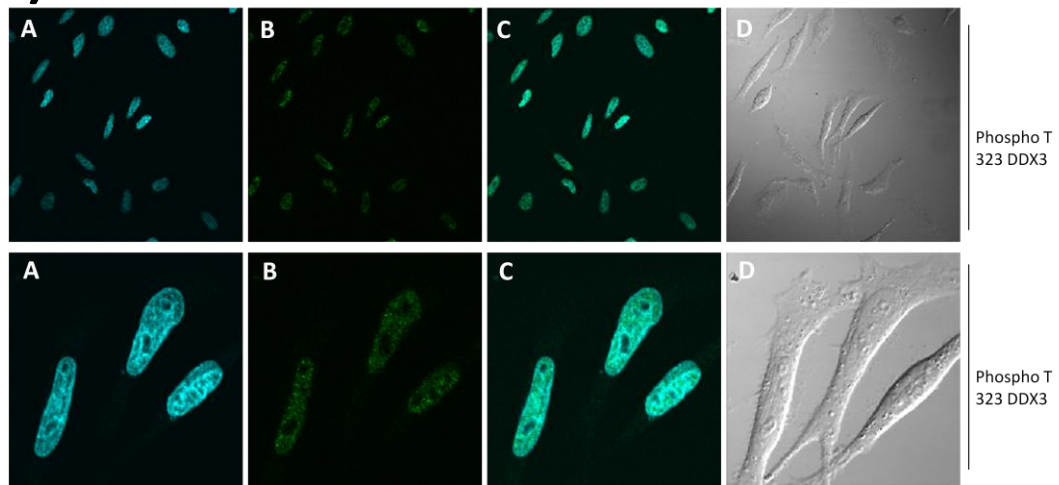
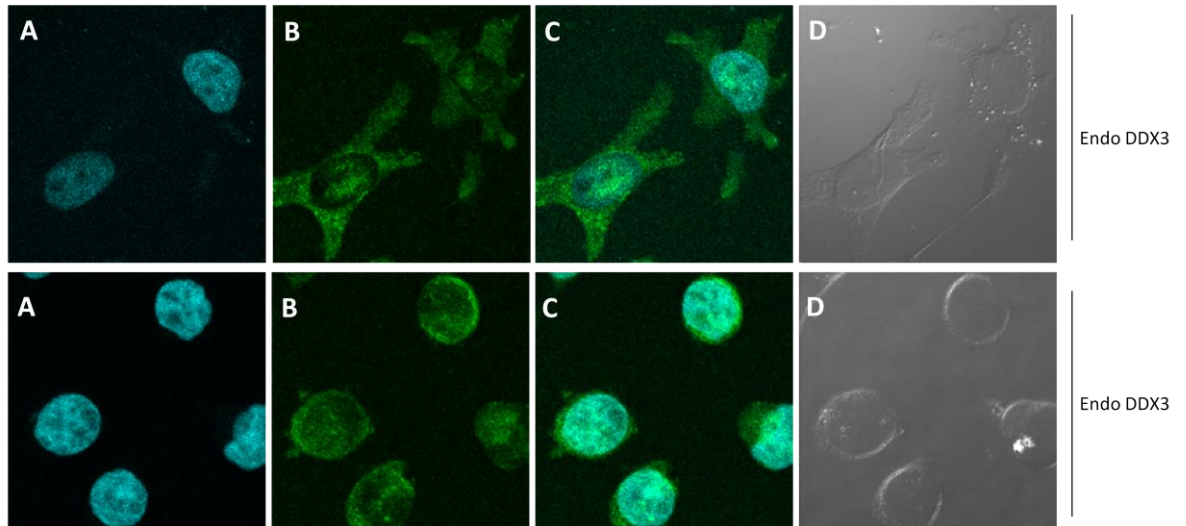


**Figure 7.6: Endogenous DDX3 is predominantly cytoplasmic and Phospho-Thr323 DDX3 is predominantly nuclear at the G1/S block.**

A double thymidine block was used to block cells at the G1/S boundary. **(1):** Cells were stained with primary  $\alpha$ - endogenous DDX3 (*Bethyl*) and secondary  $\alpha$ -rabbit Alexa Fluor-488. **(2):** Cells were stained with primary  $\alpha$ -Phospho-T323 DDX3 (*Abcam*) and secondary  $\alpha$ -rabbit Alexa Fluor-488. **Key:** A (DAPI), B ( $\alpha$ -DDX3/  $\alpha$ -Phospho-Thr323-DDX3), C (Merge A+B), D (Contrast).

**(1)**



**(2)**

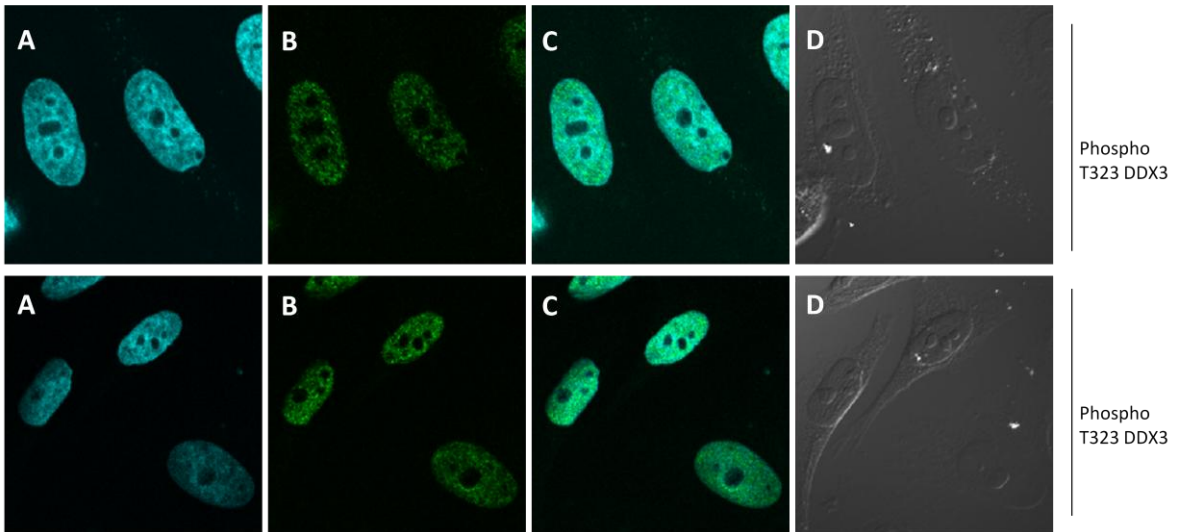


**Figure 7.7: Endogenous DDX3 becomes more nuclear and Phospho-Thr323 DDX3 remains nuclear at G2/M block.**

Cells were treated with thymidine for 24 hours followed by 3 hours release, and then treated with 100ng/ml Nocodazole for 12 hours. Nocodazole blocks cells in prometaphase. **(1)**: Cells were stained with primary  $\alpha$ -DDX3 (*Bethyl*) and secondary  $\alpha$ -rabbit Alexa Fluor-488. **(2)**: Cells were stained with primary  $\alpha$ -Phospho-T323 DDX3 (*Abcam*) and secondary  $\alpha$ -rabbit Alexa Fluor-488. **Key**: A (DAPI), B ( $\alpha$ -DDX3/  $\alpha$ -Phospho-Thr323-DDX3), C (Merge A+B), D (Contrast).

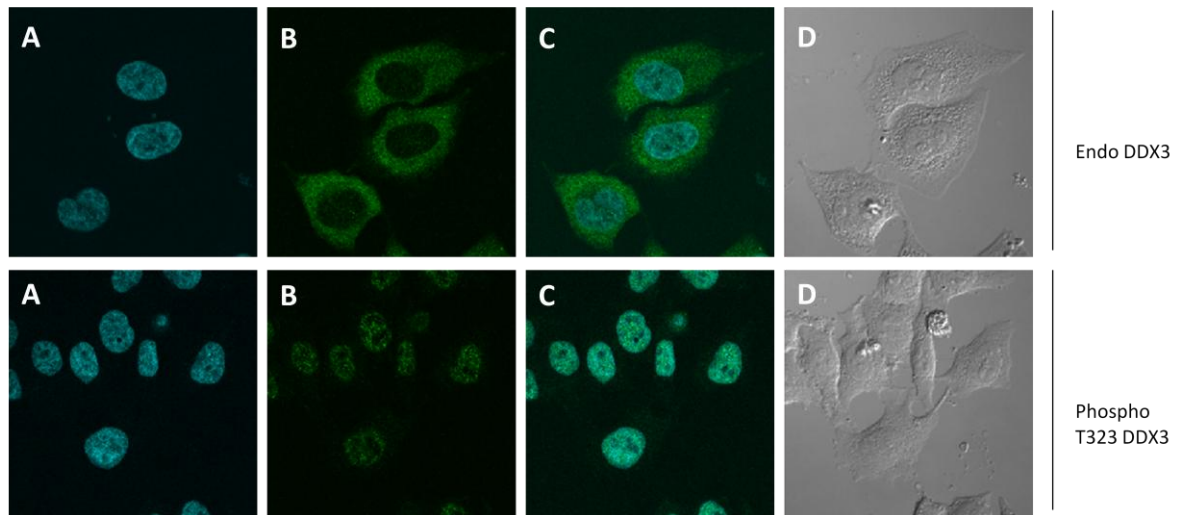


**Figure 7.8: Endogenous DDX3 is predominantly cytoplasmic and Phospho-Thr323 DDX3 predominantly nuclear at the G0/G1 block.**

A serum starvation block was used to block cells at the G0/G1 boundary. Cells were stained with primary  $\alpha$ -DDX3 (*Bethyl*), or with primary  $\alpha$ -Phospho-T323 DDX3 (*Abcam*), followed by secondary  $\alpha$ -rabbit Alexa Fluor-488. **Key:** A (DAPI), B ( $\alpha$ -DDX3/ $\alpha$ -Phospho-Thr 323-DDX3), C (Merge A+B), D (Contrast).

### 7.3.3. Phospho-Thr 323 DDX3 antibody co-localised with nuclear speckle marker

Since the Phospho-Thr 323 DDX3 antibody (*Abcam*) produced a speckled staining in the nucleus, I decided to test if it co-localised with nuclear speckle marker anti-splicing factor S35. Nuclear speckles are nuclear structures enriched in pre-mRNA splicing factors, found within the interchromatin regions of the nucleoplasm of mammalian cells (Lamond & Spector 2003). HeLa cells were grown as normal and prepared for immunofluorescence staining with Phospho-Thr-323 DDX3 (*Abcam*) and anti splicing factor SC35 (*Sigma*). As shown in Figure 7.9, Phospho-Thr-323 DDX3 co localised with the nuclear speckle marker anti splicing factor SC35, with an increase in the cytoplasmic localisation of both proteins during mitosis.

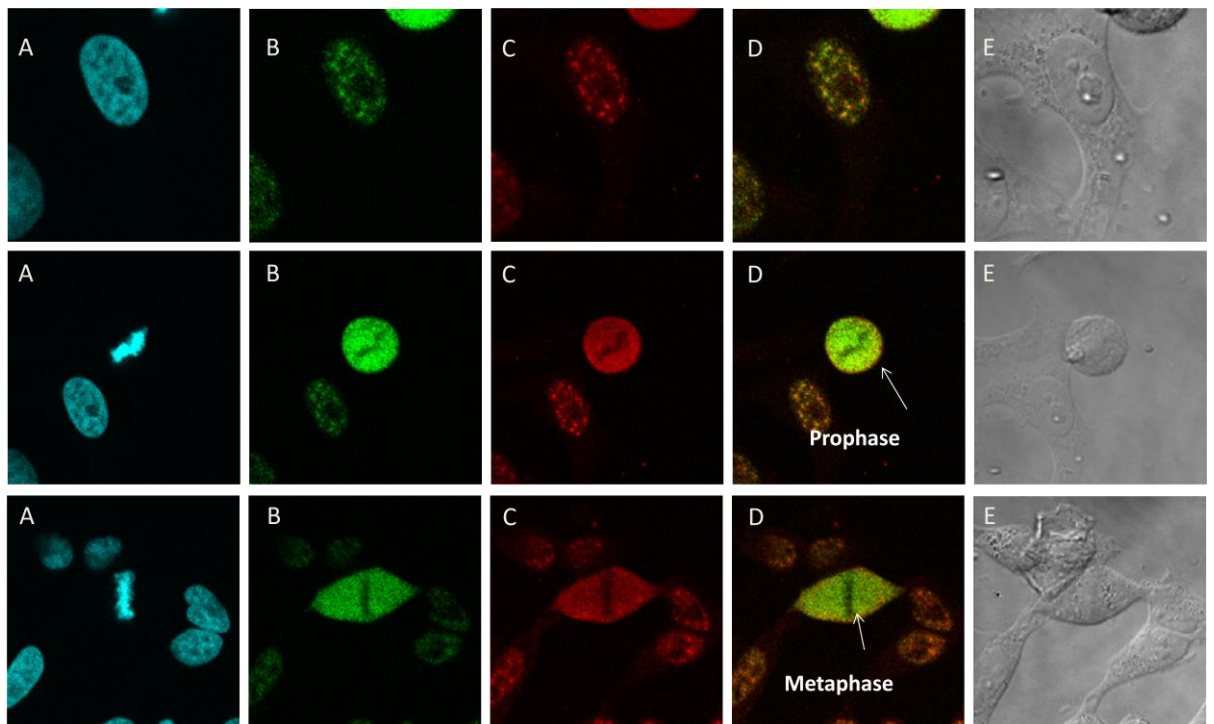


**Figure 7.9: Phospho-Thr 323 DDX3 co-localises with nuclear speckle marker anti splicing factor SC-35.**

Untreated HeLa cells were stained with an antibody against Phospho-Thr 323 DDX3 (*Abcam*) and anti-splicing factor SC-35 (*Sigma*). HeLa cells stained for PhosThr323 DDX3 and mitotic marker PhosphoHistone H3(*Cell Signalling Technologies*). **Key:** A (DAPI), B ( $\alpha$ -Phos-Thr323-DDX3), C ( $\alpha$ -PhosphoHistone H3), D (Merge B+C), E (Contrast).

#### 7.3.4. Investigating the role of Cyclin B phosphorylation of DDX3

Staining of HeLa cells showed that endogenous Phospho-T323 DDX3 (*Abcam*) localised predominantly to the nucleus in interphase cells. As stated earlier, Cyclin B has been shown to phosphorylate Thr 204 and Thr 323 of DDX3 during mitosis (Sekiguchi et al. 2007). I wanted to investigate whether phosphorylation of Thr204 and Thr323 caused nuclear accumulation of DDX3. Therefore, site mutants were created which substituted the threonines at positions 204 and 323 with alanine or phospho-mimetic aspartic acid. HeLa cells were transfected with these site mutants and stained as previously described. The T204A and T204D mutants localised predominantly to the cytoplasm, suggesting that phosphorylation of threonine 204 does not change localisation of DDX3 (Figure 7.10). The TA2 (T204A,T323A) and TD2 (T204D,T323D) double mutants also localised predominantly to the cytoplasm (Figure 7.11). To make sure that nuclear import of these site mutants was not affected, HeLa cells were transfected with expression plasmids for these mutants and treated with LMB to block nuclear export. As shown in Figure 7.11 and Figure 7.10, mutating the residues 204 and 323 to alanine or aspartic acid did not affect nuclear import. Therefore phosphorylation of DDX3 at residues 204 and 323 by Cyclin B does not seem to affect the nuclear import nor export of DDX3.

Endogenous Phospho-T323 DDX3 localised predominantly in the nucleus in interphase cells, with a cytoplasmic localisation only during mitosis, so it is unclear why our phospho-mimetic double mutant T204D/T323D remained in the cytoplasm.

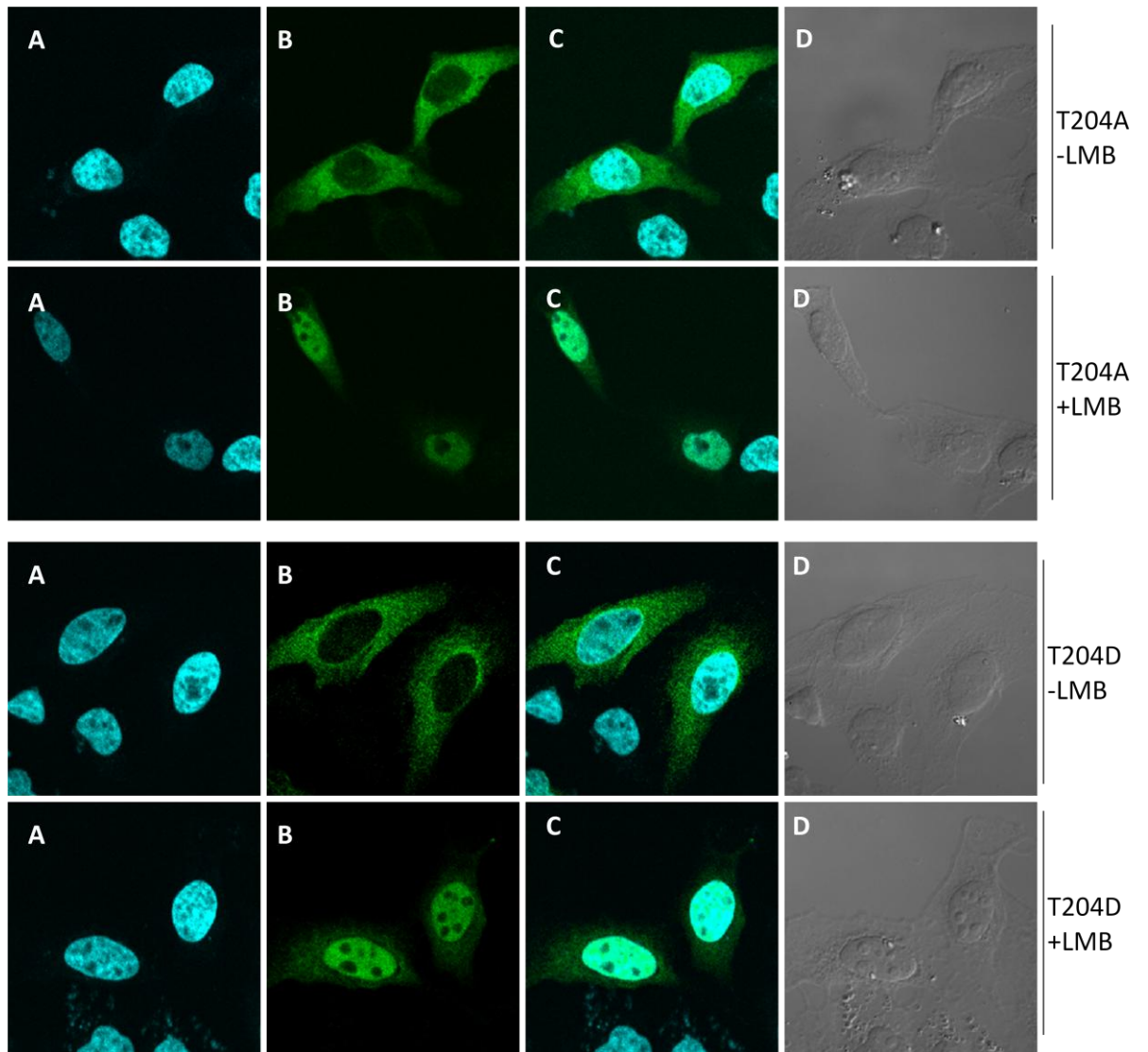


**Figure 7.10: The site mutants T204A and T204D have a predominantly cytoplasmic localisation and are exported from the nucleus in a CRM-1 dependent manner .**

HeLa cells were transfected with expression plasmids for Ha-tagged T204A and T204D mutants. Cells were treated with 20mM LMB for 2 hours or left untreated. Cells were stained with primary  $\alpha$ -Ha and secondary  $\alpha$ -mouse Alexa Fluor-488. **Key:** A(DAPI), B (Ha-DDX3), C (Merge A+B), D (Contrast).

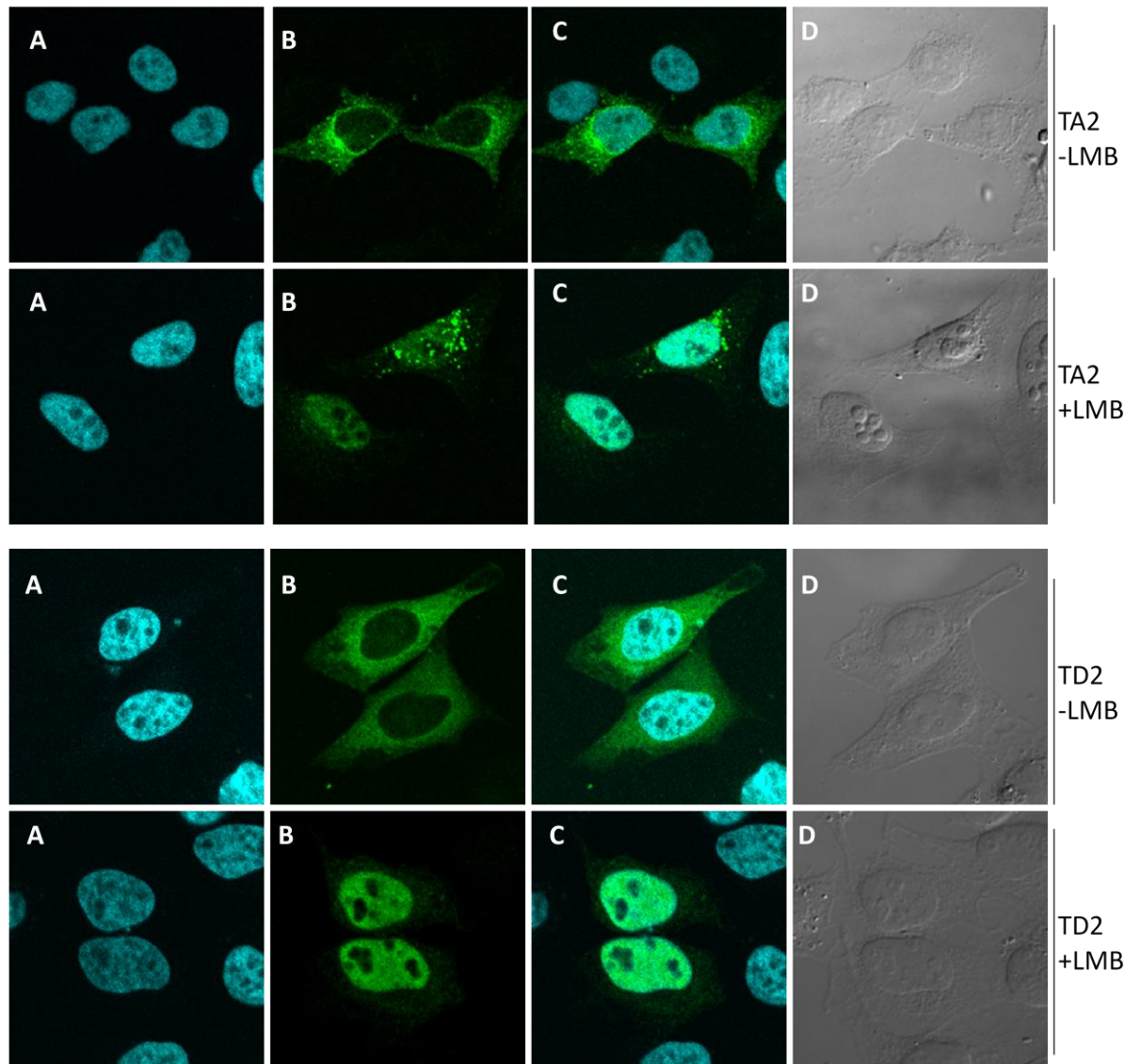


**Figure 7.11: The double site mutants TA2 and TD2 have a predominantly cytoplasmic localisation and are exported from the nucleus in a CRM-1 dependent manner.**

HeLa cells were transfected with expression plasmids for Ha-tagged TA2 and TD2 mutants. Cells were treated with 20mM LMB for 2 hours or left untreated. Cells were stained with primary  $\alpha$ -Ha and secondary  $\alpha$ -mouse Alexa Fluor-488. **Key:** A (DAPI), B (Ha-DDX3), C (Merge A+B), D (Contrast).

### 7.3.5. Investigating the expression of DDX3 during the cell cycle

A change in the localisation and a slight change in the expression levels of DDX3 and Phospho-Thr323 DDX3 (*Abcam*) was observed during the different stages of the cell cycle. I decided to investigate whether DDX3 expression levels altered in cells arrested at different stages of the cell cycle.

I used chemical blockage to arrest HeLa cells at specific stages of the cell cycle, as described previously. HeLa cell blocked at S and G0/G1 boundary had reduced levels of DDX3 (Figure 7.12). Originally I found it difficult to detect the Phospho-Thr-323 DDX3 antibody (*Abcam*) by western blotting. I was able to detect a band for Phospho-Thr-323 DDX3 in cells blocked at the G2/M boundary, however it did not correspond to the correct size, showing a band at 130kDa rather than 72kDa. This suggested that the Phospho-Thr-323 DDX3 antibody was not specific for p-DDX3.

The results of the previous experiment suggested that DDX3 levels are regulated throughout the cell cycle, I therefore decided to monitor changes in DDX3 expression during cell cycle progression.

To this end, HeLa cells were blocked at early G2/M, using a thymidine/nocodazole block and released into untreated medium and samples collected at different time points following release. Cells blocked at prometaphase had increased levels of DDX3, which decreased as the cells progressed through mitosis (Figure 7.13).

HeLa cells were also blocked at the G1/S boundary, using a double thymidine block. The double thymidine block was followed by a 21 hours release, showed that levels of DDX3 were decreased at the S and G1 phase compared to G2/M phase.

DDX3 levels increased as cells progressed through mitosis, increasing just as Cyclin B protein expression increased (Figure 7.14).

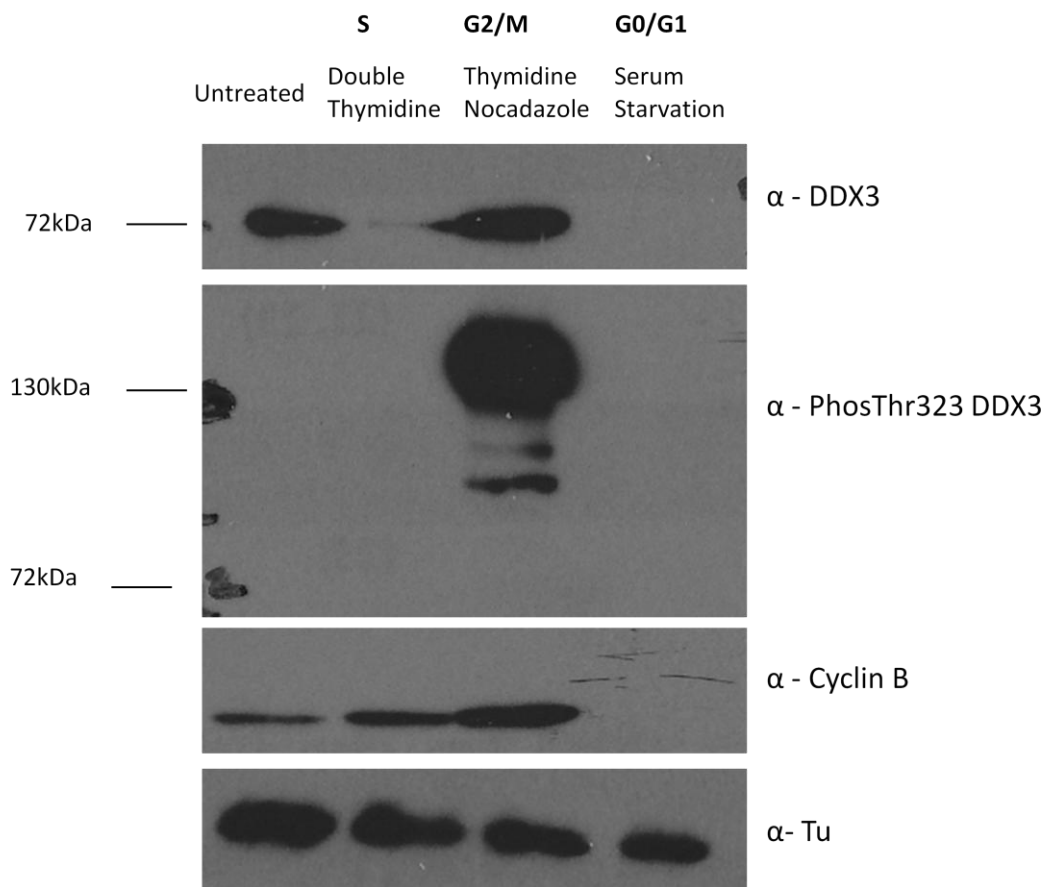


**Figure 7.12: Levels of DDX3 and Phos-Thr323-DDX3 changed during different stages of the cell cycle.**

HeLa cells were blocked in S phase, G2/M phase, G0/G1 phase as described in Chapter 2. Treated HeLa Cells and untreated control cells were lysed and immunoblotted as described in Chapter 2. Blots were probed with α-DDX3 (*Bethyl*), α-Phos-Thr323-DDX3 (*Abcam*), α-Tubulin (*Abcam*) and α-Cyclin B (*Santa Cruz*). Representative blot of three experiments.

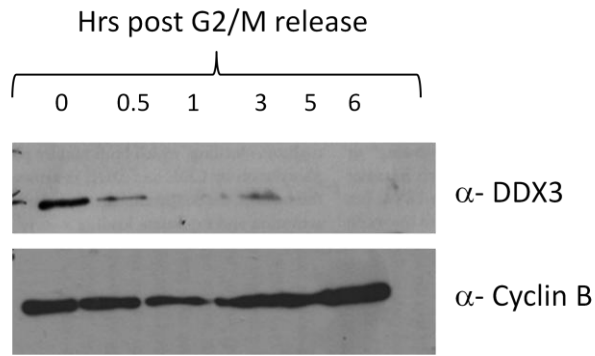


**Figure 7.13: Levels of DDX3 are increased at prometaphase.**

HeLa cells were blocked in early G2/M phase, using a Thymidine block followed by Nocodazole block. Cells were released into from block and harvested after 30 minutes, 1 hr, 3 hr, 5 hr and 6 hrs. HeLa cells were then lysed and immunoblotted as described in Chapter 2. Blots were probed with α-DDX3 (*Bethyl*) and α-Cyclin B (*Santa Cruz*).

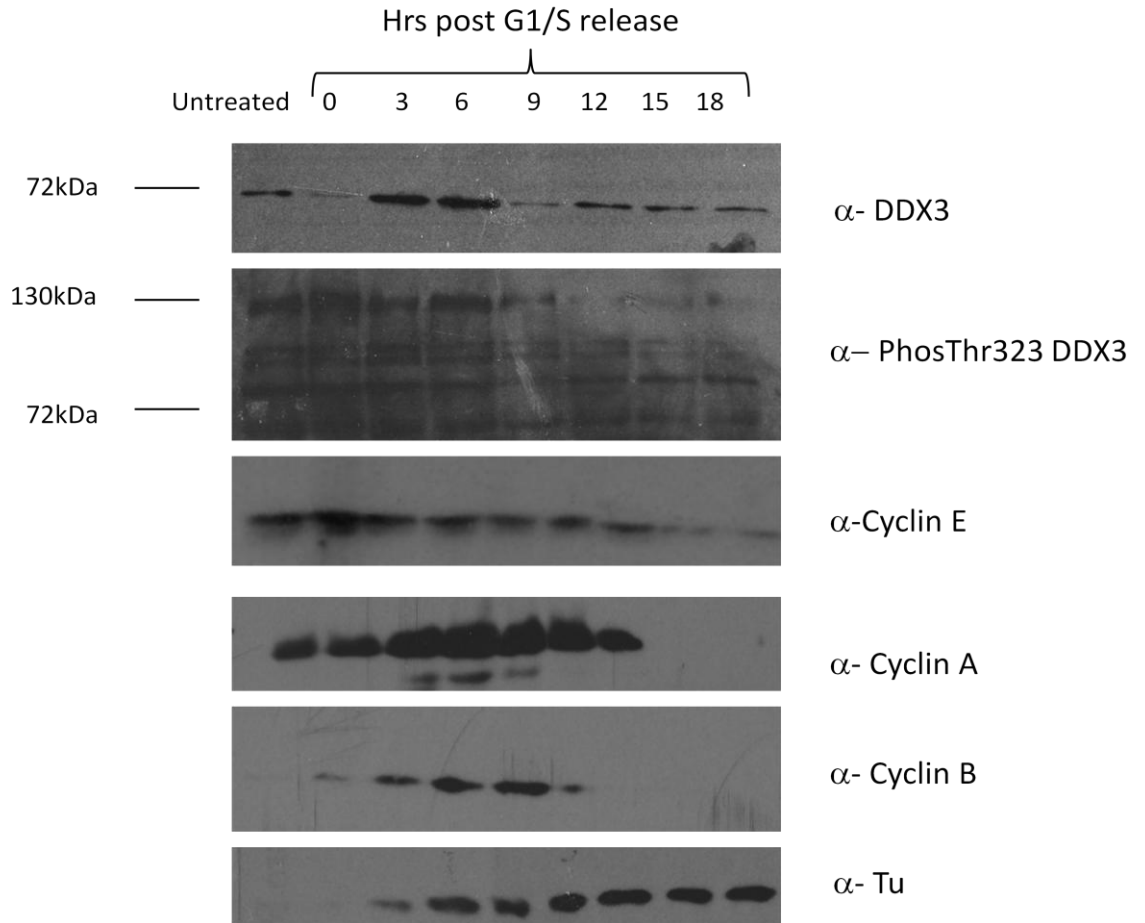


**Figure 7.14: Expression of DDX3 increases during mitosis.**

HeLa Cells were blocked in S phase using the double thymidine block as described in Chapter 2. Cells were released from the block and harvested every 3 hrs for 18 hrs. Treated HeLa Cells and untreated control cells were lysed and immunoblotted as described in Chapter 2. Blots were probed with α-DDX3 (*Bethyl*), α-Tubulin (*Abcam*), α-Cyclin B (*Santa Cruz*), α-Cyclin A (*Santa Cruz*) and α-Cyclin E (*Santa Cruz*). Representative blot of three experiments.

#### 7.4. Discussion

---

DDX3 localisation and expression seemed to change during the cell cycle. During progression through the cell cycle, I found that DDX3 protein expression was increased as cell entered mitosis and also that DDX3 became more nuclear at prometaphase. DDX3 has been shown to regulate cell cycle progression, as it is required for Cyclin A expression and translation of Cyclin E mRNA (Sekiguchi et al. 2004; Lai et al. 2010). Cyclin B has been shown to phosphorylate DDX3 during mitosis, with the authors suggesting that phosphorylation inactivates DDX3 (Sekiguchi et al. 2007). Loss of DDX3 has been shown to result in nuclear accumulation of Cyclin A mRNA, suggesting that DDX3 may play a role in export of Cyclin A mRNA (Sekiguchi et al. 2004). I had speculated that Cyclin B phosphorylation of DDX3 could lead to nuclear accumulation of DDX3, since I observed nuclear staining for the Phospho-Thr323 DDX3 antibody (Sekiguchi et al. 2004; Lai et al. 2010). However, my phospho-deficient and phospho-mimetic mutants for Thr204 and Thr323 shuttled normally, so phosphorylation of these residues does not seem to affect localisation of DDX3 in the cell. Perhaps nuclear export of Cyclin A mRNA is affected by phosphorylation, since Thr323 is situated in motif 1b which is important for RNA substrate binding. Cyclin B phosphorylation could also affect the stability levels of DDX3 protein by post-translational modifications, thereby contributing to the observed increased DDX3 levels during mitosis.

Recently, a study on phosphoproteome dynamics during the cell cycle also found DDX3 to be phosphorylated during mitosis, with phosphorylation of residues 61 and 323, and strong phosphorylation at serine 594 by Casein Kinase 1 (CK1)

during mitosis. The authors speculated that substrates of CK1 and other mitotic kinases are inactivated by phosphorylation during mitosis (Olsen et al. 2013). In another study, DDX3 has recently been shown to be a regulator of Wnt- $\beta$ -Catenin signalling by interacting with CK1 to promote its kinase activity (Cruciat et al. 2013). The Wnt- $\beta$ -Catenin pathway is highly conserved and plays an important role in development of multi-cellular organisms, and is often dis-regulated in cancer (Clevers & Nusse 2012).

DDX3 phosphorylation during mitosis might also play a role in the down-regulation of protein synthesis, since translation of cap-dependent mRNA is reduced during mitosis (Bonneaus & Sonenberg 1987). As earlier stated, loss of function DDX3 results in nuclear accumulation of Cyclin A mRNA (Fukumura 2003) and also loss of DDX3 has been associated with nuclear accumulation of PABP1 (Shih et al. 2012). Interestingly PABP1 requires mRNA to export from the nucleus (Burgess et al. 2011; Afonina 1998). Perhaps phosphorylated DDX3 has reduced affinity for mRNA and therefore DDX3's role in mRNA processing and mRNA nuclear export is impaired during mitosis.

Phosphorylation during G2/M phase of the cell cycle has been shown to regulate the interaction of DDX3 with DDX5 (Choi & Lee 2012). This DDX3/DDX5 interaction was suggested to play a role in mRNP export, and that knockdown of DDX3 affected DDX5 nuclear export. They showed that DDX3 had reduced p-Ser during G2/M phase and unchanged p-Thr and p-Tyr levels, whereas DDX5 had increased p-Ser, p-Thr and p-Tyr levels during G2/M phase. They also showed that DDX3 has a nuclear localisation at G0 and also that DDX3 levels were decreased during G2/M (Choi & Lee 2012), which is the opposite of what we found. Previous

studies have shown DDX3 to be strongly phosphorylated at Thr 323 by Cyclin B during G2/M phase (Sekiguchi et al. 2007) and Ser 594 by Ck1 (Olsen et al. 2013), which is in conflict with the above study.

DDX3 has also recently been suggested to play a role in mitotic chromosome segregation in somatic cells. The DDX3 homologue from *Drosophila* Belle and human DDX3 have both been shown to promote mitotic chromosome segregation alongside the RNA interference (RNAi) pathway (Pek & Kai 2011). The highly conserved RNAi pathway has been shown to play a role in various cellular processes, such as gene silencing and assembly of heterchromatin at centromeres (Hannon 2002), and the RNAi protein DICER is a key player in chromosomal segregation (Fukagawa et al. 2004; White & Allshire 2004). In this study DDX3 was shown to localise to chromosomes in a DICER dependent manner, and the authors suggested that DDX3 promoted chromosome segregation downstream of DICER (Pek & Kai 2011). Interestingly, they showed that DDX3 localised to condensing chromosomes in the nucleus during prophase/prometaphase, supporting our finding that DDX3 became nuclear during prometaphase.

I strongly suspect that the Phospho-Thr 323 DDX3 antibody (*Abcam*) is not specific for a phosphorylated form of DDX3, with the protein band being detected in western blot analysis (130kDa) not being the correct size for DDX3 (72kDa). The Phospho-Thr 323 DDX3 antibody (*Abcam*) band was only visible by western blotting in mitotic cells, and co-localised with the nuclear speckle marker anti-splicing factor SC-35 in immunofluorescence. The antibody was raised from a synthetic phosphopeptide derived from human DDX3 around the phosphorylation site of threonine 322 (V-A-T-P-P-G). This region is quite conserved amongst DEAD-box

proteins, therefore the Phospho-Thr323 DDX3 antibody might recognise another phosphorylated DEAD-box protein. I speculated that the antibody recognises the DEAD-box protein DD36, as it contains the (V-A-T-P-P-G) region and is found in nuclear speckles and is approximately 130kDa (Iwamoto et al. 2008). Interestingly there was an increase in the Phospho-Thr 323 during mitosis, and also the Phospho-Thr 323 antibody co-localised with the nuclear speckle marker anti splicing factor SC35.

Since there seemed to be a change in DDX3 expression levels and localisation during the cell cycle, this suggests that DDX3 might indeed play a role in regulation of the cell cycle. Further investigation is needed to fully characterise the role DDX3 plays in cell cycle regulation.

## **Chapter 8 : General Discussion**

---

DDX3 is a multifunctional protein which has been shown to play roles in various cellular processes. Recently, DDX3 has garnered a lot of interest as it has been found to be required for the replication of major viruses (Yedavalli et al. 2004; Ariumi et al. 2007), and also to be a critical component of innate immune signalling (Schröder et al. 2008; Soulat et al. 2008). DDX3 has also been implicated in tumorigenesis, with DDX3 suggested to act as both a tumour suppressor (Chao et al. 2006; Chang et al. 2005; Shih et al. 2008) and oncogene (Botlagunta et al. 2008; Botlagunta et al. 2011; Sun et al. 2011). Even though there has been a lot of research into the various functions of DDX3, there are still many questions left unanswered. Since DDX3 has been suggested as potential drug target in the fight against HIV and HCV, a better understanding of DDX3's roles in cellular processes is required.

Here I have shown that DDX3 is a nucleocytoplasmic shuttling protein which is exported from the nucleus in a CRM-1 dependent manner and that the highly conserved N-terminal NES is required and sufficient for nuclear export. I also investigated how DDX3 is imported into the nucleus, however I was unable to fully define DDX3's nuclear import. I have shown that the two rec-A like domains of DDX3 can be imported independently and that DDX3 is imported independently of Importin- $\beta$  and Calmodulin. I would hypothesise that DDX3 might import via Transportin in a PY-NLS independent manner, perhaps "piggy backing" into the nucleus with another protein or containing a non-classical Transportin NLS.

Whether DDX3's nucleocytoplasmic shuttling was regulated during innate immune signalling and by viruses was also investigated. Here the HCA showed that

triggering of PRR and pro-inflammatory cytokines did not change the localisation of DDX3. However viral proteins were able to regulate the cellular localisation of DDX3. Interestingly, I found that both HIV and HCV re-localised DDX3 to different cellular compartments, with DDX3 being enriched in the nucleolus by HIV-Rev; and DDX3 being sequestered in cytoplasmic speckles by HCV. This suggests that HIV and HCV target different nuclear and cytoplasmic functions of DDX3 to promote viral replication.

I showed that HIV-Rev caused both DDX3 and CRM-1 to accumulate in the nucleolus of cells. Yedavalli et al. showed that the C-terminus of DDX3 directly interacted with CRM-1, and also that HIV-Rev co-immunoprecipitated with DDX3. They suggested that the N-terminal NES of DDX3 was not required for CRM-1 binding, and that DDX3 worked as a CRM-1 specific effector and interacted with CRM-1 and HIV-Rev in a ternary complex. Here I have shown that the N-terminal NES of DDX3 is required for DDX3's interaction with CRM-1, and also that DDX3 can directly interact with HIV-Rev. Maybe DDX3 does not play a direct role in regulation of CRM-1 dependent export of HIV RNAs, rather DDX3 might be involved in the steps prior to RNA export. During HIV replication, it has been shown that both HIV-Tat and HIV RNA must associate with the nucleolus to mediate HIV replication (Michienzi et al. 2000; Michienzi et al. 2002). Also, DDX3 has been shown to be enriched in the nucleolus of HIV-Tat expressing cells (Jarboui et al. 2012), suggesting that DDX3 is recruited to the nucleolus by HIV-Rev and HIV-Tat. Since both DDX3 and CRM-1 are recruited to the nucleolus by HIV-Rev, maybe DDX3 plays a role in RNA processing in the nucleolus and then CRM-1 and HIV-Rev export the processed RNA from the nucleus. An insertion between motifs I and Ib of DDX3 has

been shown to interact with HIV-RNA and to be critical for HIV replication, as a peptide inhibitor for this region inhibited HIV replication (Garbelli et al. 2011). This suggests that DDX3 needs to directly interact with HIV RNA to promote replication. DDX3 has also been shown promote HIV RNA translation (Liu et al. 2011; Soto-Rifo et al. 2012; Geissler et al. 2012). Previously, DDX3 has been shown to be required for HIV IRES mediated translation (Liu et al. 2011), and was suggested to support assembly of the 80s ribosome (Geissler et al. 2012). Also DDX3 has also been shown to be required for cap-dependent translation of complex RNAs and interestingly Tar-containing HIV RNA (Soto-Rifo et al. 2012). Perhaps DDX3 is required for different functions during HIV replication, possibly having different roles depending on the stage of viral infection. Maybe DDX3 associates with HIV RNA from transcription to translation, and potentially plays a role in co-ordinating HIV RNA processes.

In this study, I also found that HCV Core protein altered the cellular localisation of DDX3 and prevented the nucleocytoplasmic shuttling of DDX3. Mis-localisation of DDX3 could have many functional consequences, since DDX3 has been shown to have important roles in both the nucleus and the cytoplasm. Here I found that HCV Core protein recruited DDX3 and eIF4E to cytoplasmic granules, similar to the oxidative stress mediated localisation of DDX3 to eIF4E-containing SG. HCV infection has been shown to regulate SGs throughout the HCV life cycle (Garaigorta et al. 2012), and to promote translation of viral RNA by recruiting components of P-bodies and SGs to lipid droplets (Ariumi, Kuroki, Kushima, et al. 2011). It is possible that the HCV Core protein might recruit DDX3 to cytoplasmic granules to promote translation of HCV RNA, while possibly inhibiting DDX3's association with "true"

SGs. It would be interesting to see if knockdown of DDX3 prevented recruitment of SG components to HCV-Core at lipid droplets, maybe DDX3 is critical for this recruitment.

Also HCV Core protein may target DDX3's different functions throughout the viral life cycle. A successful virus will maintain cell survival while promoting replication of the viral genome, so it is possible the HCV Core protein utilises DDX3's role in SGs to promote cell survival. Also HCV Core protein might inhibit type I IFN expression by targeting avSGs (Onomoto et al. 2012). DDX3 has previously been suggested to play a role in initial RNA sensing by the RIG-I/MAVS complex (Oshiumi, Sakai, et al. 2010), and avSGs have been shown to contain RIG-I and PKR, and have been shown to be critical for type I IFN induction (Onomoto et al. 2012). Since DDX3 has also been shown to be critical for type I IFN induction, it is a possibility that DDX3 is a component of avSGs. Perhaps HCV-Core protein interacts with DDX3 to prevent it from associating with IFN promoting RIG-I containing avSGs.

I have found that DDX3 is sequestered in the cytoplasm by HCV infection, therefore DDX3's role as a tumour suppressor in the nucleus could be abrogated. HCV infection is a known contributor to Hepatocellular Carcinoma (HCC) (Jahan et al. 2012). DDX3 localisation has been suggested to be cytoplasmic in transformed cells and nuclear normal primary cells (Shih et al. 2008; Miao et al. 2013; Lee et al. 2013), therefore I investigated DDX3's cellular localisation in a range of transformed cell lines and also in primary hepatocytes. I found that DDX3 has a predominantly cytoplasmic localisation in all the transformed cell lines I tested, but had a distinctly more nuclear localisation in non-transformed primary hepatocytes. This could suggest that DDX3's nuclear localisation is indeed important for its tumour

suppressor functions. Mis-localisation of tumour suppressors and oncogenes has been implicated in a range of cancers (Kau et al. 2004). Nuclear DDX3 is required for DDX3's role as a tumour suppressor. DDX3's role in p21<sup>waf1/cap1</sup> promoter activation could conceivably be affected by a loss of nuclear localisation, HBV infection has also been linked to reduced levels of DDX3 in HCC (Shih et al. 2008; Chang et al. 2005). Future work could further examine the link between DDX3 mis-localisation in transformed cells and in HCV infection, and investigate if DDX3 mis-localisation by HCV Core protein prevents DDX3 from acting as a tumour suppressor. It would be interesting to investigate if HCV Core protein inhibited DDX3's role in induction of p21<sup>waf1/cap1</sup> promoter activity.

Viral infection could also affect DDX3's role during Cell Cycle progression. We found that DDX3 expression levels changed during the cell cycle, and also that DDX3 became more nuclear during prometaphase. HCV infection has been shown to cause cell cycle arrest at G2/M, with a correlation between HCV Core protein expression and arrest at G2/M (Kannan et al. 2011). Since I found that DDX3 was sequestered in the cytoplasm during HCV infection, it would be interesting to see if HCV Core's prevention of DDX3's nucleocytoplasmic shuttling caused G2/M arrest during HCV.

In conclusion, I have found DDX3 to be a nucleocytoplasmic shuttling protein which utilises CRM-1 to be exported from the nucleus, and also to be imported to the nucleus independently of Importin- $\beta$  and Calmodulin. Interestingly, I found that DDX3's cellular localisation was targeted by HIV and HCV, with both viruses re-localising DDX3 to different cellular compartments. I also found DDX3 to associate

with SGs in response to cellular stress. I have also shown that DDX3's expression and cellular localisation changes throughout the cell cycle.

## Bibliography

---

- Ablasser, A. et al., 2009. RIG-I-dependent sensing of poly(dA:dT) through the induction of an RNA polymerase III-transcribed RNA intermediate. *Nature immunology*, 10(10), pp.1065–72.
- Afonina, E., 1998. The Human Poly(A)-binding Protein 1 Shuttles between the Nucleus and the Cytoplasm. *Journal of Biological Chemistry*, 273(21), pp.13015–13021.
- Ahmed, S. & Brickner, J.H., 2007. Regulation and epigenetic control of transcription at the nuclear periphery. *Trends in genetics : TIG*, 23(8), pp.396–402.
- Akira, S., Uematsu, S. & Takeuchi, O., 2006. Pathogen recognition and innate immunity. *Cell*, 124(4), pp.783–801.
- Anderson, P. & Kedersha, N., 2009. RNA granules: post-transcriptional and epigenetic modulators of gene expression. *Nature reviews. Molecular cell biology*, 10(6), pp.430–6.
- Anderson, P. & Kedersha, N., 2008. Stress granules: the Tao of RNA triage. *Trends in biochemical sciences*, 33(3), pp.141–50.
- Angus, A.G.N. et al., 2010. Requirement of cellular DDX3 for hepatitis C virus replication is unrelated to its interaction with the viral core protein. *The Journal of general virology*, 91(Pt 1), pp.122–32.
- Aratani, S. et al., 2001. Dual roles of RNA helicase A in CREB-dependent transcription. *Molecular and cellular biology*, 21(14), pp.4460–9.
- Aratani, S. et al., 2006. The nuclear import of RNA helicase A is mediated by importin- $\alpha$ 3. *Biochemical and biophysical research communications*, 340(1), pp.125–33.
- Arimoto, K. et al., 2008. Formation of stress granules inhibits apoptosis by suppressing stress-responsive MAPK pathways. *Nature cell biology*, 10(11), pp.1324–32.
- Ariumi, Y. et al., 2007. DDX3 DEAD-box RNA helicase is required for hepatitis C virus RNA replication. *Journal of virology*, 81(24), pp.13922–13926.
- Ariumi, Y., Kuroki, M., Kushima, Y., et al., 2011. Hepatitis C Virus Hijacks P-Body and Stress Granule Components around Lipid Droplets. *Journal of virology*, 85(14), pp.6882–92.
- Ariumi, Y., Kuroki, M., Maki, M., et al., 2011. The ESCRT system is required for hepatitis C virus production. G. M. Fimia, ed. *PloS one*, 6(1), p.e14517.

- Ashfaq, U. a et al., 2011. An overview of HCV molecular biology, replication and immune responses. *Virology journal*, 8(1), p.161.
- Askjaer, P. et al., 1999. RanGTP-regulated interactions of CRM1 with nucleoporins and a shuttling DEAD-box helicase. *Molecular and cellular biology*, 19(9), pp.6276–85.
- Askjaer, P., 1998. The Specificity of the CRM1-Rev Nuclear Export Signal Interaction Is Mediated by RanGTP. *Journal of Biological Chemistry*, 273(50), pp.33414–33422.
- Askjaer, P., Rosendahl, R. & Kjems, J., 2000. Nuclear export of the DEAD box An3 protein by CRM1 is coupled to An3 helicase activity. *The Journal of biological chemistry*, 275(16), pp.11561–8.
- Balagopal, V. & Parker, R., 2009. Polysomes, P bodies and stress granules: states and fates of eukaryotic mRNAs. *Current opinion in cell biology*, 21(3), pp.403–8.
- Bates, G.J. et al., 2005. The DEAD box protein p68: a novel transcriptional coactivator of the p53 tumour suppressor. *The EMBO journal*, 24(3), pp.543–53.
- Batlle, E. et al., 2000. The transcription factor snail is a repressor of E-cadherin gene expression in epithelial tumour cells. *Nature cell biology*, 2(2), pp.84–9.
- Bayliss, R., Littlewood, T. & Stewart, M., 2000. Structural Basis for the Interaction between FxFG Nucleoporin Repeats and Importin- $\beta$  in Nuclear Trafficking. *Cell*, 102(1), pp.99–108.
- Beckham, C. et al., 2008. The DEAD-box RNA helicase Ded1p affects and accumulates in *Saccharomyces cerevisiae* P-bodies. *Molecular biology of the cell*, 19(3), pp.984–93.
- Bernad, R. et al., 2004. Nup358/RanBP2 Attaches to the Nuclear Pore Complex via Association with Nup88 and Nup214/CAN and Plays a Supporting Role in CRM1-Mediated Nuclear Protein Export. *Molecular and Cellular Biology*, 24(6), pp.2373–2384.
- Berthelot, K. et al., 2004. Dynamics and processivity of 40S ribosome scanning on mRNA in yeast. *Molecular Microbiology*, 51(4), pp.987–1001.
- Black, B.E. et al., 2001. Nxt1 Is Necessary for the Terminal Step of Crm1-Mediated Nuclear Export. *The Journal of Cell Biology*, 152(1), pp.141–156.
- Blissenbach, M. et al., 2010. Nuclear RNA export and packaging functions of HIV-1 Rev revisited. *Journal of virology*, 84(13), pp.6598–604.

- Bonneaus, A. & Sonenberg, N., 1987. Involvement of the 24-kDa Cap-binding Protein in Regulation of Protein Synthesis in Mitosis. *The Journal of biological chemistry*, 262(15), pp.11134–11139.
- Botlagunta, M. et al., 2011. Expression of DDX3 is directly modulated by hypoxia inducible factor-1 alpha in breast epithelial cells. *PloS one*, 6(3), p.e17563.
- Botlagunta, M. et al., 2008. Oncogenic role of DDX3 in breast cancer biogenesis. *Oncogene*, 27(28), pp.3912–22.
- Boulant, S. et al., 2005. Hepatitis C virus core protein is a dimeric alpha-helical protein exhibiting membrane protein features. *Journal of virology*, 79(17), pp.11353–65.
- Boulant, S. et al., 2006. Structural determinants that target the hepatitis C virus core protein to lipid droplets. *The Journal of biological chemistry*, 281(31), pp.22236–47.
- Boulant, S., Targett-Adams, P. & McLauchlan, J., 2007. Disrupting the association of hepatitis C virus core protein with lipid droplets correlates with a loss in production of infectious virus. *The Journal of general virology*, 88(Pt 8), pp.2204–13.
- Bowie, A.G. & Unterholzner, L., 2008. Viral evasion and subversion of pattern-recognition receptor signalling. *Nature reviews. Immunology*, 8(12), pp.911–22.
- Braun, I.C. et al., 1999. TAP binds to the constitutive transport element (CTE) through a novel RNA-binding motif that is sufficient to promote CTE-dependent RNA export from the nucleus. *The EMBO journal*, 18(7), pp.1953–65.
- Browne, S.K. et al., 2006. Differential IFN-gamma stimulation of HLA-A gene expression through CRM-1-dependent nuclear RNA export. *Journal of immunology*, 177(12), pp.8612–9.
- Bukh, J., Purcell, R.H. & Miller, R.H., 1994. Sequence analysis of the core gene of 14 hepatitis C virus genotypes. *Proceedings of the National Academy of Sciences of the United States of America*, 91(17), pp.8239–43.
- Bürckstümmer, T. et al., 2009. An orthogonal proteomic-genomic screen identifies AIM2 as a cytoplasmic DNA sensor for the inflammasome. *Nature immunology*, 10(3), pp.266–72.
- Burden, D.A. & Osheroff, N., 1998. Mechanism of action of eukaryotic topoisomerase II and drugs targeted to the enzyme. *Biochimica et biophysica acta*, 1400(1-3), pp.139–54.

- Burgess, H.M. et al., 2011. Nuclear relocalisation of cytoplasmic poly(A)-binding proteins PABP1 and PABP4 in response to UV irradiation reveals mRNA-dependent export of metazoan PABPs. *Journal of cell science*, 124(Pt 19), pp.3344–55.
- Caillaud, A. et al., 2005. Regulatory serine residues mediate phosphorylation-dependent and phosphorylation-independent activation of interferon regulatory factor 7. *The Journal of biological chemistry*, 280(18), pp.17671–7.
- Carrillo-Infante, C. et al., 2007. Viral infections as a cause of cancer (review). *International journal of oncology*, 30(6), pp.1521–8.
- Chan, C.K. et al., 1998. Mutual exclusivity of DNA binding and nuclear localization signal recognition by the yeast transcription factor GAL4: implications for nonviral DNA delivery. *Gene therapy*, 5(9), pp.1204–12.
- Chang et al., 2006. DDX3, a DEAD box RNA helicase, is deregulated in hepatitis virus-associated hepatocellular carcinoma and is involved in cell growth control. *Oncogene*, 25(14), pp.1991–2003.
- Chang, P. et al., 2005. DDX3, a DEAD box RNA helicase, is deregulated in hepatitis virus-associated .... *Oncogene*.
- Chang, T.-H. & Tarn, W.-Y., 2009. The current understanding of Ded1p/DDX3 homologs from yeast to human. *RNA Biology*, 6(1), pp.17–20.
- Chao, C.-H. et al., 2006. DDX3, a DEAD box RNA helicase with tumor growth-suppressive property and transcriptional regulation activity of the p21waf1/cip1 promoter, is a candidate tumor suppressor. *Cancer research*, 66(13), pp.6579–88.
- Chevalier, S.A. et al., 2005. Presence of a functional but dispensable nuclear export signal in the HTLV-2 Tax protein. *Retrovirology*, 2, p.70.
- Chinnasamy, D. et al., 2000. Lentiviral-mediated gene transfer into human lymphocytes: role of HIV-1 accessory proteins. *Blood*, 96(4), pp.1309–16.
- Choi, Y.-J. & Lee, S.-G., 2012. The DEAD-box RNA helicase DDX3 interacts with DDX5, co-localizes with it in the cytoplasm during the G2/M phase of the cycle, and affects its shuttling during mRNP export. *Journal of cellular biochemistry*, 113(3), pp.985–96.
- Cingolani, G. et al., 2002. Molecular basis for the recognition of a nonclassical nuclear localization signal by importin beta. *Molecular cell*, 10(6), pp.1345–53.
- Cingolani, G. et al., 1999. Structure of importin-beta bound to the IBB domain of importin-alpha. *Nature*, 399(6733), pp.221–9.

- Clevers, H. & Nusse, R., 2012. Wnt/ $\beta$ -catenin signaling and disease. *Cell*, 149(6), pp.1192–205.
- Clouse, K.N. et al., 2001. A Ran-independent pathway for export of spliced mRNA. *Nature cell biology*, 3(1), pp.97–9.
- Conti, E. et al., 1998. Crystallographic Analysis of the Recognition of a Nuclear Localization Signal by the Nuclear Import Factor Karyopherin  $\alpha$ . *Cell*, 94(2), pp.193–204.
- La Cour, T. et al., 2004. Analysis and prediction of leucine-rich nuclear export signals. *Protein engineering, design & selection : PEDS*, 17(6), pp.527–36.
- Cruciat, C.-M. et al., 2013. RNA Helicase DDX3 Is a Regulatory Subunit of Casein Kinase 1 in Wnt/ $\beta$ -Catenin Signaling. *Science (New York, N.Y.)*.
- Cullen, B.R., 2003. Nuclear RNA export. *Journal of Cell Science*, 116(4), pp.587–597.
- Daelemans, D. et al., 2002. A synthetic HIV-1 Rev inhibitor interfering with the CRM1-mediated nuclear export. *PNAS*, 99(22), pp.14440–14445.
- Dang, Y. et al., 2009. Inhibition of nonsense-mediated mRNA decay by the natural product pateamine A through eukaryotic initiation factor 4AIII. *The Journal of biological chemistry*, 284(35), pp.23613–21.
- Dias, S.M.G. et al., 2009. The molecular basis for the regulation of the cap-binding complex by the importins. *Nature structural & molecular biology*, 16(9), pp.930–7.
- Dundr, M. et al., 1995. The roles of nucleolar structure and function in the subcellular location of the HIV-1 Rev protein. *J. Cell Sci.*, 108(8), pp.2811–2823.
- Emerman, M. & Malim, M.H., 1998. HIV-1 regulatory/accessory genes: keys to unraveling viral and host cell biology. *Science (New York, N.Y.)*, 280(5371), pp.1880–4.
- Endoh, H. et al., 1999. Purification and Identification of p68 RNA Helicase Acting as a Transcriptional Coactivator Specific for the Activation Function 1 of Human Estrogen Receptor alpha. *Mol. Cell. Biol.*, 19(8), pp.5363–5372.
- Englmeier, L. et al., 2001. RanBP3 influences interactions between CRM1 and its nuclear protein export substrates. *EMBO reports*, 2(10), pp.926–32.
- Englmeier, L., Olivo, J.-C. & Mattaj, I.W., 1999. Receptor-mediated substrate translocation through the nuclear pore complex without nucleotide triphosphate hydrolysis. *Current Biology*, 9(1), pp.30–41.

- Fagerlund, R. et al., 2002. Arginine/lysine-rich nuclear localization signals mediate interactions between dimeric STATs and importin alpha 5. *The Journal of biological chemistry*, 277(33), pp.30072–8.
- Fahrenkrog, B. & Aebi, U., 2003. The nuclear pore complex: nucleocytoplasmic transport and beyond. *Nature reviews. Molecular cell biology*, 4(10), pp.757–66.
- Fanara, P. et al., 2000. Quantitative analysis of nuclear localization signal (NLS)-importin alpha interaction through fluorescence depolarization. Evidence for auto-inhibitory regulation of NLS binding. *The Journal of biological chemistry*, 275(28), pp.21218–23.
- Feitelson, M.A. et al., 2002. Genetic mechanisms of hepatocarcinogenesis. *Oncogene*, 21(16), pp.2593–604.
- Frankel, A.D. & Young, J.A., 1998. HIV-1: fifteen proteins and an RNA. *Annual review of biochemistry*, 67, pp.1–25.
- Fraser, C.S., Pain, V.M. & Morley, S.J., 1999. Cellular stress in xenopus kidney cells enhances the phosphorylation of eukaryotic translation initiation factor (eIF)4E and the association of eIF4F with poly(A)-binding protein. *The Biochemical journal*, 342 Pt 3, pp.519–26.
- Freed, E.O., 2004. HIV-1 and the host cell: an intimate association. *Trends in microbiology*, 12(4), pp.170–7.
- Fribourg, S. et al., 2001. Structural basis for the recognition of a nucleoporin FG repeat by the NTF2-like domain of the TAP/p15 mRNA nuclear export factor. *Molecular cell*, 8(3), pp.645–56.
- Fridell, R. et al., 1997. Nuclear import of hnRNP A1 is mediated by a novel cellular cofactor related to karyopherin-beta. *Journal of cell science*, 110(11), pp.1325–1331.
- Fried, H. & Kutay, U., 2003. Nucleocytoplasmic transport: taking an inventory. *Cellular and molecular life sciences : CMLS*, 60(8), pp.1659–88.
- Fujii, R. et al., 2001. A Role of RNA Helicase A in cis-Acting Transactivation Response Element-mediated Transcriptional Regulation of Human Immunodeficiency Virus Type 1. *The Journal of biological chemistry*, 276(8), pp.5445–51.
- Fukagawa, T. et al., 2004. Dicer is essential for formation of the heterochromatin structure in vertebrate cells. *Nature cell biology*, 6(8), pp.784–91.
- Fukumura, J., 2003. A Temperature-Sensitive Mutant of the Mammalian RNA Helicase, DEAD-BOX X Isoform, DBX, Defective in the Transition from G1 to S Phase. *Journal of Biochemistry*, 134(1), pp.71–82.

- Fukushima, K. et al., 2001. Correlation between p21(waf1) and p16(INK4a) expression in hepatocellular carcinoma. *Hepatology research : the official journal of the Japan Society of Hepatology*, 20(1), pp.52–67.
- Fuller-Pace, F. V., 2006. DExD/H box RNA helicases: multifunctional proteins with important roles in transcriptional regulation. *Nucleic acids research*, 34(15), pp.4206–15.
- Fuller-Pace, F. V & Ali, S., 2008. The DEAD box RNA helicases p68 (Ddx5) and p72 (Ddx17): novel transcriptional co-regulators. *Biochemical Society transactions*, 36(Pt 4), pp.609–12.
- Garaigorta, U. et al., 2012. Hepatitis C Virus Induces the Formation of Stress Granules whose Proteins Regulate HCV RNA Replication, Virus Assembly and Egress. *Journal of virology*, 86(20), pp.11043–11056.
- Garbelli, A. et al., 2011. A motif unique to the human DEAD-box protein DDX3 is important for nucleic acid binding, ATP hydrolysis, RNA/DNA unwinding and HIV-1 replication. A.-K. Bielinsky, ed. *PLoS one*, 6(5), p.e19810.
- Gardy, J.L. et al., 2005. PSORTb v.2.0: expanded prediction of bacterial protein subcellular localization and insights gained from comparative proteome analysis. *Bioinformatics (Oxford, England)*, 21(5), pp.617–23.
- Gartel, A.L. et al., 2000. Sp1 and Sp3 activate p21 (WAF1/CIP1) gene transcription in the Caco-2 colon adenocarcinoma cell line. *Oncogene*, 19(45), pp.5182–8.
- Gavet, O. & Pines, J., 2010. Activation of cyclin B1-Cdk1 synchronizes events in the nucleus and the cytoplasm at mitosis. *The Journal of cell biology*, 189(2), pp.247–59.
- Geetha, T. et al., 2005. TRAF6-mediated ubiquitination regulates nuclear translocation of NRIF, the p75 receptor interactor. *The EMBO journal*, 24(22), pp.3859–68.
- Geissler, R., Golbik, R.P. & Behrens, S.-E., 2012. The DEAD-box helicase DDX3 supports the assembly of functional 80S ribosomes. *Nucleic acids research*, 40(11), pp.4998–5011.
- Goldfarb, D.S. et al., 2004. Importin alpha: a multipurpose nuclear-transport receptor. *Trends in cell biology*, 14(9), pp.505–14.
- Görlich, D. et al., 1995. Two different subunits of importin cooperate to recognize nuclear localization signals and bind them to the nuclear envelope. *Current biology : CB*, 5(4), pp.383–92.

- Goto, H. et al., 1999. Identification of a novel phosphorylation site on histone H3 coupled with mitotic chromosome condensation. *The Journal of biological chemistry*, 274(36), pp.25543–9.
- Grakoui, A. et al., 1993. Expression and Identification of Hepatitis C Virus Polyprotein Cleavage Products. *Journal of virology*, 67(3).
- Güttinger, S. et al., 2004. Transportin2 functions as importin and mediates nuclear import of HuR. *Proceedings of the National Academy of Sciences of the United States of America*, 101(9), pp.2918–23.
- Güttler, T. et al., 2010. NES consensus redefined by structures of PKI-type and Rev-type nuclear export signals bound to CRM1. *Nature structural & molecular biology*, 17(11), pp.1367–76.
- Hagting, A. et al., 1999. Translocation of cyclin B1 to the nucleus at prophase requires a phosphorylation-dependent nuclear import signal. *Current biology : CB*, 9(13), pp.680–9.
- Hannon, G.J., 2002. RNA interference. *Nature*, 418(6894), pp.244–51.
- Hanover, J.A. et al., 2007. The High Mobility Group Box Transcription Factor Nhp6Ap enters the nucleus by a calmodulin-dependent, Ran-independent pathway. *The Journal of biological chemistry*, 282(46), pp.33743–51.
- Hanover, J.A., Love, D.C. & Prinz, W.A., 2009. Calmodulin-driven nuclear entry: trigger for sex determination and terminal differentiation. *The Journal of biological chemistry*, 284(19), pp.12593–7.
- Harper, J.W. et al., 1993. The p21 Cdk-interacting protein Cip1 is a potent inhibitor of G1 cyclin-dependent kinases. *Cell*, 75(4), pp.805–16.
- Hautbergue, G.M. et al., 2008. Mutually exclusive interactions drive handover of mRNA from export adaptors to TAP. *Proceedings of the National Academy of Sciences of the United States of America*, 105(13), pp.5154–9.
- Henderson, B.R. & Percipalle, P., 1997. Interactions between HIV Rev and nuclear import and export factors: the Rev nuclear localisation signal mediates specific binding to human importin-beta. *Journal of molecular biology*, 274(5), pp.693–707.
- Henzel, M.J. et al., 1997. Mitosis-specific phosphorylation of histone H3 initiates primarily within pericentromeric heterochromatin during G2 and spreads in an ordered fashion coincident with mitotic chromosome condensation. *Chromosoma*, 106(6), pp.348–60.

- Herold, A. et al., 2000. TAP (NXF1) belongs to a multigene family of putative RNA export factors with a conserved modular architecture. *Molecular and cellular biology*, 20(23), pp.8996–9008.
- Hetzer, M.W. & Wente, S.R., 2009. Border control at the nucleus: biogenesis and organization of the nuclear membrane and pore complexes. *Developmental cell*, 17(5), pp.606–16.
- Hiscox, J.A., 2007. RNA viruses: hijacking the dynamic nucleolus. *Nature reviews. Microbiology*, 5(2), pp.119–27.
- Horton, P. & Nakai, K., 1997. Better prediction of protein cellular localization sites with the k nearest neighbors classifier. *Proceedings / ... International Conference on Intelligent Systems for Molecular Biology ; ISMB. International Conference on Intelligent Systems for Molecular Biology*, 5, pp.147–52.
- Howitt, J. et al., 2012. Ndfip1 regulates nuclear Pten import in vivo to promote neuronal survival following cerebral ischemia. *The Journal of cell biology*, 196(1), pp.29–36.
- Huang, Chao & Su, 2004. Diverse cellular transformation capability of overexpressed genes in human hepatocellular carcinoma. *Biochemical and biophysical research communications*, 315(4), pp.950–958.
- Hutten, S. & Kehlenbach, R.H., 2007. CRM1-mediated nuclear export: to the pore and beyond. *Trends in cell biology*, 17(4), pp.193–201.
- Hutten, S. & Kehlenbach, R.H., 2006. Nup214 is required for CRM1-dependent nuclear protein export in vivo. *Molecular and cellular biology*, 26(18), pp.6772–85.
- Ishaq, M. et al., 2008. Knockdown of cellular RNA helicase DDX3 by short hairpin RNAs suppresses HIV-1 viral replication without inducing apoptosis. *Molecular biotechnology*, 39(3), pp.231–8.
- Iwamoto, F. et al., 2008. Transcription-dependent nucleolar cap localization and possible nuclear function of DExH RNA helicase RHAU. *Experimental cell research*, 314(6), pp.1378–91.
- Izaurralde, E., 2002. A novel family of nuclear transport receptors mediates the export of messenger RNA to the cytoplasm. *European journal of cell biology*, 81(11), pp.577–84.
- Jahan, S. et al., 2012. Hepatitis C virus to hepatocellular carcinoma. *Infectious agents and cancer*, 7(1), p.2.

- Jäkel, S. & Görlich, D., 1998. Importin beta, transportin, RanBP5 and RanBP7 mediate nuclear import of ribosomal proteins in mammalian cells. *The EMBO journal*, 17(15), pp.4491–502.
- Jang, D., Guo, M. & Wang, D., 2007. Proteomic and Biochemical Studies of Calcium- and Phosphorylation-Dependent Calmodulin Complexes in Mammalian Cells research articles. , pp.3718–3728.
- Jarboui, M.A. et al., 2012. Nucleolar Protein Trafficking in Response to HIV-1 Tat: Rewiring the Nucleolus B. Verhasselt, ed. *PLoS ONE*, 7(11), p.e48702.
- Jarboui, M.A. et al., 2011. Proteomic profiling of the human T-cell nucleolus. *Molecular immunology*, 49(3), pp.441–52.
- Kang, J.-I., Kwon, Y.-C. & Ahn, B.-Y., 2012. Modulation of the type I interferon pathways by culture-adaptive hepatitis C virus core mutants. *FEBS letters*, 586(9), pp.1272–8.
- Kang, Y. & Cullen, B.R., 1999. The human Tap protein is a nuclear mRNA export factor that contains novel RNA-binding and nucleocytoplasmic transport sequences. *Genes & development*, 13(9), pp.1126–39.
- Kann, M. et al., 1999. Phosphorylation-dependent binding of hepatitis B virus core particles to the nuclear pore complex. *The Journal of cell biology*, 145(1), pp.45–55.
- Kannan, R.P. et al., 2011. Hepatitis C virus infection causes cell cycle arrest at the level of initiation of mitosis. *Journal of virology*, 85(16), pp.7989–8001.
- Kato, H. et al., 2008. Length-dependent recognition of double-stranded ribonucleic acids by retinoic acid-inducible gene-I and melanoma differentiation-associated gene 5. *The Journal of experimental medicine*, 205(7), pp.1601–10.
- Kato, N., 2000. Genome of human hepatitis C virus (HCV): gene organization, sequence diversity, and variation. *Microbial & comparative genomics*, 5(3), pp.129–51.
- Kau, T.R., Way, J.C. & Silver, P. a, 2004. Nuclear transport and cancer: from mechanism to intervention. *Nature reviews. Cancer*, 4(2), pp.106–17.
- Kaur, G. et al., 2010. Calmodulin-dependent nuclear import of HMG-box family nuclear factors: importance of the role of SRY in sex reversal. *The Biochemical journal*, 430(1), pp.39–48.
- Kay, A. & Zoulim, F., 2007. Hepatitis B virus genetic variability and evolution. *Virus research*, 127(2), pp.164–76.

- Kedersha, N. et al., 2002. Evidence that ternary complex (eIF2-GTP-tRNA(i)(Met))-deficient preinitiation complexes are core constituents of mammalian stress granules. *Molecular biology of the cell*, 13(1), pp.195–210.
- Kedersha, N. et al., 2005. Stress granules and processing bodies are dynamically linked sites of mRNP remodeling. *The Journal of cell biology*, 169(6), pp.871–84.
- Khapersky, D.A., Hatchette, T.F. & McCormick, C., 2012. Influenza A virus inhibits cytoplasmic stress granule formation. *FASEB journal : official publication of the Federation of American Societies for Experimental Biology*, 26(4), pp.1629–39.
- Kim, T. et al., 2010. Aspartate-glutamate-alanine-histidine box motif (DEAH)/RNA helicase A helicases sense microbial DNA in human plasmacytoid dendritic cells. *Proceedings of the National Academy of Sciences of the United States of America*, 107(34), pp.15181–6.
- Kim, W.J. et al., 2005. Sequestration of TRAF2 into stress granules interrupts tumor necrosis factor signaling under stress conditions. *Molecular and cellular biology*, 25(6), pp.2450–62.
- Kimura, M. et al., 2012. Identification of cargo proteins specific for the nucleocytoplasmic transport carrier transportin by combination of an in vitro transport system and SILAC-based quantitative proteomics. *Molecular & Cellular Proteomics*, (12), pp.145–157.
- Kimura, T. et al., 2004. CRM1-dependent, but not ARE-mediated, nuclear export of IFN- $\alpha$ 1 mRNA. *Journal of cell science*, 117(Pt 11), pp.2259–70.
- Kitamura, R. et al., 2006. Nuclear import of Epstein-Barr virus nuclear antigen 1 mediated by NPI-1 (Importin  $\alpha$ 5) is up- and down-regulated by phosphorylation of the nuclear localization signal for which Lys379 and Arg380 are essential. *Journal of virology*, 80(4), pp.1979–91.
- Von Knethen, A. et al., 2010. Casein-kinase-II-dependent phosphorylation of PPAR $\gamma$  provokes CRM1-mediated shuttling of PPAR $\gamma$  from the nucleus to the cytosol. *Journal of cell science*, 123(Pt 2), pp.192–201.
- Kosugi, S. et al., 2008. Design of peptide inhibitors for the importin  $\alpha$ /beta nuclear import pathway by activity-based profiling. *Chemistry & biology*, 15(9), pp.940–9.
- Kudo, N. et al., 1999. Leptomycin B inactivates CRM1/exportin 1 by covalent modification at a cysteine residue in the central conserved region. *Proceedings of the National Academy of Sciences of the United States of America*, 96(16), pp.9112–7.

- Kutay, U. & Güttinger, S., 2005. Leucine-rich nuclear-export signals: born to be weak. *Trends in cell biology*, 15(3), pp.121–4.
- Lahn, B.T. & Page, D.C., 1997. Functional coherence of the human Y chromosome. *Science*, 278(5338), pp.675–80.
- Lai, Lee & Tarn, 2008. The DEAD-box RNA helicase DDX3 associates with export messenger ribonucleoproteins as well as tip-associated protein and participates in translational control. *Molecular biology of the cell*, 19(9), pp.3847–58.
- Lai, M.-C. et al., 2010. DDX3 regulates cell growth through translational control of cyclin E1. *Molecular and cellular biology*, 30(22), pp.5444–5453.
- Lamm, G., 1996. p72: a human nuclear DEAD box protein highly related to p68. *Nucleic Acids Research*, 24(19), pp.3739–3747.
- Lamond, A.I. & Spector, D.L., 2003. Nuclear speckles: a model for nuclear organelles. *Nature reviews. Molecular cell biology*, 4(8), pp.605–12.
- Lange, A. et al., 2007. Classical nuclear localization signals: definition, function, and interaction with importin alpha. *The Journal of biological chemistry*, 282(8), pp.5101–5.
- Lee et al., 2006. Rules for nuclear localization sequence recognition by karyopherin beta 2. *Cell*, 126(3), pp.543–58.
- Lee et al., 2003. The structure of importin-beta bound to SREBP-2: nuclear import of a transcription factor. *Science*, 302(5650), pp.1571–5.
- Lee, C.-H. et al., 2013. Low/negative expression of DDX3 might predict poor prognosis in non-smoker patients with oral cancer. *Oral diseases*, 4, pp.1–8.
- Lee, C.-S. et al., 2008. Human DDX3 functions in translation and interacts with the translation initiation factor eIF3. *Nucleic acids research*, 36(14), pp.4708–18.
- Li, J. et al., 1999. A role for RNA helicase A in post-transcriptional regulation of HIV type 1. *Proceedings of the National Academy of Sciences of the United States of America*, 96(2), pp.709–14.
- Liang, S.-H., 1999. A Bipartite Nuclear Localization Signal Is Required for p53 Nuclear Import Regulated by a Carboxyl-terminal Domain. *Journal of Biological Chemistry*, 274(46), pp.32699–32703.
- Liao, B., Paschal, B.M. & Luby-Phelps, K., 1999. Mechanism of Ca<sup>2+</sup>-dependent nuclear accumulation of calmodulin. *Proceedings of the National Academy of Sciences of the United States of America*, 96(11), pp.6217–22.

- Liker, E. et al., 2000. The structure of the mRNA export factor TAP reveals a cis arrangement of a non-canonical RNP domain and an LRR domain. *The EMBO journal*, 19(21), pp.5587–98.
- Lin, J.-C., Hsu, M. & Tarn, W.-Y., 2007. Cell stress modulates the function of splicing regulatory protein RBM4 in translation control. *Proceedings of the National Academy of Sciences of the United States of America*, 104(7), pp.2235–40.
- Lindenbach, B.D. et al., 2005. Complete replication of hepatitis C virus in cell culture. *Science (New York, N.Y.)*, 309(5734), pp.623–6.
- Linder, P. et al., 1989. Birth of the D-E-A-D box. *Nature*, 337(6203), pp.121–2.
- Linder, P., 2006. Dead-box proteins: a family affair--active and passive players in RNP-remodeling. *Nucleic acids research*, 34(15), pp.4168–80.
- Linder, P. & Jankowsky, E., 2011. From unwinding to clamping — the DEAD box RNA helicase family. *Nature Reviews Molecular Cell Biology*, 12(8), pp.505–516.
- Liu, J. et al., 2011. Translational regulation of HIV-1 replication by HIV-1 Rev cellular cofactors Sam68, eIF5A, hRIP, and DDX3. *Journal of neuroimmune pharmacology : the official journal of the Society on NeuroImmune Pharmacology*, 6(2), pp.308–21.
- Loeb, K., Kostner, H. & Firpo, E., 2005. A mouse model for cyclin E-dependent genetic instability and tumorigenesis. *Cancer Cell*, 8(1), pp.35–47.
- Lotan, R. et al., 2005. The RNA polymerase II subunit Rpb4p mediates decay of a specific class of mRNAs. *Genes & development*, 19(24), pp.3004–16.
- Lund, M.K. & Guthrie, C., 2005. The DEAD-box protein Dbp5p is required to dissociate Mex67p from exported mRNPs at the nuclear rim. *Molecular cell*, 20(4), pp.645–51.
- Macara, I.G., 2001. Transport into and out of the nucleus. *Microbiology and molecular biology reviews : MMBR*, 65(4), pp.570–94, table of contents.
- Malim, M.H. et al., 1989. The HIV-1 rev trans-activator acts through a structured target sequence to activate nuclear export of unspliced viral mRNA. *Nature*, 338(6212), pp.254–7.
- Mamiya, N. & Worman, H.J., 1999. Hepatitis C Virus Core Protein Binds to a DEAD Box RNA Helicase. *Journal of Biological Chemistry*, 274(22), pp.15751–15756.
- Marfori, M. et al., 2012. Structural Basis of High-Affinity Nuclear Localization Signal Interactions with Importin- $\alpha$ . *Traffic (Copenhagen, Denmark)*, pp.532–548.

- Marsden, S. et al., 2006. Unwinding single RNA molecules using helicases involved in eukaryotic translation initiation. *Journal of molecular biology*, 361(2), pp.327–35.
- Matunis, M.J., Wu, J. & Blobel, G., 1998. SUMO-1 modification and its role in targeting the Ran GTPase-activating protein, RanGAP1, to the nuclear pore complex. *The Journal of cell biology*, 140(3), pp.499–509.
- McLauchlan, J., 2000. Properties of the hepatitis C virus core protein: a structural protein that modulates cellular processes. *Journal of viral hepatitis*, 7(1), pp.2–14.
- Medzhitov, R., 2001. Toll-like receptors and innate immunity. *Nature reviews. Immunology*, 1, pp.135–145.
- Mehdi, A.M. et al., 2011. A probabilistic model of nuclear import of proteins. *Bioinformatics (Oxford, England)*, 27(9), pp.1239–46.
- Melen, K., Kinnunen, L. & Julkunen, I., 2001. Arginine/lysine-rich structural element is involved in interferon-induced nuclear import of STATs. *The Journal of biological chemistry*, 276(19), pp.16447–55.
- Merz, C. et al., 2007. Protein composition of human mRNPs spliced in vitro and differential requirements for mRNP protein recruitment. *RNA (New York, N.Y.)*, 13(1), pp.116–28.
- Meylan, E. et al., 2005. Cardif is an adaptor protein in the RIG-I antiviral pathway and is targeted by hepatitis C virus. *Nature*, 437(7062), pp.1167–72.
- Miao, X. et al., 2013. Nectin-2 and DDX3 are biomarkers for metastasis and poor prognosis of squamous cell/adenosquamous carcinomas and adenocarcinoma of gallbladder. *International journal of clinical and experimental pathology*, 6(2), pp.179–90.
- Michienzi, A. et al., 2002. A nucleolar TAR decoy inhibitor of HIV-1 replication. *Proceedings of the National Academy of Sciences of the United States of America*, 99(22), pp.14047–52.
- Michienzi, A. et al., 2000. Ribozyme-mediated inhibition of HIV 1 suggests nucleolar trafficking of HIV-1 RNA. *Proceedings of the National Academy of Sciences*, 97(16), pp.8955–8960.
- Miyanari, Y. et al., 2007. The lipid droplet is an important organelle for hepatitis C virus production. *Nature cell biology*, 9(9), pp.1089–97.
- Myöhänen, S. & Baylin, S.B., 2001. Sequence-specific DNA binding activity of RNA helicase A to the p16INK4a promoter. *The Journal of biological chemistry*, 276(2), pp.1634–42.

- Nardozi, J.D., Lott, K. & Cingolani, G., 2010. Phosphorylation meets nuclear import: a review. *Cell communication and signaling : CCS*, 8(1), p.32.
- Nemergut, M.E. et al., 2002. Ran-binding protein 3 links Crm1 to the Ran guanine nucleotide exchange factor. *The Journal of biological chemistry*, 277(20), pp.17385–8.
- Nguyen, H., Sankaran, S. & Dandekar, S., 2006. Hepatitis C virus core protein induces expression of genes regulating immune evasion and anti-apoptosis in hepatocytes. *Virology*, 354(1), pp.58–68.
- Nichols, R.C. et al., 2000. The RGG domain in hnRNP A2 affects subcellular localization. *Experimental cell research*, 256(2), pp.522–32.
- Nieto, M.A., 2002. The snail superfamily of zinc-finger transcription factors. *Nature reviews. Molecular cell biology*, 3(3), pp.155–66.
- Nonhoff, U. et al., 2007. Ataxin-2 interacts with the DEAD/H-box RNA helicase DDX6 and interferes with P-bodies and stress granules. *Molecular biology of the cell*, 18(4), pp.1385–96.
- Oda, S. et al., 2009. Structural basis for targeting of human RNA helicase DDX3 by poxvirus protein K7. *Structure*, 17(11), pp.1528–37.
- De Oliveria Andrade, L.J. et al., 2009. Association between hepatitis C and hepatocellular carcinoma. *Journal of global infectious diseases*, 1(1), pp.33–7.
- Olsen, J. V et al., 2013. Quantitative Phosphoproteomics Reveals Widespread Full Phosphorylation Site Occupancy During Mitosis. , (January 2010).
- Onder, T.T. et al., 2008. Loss of E-cadherin promotes metastasis via multiple downstream transcriptional pathways. *Cancer research*, 68(10), pp.3645–54.
- Onomoto, K. et al., 2012. Critical role of an antiviral stress granule containing RIG-I and PKR in viral detection and innate immunity. *PloS one*, 7(8), p.e43031.
- Oshiumi, H., Sakai, K., et al., 2010. DEAD/H BOX 3 (DDX3) helicase binds the RIG-I adaptor IPS-1 to up-regulate IFN-beta-inducing potential. *European journal of immunology*, 40(4), pp.940–8.
- Oshiumi, H., Ikeda, M., et al., 2010. Hepatitis C virus core protein abrogates the DDX3 function that enhances IPS-1-mediated IFN-beta induction. *PloS one*, 5(12), p.e14258.
- Owsianka, A.M. & Patel, A.H., 1999. Hepatitis C virus core protein interacts with a human DEAD box protein DDX3. *Virology*, 257(2), pp.330–40.

- Pek, J.W. & Kai, T., 2011. DEAD-box RNA helicase Belle/DDX3 and the RNA interference pathway promote mitotic chromosome segregation. *Proceedings of the National Academy of Sciences of the United States of America*, p.1106245108–.
- Pemberton, L.F. & Paschal, B.M., 2005. Mechanisms of receptor-mediated nuclear import and nuclear export. *Traffic (Copenhagen, Denmark)*, 6(3), pp.187–98.
- Pérez-Vilaró, G. et al., 2012. Hepatitis C virus infection alters p-body composition but is independent of p-body granules. *Journal of virology*, 86(16), pp.8740–9.
- Petosa, C. et al., 2004. Architecture of CRM1/Exportin1 suggests how cooperativity is achieved during formation of a nuclear export complex. *Molecular cell*, 16(5), pp.761–75.
- Pichler, A. & Melchior, F., 2002. Ubiquitin-related modifier SUMO1 and nucleocytoplasmic transport. *Traffic (Copenhagen, Denmark)*, 3(6), pp.381–7.
- Pines, J. & Hunter, T., 1994. The differential localization of human cyclins A and B is due to a cytoplasmic retention signal in cyclin B. *The EMBO journal*, 13(16), pp.3772–81.
- Pollard, V.W. & Malim, M.H., 1998. The HIV-1 Rev protein. *Annual review of microbiology*, 52, pp.491–532.
- Poon, I.K.H. & Jans, D. a, 2005. Regulation of nuclear transport: central role in development and transformation? *Traffic (Copenhagen, Denmark)*, 6(3), pp.173–86.
- Preuss, U., Landsberg, G. & Scheidtmann, K.H., 2003. Novel mitosis-specific phosphorylation of histone H3 at Thr11 mediated by Dlk/ZIP kinase. *Nucleic acids research*, 31(3), pp.878–85.
- Rabe, B. et al., 2003. Nuclear import of hepatitis B virus capsids and release of the viral genome. *Proceedings of the National Academy of Sciences of the United States of America*, 100(17), pp.9849–54.
- Rajendran, R.R. et al., 2003. Regulation of nuclear receptor transcriptional activity by a novel DEAD box RNA helicase (DP97). *The Journal of biological chemistry*, 278(7), pp.4628–38.
- Rocak, S. & Linder, P., 2004. DEAD-box proteins: the driving forces behind RNA metabolism. *Nature reviews. Molecular cell biology*, 5(3), pp.232–41.
- Rodríguez-Vilarrupla, A. et al., 2005. Binding of calmodulin to the carboxy-terminal region of p21 induces nuclear accumulation via inhibition of protein kinase C-mediated phosphorylation of Ser153. *Molecular and cellular biology*, 25(16), pp.7364–74.

- Rogers, G.W., Komar, A.A. & Merrick, W.C., 2002. eIF4A: the godfather of the DEAD box helicases. *Progress in nucleic acid research and molecular biology*, 72, pp.307–31.
- Rothenbusch, U. et al., 2012. Sumoylation regulates Kap114-mediated nuclear transport. *The EMBO journal*, 31(11), pp.2461–72.
- Rousseau, D. et al., 1999. Growth inhibition by CDK-cyclin and PCNA binding domains of p21 occurs by distinct mechanisms and is regulated by ubiquitin-proteasome pathway. *Oncogene*, 18(30), pp.4313–25.
- Ruggieri, A. et al., 2012. Dynamic oscillation of translation and stress granule formation mark the cellular response to virus infection. *Cell host & microbe*, 12(1), pp.71–85.
- Sachdev, S. et al., 2000. Nuclear Import of I $\kappa$ B $\alpha$  Is Accomplished by a Ran-Independent Transport Pathway. *Molecular and cellular biology*, 20(5), pp.1571–1582.
- Sasaki, T. et al., 2006. Spatiotemporal regulation of c-Fos by ERK5 and the E3 ubiquitin ligase UBR1, and its biological role. *Molecular cell*, 24(1), pp.63–75.
- Sato, S. et al., 2006. Proteomic profiling of lipid droplet proteins in hepatoma cell lines expressing hepatitis C virus core protein. *Journal of biochemistry*, 139(5), pp.921–30.
- Schröder, M., 2010. Human DEAD-box protein 3 has multiple functions in gene regulation and cell cycle control and is a prime target for viral manipulation. *Biochemical pharmacology*, 79(3), pp.297–306.
- Schröder, M., 2011. Viruses and the human DEAD-box helicase DDX3: inhibition or exploitation? *Biochemical Society transactions*, 39(2), pp.679–683.
- Schröder, M., Baran, M. & Bowie, A.G., 2008. Viral targeting of DEAD box protein 3 reveals its role in TBK1/IKK $\epsilon$ -mediated IRF activation. *The EMBO journal*, 27(15), pp.2147–57.
- Sekiguchi, T. et al., 2004. Human DDX3Y, the Y-encoded isoform of RNA helicase DDX3, rescues a hamster temperature-sensitive ET24 mutant cell line with a DDX3X mutation. *Experimental cell research*, 300(1), pp.213–22.
- Sekiguchi, T., Kurihara, Y. & Fukumura, J., 2007. Phosphorylation of threonine 204 of DEAD-box RNA helicase DDX3 by cyclin B/cdc2 in vitro. *Biochemical and biophysical research communications*, 356(3), pp.668–73.
- Sharma, D. & Bhattacharya, J., 2010. PLoS ONE: Evolutionary Constraints Acting on DDX3X Protein Potentially Interferes with Rev-Mediated Nuclear Export of HIV-1 RNA W. Delpont, ed. *PloS one*, 5(3), p.e9613.

- Sharma, S. et al., 2003. Triggering the interferon antiviral response through an IKK-related pathway. *Science*, 300(5622), pp.1148–51.
- Shen, X. et al., 2005. Scanning the human proteome for calmodulin-binding proteins. *Proceedings of the National Academy of Sciences of the United States of America*, 102(17), pp.5969–74.
- Shih, J.-W. et al., 2008. Candidate tumor suppressor DDX3 RNA helicase specifically represses cap-dependent translation by acting as an eIF4E inhibitory protein. *Oncogene*, 27(5), pp.700–14.
- Shih, J.-W. et al., 2012. Critical roles of RNA helicase DDX3 and its interactions with eIF4E/PABP1 in stress granule assembly and stress response. *The Biochemical journal*, 441(1), pp.119–29.
- Simmonds, P. et al., 1993. Classification of hepatitis C virus into six major genotypes and a series of subtypes by phylogenetic analysis of the NS-5 region. *The Journal of general virology*, 74 ( Pt 11, pp.2391–9.
- Smith, G.L. et al., 1997. Vaccinia virus immune evasion. *Immunological reviews*, 159, pp.137–54.
- Smith, J.A. et al., 2006. Reovirus Induces and Benefits from an Integrated Cellular Stress Response. *Journal of virology*, 80(4), pp.2019–2033.
- Soderholm, J.F. et al., 2011. Importazole, a small molecule inhibitor of the transport receptor importin- $\beta$ . *ACS chemical biology*, 6(7), pp.700–8.
- Solomon, S. et al., 2007. Distinct structural features of caprin-1 mediate its interaction with G3BP-1 and its induction of phosphorylation of eukaryotic translation initiation factor 2 $\alpha$ , entry to cytoplasmic stress granules, and selective interaction with a subset of mRNAs. *Molecular and cellular biology*, 27(6), pp.2324–42.
- Soto-Rifo, R. et al., 2012. DEAD-box protein DDX3 associates with eIF4F to promote translation of selected mRNAs. *The EMBO journal*, 31(18), pp.3745–3756.
- Soulat, D. et al., 2008. The DEAD-box helicase DDX3X is a critical component of the TANK-binding kinase 1-dependent innate immune response. *The EMBO*, 27(15), pp.2135–2146.
- Spriggs, K. a et al., 2008. Re-programming of translation following cell stress allows IRES-mediated translation to predominate. *Biology of the cell / under the auspices of the European Cell Biology Organization*, 100(1), pp.27–38.
- Spruck, C., 1999. Deregulated cyclin E induces chromosome instability. *Nature*.

- Srivastava, S.P., 1998. Phosphorylation of Eukaryotic Translation Initiation Factor 2 Mediates Apoptosis in Response to Activation of the Double-stranded RNA-dependent Protein Kinase. *Journal of Biological Chemistry*, 273(4), pp.2416–2423.
- Stevens, S.W. et al., 2002. Composition and Functional Characterization of the Yeast Spliceosomal Penta-snRNP. *Molecular Cell*, 9(1), pp.31–44.
- Stevenson, N.J. et al., 2011. Ribavirin enhances IFN- $\alpha$  signalling and MxA expression: a novel immune modulation mechanism during treatment of HCV. *PloS one*, 6(11), p.e27866.
- Stewart, M., 2007. Molecular mechanism of the nuclear protein import cycle. *Nature reviews. Molecular cell biology*, 8(3), pp.195–208.
- Strambio-De-Castillia, C., Niepel, M. & Rout, M.P., 2010. The nuclear pore complex: bridging nuclear transport and gene regulation. *Nature reviews. Molecular cell biology*, 11(7), pp.490–501.
- Stutz, F., 2003. The interplay of nuclear mRNP assembly, mRNA surveillance and export. *Trends in Cell Biology*, 13(6), pp.319–327.
- Sun, M. et al., 2011. The role of DDX3 in regulating Snail. *Biochimica et biophysica acta*, 1813(3), pp.438–47.
- Svitkin, Y. V et al., 1996. General RNA binding proteins render translation cap dependent. *The EMBO journal*, 15(24), pp.7147–55.
- Sweitzer, T.D. & Hanover, J.A., 1996. Calmodulin activates nuclear protein import: a link between signal transduction and nuclear transport. *Proceedings of the National Academy of Sciences of the United States of America*, 93(25), pp.14574–9.
- Takaoka, A. et al., 2007. DAI (DLM-1/ZBP1) is a cytosolic DNA sensor and an activator of innate immune response. *Nature*, 448(7152), pp.501–5.
- Takizawa, C.G., Weis, K. & Morgan, D.O., 1999. Ran-independent nuclear import of cyclin B1-Cdc2 by importin beta. *Proceedings of the National Academy of Sciences of the United States of America*, 96(14), pp.7938–43.
- Tang, H. et al., 1997. A cellular cofactor for the constitutive transport element of type D retrovirus. *Science (New York, N.Y.)*, 276(5317), pp.1412–5.
- Targett-Adams, P. et al., 2008. Maturation of hepatitis C virus core protein by signal peptide peptidase is required for virus production. *The Journal of biological chemistry*, 283(24), pp.16850–9.

- Taulés, M. et al., 1999. Calmodulin binds to p21(Cip1) and is involved in the regulation of its nuclear localization. *The Journal of biological chemistry*, 274(35), pp.24445–8.
- Taulés, M. et al., 1998. Calmodulin is essential for cyclin-dependent kinase 4 (Cdk4) activity and nuclear accumulation of cyclin D1-Cdk4 during G1. *The Journal of biological chemistry*, 273(50), pp.33279–86.
- Tourrière, H. et al., 2003. The RasGAP-associated endoribonuclease G3BP assembles stress granules. *The Journal of cell biology*, 160(6), pp.823–31.
- Tran, E.J. et al., 2007. The DEAD-box protein Dbp5 controls mRNA export by triggering specific RNA:protein remodeling events. *Molecular cell*, 28(5), pp.850–9.
- Tran, E.J. & Wenthe, S.R., 2006. Dynamic nuclear pore complexes: life on the edge. *Cell*, 125(6), pp.1041–53.
- Trotman, L.C. et al., 2007. Ubiquitination regulates PTEN nuclear import and tumor suppression. *Cell*, 128(1), pp.141–56.
- Truant, R., 1999. The Human Tap Nuclear RNA Export Factor Contains a Novel Transportin-dependent Nuclear Localizatoin Signal That Lacks Nuclear Export Signal Function. *Journal of Biological Chemistry*, 274(45), pp.32167–32171.
- Truant, R. & Cullen, B.R., 1999. The Arginine-Rich Domains Present in Human Immunodeficiency Virus Type 1 Tat and Rev Function as Direct Importin beta - Dependent Nuclear Localization Signals. *Mol. Cell. Biol.*, 19(2), pp.1210–1217.
- Unterholzner, L. et al., 2010. IFI16 is an innate immune sensor for intracellular DNA. *Nature immunology*, 11(11), pp.997–1004.
- Vashist, S. et al., 2012. Identification of RNA-protein interaction networks involved in the norovirus life cycle. *Journal of virology*, 86(22), pp.11977–90.
- Vetter, I.R. et al., 1999. Structural View of the Ran–Importin  $\beta$  Interaction at 2.3 Å Resolution. *Cell*, 97(5), pp.635–646.
- Wang, H., Gao, X., et al., 2009. P68 RNA helicase is a nucleocytoplasmic shuttling protein. *Cell research*, 19(12), pp.1388–400.
- Wang, H., Kim, S. & Ryu, W.-S., 2009. DDX3 DEAD-Box RNA helicase inhibits hepatitis B virus reverse transcription by incorporation into nucleocapsids. *Journal of virology*, 83(11), pp.5815–24.
- Wang, H. & Ryu, W.-S., 2010. Hepatitis B virus polymerase blocks pattern recognition receptor signaling via interaction with DDX3: implications for immune evasion. *PLoS pathogens*, 6(7), p.e1000986.

- White, J.P. & Lloyd, R.E., 2012. Regulation of stress granules in virus systems. *Trends in microbiology*, 20(4), pp.175–83.
- White, S.A. & Allshire, R.C., 2004. Loss of Dicer fowls up centromeres. *Nature cell biology*, 6(8), pp.696–7.
- Wieland, S.F. & Chisari, F. V, 2005. Stealth and cunning: hepatitis B and hepatitis C viruses. *Journal of virology*, 79(15), pp.9369–80.
- Wilson, V.G. & Rangasamy, D., 2001. Intracellular targeting of proteins by sumoylation. *Experimental cell research*, 271(1), pp.57–65.
- Wood, L.D. et al., 2003. Small ubiquitin-like modifier conjugation regulates nuclear export of TEL, a putative tumor suppressor. *Proceedings of the National Academy of Sciences of the United States of America*, 100(6), pp.3257–62.
- Wu, D.-W., Liu, W.-S., et al., 2011. Reduced p21(WAF1/CIP1) via alteration of p53-DDX3 pathway is associated with poor relapse-free survival in early-stage human papillomavirus-associated lung cancer. *Clinical cancer research : an official journal of the American Association for Cancer Research*, 17(7), pp.1895–905.
- Wu, K., Yan, H., et al., 2011. Mono-ubiquitination drives nuclear export of the human DCN1-like protein hDCNL1. *The Journal of biological chemistry*, 286(39), pp.34060–70.
- Yan, X. et al., 2003. A Novel Domain within the DEAD-Box Protein DP103 Is Essential for Transcriptional Repression and Helicase Activity. *Molecular and Cellular Biology*, 23(1), pp.414–423.
- Yang, P. et al., 2010. The cytosolic nucleic acid sensor LRRFIP1 mediates the production of type I interferon via a beta-catenin-dependent pathway. *Nature immunology*, 11(6), pp.487–94.
- Yashiroda, Y. & Yoshida, M., 2003. Nucleo-cytoplasmic transport of proteins as a target for therapeutic drugs. *Current medicinal chemistry*, 10(9), pp.741–8.
- Yedavalli, V. et al., 2004. Requirement of DDX3 DEAD box RNA helicase for HIV-1 Rev-RRE export function. *Cell*, 119(3), pp.381–392.
- Yoneyama, M. & Fujita, T., 2007. Function of RIG-I-like receptors in antiviral innate immunity. *The Journal of biological chemistry*, 282(21), pp.15315–8.
- You, L.-R. et al., 1999. Hepatitis C Virus Core Protein Interacts with Cellular Putative RNA Helicase. *Journal of virology*, 73(4), pp.2841–2853.
- Yu, S. et al., 2010. Hepatitis B virus polymerase inhibits RIG-I- and Toll-like receptor 3-mediated beta interferon induction in human hepatocytes through

interference with interferon regulatory factor 3 activation and dampening of the interaction between TBK1/IKKepsilon and . *The Journal of general virology*, 91(Pt 8), pp.2080–90.

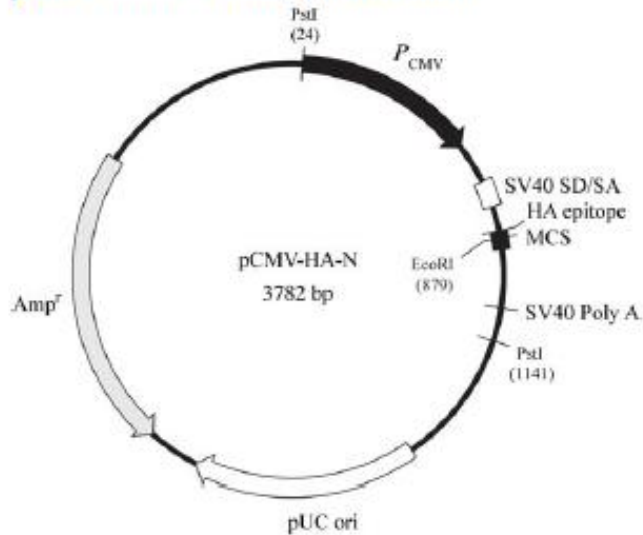
Zhang, Z. et al., 2011. The helicase DDX41 senses intracellular DNA mediated by the adaptor STING in dendritic cells. *Nature immunology*, 12(10), pp.959–65.

Zhou, Z. et al., 2002. Comprehensive proteomic analysis of the human spliceosome. *Nature*, 419(6903), pp.182–5.

Zolotukhin, A.S. & Felber, B.K., 1999. Nucleoporins nup98 and nup214 participate in nuclear export of human immunodeficiency virus type 1 Rev. *Journal of virology*, 73(1), pp.120–7.

## Appendix I

### pCMV-HA-N Vector Information



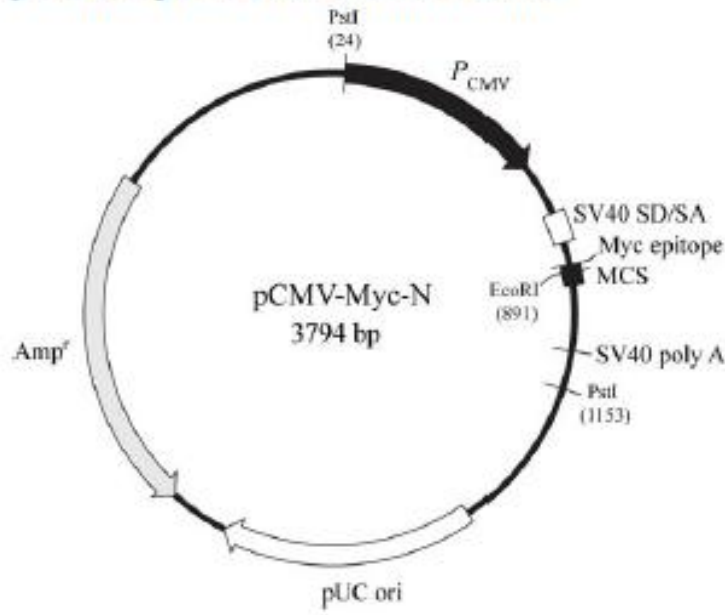
	Hemagglutinin (HA) epitope												SfiI		
829	ATG	TAC	CCA	TAC	GAT	GTT	CCA	GAT	TAC	GCT	CTT	ATG	GCC	ATG	GAG
	TAC	ATG	GGT	ATG	CTA	CAA	GGT	CTA	ATG	CGA	GAA	TAC	CGG	TAC	CTC
	SfiI						XhoI						NotI		
			EcoRI		Sall		BglII		KpnI						
874	GCC	CGA	ATT	CGG	TCG	ACC	GAG	ATC	TCT	CGA	GGT	ACC	GCG	GCC	GC
	CGG	GCT	TAA	GCC	AGC	TGG	CTC	TAG	AGA	GCT	CCA	TGG	CGC	CGG	CG

**Figure I: Map of pCMV-Ha vector.**

Adapted from

[http://www.clontech.com/IE/Products/Protein\\_Expression\\_and\\_Purification/Myc-Tagged\\_Protein\\_Purification/Myc\\_and\\_HA\\_Vectors?sitex=10023:22372:US](http://www.clontech.com/IE/Products/Protein_Expression_and_Purification/Myc-Tagged_Protein_Purification/Myc_and_HA_Vectors?sitex=10023:22372:US)

## pCMV-Myc-N Vector Information



	Myc epitope												SfiI				
838	ATG	GAG	CAG	AAG	CTG	ATC	TCA	GAG	GAG	GAC	CTG	CTT	ATG	GCC	ATG	GAG	
	TAC	CTC	GTC	TTC	GAC	TAG	AGT	CTC	CTC	CTG	GAC	GAA	TAC	CGG	TAC	CTC	
	SfiI			EcoRI			Sall			BglII		XhoI		KpnI		NotI	
886	GCC	CGA	ATT	CGG	TCG	ACC	GAG	ATC	TCT	CGA	GGT	ACC	GCG	GCC	GC		
	CGG	GCT	TAA	GCC	AGC	TGG	CTC	TAG	AGA	GCT	CCA	TGG	CGC	CGG	CG		

**Figure II: Map of pCMV-Myc vector.**

Adapted from

[http://www.clontech.com/IE/Products/Protein\\_Expression\\_and\\_Purification/Myc-Tagged\\_Protein\\_Purification/Myc\\_and\\_HA\\_Vectors?sitex=10023:22372:US](http://www.clontech.com/IE/Products/Protein_Expression_and_Purification/Myc-Tagged_Protein_Purification/Myc_and_HA_Vectors?sitex=10023:22372:US)

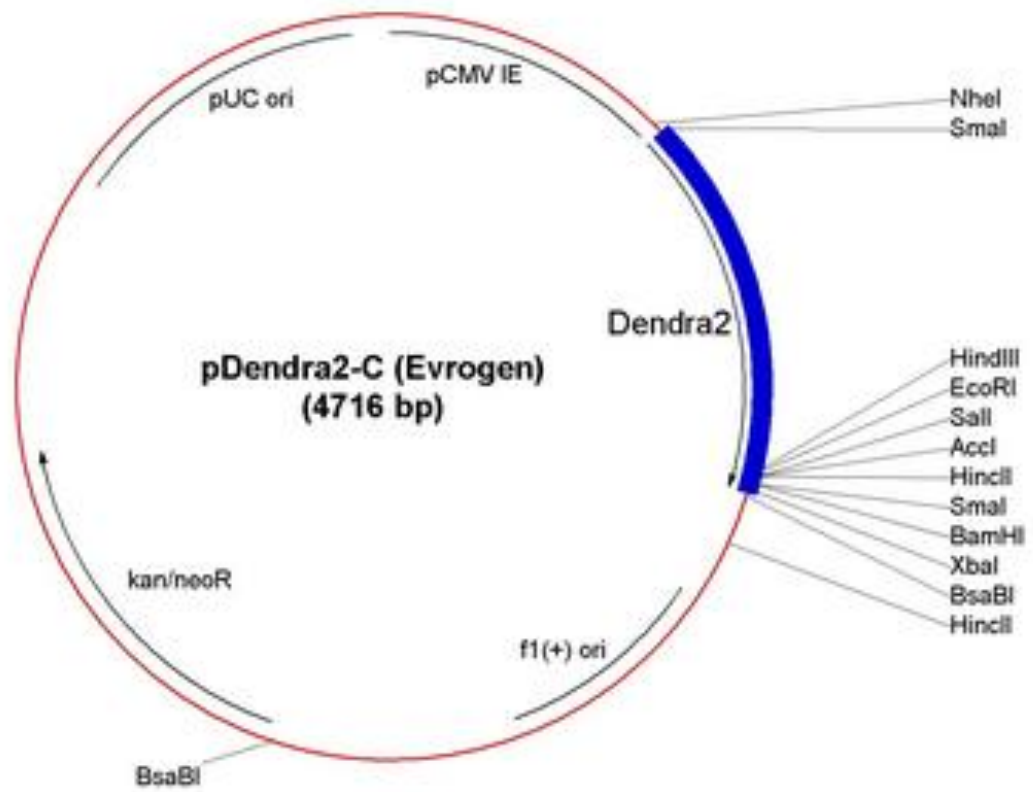


**Figure III: Map of pDendra2-c vector.**

Adapted from <http://www.bioss.uni-freiburg.de/toolbox/products.php?PL-47&osCsid=rrvmcoj3iotn80h0a2orgt36ofp918nc>

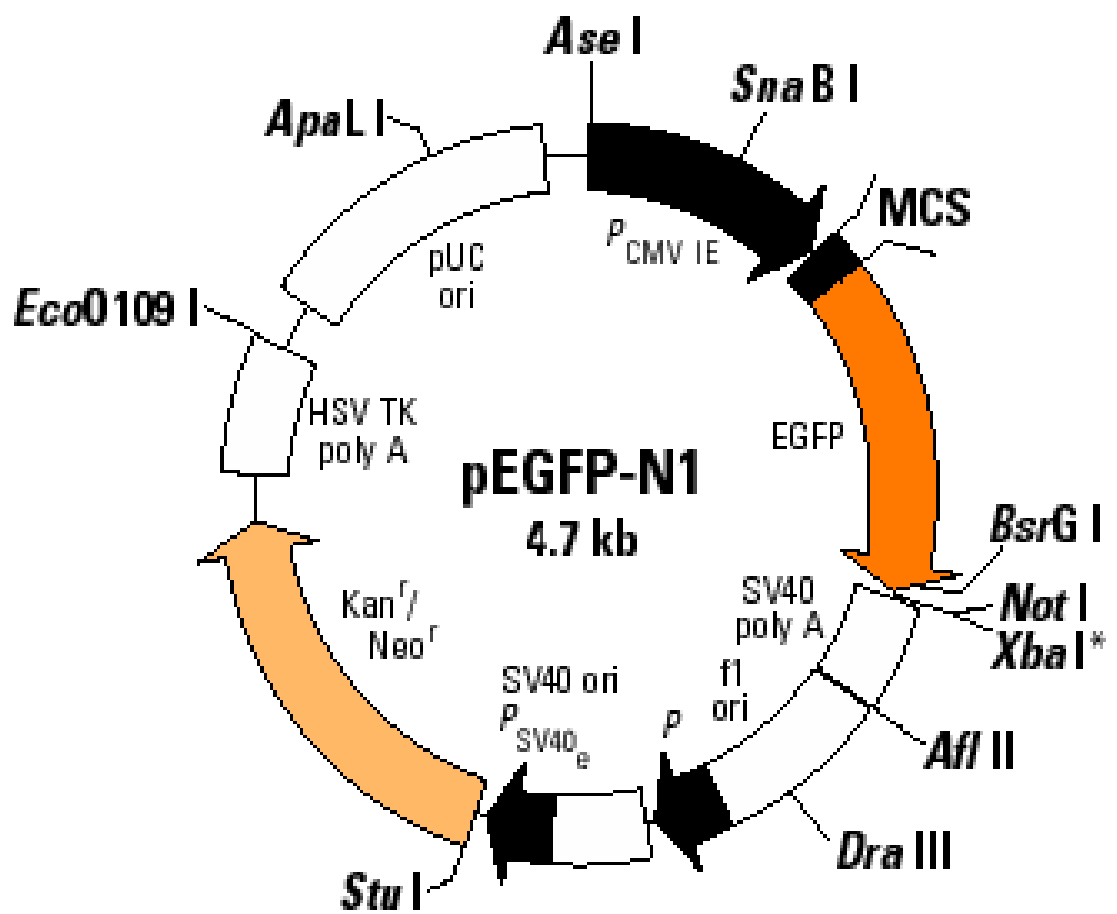
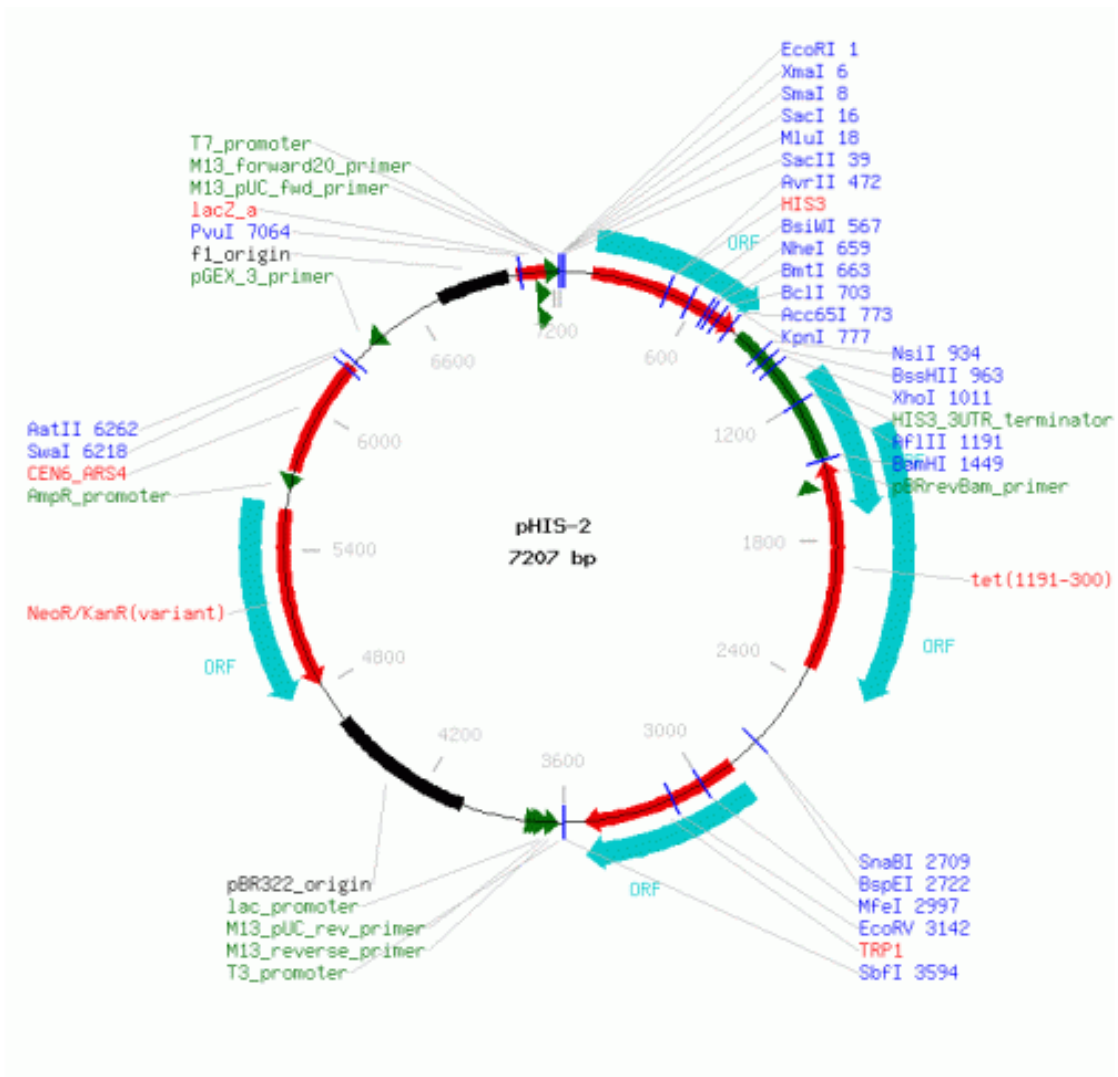


Figure IV: Map of pEGFP-N1.

Adapted from <http://www.liv.ac.uk/physiology/ncs/catalogue/Cloning/pEGFP-N1.htm>



**Figure V: Map of pHis-parallel 2.**

Adapted from

[https://www.lablife.org/g?a=seqa&id=vdb\\_g2.VpMokesmWHgT6U13nMsJHQywkHa-\\_sequence\\_e14dbd80224e8db3bff633927c255c87e2f06104\\_10](https://www.lablife.org/g?a=seqa&id=vdb_g2.VpMokesmWHgT6U13nMsJHQywkHa-_sequence_e14dbd80224e8db3bff633927c255c87e2f06104_10)

<b>DDX3 plasmids</b>	pDendra2- DDX3
pCMV-Ha DDX3 1-662	NLS1 1-662
pCMV-Ha DDX3 22-662	NLS1 1-408
pCMV-Ha DDX3 44-662	NLS2-1 1-408
pCMV-Ha DDX3 80-662	NLS2-2 139-408
pCMV-Ha DDX3 110-662	T204D
pCMV-Ha DDX3 120-662	T323D
pCMV-Ha DDX3 130-662	T204A
pCMV-Ha DDX3 1-408	T323A
pCMV-Ha DDX3 1-139	TA2
pCMV-Ha DDX3 139-408	TD2
pCMV-Ha DDX3 139-662	<b>HIV plasmids</b>
pCMV-Ha DDX3 409-662	pCMV-Ha-Rev
pCMV-Myc 1-662	GAG-RRE
pCMV-Myc DDX3 1-408	GAG-CTE
pCMV-Myc 1-139	HIV rev- ha tagged
pCMV-Myc 139-408	RRE promoter
pCMV-Myc 139-662	<b>HCV plasmids</b>
pCMV-Myc 409-662	pCMV-Ha HCV Core Con1
pCMV-Myc K230E	pCMV-Ha HCV Core Con1 Y35A
DDX3 NES-44-662 Ha	pCMV-Ha HCV Core JC1
DDX3 NES-130-662 myc	pCMV-Ha HCV Core H77
DDX3 NES-80-662 myc	pBRTM/HCV1-3011 DNA construct
DDX3 NES-110-408 Ha	<b>Bimax Plasmids</b>
DDX3 NES-100-408 Ha	pCMV-GRX-flag Bimax 1
DDX3 NES-100-662 Ha	pCMV-GRX-flag Bimax 2
	SV40 NLS GFP
	pCMV-GRX-flag

**Table I: Expression constructs used for the project.**

## Appendix II

### One-dimensional SDS PAGE buffers

Solution	Reagent
<b>Resolving Gel Buffer (1.5M Tris,pH8.8)</b>	90.75g Tris Add 400ml dH <sub>2</sub> O Adjust pH 8.8 with HCl Make up to 500ml
<b>Stacking Gel buffer(0.5M Tris,pH6.8)</b>	15g Tris Add 150ml dH <sub>2</sub> O Adjust to pH 6.8 with HCl Make up to 250ml
<b>10% Resolving Gel for 2 gels</b>	4.1ml dH <sub>2</sub> O 3.3ml 30% acrylamide 2.5ml 1.5Tris (pH 8.8) 100 µl 10% SDS 50µl APS Temed 5 µl
<b>5% Stacking Gel for 2 gels</b>	3.4ml dH <sub>2</sub> O 1ml 30% acrylamide 1.5ml 1.5Tris (pH 8.8) 60 µl 10% SDS 60µl APS Temed 6 µl
<b>10x Running buffer</b>	30.3g Trizma Base 144g Glycine 10g SDS Make up to 1L with dH <sub>2</sub> O
<b>10x Transfer Buffer</b>	30.3 Tris 144g Glycine Make up to 1L with dH <sub>2</sub> O
<b>1x Transfer Buffer</b>	50ml 10X Transfer Bufer 75ml Methanol (15%) Make up to 500ml with dH <sub>2</sub> O
<b>2x Laemmli sample buffer</b>	2ml 0.5M Tris/Cl pH 6.8 2% SDS (use 10% stock) 10ml Glycerol 200µl bromophenol blue (1% stock in ethanol) 2ml 1M DTT Make up to 20ml with dH <sub>2</sub> O
<b>PBS/Tween</b>	1x PBS 0.1 % Tween-20 (1ml in 1L)
<b>ECL A</b>	1 ml luminol solution 0.44 ml coumaric acid solution 10 ml Tris-HCl 1M, pH 8.5 Distilled water up to a final volume of 100 ml
<b>ECL B</b>	10 ml Tris-HCl 1M, pH 8.5 Distilled water up to a final volume of 100 ml

## Cell Lysis Buffers

Buffers	Reagent
Subcellular fractionation buffer	250 mM Sucrose 20 mM HEPES (7.4) 10 mM KCl 1.5 mM MgCl <sub>2</sub> 1 mM EDTA 1 mM EGTA
IP Lysis Buffer	50mM HEPES pH 7.5 (or Tris/HCl pH 7.5) 150mM NaCl 1mM EDTA 10% Glycerol 0.5% NP-40 (or 1% NP-40) Store in fridge
Protease and phosphatase inhibitors	Aprotinin (20µl/ml) 1 mM sodium orthovanadate (10µl/ml) 1 mM PMSF (10µl/ml)

## Immunohistochemistry buffers

Buffers	Reagents
Fixation solution	100ml PBS (1x) 4g Paraformaldehyde Heat to 68°C on hotplate with constant stirring in a fume hood. Once cooled, filter sterilize. Aliquot and store at -20°C
Permeabilisation solution	0.5% Triton-X in PBS
Blocking buffer	5% BSA in PBS-Tween (0.05%)

## DNA technology Buffers

Buffers	Reagent
50X TAE	242g Tris Base 57.1ml glacial acetic acid 100ml 0.5M EDTA (pH 8.0) Make up with dH <sub>2</sub> O to 1L
0.8% Agarose gel	0.2g Agarose 25ml 1X TAE 10,000X GelRed or 10,000X Etidium Bromide
6x Loading Dye	3ml glycerol (30%) 25mg bromophenol blue 0.25%) Make up to dH <sub>2</sub> O to 10mL

## DNA transfection Reagents

Buffers	Reagent
2x HBS buffer:	42mM HEPES 10mM KCL 12mM dextrose 1.5mM Na <sub>2</sub> HPO <sub>4</sub> ·7H <sub>2</sub> O 280mM NaCl
2.5M CaCl <sub>2</sub> :	36.75g CaCl <sub>2</sub> ·2H <sub>2</sub> O Make up with dH <sub>2</sub> O to 100ml

## Buffers for Preparing Competant cells

Buffers	Reagent
Transformation Buffer	55 mM MnCl <sub>2</sub> ·4H <sub>2</sub> O 15 mM CaCl <sub>2</sub> ·2H <sub>2</sub> O 250 mM KCl 10 mM PIPES (0.5M, pH 6.7) Chilled to 0°C before use.

## Buffers for His-tagged protein production

Buffers	Reagent
<b>Lysis Buffer (pH 8.0)</b>	50mM Na <sub>2</sub> HPO <sub>4</sub> 300mM NaCl 10mM Imidazole 20mM β-mercaptoethanol (added just before use) 1 mM PMSF (added just before use)
<b>Lysis Buffer (pH 8.0) Protein greater than 70kDa</b>	1x TBS 500mM NaCl 5mM MgCl <sub>2</sub> 250mM Sucrose 10% Glycerol 1% Triton X 10mM Imidazole 20mM β-mercaptoethanol (added just before use) 1 mM PMSF (added just before use)
<b>Wash buffer I</b>	Lysis buffer (pH 8.0) 20mM Imidazole
<b>Wash buffer II</b>	Lysis buffer (pH 8.0) 40mM Imidazole
<b>Elution buffer</b>	Lysis buffer (pH8.0) 250mM Imidazole

## Antibody information

<b>Antibody</b>	<b>Company</b>	<b>Western Blotting Dilution in 5% Milk</b>	<b>Confocal Microcopy Dilution in 5% BSA</b>
<b>α-Ha</b>	Cambridge Biosciences	1:1000	1:500
<b>α-Myc</b>	Sigma	1:1000	1:500
<b>α-CRM-1</b>	Novus	1:1000	1:500
<b>α-DDX3</b>	Santa Cruz	1:500	1:100
<b>α-DDX3</b>	Bethyl Laboratories	1:1000	1:250
<b>α-PhosT323 DDX3</b>	Abcam	1:200	1:250
<b>α-PhosHis H2A.2</b>	Cell Signalling	-	1:250
<b>α- eIF4E</b>	Abcam	1:500	1:250
<b>α- polyHistidine</b>	Sigma	1:1000	-
<b>α-Tubulin</b>	Abcam	1:1000	1:500
<b>α-PhosHis Ser H10</b>	Cell signalling	-	1:500
<b>α-Cyclin B</b>	Santa Cruz	1:250	1:100
<b>α-Cyclin E</b>	Santa Cruz	1:250	1:100
<b>α-Cyclin A</b>	Santa Cruz	1:250	1:100
<b>α-Cyclin D</b>	Santa Cruz	1:250	1:100
<b>α-Ha AlexaFluor 594</b>	Invitrogen	-	1:500
<b>α-HCV Core</b>	Abcam	-	1:500

**Table II:** Primary antibodies used for western blotting, immunofluorescent staining or immunoprecipitations.